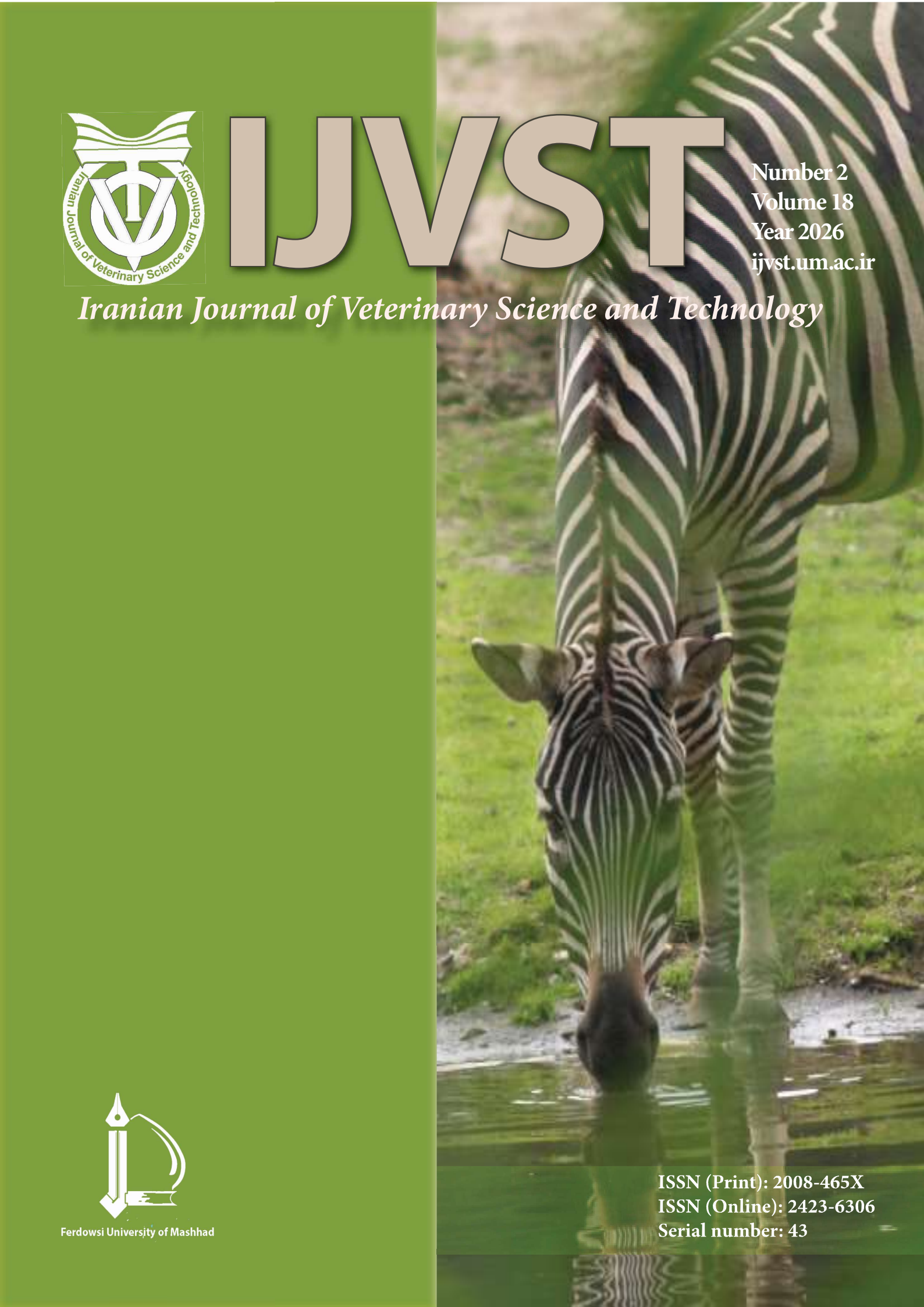

IJVST

Number 2
Volume 18
Year 2026
ijvst.um.ac.ir

Iranian Journal of Veterinary Science and Technology

Ferdowsi University of Mashhad

ISSN (Print): 2008-465X
ISSN (Online): 2423-6306
Serial number: 43

In the Name of God, the Compassionate, the Merciful

Iranian Journal *of* Veterinary Science and Technology

Editorial Office:
Faculty of Veterinary Medicine,
Ferdowsi University of Mashhad,
Azadi Square, Mashhad, IRAN
P.O. Box: 1793; Postal Code: 9177948974

Tel: +98 51 3880 3742 ***Fax:*** +98 51 3876 3852
Web: ijvst.um.ac.ir ***Email:*** ijvst@um.ac.ir

FERDOWSI UNIVERSITY OF MASHHAD PRESS

GENERAL INFORMATION

ISSN Print Edition: 2008-465X
ISSN Online Edition: 2423-6306

Journal Homepage:
ijvst.um.ac.ir

Abstracting and Indexing:
Scopus, ISI Master Journal List, Zoological Record; EMBASE, EBSCO, MIAR, Scientific Information Database (SID); Islamic World Science Citation Database (ISC); Magiran; Google Scholar; Centre for Agriculture and Biosciences International (CABI), DOAJ.

This journal has achieved the rating of:
- "Scientific-Research", by Commission of Evaluation of Iranian Scientific Journals, the Ministry of Science, Research and Technology, from Vol.7, No. 1, July 2015 onward.
- "International", by Commission of Evaluation of Iranian Scientific Journals, the Ministry of Science, Research and Technology, from Vol.13, No. 2, 2021 onward.

Publication Date:
Iranian Journal of Veterinary Science and Technology (IJVST) is published 4 times a year. Volume 14 with 4 issues appear in 2022.

Managing Director:
Abolghassem Naghibi, DVM, PhD

Editorial Officer:
Monir Taheri

Logo Design and Illustration:
Dr. Behrooz Fathi, Taraneh Ebnalnassir

Language Editors:
Kiarash Ebrahimi

SCOPE

Iranian Journal of Veterinary Science and Technology (IJVST) publishes important research advances in veterinary medicine and subject areas relevant to veterinary medicine including anatomy, physiology, pharmacology, bacteriology, biochemistry, biotechnology, food hygiene, public health, immunology, molecular biology, parasitology, pathology, virology, large and small animal medicine, poultry diseases, diseases of equine species, and aquaculture. Articles can comprise research findings in basic sciences, as well as applied veterinary findings and experimental studies and their impact on diagnosis, treatment, and prevention of diseases. IJVST publishes four kinds of manuscripts: Research Article, Review Article, Short Communication, and Case Report.

ON THE COVER

The plains zebra (Equus quagga) is one of the four zebra species (see page 81). Cover image: photograph from Pixabay, available under the Public Domain CC0 licens

Editorial Office:
Faculty of Veterinary Medicine,
Ferdowsi University of Mashhad,
Azadi Square, Mashhad, IRAN
P.O. Box: 1793; Postal Code: 9177948974

Tel: +98 51 3880 3742 ***Fax:*** +98 51 3876 3852
Web: ijvst.um.ac.ir ***Email:*** ijvst@um.ac.ir

FERDOWSI UNIVERSITY OF MASHHAD PRESS

TABLE OF CONTENTS

IRANIAN JOURNAL OF VETERINARY SCIENCE AND TECHNOLOGY

Editorial Office:
Faculty of Veterinary Medicine, Ferdowsi University of Mashhad,
Azadi Square, Mashhad, IRAN
P.O. Box: 1793; Postal Code: 9177948974

Tel: +98 51 3880 3742 ***Fax:*** +98 51 3876 3852
Web: ijvst.um.ac.ir ***Email:*** ijvst@um.ac.ir

TABLE OF CONTENTS

IRANIAN JOURNAL OF VETERINARY SCIENCE AND TECHNOLOGY

Editorial Office:
Faculty of Veterinary Medicine, Ferdowsi University of Mashhad,
Azadi Square, Mashhad, IRAN
P.O. Box: 1793; Postal Code: 9177948974

Tel: +98 51 3880 3742 ***Fax:*** +98 51 3876 3852
Web: ijvst.um.ac.ir ***Email:*** ijvst@um.ac.ir

Iranian Journal of Veterinary Science and Technology

Received: 2025- Sep-04
Accepted after revision: 2026- Feb-09
Published online: 2026- Feb-10

RESEARCH ARTICLE

DOI:10.22067/ijvst.2026.94932.1590

Morphological and molecular identification of common *Eimeria* species in sheep and goats of Bajestan area, Khorasan Razavi Province

Mohammad Abdollahi[a], Asma Keyvanlou[b], Gholamreza Razmi[c]

[a] Graduated in Doctor of Veterinary Medicine, Department of Pathobiology, Faculty of Veterinary Medicine, Ferdowsi University of Mashhad, Mashhad, Iran.
[b] Graduated in Veterinary Parasitology, Department of Pathobiology, Faculty of Veterinary Medicine, Ferdowsi University of Mashhad, Mashhad, Iran.
[c] Department of Pathobiology, Faculty of Veterinary Medicine, Ferdowsi University of Mashhad, Mashhad, Iran.

ABSTRACT

Coccidiosis is a gastrointestinal disease caused by *Eimeria* spp in small ruminants. Limited information is available regarding the identified *Eimeria* species in sheep flocks in Khorasan Razavi Province. The present study aimed to identify the common *Eimeria* species and detect the pathogenic species in sheep and goats flocks in the Bajestan area. Between September 2021 to June 2022, a total of 400 fecal samples were collected from the rectum of sheep and goats. Samples initially were examined using the Willis method for the presence of *Eimeria* infestation, and then the Oocyst per gram (OPG) OPG level was determined using the Clayton Lane method. Samples with high OPG values were cultured in a 2.5% potassium dichromate solution. After the sporulation of the cultured sample, the *Eimeria* species was identified by the morphological characteristics. Additionally, the DNA of sporulated *Eimeria* oocysts from sheep and goats was extracted and tested using the PCR method. Two positive samples of each of these animals were selected and submitted for sequencing. In the present study, the prevalence of *Eimeria* spp infection was 69.5% (139/200) in sheep and 69% (138/200) in goats. In morphological studies, *Eimeria* faurei and *Eimeria* ovinoidalis were identified in sheep, and *Eimeria* alijevi, *Eimeria* hirci, and *Eimeria* christenseni were identified in goats. PCR amplification confirmed the presence of *Eimeria* spp in positive samples. The findings indicate a high prevalence of mixed *Eimeria* spp. infection in sheep and goats in the Bajestan area. In addition, two *Eimeria* species in sheep and three species in goats were morphologically identified.

Keywords

Prevalence, Identification, Eimeria; goat, sheep

Number of Figures: 3
Number of Tables: 1
Number of References:: 42
Number of Pages: 7

Abbreviations

OPG: Oocyst per gram

PCR : polymerase chain reaction

Corresponding author: Gholamreza Razmi
Email: razmi@um.ac.ir
Tel: +98(51)3876-3853

Introduction

Coccidiosis is one of the most common worldwide gastrointestinal disease affecting ruminants and poultry [1]. Coccidiosis caused by *Eimeria* spp. is a high-morbidity parasitic disease affecting various animal species, including sheep and goats [2]. *Eimeria* spp. Infections may result in either acute or chronic intestinal disorders in small ruminants and are responsible for significant economic losses worldwide [3].

Eimeria spp. is host-specific, which means an *Eimeria* species that infects goats does not infect sheep, and vice versa [4]. Many species of *Eimeria* have been identified in sheep and goats.

Among these species, three species of *E. ovinoidalis, E. ahsata,* and *E. crandalis* are known as pathogenic species in sheep, and four species of *E. caprina, E. ninakohlyakimovi, E. christenseni*, and *Eimeria* arloingi are known as pathogenic species in goats [5]. Among the known pathogenic species of *Eimeria* in goats are *E. arloingi* and *E. ninakohlyakimovi* that are known as the dominant pathogenic species in Iran as well as many other parts of the world [6].

Environmental and climatic factors are crucial in development, survival, and transmission of coccidiosis. *Eimeria* oocysts can survive in the environment for extended periods, ranging from a few weeks to several months, under favorable conditions moderate temperature and adequate humidity [7].

Coccidiosis is primarily spread through the ingestion of sporulated oocysts of *Eimeria* spp [8]. The life cycle of *Eimeria* consists of three main stages: asexual reproduction (schizogony) and sexual reproduction (gametogony) within the host's body, and sporogony outside the host in the external environment [9]. The location of these stages, whether in the small or large intestine, depends on the *Eimeria* species involved [4].

Coccidiosis in small ruminants occurs in both clinical and subclinical forms [10]. The clinical form is associated with diarrhea and death, while the subclinical form shows weight loss and reduction in animal production both in sheep and goats [7,11]. Studies indicate that most domestic ruminants become infected with coccidiosis at some point during their lifetime [7,12], with lambs between 1 and 6 months of age being the most susceptible [13]. Adult animals generally exhibit milder clinical signs due to high immunity from repeated infections [4,14].

Eating colostrum in lambs on the first day of birth creates immunity against the disease for several weeks after birth [15,16]. Nevertheless, when animals ingest large number of sporulated oocysts, the invasive stages of *Eimeria* spp. can cause enteritis and diarrhea [4,17]. This invasion cause destruction of intestinal mucosal cells, and cell rupture and may lead to diarrhea and dehydration. Also, it may disrupt the absorption of nutrients, albumin and electrolytes, and, in severe cases anemia, hypoalbuminemia and electrolyte imbalance [4].

Coccidiosis primarily affects young and immature ruminants, and its clinical manifestation includes symptoms such as diarrhea, anorexia, poor growth, and weight loss [18]. Although hemorrhagic diarrhea due to coccidiosis is less common in lambs and kids, it is more prevalent in calves [4,19]. Necropsy findings in affected small ruminants may include catarrhal enteritis, bleeding, and inflammation of the mucous membranes of the small and large intestines [20]. Coccidiosis is often a self-limiting disease and sometimes improves without specific treatment [21]. Numerous drugs are prescribed to treat and prevent coccidiosis, including amprolium, sulfonamides, lasalocid, and monensin. Environmental hygiene should be observed to avoid the disease, and rotation of grazing animals is effective; drugs can also be used for prevention [22,23].

According to studies, *Eimeria* parasites' prevalence in different parts of Iran varies between 16% and 89.91 %, and infection with more than one *Eimeria* species has also been reported between 56% and 100% of positive samples in different herds [24,25, 26,27,28,29]. Despite the importance of sheep and goat breeding in Khorasan province, limited studies have investigated the species composition of *Eimeria* species in this region. Therefore, the present study aimed to identify common morphological species of *Eimeria* and molecular confirmation of pathogenic species in sheep and goats in the Bajestan area.

Results

Out of 200 fecal samples collected from sheep in the study area , 139 samples were positive for *Eimeria* oocysts, representing a prevalence rate of 69.5%. Similarly, among the 200 fecal samples obtained from goats, 138 samples were positive, indicating a prevalence rate of 69%. The Clayton lane method was used to determine the OPG values in samples that tested positive for *Eimeria* oocysts. The mean OPG values (± standard deviation) recorded for sheep and goats during different months are presented in Table 1.

Using the morphological identification keys available for *Eimeria* species in goats, *E. christenseni* (5.5%), *E. elijoi* (13.63%), and *E. hirci* (0.5%) were identified. However, due to the similarity in morphology between the three species of *E.caprina*, *E. caprovina*, and *E. sefronika* (46.96%), and the similarity between the two species of *E.arloingi* and *E.jolchijovi* (16.16%), it was not possible to distinguish these species from each other. Accurate identification of these species re-

Table 1.
OPG level of fecal samples in sheep and goats in different months

Results of OPG Month	Sheep	Goat
	Mean ± SD	Mean ± SD
November	51.45 ± 104	85.46 ± 40
December	71.07 ± 57	38.83 ± 47
January	56.65 ± 39	162.45 ± 61
February	64.23 ± 37	338 ± 304.
March	13.51 ± 12	131.24 ± 81

quired molecular testing, as shown in Figure 1.

Also, based on the observations made, two species of *E.faurei* (74.74%) and *E. ovinoidalis* (8.08%) were identified in sheep. However, due to the similarity in morphology between the species of *E. ahsata, E. bacquensis,* and *E. granulosa* (5.05%), it is not possible to definitively distinguish these species from each other through morphological methods, and accurate identification requires molecular testing as shown in (Figure 2).

In this study, two DNA samples extracted from *Eimeria* oocysts collected from goats and sheep were tested by PCR along with positive and negative controls. Both sheep and goat samples showed a band slightly larger than 300 bp (Figure 3).

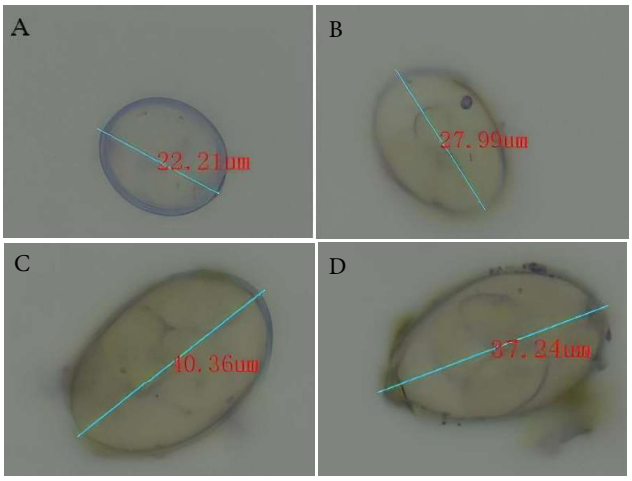

Figure 1.
A: *E.elijoi,* B: *E. arloingi* or *E. jolchijovi, C: E. caprina* or *E. sefronika*, D: *E.christenseni* in goats.

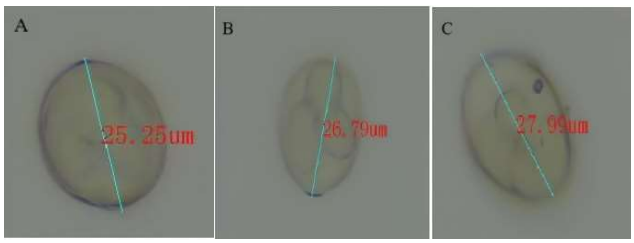

Figure 2.
A: *E. ahsata* or *E.bacquensis*, B: *E. faurei*, C: *E.ovinoidalis* in sheep.

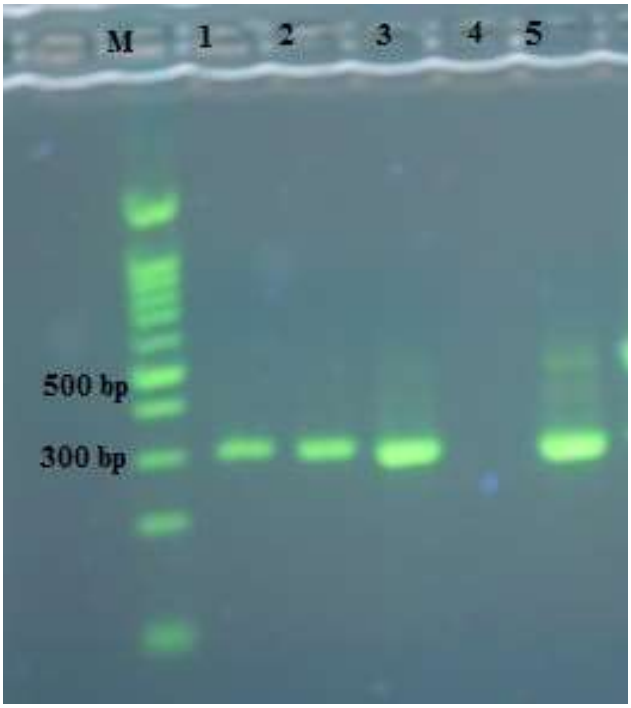

Figure 3.
Electrophoresis results of PCR with special primers; M: Marker 100 bp, 1, 2: positive sample(goat), 3: positive sample(sheep), 4: negative control, 5: positive control.

Discussion

The present study revealed a prevalence of coccidiosis of 69.5% in sheep and 69% in goats in the Bajestan area w of Khorasan Razavi Province. The prevalence of coccidiosis has been reported in sheep and goats in different studies conducted in various countries and regions. The prevalence rates vary from 54% to 90.09%, depending on the location, climate, and diagnostic methods. The highest prevalence (90.09%) has been reported in China, while the lowest prevalence was recorded in Ordon [34,35,36].

In Iran, Yakhchali et al. reported a 16.7% prevalence of coccidiosis in sheep in Tabriz [37]. Nourollahifar et al. reported a 63% prevalence of coccidiosis in sheep in Rudsar [38]. Many *Eimeria* species have been identified in sheep and goats, some of which can cause disease. According to studies, *E.ovina* has the highest pathogenicity in sheep; *E. ahhsata* and *E. crandalis* are next in line, and *E. faurei*, has low pathogenicity [39]. In goats, *E. ninakohlyakimoi* and *E.caprina* have the highest pathogenicity, and *E. arloingi* has low pathogenicity [40]. In the present study, morphological examination identified *E.faurei* and *E. ovina* in sheep. However, due to the morphological similarities among *E.ahhsata*, *E.granulosa*, and *E. bukidnonensis*, a conclusive identification solely based on morphological characteristics was not possible.

Additionally, in goats, species such as *E. elijoyi, E. christenseni,* and *E. hirci* were identified using available morphological keys. However, the close morphologi-

cal resemblance between *E. arloingi* and *E. jolchijovi,* along with similarities among *E. caprina, E. caprovina*, and *E.espinosa*, prevented an accurate diagnosis from being made using the morphological approach[31].

In research carried out by Yakhchali et al. involving sheep fecal samples from Malayer region, *E. faurei* was found to be the most common species among lambs younger than six months of age, and the second most common species overall after *E. intracata*, [25].

Vasilkova et al. identified *E.elijoyi* and *E. arloingi* as dominant species in goats following examination of various *Eimeria* species in sheep and goats [41]. In this study, the highest prevalence in sheep was related to E. faurei, and in goats was related to one of *E. caprina, E.caprovina,* or *E. espheronica.*

Interestingly, *E. ovinoidea* frequently reported as a dominant species in sheep in many studies, was reported with low prevalence in this study. In goats, *E. ninakohlyakimoi* was reported with high prevalence in various studies, but was not identified in this study. The OPG level recorded in this study did not follow a specific pattern during different months and fluctuated during different months. According to studies, the OPG level observed in sheep and goats in Bajestan were lower compared to those reported in other regions of Iran and the worldwide. Standard methods for identifying different *Eimeria* species, including morphological and histological approaches, are time-consuming and often lack sufficient sensitivity. Overlapping morphological characteristics between *Eimeria* species further complicate accurate identification. Therefore, the development and evolution of molecular diagnostics for identifying and determining the characteristics of parasites have been very helpful [42].

The 18S rRNA gene has been used as a molecular target to distinguish closely related *Eimeria* species and for conducting phylogenetic analyses. Amplification of fragments ranging between 384 and 546 bp has been effectively amplified using primer sets targeting the 3' end of the 18S rRNA gene and the 5' end of the 5.8S rRNA gene within the ITS-1 regions of the Eimaria genus [32]. In the present study, PCR results confirmed the presence of *Eimeria* spp in fecal samples in sheep and goats. however, sequencing of the PCR samples yielded low quality results, which prevented the identification of the dominant species of sheep and goats in the Bajestan area. Consequently, it is essential to gather a larger number of representative samples of various *Eimeria* species from sheep and goats; sequencing these samples can facilitate phylogenetic analysis and precise identification of morphologically similar *Eimeria* species.

In conclusion, the present study identified *E. faurei* and *E. ovinoidalis* as the predominant species in sheep and *E. elijoyi, E. christenseni,* and *E. hirci in* goats based on morphological examination. Although, PCR amplification of ITS1 region was successfully performed for positive samples, sequencing samples had low quality and results were insufficient for phylogenetic analysis.

Materials & Methods

Declaration of Generative AI and AI-assisted technologies in the writing process

To reduce noise and preserve fine details in microscopic images, AI-based image enhancement methods were employed."

Sampling

This study was conducted from September 2021 to June 2022, and fecal samples of sheep and goats were collected to determine the frequency of *Eimeria* spp infection and identify *Eimeria* species in Bajestan, Khorasan Razavi province, Iran.

The sample size was calculated based on a previously reported prevalence rate of 20% in Zabol area [28,29]. Accordingly, 200 fecal samples per animal were collected. Each month, fecal samples of 40 sheep and 40 goats were collected directly from the rectum in special containers and transferred to the parasitology laboratory of the Faculty of Veterinary Medicine at Ferdowsi University of Mashhad.

Microscopic examination

The fecal samples were examined by the Willis method [30]. Samples that tested positive were separated and preserved for further testing. Oocysts per gram (OPG) were determined quantitatively by the Clayton Lane method [30]. After examination, oocysts were purified and transferred into 2.5% (w/v) potassium dichromate solution to allow sporulated at room temperature [30]. Species identification was performed based on oocyst size and morphology (shape, color, form index, presence or absence of micropyle and its cap, presence or absence of residual, polar, and Stieda bodies of the oocysts and sporocysts). One hundred sporulated oocysts were identified using the available morphological keys [30,31]. The size of *Eimeria* oocysts was determined using a digital microscope.

DNA extraction and PCR test

Positive Samples were isolated, examined under light microscope, and preserved for molecular detection. DNA was extracted from the fecal samples using Genomic DNA Purification kit (denazist Co, Mashhad) following the manufacturer's instructions. DNA samples were kept at −20 °C until processed for PCR assay.

The ITS-1 region of *Eimeria* spp. from each positive sample was amplified using PCR and the cycling conditions and primer sequences of the forward and reverse primers were as follows:

Forward: 5'-GCAAAAGTCGTAACACGGTTTCC-3',
Reverse: 5'CTGCAATTCACAATGCGTATCG-3

Cycling conditions were: initial denaturation at 94'C for 5 min followed by 35 cycles of 94°C for 45 s, 65°C for 1 min and 72°C for 1 min, this was followed by a final extension at 72°C for 7 min. The amplification products from ITS-1 rRNA were separated on a 1.8% agarose gel containing 1 µl/mL of green viewer for 40–60 min, and then imaged. From the PCR products, one positive sample from sheep, and

one from goat were selected and sent for sequencing [32, 33].

Sequencing

PCR positive samples using the primers were submitted for sequencing to a company in Iran (Topaz- Genekaush Co, Karaj, Iran). The submitted samples were sequenced using the MEGA-4 software, and after performing a blast, the sequenced samples from sheep and goats did not match any of the registered samples in the gene bank.

Statistical analysis

The prevalence of *Eimeria* spp infection in sheep and goats was calculated by SPSS software version 22(IBM company.USA)

Authors' Contributions

Conceptualization: G.R.R., Methodology: M.A., A.K, Investigation: M.A, A.K, G.R.R, Writing - original draft preparation: M.A., A.K., Writing - review and editing: G.R., Funding acquisition: G.R.R., Supervision: G.R.R.

Acknowledgements

The authors thank Mr Hamid Eshrati for his assistance with the laboratory examination. This study was supported by grant No 3/57226 from the Vice President of Research and Technology of Ferdowsi University of Mashhad, Iran.

Conflict of interest

The authors declare that there is no conflict of interest.

References

1. Ashfaq K, Asghar AY, Hashmi SS, Abbas A. Bovine Cocvidiosis: A formidable challenge to cattle industry. Int J Res Adv Agric Sci. 2023;2(2):34–42.

2. Hafeez MA, Sattar A, Khalid K, Khalid AR, Mahmood MS, Aleem MT, et al. Molecular and morphological characterization of Eimeria crandallis isolated from deer (Cervidae) in different captive animals. Life. 2022;12(10):1621. Doi:10.3390/life12101621.

3. de Macedo LO, Bezerra-Santos MA, de Mendonça CL, Alves LC, Ramos RAN, de Carvalho GA. Prevalence and risk factors associated with infection by Eimeria spp. in goats and sheep in Northeastern Brazil. J Parasit Dis. 2020;44(3):607–12. Doi:10.1007/s12639-020- 01235-3.

4. Bangoura B, Bardsley KD. Ruminant coccidiosis. Vet Clin Food Anim Pract. 2020;36(1):187–203.

5. Shaheed HA, Al-Aziz SA. Eimeriosis is small ruminants in Basrah province/southern Iraq. One Heal Triad. 2023; 3:60–68. Doi:10.47278/book.oht/2023.78.

6. Soe AK. Coccidia (Protozoa: Apicomplexa) of the domesticated goat Capra hircus in New Zealand: a thesis presented in partial fulfilment of the requirements for the degree of Master of Philosophy in veterinary science at Massey University. Massey University, 1989.

7. Bangoura B, Bhuiya MAI, Kilpatrick M. Eimeria infections in domestic and wild ruminants with reference to control options in domestic ruminants. Parasitol Res. 2022;121(8):2207–32. Doi:10.1007/s00436-022-07564-x

8. Zhang K, Liang G, Lang J, Qin Z, Zhang Y, Wang Y, et al. Eimeria spp. (Eimeriidae) in the migratory whooper swan (Cygnus cygnus) Linnaeus, 1758 (Anatidae) from Sanmenxia Swan Lake National Urban Wetland Park in the middle reaches of the Yellow River in China. Parasitol Res. 2022;121(10):2967–77. Doi:10.1007/s00436-022-07629-x.

9. Pandian TJ. Evolution and speciation in Protozoa. CRC Press; 2023. Doi:10.1201/9781003323716.

10. Elazazy OM. Eimeria species infection in small ruminants in Kuwait. Egypt Vet Med Soc Parasitol J. 2023;19(1):36–42. Doi:10.21608/evmspj.2023.305397.

11. Mohamed HI, Arafa WM, El-Dakhly KM. Ovine coccidiosis and associated risk factors in Minya, Egypt. Beni-Suef Univ J Basic Appl Sci. 2022;11(1):137. Doi:10.1186/s43088-022-00318-9.

12. Hatam-Nahavandi K, Carmena D, Rezaeian M, Mirjalali H, Rahimi HM, Badri M, et al. Gastrointestinal parasites of domestic mammalian hosts in Southeastern Iran. Vet Sci. 2023;10(4):261. Doi:10.3390/vetsci10040261.

13. Barre A, Hirabe AM, Mohamed AA, Ibrahim AA, Mohamed HE, Adan MA, et al. Prevalence, public health and associated risk factors of coccidiosis in small ruminants at Deyniile sub-district in Mogadishu, Somalia. J Vet Med Anim Sci. 2023;6(1):1–6.

14. Sule IF, Kingsley DG, Adamu NM. Prevalence of coccidia in sheep at the Bauchi Abattoir, Inkil, Bauchi state. Int J Zool Appl Biosci. 2021;6(6):288–92.

15. van Rooyen J. The principles of good lamb survival. Stockfarm. 2022;12(2):50–1.

16. van Wyngaard J. Caring for lambs. Farmer's Weekly. 2021;2021(21030):40–2.

17. Ashraf A, Shahardar RA, Bulbul KH, Wani ZA, Allaie IM, Mir AQ. Efficacy of amprolium against goats in central Kashmir. J Entomol Zool Stud. 2020;8(3):1667–70. Doi:10.22271/j.ento.2020.v8.i3z.6978.

18. Kaur S, Singla LD, Sandhu BS, Bal MS, Kaur P. Coccidiosis in goats: pathological observations on intestinal developmental stages and anticoccidial efficacy of amprolim. Indian J Anim Res. 2019;53(2):245–9.

19. Durgut MK, Ok M. Evaluation of Some Intestinal Biomark-

ers in the Determination of Intestinal Damage in Calves with Coccidiosis. Trop Anim Sci J. 2023;46(2):221–30. Doi:10.5398/tasj.2023.46.2.221.

20. Van Metre DC, Tyler JW, Stehman SM. Diagnosis of enteric disease in small ruminants. Vet Clin North Am Food Anim Pract. 2000;16(1):87–115. Doi:10.1016/S0749-0720(15)301389.

21. Adolph C. Coccidia. Clin Small Anim Intern Med. 2020;1023–7. Doi: 10.1002/9781119501237.ch111.

22. Noack S, Chapman HD, Selzer PM. Anticoccidial drugs of the livestock industry. Parasitol Res. 2019;118(7):2009–26. Doi:10.1007/s00436-019-06343-5.

23. Constable PD, Hinchcliff KW, Done SH, Gruenberg W. A textbook of the diseases of cattle, horses, sheep, pigs, and goats. Vet Med. 2017; pp:2045.

24. Hashemnia M, Rezaei F, Chalechale A. Prevalence, intensity, and pathological lesions of Eimeria infection in goats in western Iran. Comp Clin Path. 2015;24(4):805–10. Doi: 10.1007/s00580-014-1986-7.

25. Yakhchali M, Golami E. Eimeria infection (Coccidia: Eimeriidae) in sheep of different age groups in Sanandaj city, Iran. Vet Arh. 2008;78(1):57-64.

26. Kheirandish R, Nourollahi-Fard SR, Yadegari Z. Prevalence and pathology of coccidiosis in goats in southeastern Iran. J Parasit Dis. 2014;38(1):27–31. Doi:10.1007/s12639-012-0186-0.

27. Radfar MH, Sakhaee E, Shamsaddini BM, HAJ MH. Study on gastrointestinal parasitic infection in Raeini goats. Iran J Vet Res Shiraz Univ. 2011;12(1):76–80.

28. Mirzaei M, Dahmardeh E. The prevalence of Eimeria species in sheep in Zabol city, Iran. Iran Vet J. 2016;11(4):98–105. Doi:10.22055/ivj.2016.13021.

29. Lwanga SK, Lemeshow S. Sample size determination in health studies. Geneva World Health Organ. 1991;1.

30. E. J. L. Soulsby. Helminths, arthropods, and protozoa of domesticated animals. London: Baillière Tindall; 1982. 809 pp.

31. Eckert J, Braun R, Shirley MW CP. Biotechnology: guidelines on techniques in coccidiosis research. 1st ed. Luxembourg: Office for Official Publications of the European Communities; 1995. 660 pp.

32. Kawahara F, Zhang G, Mingala CN, Tamura Y, Koiwa M, Onuma M, et al. Genetic analysis and development of species-specific PCR assays based on the ITS-1 region of rRNA in bovine Eimeria parasites. Vet Parasitol. 2010;174(1–2):49–57. Doi:10.1016/j.vetpar.2010.08.001.

33. Khodakaram-Tafti A, Hashemnia M, Razavi SM, Sharifiyazdi H, Nazifi S. Genetic characterization and phylogenetic analysis of Eimeria arloingi in Iranian native kids. Parasitol Res. 2013;112(9):3187–92. Doi: 10.1007/s00436-013-3494-0.

34. Wang CR, Xiao JY, Chen AH, Chen J, Wang Y, Gao JF, et al. Prevalence of coccidial infection in sheep and goats in northeastern China. Vet Parasitol. 2010;174(3–4):213–7. Doi:10.1016/j.vetpar.2010.08.026.

35. Souza LEB de, Cruz JF da, Teixeira MR, Albuquerque GR, Melo ADB, Tapia DMT. Epidemiology of Eimeria infections in sheep raised extensively in a semiarid region of Brazil. Rev. Bras. Parasitol. Veterinária. 2015;24(4):410–5. Doi:10.1590/S1984-29612015070.

36. Abo-Shehada MN, Abo-Farieha HA. Prevalence of Eimeria species among goats in northern Jordan. Small Rumin Res. 2003;49(2):109–13. Doi:10.1016/S0921-4488(03)00078-6.

37. Yakhchali, M., Zarei, MR. Prevalence of Eimeria infection in sheep of Tabriz suburb, Iran. Iran J Vet Res. 2008;9(3):277–80.

38. Nourollahi-Fard SR, Khedri J, Ghashghaei O, Mohammadyari N, Sharifi H. The prevalence of ovine Eimeria infection in Rudsar, North of Iran, (2011–2012). J Parasit Dis [Internet]. 2016;40(3):954–7. Doi:10.1007/s12639-014-0613-5.

39. J. P. Dubey. Coccidiosis in Livestock, Poultry, Companion Animals, and Humans. 1st ed. Boca Raton: CRC Press; 2019. 394 pp.

40. Yakhchali M, Rezaei AA. The prevalence and intensity of Eimeria spp. infection in sheep of Malayer suburb, Iran. Arch Razi Inst. 2010;65(1):27–32.

41. Vasilková Z, Krupicer I, Legáth J, Kovalkovičová N, Peťko B. Coccidiosis of small ruminants in various regions of Slovakia. Acta Parasitol. 2004 Dec 1; 49:272–5.

42. Al-Habsi K, Yang R, Ryan U, Miller DW, Jacobson C. Morphological and molecular characterization of three Eimeria species from captured rangeland goats in Western Australia. Vet Parasitol Reg Stud Reports. 2017; 9:75–83. Doi:10.1016/j.vprsr.2017.05.001.

How to cite this article
Abdollahi M, Keyvanlou A, Razmi Gh. Morphological and molecular identification of common Eimeria species in sheep and goats of Bajestan area, Khorasan Razavi Province. Iran J Vet Sci Technol.2026; 18(2): 1-7
DOI: https://doi.org/10.22067/ijvst.2026.94932.1590
URL: https://ijvst.um.ac.ir/article_47906.html

Iranian Journal of Veterinary Science and Technology

Received: 2025- Jul-13
Accepted after revision: 2025- Nov-29
Published online: 2025- Dec-01

RESEARCH ARTICLE

DOI: 110.22067/ijvst.2025.93330.1533

Cryo-infarction: a method of choice for the establishment of a rat model of myocardial infarction

Alireza Karimi[a], Maryam M. Matin[a,b], Azadeh Haghighitalab[a,c], Hossein Kazemi Mehrjerdi[d], Masoud Rajabioun[d], Mehrdad Aghasizadeh[a], Ahmad Reza Bahrami[a,b]

[a] Department of Biology, Faculty of Science, Ferdowsi University of Mashhad, Mashhad, Iran.
[b] Institute of Biotechnology, Ferdowsi University of Mashhad, Mashhad, Iran.
[c] Stem Cells and Regenerative Medicine Department, Academic Center for Education, Culture, and Research (ACECR) - Khorasan Razavi, Iran.
[d] Department of Clinical Sciences, Faculty of Veterinary Medicine, Ferdowsi University of Mashhad, Mashhad, Iran.

ABSTRACT

Ligation of the left anterior descending (LAD) coronary artery is a widely used method for inducing myocardial infarction (MI) in experimental models; however, it is associated with substantial limitations, including high mortality rates, excessive bleeding and variability in infarct size. Cryo-infarction has emerged as a promising alternative that may overcome these challenges by providing improved survival and reproducibility. In the present study, we aimed to refine the cryo-infarction method as a reliable and practical rat model for MI. Adult male Wistar rats underwent open-chest surgery under mechanical ventilation, followed by either LAD ligation or cryo-induced infarction. Model validation was performed using TTC (2,3,5-triphenyltetrazolium chloride) staining and immunofluorescence analysis, serum troponin I measurement, and electrocardiography assessment. Infarct severity was further evaluated by echocardiography, hematoxylin, and eosin staining, and Masson's trichrome staining. Our findings demonstrate that cryo-infarction provides several advantages over conventional ligation, including simplicity, reproducibility, and reduced mortality. These results highlight the potential of cryo-infarction as a standard approach for developing robust animal models, benefiting both basic and translational cardiovascular research.

Keywords

Heart, Myocardial infarction, Cryo-infarction, LAD, Rat model

Number of Figures: 9
Number of Tables: 1
Number of References:: 33
Number of Pages: 14

Abbreviations

AAR: Area at risk

AS: Atherosclerosis

Corresponding author: Ahmad Reza Bahrami
Email: ar-bahrami@um.ac.ir
Tel: +98(51)3880-5505

Introduction

Myocardial infarction, commonly referred to as a heart attack, is acute ischemia condition that results in irreversible damage to cardiac muscle tissue. This is commonly caused by blood clots that obstruct a coronary artery [1][2]. The clot formation or thrombosis that triggers myocardial infarction may arise from disrupted endothelial function, platelet activation, or coagulation factor imbalances, among other factors. The resulting ischemic injury to cardiomyocytes leads to cardiac dysfunction and potential complications such as arrhythmias, heart failure, or sudden cardiac death [3][4]. Researchers often seek to replicate myocardial infarction in laboratory animals to study its causes and explore therapeutic interventions. To study the process of the disease in detail, animal models have played a very important role in laboratory investigations for many decades [5]. Among available laboratory species, rats are widely used due to their cost-effectiveness, ease of handling, and genetic similarities to humans. These animals have helped researchers to create MI models and develop many novel therapeutic methods [6]. A variety of approaches have been developed to induce MI model and the success rate of the investigators depends on each method. The common procedures for the MI induction include: permanent ligation (PL), chemical methods (isoproterenol-induced MI model), and cryoinjury. Additionally, the high-fat diet method is used to study the pathology of coronary artery diseases (CADs) in animals. This approach involves feeding experimental animals with cholesterol-rich foods for a relatively long time, inducing hyperlipidemia, atherosclerosis (AS), and sclerotic plaques, resulting in stenosis in blood vessels and myocardial ischemia. Although animal models created with a high-fat diet closely mimic the natural progression of human CAD patients, this approach is labor-intensive and presents challenges in precisely controlling myocardial ischemia [6]. Rats are frequently selected for CAD studies because they are easy to maintain, have high survival rates, and are inexpensive to keep. However, the absence of a gallbladder and a natural resistance to spontaneous anti-AS formation limit their suitability as ideal CAD models. This character makes it difficult to induce AS lesions by a high-fat diet alone. Therefore, most researchers prefer to use a combination of drugs and/or injury to form AS lesions. Although the morphology of AS lesions and plaque rupture positions in rats are similar to those in humans, the underlying pathogenesis still differs from that observed in human CAD [6][7]. Pharmacological induction is relatively simple and usually uses abdominal, caudal, or sublingual vein injection of pituitrin or isoproterenol (ISO), which can result in short-term MI. The isoproterenol-induced acute myocardial infarction (AMI) model is a widely used and well-established non-surgical approach in rats. ISO is a chemical compound that produces extensive necrosis in the ventricular subendocardial region and interventricular septum. This model offers several advantages over surgical models, including low mortality rate, technical simplicity, and absence of post-surgical infections. Rats are commonly preferred for this model, but several other species, like mice and rabbits, are also reported to be used. The ISO-induced MI model is widely used in assessing the cardio-protective activity of natural as well as synthetic compounds [6][8]. However, this model is unsuitable for investigating autolysis recanalization in clinical settings. In the PL technique, an anesthetized rat undergoes left thoracotomy followed by LAD occlusion. This method requires surgical left thoracotomy in anesthetized rats, where the LAD is ligated [9][10]. LAD ligation induces complete ischemia, leading to irreversible oxygen deprivation, significant Area at risk (AAR) infarction, and permanent scar formation. This scar tissue is susceptible to pathological remodeling, ultimately contributing to the progression of heart failure. Furthermore, the anatomical site of coronary occlusion significantly influences the infarction extent, with proximal ligations producing larger infarcts than distal occlusions; occlusion closer to the heart's base results in a larger and more severe injury. The PL technique typically produces extensive myocardial damage, with infarcts generally encompassing 30-40% of the total myocardial area [6][11]. A major advantage of employing the PL method is that it results in a substantial infarction, leading to clearer distinctions in cardiac function between sham-operated and MI animals [12]. The surgical ligation model is a widely used method for inducing AMI by ligating different regions of the coronary artery, with the LAD coronary artery ligation being the most common. This method was first introduced by Johns and Olson in 1954 and has since been adapted for use in both small and large animal species. Mice and rats are commonly employed

Abbreviations-Cont'd

CAD: Coronary artery disease
EF: Ejection fraction
ECG: Electrocardiography
FS: Fractional shortening
ISO: Isoproterenol
LAD: Left anterior descending
LDL: Low-density lipoprotein
LV: Left ventricle
MI: Myocardial infarction
PL: Permanent ligation
ROS: Reactive oxygen species
TBS: Tris-buffered saline

in laboratory settings for surgical ligation due to their numerous benefits compared to larger animals. The main limitations of LAD model are high mortality rate, post-surgical infection, variation in infarct size from 4-59%, requirement of expert hands, and an artificial ventilator. Performing this technique on mice is challenging and necessitates advanced surgical proficiency with microsurgical techniques. Complications can arise due to tissue damage, high perioperative mortality rates, intraoperative bleeding, lung damage or collapse, ligation errors, or inadequate ventilation. Cryoinjury represents an alternative method for inducing permanent myocardial injury. In this model, a pre-cooled rod at -196°C is applied to the heart, for multiple times, to cause injury. Cryoinjury leads to progressive structural reorganization and volumetric expansion of the left ventricular chamber [12]. The cryoinjury technique models myocardial infarction through controlled focal freezing of cardiac tissue. The cryo-infarction technique has been explored as a viable method for inducing MI in experimental models. The cryoinjury model produces well-defined myocardial damage characterized by histological features typical of infarction, including coagulation necrosis, hemorrhagic regions, inflammatory responses, and subsequent tissue repair with scar formation. This pathological progression ultimately results in heart failure, closely mimicking the outcomes observed in LAD ligation models, while providing a valuable alternative for investigating cardiac injury. Compared to surgical occlusion techniques, the cryodamage approach demonstrates superior technical simplicity and experimental reproducibility, as it eliminates the need for intricate vascular interventions [4]. In the present study, we propose that cryoinjury provides an optimal balance between reproducibility and physiological relevance for modeling MI and associated immune responses in rats. To our knowledge, no previous study has systematically compared cryoinjury with established MI induction methods.

Results

Cryo-induced myocardial infarction produces localized necrosis comparable to LAD ligation

The cryo method successfully induced myocardial infarction in rats. Post-procedure, a bright white and sunken region was observed at the site of cryo-injury, confirming the induction of localized infarction. Notably, this color change closely resembled the pale necrotic regions typically observed in LAD-ligation models, indicating a comparable loss of tissue viability. Quantitative analysis using TTC-stained sections revealed an infarct size of 12.52% in cryo-MI hearts (Figure 1A, B).

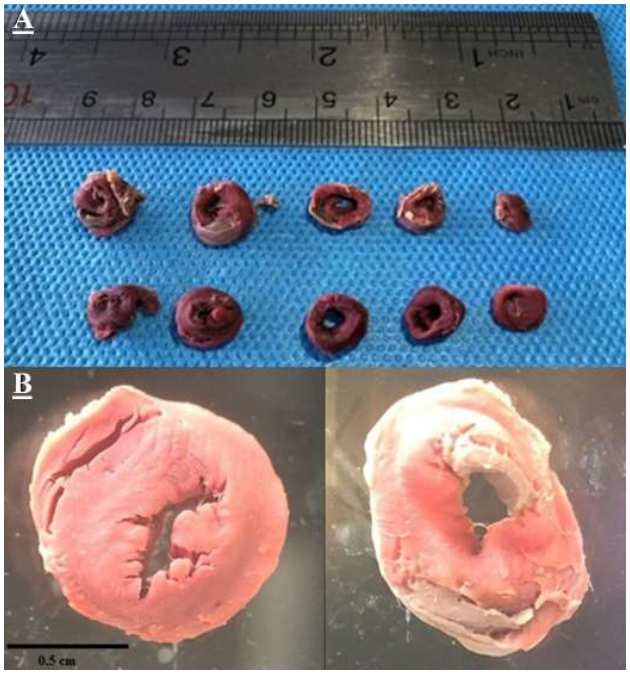

Figure 1.
Cryo-induced myocardial infarction shows pale necrotic regions compared to uniform red tissue in sham hearts. (A) The top row shows cryo-induced myocardial infarction, characterized by pale regions indicating infarcted tissue, while the bottom row represents the sham group with uniformly red myocardium, consistent with viable tissue. (B) Higher magnification of representative TTC-stained heart sections from sham (left) and cryo-MI (right) groups, 24 h post-surgery. The infarcted area in the cryo-MI sample was quantified as 12.52% using ImageJ software. Scale bar = 0.5 cm.

Cryo-induced myocardial infarction is associated with increased apoptosis and macrophage infiltration compared to sham

Immunofluorescence analysis revealed an increased accumulation of caspase-3 positive cells and expression of the macrophage marker CD68, in cryo-MI hearts compared to sham operated controls, indicating enhanced apoptosis and macrophage infiltration (Figures 2, 3). Quantitative analysis confirmed significant differences between groups ($p < 0.001$ for caspase-3; and $p < 0.01$ for CD68).

Cryo-induced myocardial infarction exhibits higher early survival than LAD ligation

Qualitative troponin testing was positive in all animals subjected to cryo-MI and LAD-MI procedures, whereas sham operated rats consistently tested negative. Survival analysis revealed a marked difference in early mortality between the two surgical approaches. Within the first 24 h post-surgery, 28 of 95 rats in the cryo-MI group died, corresponding to a survival rate of 70.59%. In contrast, 64 out of 102 rats in the LAD-

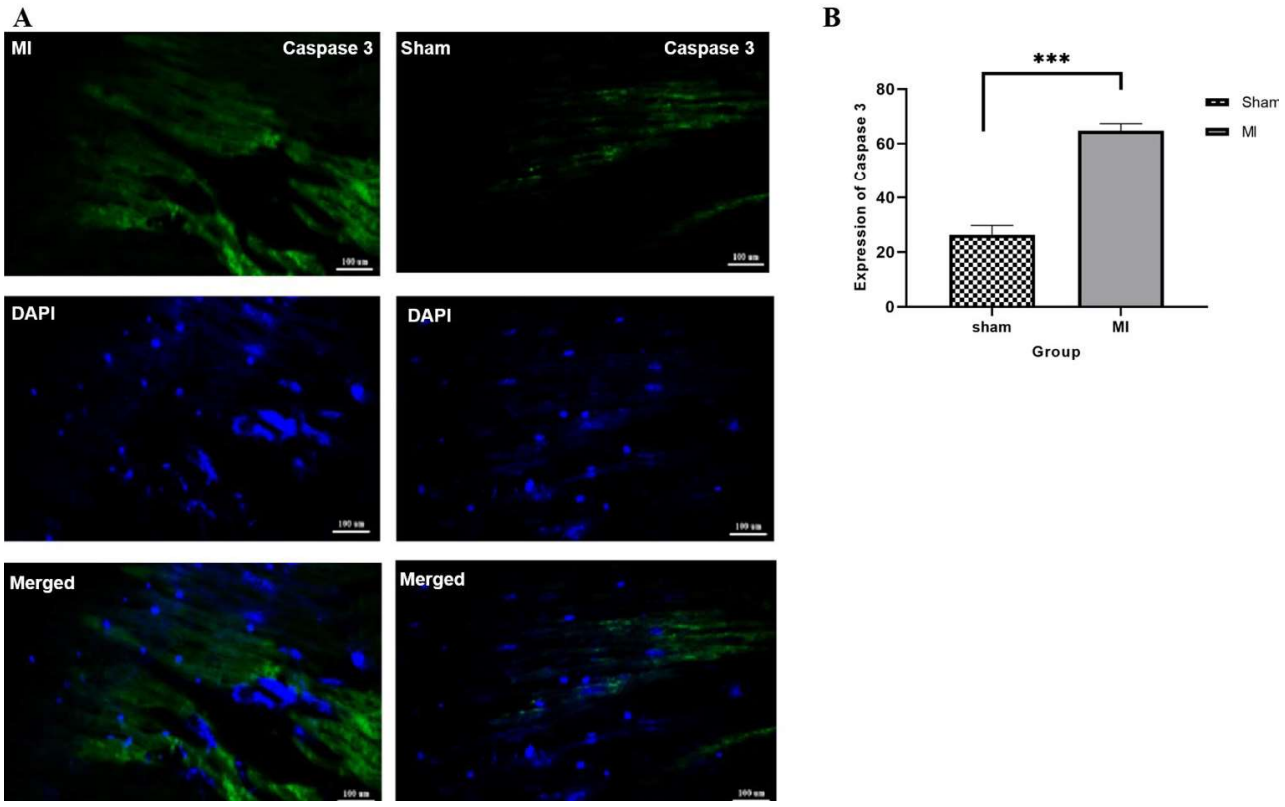

Figure 2.
Immunofluorescence detection and quantification of caspase-3 positive cells in sham and cryo-MI hearts. (A) Immunofluorescence staining of caspase 3 positive cells in sham and cryo-MI groups. Caspase-3 positive cells appear green, and nuclei are counterstained with DAPI (blue). Merged images show colocalization. Scale bar represents 100 µm. (B) Quantification was expressed as the percentage of caspase-3 positive cells relative to total nuclei. Quantitative analysis reveals a significant increase in caspase-3 expression in the cryo-MI group compared to sham ($p < 0.001$) (48 h after MI).

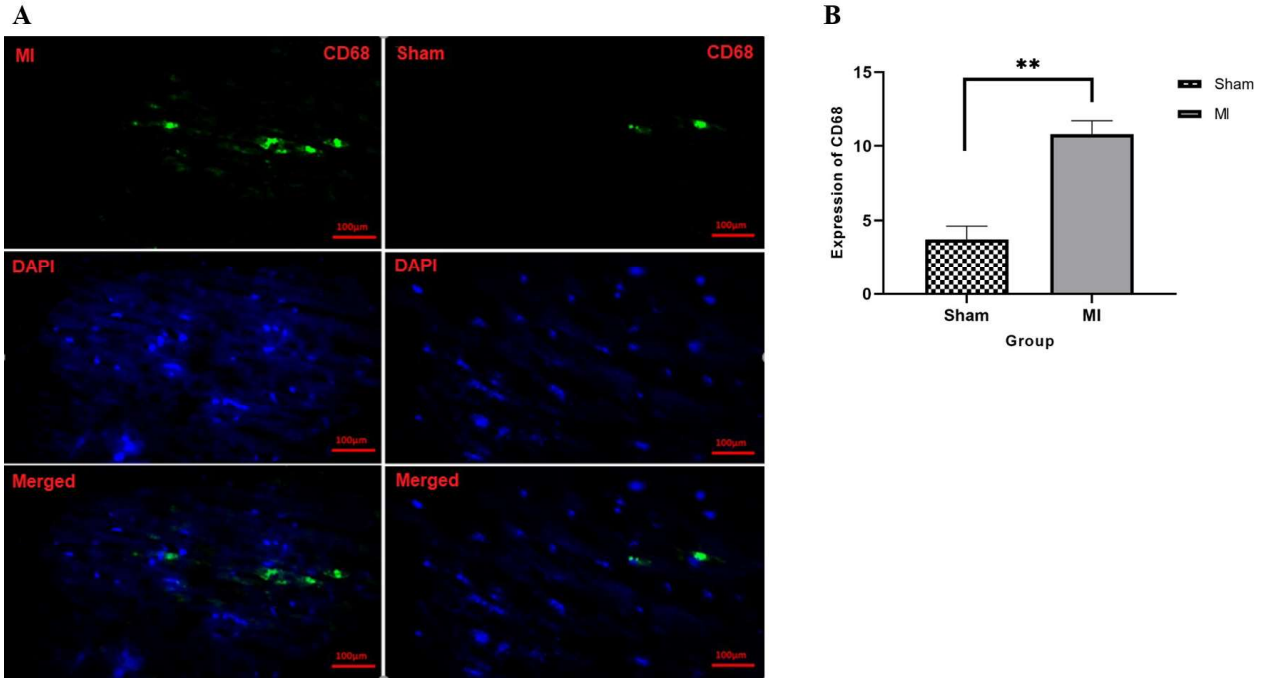

Figure 3.
Increased CD68⁺ macrophage infiltration in cryo-induced myocardial infarction compared to sham controls. (A) Immunofluorescence staining of CD68⁺ macrophages in sham and cryo-MI groups. CD68⁺ cells are shown in green, and nuclei are counterstained with DAPI (blue). Merged images illustrate macrophage localization within cardiac tissue. (B) Quantification was expressed as the percentage of CD68⁺ cells relative to total nuclei. Bar graph showing a significant increase in CD68⁺ macrophage infiltration in the cryo-MI group compared to sham controls ($p < 0.01$) (48 h after MI). Scale bar represents 100 µm.

MI group died during the same period, resulting in a substantially lower survival rate of 38.76% (Table 1), indicating higher early mortality in LAD-MI.

Cryo- and LAD-induced myocardial infarction cause ST-segment elevation and rhythm alterations

ECG recordings demonstrated pronounced ST-segment elevation in both cryo-MI and LAD-MI groups compared with sham controls (Figure 4). LAD-MI produced severe rhythm disturbances and high-amplitude changes, whereas cryo-MI exhibited abnormal but less pronounced alterations, consistent with localized myocardial damage.

Table 1.
Survival ration of surgical procedures.

Type of surgery	Total number of rats	Number of surviving rats 24 h after surgery	Survival percentage of rats 24 h after surgery
Cryo	95	67	70.52
LAD	102	38	38.76

Cryo- and LAD-induced myocardial infarction cause persistent decline in cardiac function

Serial echocardiography demonstrated significant reductions in fractional shortening (FS) and ejection fraction (EF) in both cryo-MI and LAD-MI groups compared with sham controls (Figure 5 A, B). Both MI models exhibited a sharp decline in FS and EF as early as day 1 post-surgery, followed by partial functional recovery by day 28 and persistent dysfunction through day 55. In contrast, sham-operated animals maintained stable FS and EF values throughout the study, indicating that cryo- and LAD-induced infarction result in sustained impairment of cardiac contractility.

Cryo-induced MI causes greater fibrotic remodeling than LAD ligation

Histological analysis revealed normal myocardial architecture, characterized by intact cardiomyocytes and preserved tissue organization in sham hearts (Figure 6I, 6II). In contrast, LAD-MI hearts at day 7 post-infarction, exhibited severe pathological alterations, including interstitial edema, mixed inflammatory infiltrates within the pericardium, cardiomyocyte

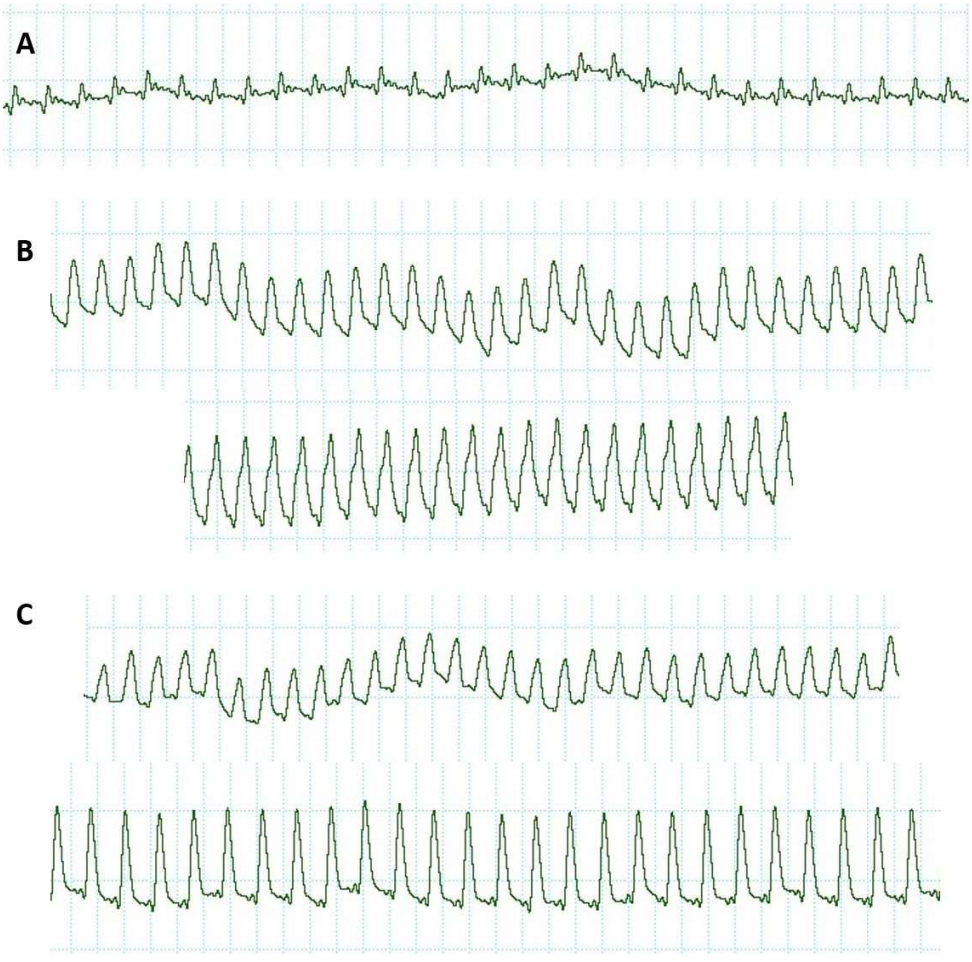

Figure 4.
Representative ECG waveforms in sham and MI models of myocardial infarction.
(A) Normal ECG pattern from sham-operated rats. (B) ECG waveform following LAD-induced myocardial infarctionin two rats, showing marked alterations in rhythm and amplitude. (C) ECG waveform following cryo-induced myocardial infarction in two rats, demonstrating distinct changes compared to sham controls. Compared to sham, LAD ligation produces severe rhythm disturbances and high-amplitude changes, while cryo-induced MI shows abnormal but less pronounced alterations, reflecting localized rather than extensive damage.

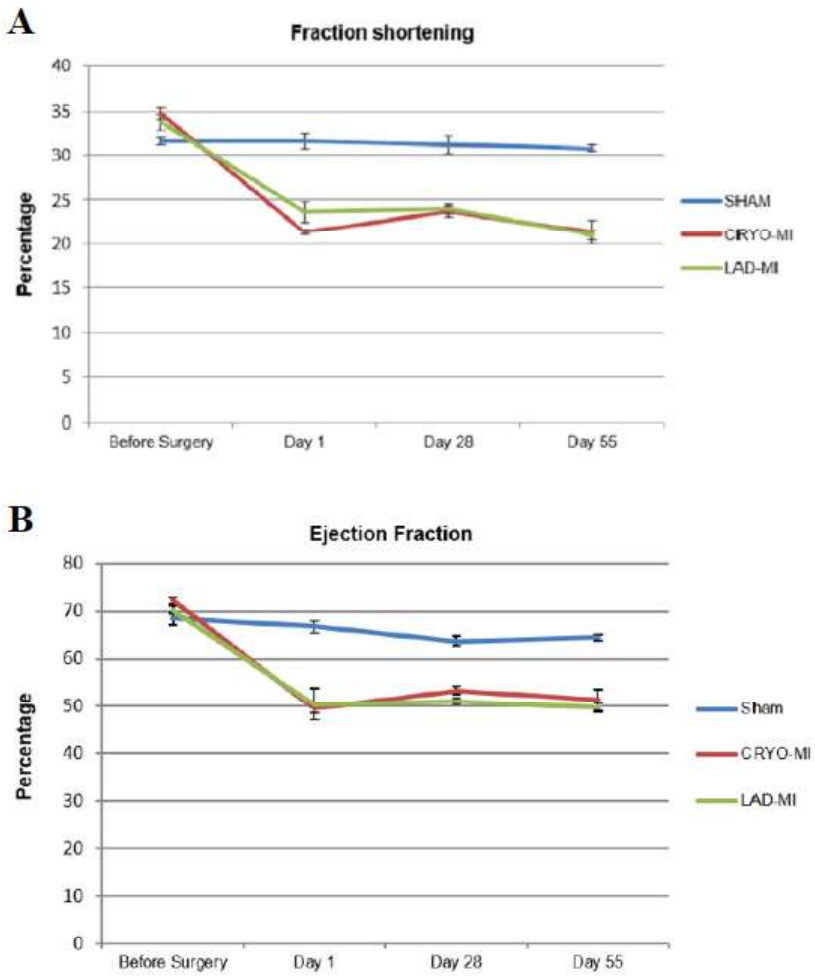

Figure 5.
Longitudinal decline in fractional shortening and ejection fraction after myocardial infarction. (A) FS was measured at baseline (pre-surgery), day 1, day 28, and day 55 post-procedure in sham (n = 5), LAD-MI (n = 3), and cryo-MI (n = 3) groups. Both LAD-MI and cryo-MI models exhibited a sharp reduction in FS by day 1, followed by partial recovery at day 28 and sustained impairment through day 55, whereas sham animals maintained stable FS values throughout. (B) EF was measured at baseline (pre-surgery), day 1, day 28, and day 55 post-procedure in sham (n = 4), LAD-MI (n = 3), and cryo-MI (n = 3) groups. Both LAD-MI and cryo-MI models exhibited a sharp reduction in EF by day 1, followed by minimal recovery at day 28 and persistent dysfunction through day 55, whereas sham animals maintained near-normal EF values throughout.

degeneration and necrosis, and hemorrhagic necrosis localized to the infarct border zone (Figure 6IIIA–F). In comparison, cryo-MI hearts at the same time point displayed focal necrosis accompanied by mixed inflammatory cell infiltration, interstitial edema, and eosinophilic changes confined to the cryo-injured region (Figure 6IVA-D). By day 55, chronic remodeling was evident in both models. LAD-MI hearts demonstrated granulation tissue formation, fibroblast proliferation, and early collagen deposition, along with pericardial thickening and fibrosis (Figure 7A-E). In contrast, cryo-MI hearts developed large, pale, homogeneous regions composed of acellular, densely collagenous scar tissue replacing functional myocardium, with adjacent hypertrophied cardiomyocytes indicative of compensatory remodeling (Figure 8). Masson's trichrome staining at day 56 confirmed extensive fibrotic replacement and pronounced ventricular wall thinning in cryo-MI hearts, whereas LAD-MI hearts exhibited localized collagen deposition restricted to the infarct zone, with relative preservation of overall chamber geometry (Figure 9). Quantitative analysis demonstrated significantly greater collagen deposition in cryo-MI hearts (10.99%) compared to LAD-MI hearts (6.19%), highlighting the more pronounced fibrotic remodeling associated with cryo-induced infarction.

Discussion

This study aimed to further investigate the cryo-infarction technique as a reliable approach for establishing a MI model in rats and to compare its outcomes with those obtained using the LAD coronary artery ligation method. Cryoinjury and LAD ligation are among the most commonly employed techniques for inducing MI in rodent models. Cryoinjury relies on the controlled application of subzero temperatures using a cryoprobe, resulting in localized necrosis through ice crystal formation and cellular disruption. A key advantage of this approach is the ability to precisely target specific myocardial regions and generate highly reproducible infarcts by adjusting probe temperature and contact duration. In contrast, LAD ligation induces MI through occlusion of the left anterior descending coronary artery, a major vessel supplying oxygenated blood to the myocardium, thereby producing ischemia that leads to extensive infarction, and closely resembles clinical coronary occlusion [13][14].

Figure 6.
Histopathological changes in sham, LAD-MI, and cryo-MI hearts. (I, II) Sham group shows normal myocardial architecture with intact cardiomyocytes and preserved tissue organization (400×, scale bar represents 50 µm). III (A-F) LAD-MI hearts at day 7 exhibit severe pathological changes, including interstitial edema, pericardial mixed inflammatory infiltrates, cardiomyocyte degeneration and necrosis, hemorrhagic necrosis, and co-localization of necrosis with inflammation and edema (100×, scale bar represents 200 µm–400×, scale bar represents 50 µm). (A) Interstitial edema with widened intramuscular spaces (arrow; H&E, 400×, scale bar represents 50 µm). (B) Pericardial mixed inflammatory infiltrate (arrows; H&E, 100×, scale bar represents 200 µm). (C, D) Cardiomyocyte degeneration and necrosis with mononuclear cell infiltration (arrows; H&E, 400×, scale bar represents 50 µm). (E) Co-localization of myocyte necrosis (black arrow), inflammatory infiltrate (blue arrow), and interstitial edema (stars; H&E, 400×, scale bar represents 50 µm). (F) Hemorrhagic necrosis showing degenerated cardiomyocytes (yellow arrow), hemorrhage (black arrow), inflammation (blue arrow), and edema (star; H&E, 400×). All images represent characteristic findings from the infarct border zone. IV (A-D) Cryo-MI hearts at day 7 display focal necrosis with mixed inflammatory cell infiltration, interstitial edema, and eosinophilic changes in the cryoinjured region (100×, scale bar represents 200 µm–400×, scale bar represents 50 µm). (A, B) Necrotic cardiomyocytes with mixed inflammatory infiltrate (mononuclear and polymorphonuclear leukocytes, arrows; H&E, 100×, scale bar represents 200 µm). (C) High-magnification view of necrotic myocardium with leukocyte infiltration (H&E, 400×, scale bar represents 50 µm). (D) Pericardial mixed inflammatory cell infiltration (H&E, 400×, scale bar represents 50 µm). All sections show characteristic interstitial edema and eosinophilic changes in the cryoinjured region.

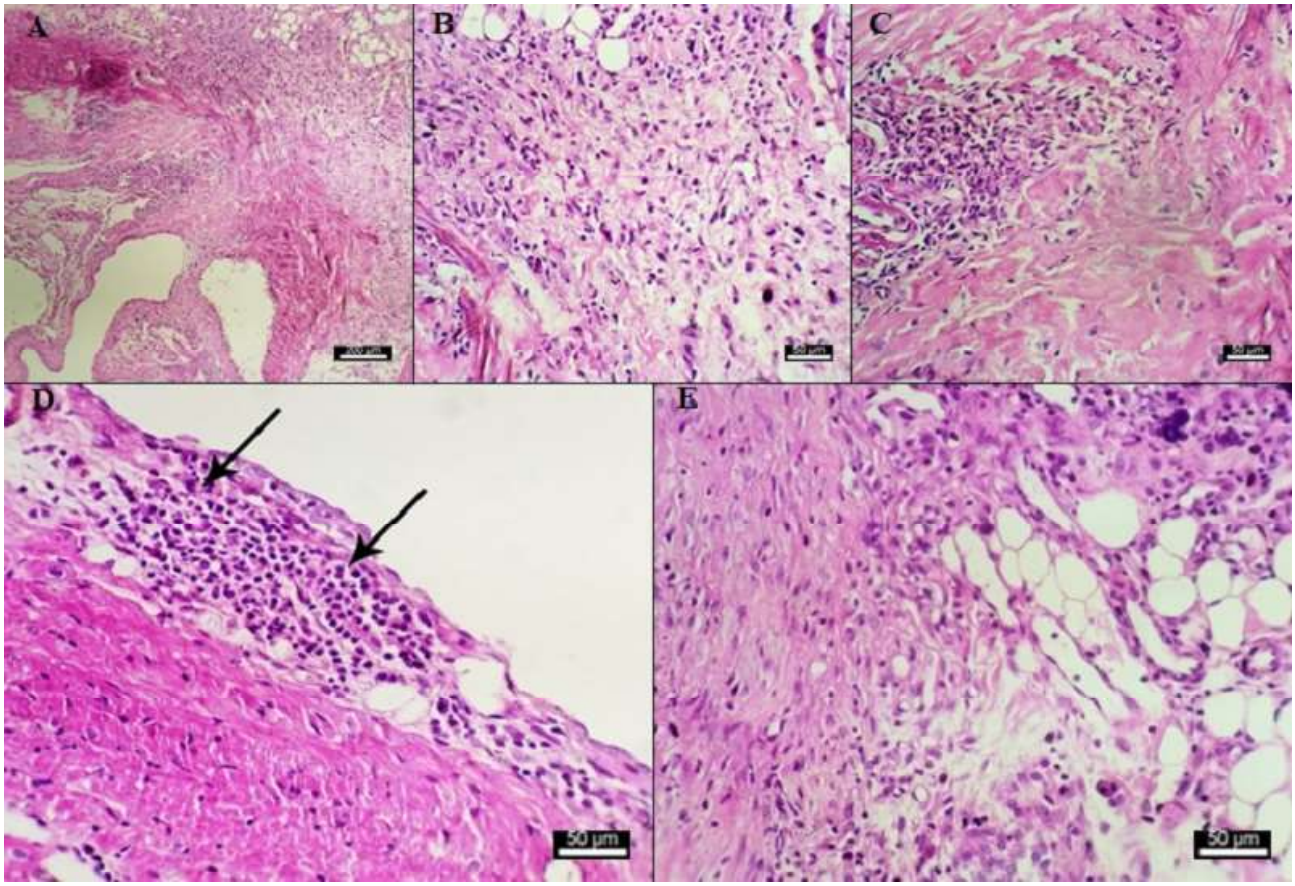

Figure 7.
Chronic histopathological changes in LAD-myocardial infarction at day 55.
(A–C) Cardiomyocyte necrosis with granulocyte and mononuclear cell infiltration, accompanied by granulation tissue formation, fibroblast proliferation, and early collagen deposition (100×- scale bar represents 200 µm, 400×-scale bar represents 50 µm). (D) Mixed inflammatory cell infiltration in the pericardium (arrows; 400×, scale bar represents 50 µm). (E) Thickened, fibrotic pericardium with dense inflammatory infiltrate (400×, scale bar represents 50 µm).

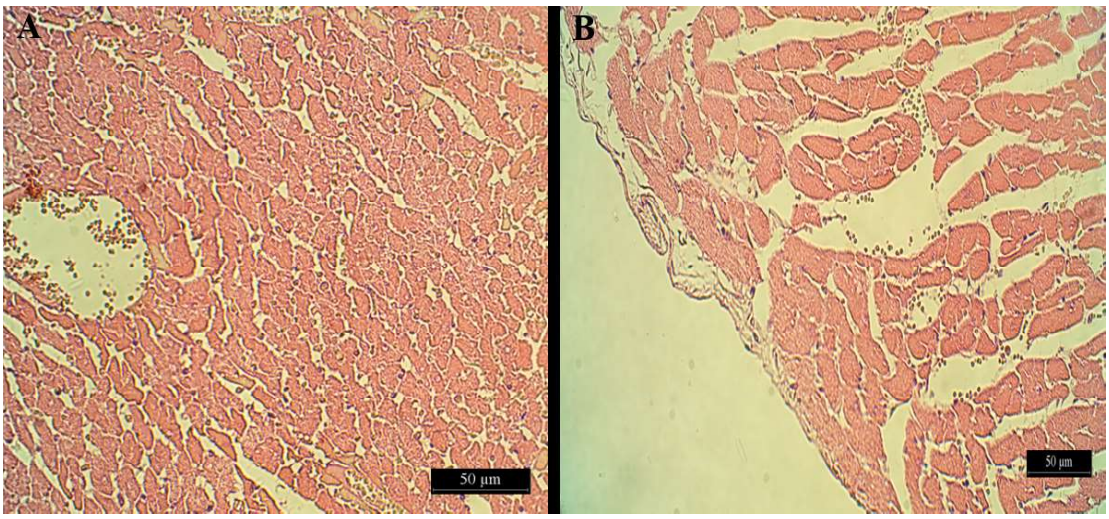

Figure 8.
Chronic structural remodeling in cryo-induced myocardial infarction at day 55. (A) Large, pale, homogeneous region representing an acellular, densely collagenous scar replacing functional myocardium. (B) Adjacent viable myocardium exhibiting hypertrophied cardiomyocytes, indicative of compensatory remodeling under increased hemodynamic load (400×, scale bar represents 50 µm).

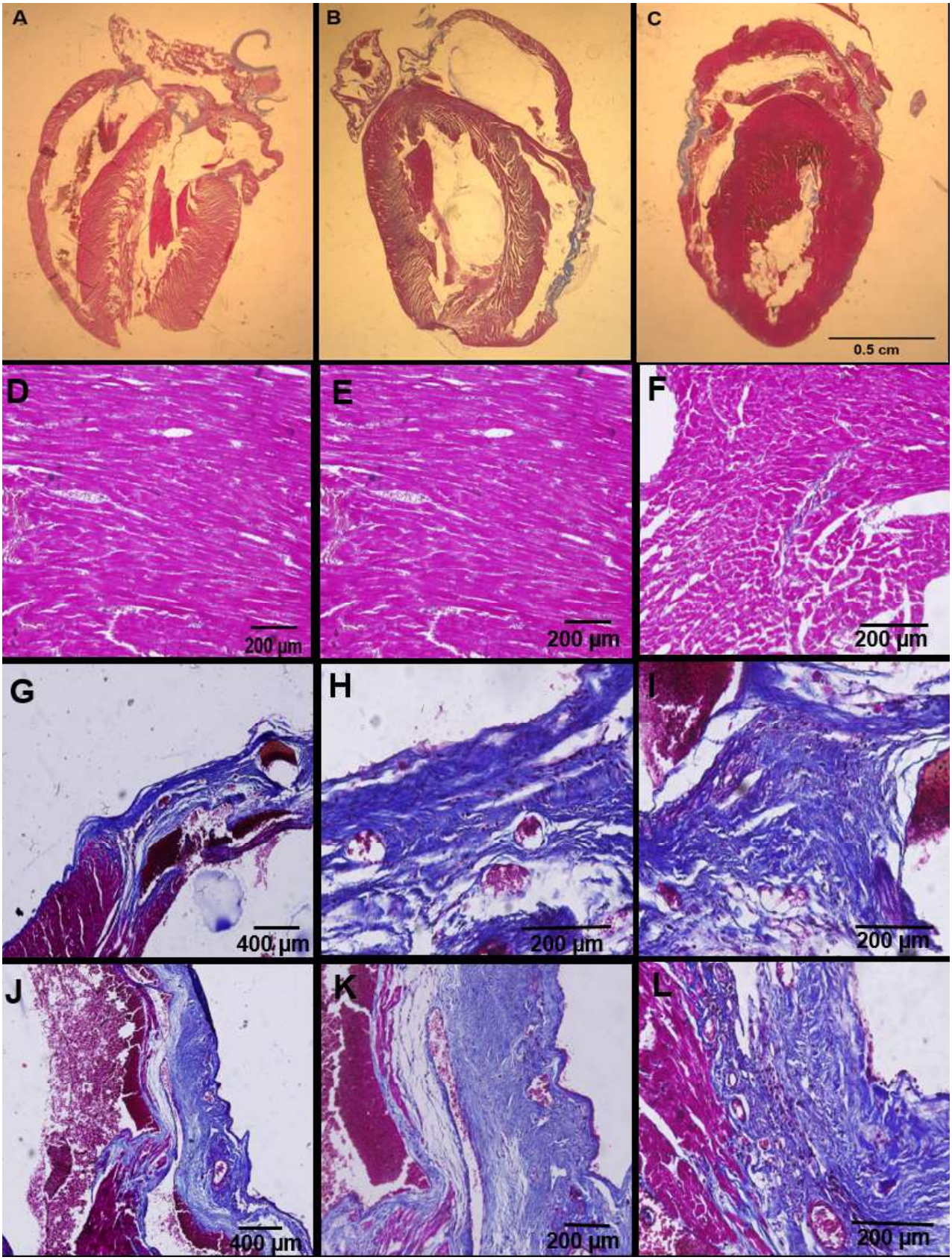

Figure 9.
Fibrotic remodeling at 56 days post-myocardial infarction, visualized using Masson's trichrome staining. (A) Sham group: No detectable collagen deposition (blue), indicating preserved myocardial architecture. (B) Cryo-MI group: Extensive fibrotic replacement (blue) accompanied by marked ventricular wall thinning. (C) LAD-MI group: Prominent collagen deposition (blue) localized to the infarct zone, consistent with scar formation. Cryo-MI hearts exhibit extensive, transmural fibrosis accompanied by pronounced ventricular wall thinning, whereas LAD-MI hearts show scar formation restricted to the infarct territory, preserving overall chamber geometry. Magnified view of each experimental group is provided in D-L. (D-F) Sham group: Normal myocardial architecture without detectable collagen deposition. (G-I) Cryo-MI group: Extensive, transmural fibrotic replacement (blue) accompanied by pronounced ventricular wall thinning. (J-L) LAD-MI group: Collagen deposition (blue) restricted to the infarct territory, preserving overall ven-

Each method presents distinct advantages and limitations. LAD ligation is well established and widely accepted, but it requires advanced microsurgical expertise, stereomicroscopic visualization, and precision instrumentation. Importantly, infarct size in the LAD model is highly operator dependent, ranging from 10–45% of the LV in inexperienced hands, while experienced operators achieve consistent infarcts (~35 ± 5%). Moreover, LAD ligation carries a high risk of procedural complications, including cardiac perforation and hemorrhage, contributing to elevated perioperative mortality. In the present study, early mortality was significantly higher in LAD-MI rats (70.59%) compared to cryo-MI rats (38.76%), underscoring the safety advantage of cryoinjury [15][12][16]. By comparison, cryoinjury offers superior control over infarct localization and size, thereby minimizing variability and reducing procedural complexity. Importantly, cryo-MI minimizes bleeding risk and allows reproducible induction of focal myocardial damage, making it particularly suitable for studies requiring localized injury. However, LAD ligation produces extensive infarctions and severe LV dilation, which may be advantageous for investigating advanced heart failure mechanisms. It is also important to recognize that rodent exhibit compensatory hypertrophy following MI, which often preserves ejection fraction despite large infarct sizes (>30% LV), a response that differs from human pathophysiology. This limitation should be considered when translating findings from rodent MI models to clinical settings [16][15][12]. In the present study, MI induction was confirmed by elevated troponin I levels, ECG abnormalities, and echocardiographic evidence of impaired cardiac function, consistent with Global MI Task Force criteria. Troponin I, a highly specific biomarker of myocardial injury, was positive in all cryo-MI and LAD-MI rats, validating successful infarction. Following myocardial damage, cTnI is released into the circulation within 4 to 6 h of injury, and its exceptional tissue specificity and diagnostic sensitivity has established it as the clinical gold-standard for MI diagnosis. The rapid troponin I assay employed in this study utilizes antibody coated particles and a marker reagent capable of detecting troponin I in whole blood or serum with a detection threshold of 1 ng/ml. In healthy rats, FS and EF typically range between 30-35% and 65-75%, respectively. However, the post-MI echocardiography analyses in the present study indicated that both cryo- and LAD-MI animals exhibited a marked reduction in FS (to 20-25%) and EF (to approximately 50%), with persistent dysfunction observed through day 55. Histological analysis demonstrated acute necrosis and inflammatory infiltration in both models, with cryo-MI hearts exhibiting focal injury and LAD-MI hearts showing extensive hemorrhagic necrosis. Chronic remodeling differed substantially as Masson's trichrome staining revealed greater collagen deposition and transmural fibrosis in cryo-MI hearts (10.99%) compared to LAD-MI hearts (6.19%), accompanied by ventricular wall thinning and hypertrophy of adjacent myocardium [8][17][18][19][20]. Immunofluorescence analysis further confirmed these observations, revealing increased caspase-3 expression and enhanced $CD68^{+}$ macrophage infiltration in cryo-MI hearts. These findings indicate robust apoptotic activity and inflammatory response. Our results suggest that cryoinjury induces localized but severe cellular stress, triggering apoptosis and immune cell recruitment. While such inflammatory responses may contribute to progressive fibrosis, they also provide a controlled microenvironment for studying post-MI remodeling processes and evaluating therapeutic interventions [21][22]. Overall, these data demonstrate that cryoinjury represents a reproducible, technically less demanding, and safer alternative to LAD ligation for inducing MI in rats, particularly when localized infarction and reduced mortality are desired. Conversely, LAD ligation remains the preferred approach for modeling large infarcts and advanced heart failure studies. Thus, selection of the appropriate MI model should be guided by experimental objectives, balancing infarct size, reproducibility, and translational relevance [12][17]. In summary, although cryoinjury and LAD ligation both result in comparable long-term LV dysfunction, cryoinjury offers distinct advantages. This method resulted in attenuated remodeling, formation of more compact and uniform scar tissue, and significantly higher survival rates compared to LAD ligation. Importantly, cryoinjury scars persist indefinitely, providing a stable and reproducible platform for investigating scar-region pathophysiology and long-term remodeling. Furthermore, cryoinjury consistently generates infarcts of uniform size and shape with precise spatial localization, making it an attractive model for preclinical studies focused on therapeutic interventions and mechanistic research [23][24][4][12].

Materials & Methods

Ethical approval

This study was conducted in accordance with ethical standards and received approval from the Ferdowsi University of Mashhad (FUM) Research Ethics Committee [Approval No: IR.UM.REC.1401.269].

Animal subjects

Adult male Wistar rats (250-300 g) were kept under standard conditions (23 ± 2°C; a 12-h light/dark cycle) with ad libitum access to standard food and water. The rats were bred and maintained in the animal house of FUM. All experimental procedures were conducted

in accordance with applicable guidelines and regulations, including the ARRIVE 2.0 guidelines. Fifteen male rats aged 60-90 days were randomly assigned into three groups: sham operated controls (group 1, n=5), LAD group (group 2, n=5), and Cryo group (group 3, n=5). During the experiments, the animals were randomly divided into three groups using Excel software (version 2016).

Prior to anesthesia, body weight and temperature were recorded for all animals. Anesthesia was induced via injection of ketamine (100 mg/kg; Alfasan 10%) and xylazine (10 mg/kg; Interchemie 2%) mixed in a 2:1 ratio. Additionally, meloxicam (1 mg/kg; RazakPharma 2%) was administered intramuscularly as a preemptive analgesic. Adequate depth of anesthesia was confirmed by the absence of the toe-pinch reflex and was monitored throughout the surgical procedure. Endotracheal intubation was performed by placing an angiocath (Vaccess I.V. Cannula green) in the trachea, with visualization aided by a flashlight in a darkened room. Mechanical ventilation was performed by connecting the endotracheal tube to the modified Babylog 8000 Drager ventilator (O_2 Vol=60, insp. Flow V=2 (l/min), Pinsp=30 (mbar), (TI=0.2 s). The aseptic condition was maintained during the survival surgery. Before surgery, ophthalmic ointment was applied to prevent corneal desiccation. After the surgery, animals were monitored for body temperature, heart rate, and signs of pain until full recovery. Rats were removed from ventilator and placed in individual cages with a heating pad positioned at one end to maintain normothermia. Water was made freely available. Sterile saline (0.5 ml) was administered subcutaneously following the surgery. Enrofloxacin (10 mg/kg) was administered immediately after the surgery and continued during recovery [4][25]. Antibiotic injections were given every 12 h and analgesics were administered every 24 h for 3 consecutive days following surgery [25][26].

Induction of myocardial infarction

Animals were left to reach steady breathing and their chests were opened at the fourth left intercostal space using surgical scissors. The space was opened without cutting muscle tissue to minimize bleeding. Then a chest retractor was placed to maintain exposure. The pericardium was opened but preserved whenever possible [25][27]. The LAD was identified and tied using a 6-0 Prolene (polypropylene blue monofilament 209127) suture [28]. In the cryo-MI group, a cryoprobe consisting of a 3 mm diameter copper rod, was immersed in liquid nitrogen for two min. After exposure of the heart and opening of the pericardium, the cryo-infarction was induced by applying the cryoprobe tip to the anterior wall of the left ventricle for 10 seconds [4]. Sham control animals underwent the same surgical exposure without LAD ligation or cryo application. After completion of the procedure, the chest retractor was removed and the ribs were sutured using 4-0 Prolene (20 mm polyglycolate coated violet) suture. After closing the ribs, the ventilator output was briefly interrupted (1-2 seconds) to ensure proper breathing. The skin was closed using continuous 20 mm 4-0 Prolene sutures [28].

Infarct size measurement

Myocardial infarction size was assessed using 2,3,5-triphenyltetrazolium chloride (TTC) staining. Hearts were rapidly excised, flash-frozen at -80°C, and transversely sectioned into 2 mm-thick slices. Sections were incubated in 2% TTC solution at 37°C, for 30 min, followed by fixation in 10% neutral buffered formalin for 24 h. After rinsing with saline, the unstained infarcted regions were clearly demarcated from viable brick-red stained myocardium, enabling precise topographic documentation of ischemic damage [29][30].

Immuno-histochemistry analysis

Excised tissues were fixed in 10% neutral buffered formalin for 24–72 h, dehydrated through graded ethanol series (70%, 80%, 90%, 100%; 50 min each), cleared in xylene, and embedded in paraffin. Sections (5 µm thick) were prepared using a Leica RM2135 microtome and mounted on silanized slides. Antigen retrieval was performed by microwaving sections in 1× Tris-buffered saline (TBS; Sigma, T5912) until boiling, followed by incubation for 20 min in the heated solution. After three washes in phosphat buffer saline (PBS) (5 min each), sections were permeabilized with 0.3% Triton X-100 (Sigma, T8787) for 30 min and blocked with 10% goat serum (Sigma, G9023) for 45 min. Primary antibodies against caspase-3 (orb10237) and CD68 (orb388936) were applied at a dilution of 1:100 in PBS and incubated for 24 h at 2–8°C in a humidified chamber. Sections were washed four times (5 min each) and incubated with secondary antibodies (CD68: orb688924, caspase3: orb688925; 1:150 dilution) at 37°C for 1.5 h in the dark, then washed three times. DAPI (Sigma-D9542) was applied for 20 min, followed by PBS washing steps. Slides were mounted with glycerol and PBS and examined using a fluorescent microscope (Olympus).

Biochemical analysis of troponin in serum

Blood samples were collected 24 h post surgery from the retroorbital sinus and centrifuged at 3000 × *g* for 5 min at 4°C. Serum samples were immediately analyzed for troponin I using the Cardiac Troponin I Cassette Tape (Vitrotec CTN00-08), a rapid immunochromatographic assay for whole blood or serum. For analysis, 50 µl of serum was added to the sample, followed by 40 µl of cTnI buffer provided in the kit. A control line indicated proper test performance and sufficient sample volume.

Hematoxylin-Eosin staining

H&E staining was performed to assess cardiac morphology and confirm myocardial infarction. Heart tissues were collected at 7 and 55 days post-surgery, fixed in 10% formalin, sectioned at 5 µm, and stained with hematoxylin and eosin. Necrotic areas were examined using an Olympus BX-51 microscope equipped with a digital camera.

Electrocardiography and echocardiography

On day 7, rats underwent ECG recording under anesthesia (ketamine 75 mg/kg, xylazine 10 mg/kg) using the PowerLab Electrophysiological System (ML11, ADInstruments, Australia). Electrodes were placed on the right and left forelimbs. FS, and EF were assessed as indicators of left ventricular function. FS reflects the percentage reduction in ventricular diameter during systole, while EF represents the proportion of blood ejected from the left ventricle per heartbeat, calculated as:

EF="Stroke Volume" /"End-Diastolic Volume" ×100

Normal EF in rats ranges from 65–75%, with reductions indicating impaired cardiac performance [31]. Echocardiography (MyLab 30Gold VET, 8–10 MHz transducer) was performed after chest hair removal one day before surgery and on days 1, 28, and 55 post-surgery to monitor cardiac performance on anesthetized rats.

Masson's trichrome staining for collagen detection

Masson's trichrome staining was used to evaluate collagen deposition in cardiac tissue. In this method, collagen fibers appear blue, nuclei black, and cytoplasmic components red. Heart tissues were harvested 55 days post-surgery, fixed in 10% neutral buffered formalin for 24 h, and embedded in paraffin. Serial sections (5 µm) were prepared from regions of interest using a microtome. Images were captured using an OLYMPUS stereomicroscope (SZH-ILLK, Japan) [32][33].

Statistical analysis

Quantification of caspase-3 and CD68 expression was performed using ImageJ software. Statistical analyses were conducted using GraphPad Prism 10.3. Analyses included both sham and cryo-MI groups.

Authors' Contributions

AK: Investigation, Visualization, Software, Formal analysis, Data acquisition, Methodology, Writing - original draft preparation. MMM: Funding acquisition, Project administration, Supervision, Methodology, Validation, Resources. AH: Project administration, Supervision, Methodology, Investigation, Validation. HKM: Supervision, Methodology, Validation. MR: Supervision, Methodology, Data Acquisition, Visualization. MA: Methodology, Data acquisition, Visualization. ARB: Conceptualization, Funding acquisition, Project administration, Supervision, Methodology, Validation, Visualization, Resources. All authors were involved in writing, reviewing, and editing, and approved the final version.

Acknowledgements

We would like to express our sincere gratitude to the staff of the Mashhad Academic Jahad Medical Diagnostic Laboratory and the Veterinary Clinic, especially Mr. Barati, for their invaluable support. We also extend our special thanks to Mohammad-Hasan Mollaei, Dr. Hamidreza Kazerani and Navid Nateghi for their assistance and contributions throughout this study. We also extend our thanks to the laboratory technicians and postgraduate students in the Molcular Biology Laboratory of FUM for their assistance. This work was supported by Ferdowsi University of Mashhad)Grant No. 59386(and the National Institute for Medical Research Development (NIMAD, Grant No. 957797). The funding body had no role in study design, data collection and analysis, decision to publish, or preparation of the manuscript.

Conflict of interest

The authors declare that there is no conflict of interest.

References

1. Fathima SN. An update on myocardial infarction. Curr Res Trends Med Sci Technol. 2021;1:95.

2. Choo EH, Chang K, Lee KY, Lee D, Kim JG, Ahn Y, et al. Prognosis and predictors of mortality in patients suffering myocardial infarction with non-obstructive coronary arteries. J Am Heart Assoc. 2019;8(14):e011990. Doi:10.1161/JAHA.119.011990.

3. Mirzavi F, Ebrahimi S, Ghazvini K, Mehr SMH, Hashemy SI. Diagnostic, prognostic, and therapeutic potencies of circulating miRNAs in acute myocardial infarction. Crit Rev Eukaryot Gene Expr. 2019;29(4).Doi:10.1615/CritRevEukaryotGeneExpr.2019028211.

4. Alonzo M, Delgado M, Cleetus C, Kumar SA, Thakur V, Chattopadhyay M, et al. Methods for histological characterization of cryo-induced myocardial infarction in a rat model. Acta Histochem. 2020;122(7):151624. Doi:10.1016/j.acthis.2020.151624.

5. van der Velden J, Asselbergs FW, Bakkers J, Batkai S, Bertrand L, Bezzina CR, et al. Animal models and animal-free innovations for cardiovascular research: current status and routes to be explored. Consensus document of the ESC Working Group on Myocardial Function and the ESC Working Group on Cellular Biology of the Heart. Cardiovasc Res. 2022;118(15):3016–51. Doi:10.1093/cvr/cvab370.

6. Tang Y ping, Liu Y, Fan Y jie, Zhao Y yang, Feng J qun, Liu Y. To develop a novel animal model of myocardial infarction: A research imperative. Anim Model Exp Med. 2018;1(1):36–9. Doi:10.1002/ame2.12010.

7. Liao J, Huang W, Liu G. Animal models of coronary heart disease. J Biomed Res. 2016;31(1):3.Doi:10.7555/JBR.30.20150051.

8. Kumar M, Kasala ER, Bodduluru LN, Dahiya V, Sharma D, Kumar V, et al. Animal models of myocardial infarction: Mainstay in clinical translation. Regul Toxicol Pharmacol. 2016;76:221–30. Doi:10.1016/j.yrtph.2016.03.005.

9 Nugroho J, Yuniarti WM, Wardhana A, Ghea C. Modification on acute myocardial infarction model through left anterior descending coronary artery ligation: An experimental study on rats (*Rattus norvegicus*) using readily available materials. Vet World. 2019;(9):1448. Doi: 10.14202/vetworld.2019.1448-1453.

10. Kolk MV V, Meyberg D, Deuse T, Tang-Quan KR, Robbins RC, Reichenspurner H, et al. LAD-ligation: a murine model of myocardial infarction. J Vis Exp. 2009;14(32):1438. Doi: 10.3791/1438.

11. De Villiers C, Riley PR. Mouse models of myocardial infarction: comparing permanent ligation and ischaemia-reperfusion. Dis Model Mech. 2020;13(11):dmm046565. Doi:10.1242/dmm.046565.

12. Martin TP, MacDonald EA, Elbassioni AAM, O'toole D, Zaeri AAI, Nicklin SA, et al. Preclinical models of myocardial infarction: from mechanism to translation. Br J Pharmacol. 2022;179(5):770–91. Doi:10.1111/bph.15595.

13. Duerr GD, Elhafi N, Bostani T, Ellinger J, Swieny L, Kolobara E, et al. Comparison of myocardial remodeling between cryo-infarction and reperfused infarction in mice. Biomed Res Int. 2011;2011(1):961298. Doi:10.1155/2011/961298.

14. Gao E, Koch WJ. A novel and efficient model of coronary artery ligation in the mouse. In: Wound Regeneration and Repair: Methods and Protocols. Springer; 2013. p. 299–311. Doi:10.1007/978-1-62703-505-7_17.

15. Lim GB. Clonal haematopoiesis induces a pro-inflammatory monocyte phenotype in HF. Nat Rev Cardiol. 2021;18(2):74.

Doi:10.1038/s41569-020-00481-5.

16. Bayat H, Swaney JS, Ander AN, Dalton N, Kennedy BP, Hammond HK, et al. Progressive heart failure after myocardial infarction in mice. Basic Res Cardiol. 2002;97:206–13. Doi:10.1007/s003950200013.

17. Reichert K, Colantuono B, McCormack I, Rodrigues F, Pavlov V, Abid MR. Murine left anterior descending (LAD) coronary artery ligation: an improved and simplified model for myocardial infarction. J Vis Exp. 2017;(122):55353. Doi:10.3791/55353.

18. Esmaeili R, Sadeghpour A, Darbandi-Azar A, Majidzadeh-A K, Vajhi A, Sadeghizadeh M. Echocardiographic assessment of myocardial infarction: comparison of a rat model in two strains. Iran J Vet Res. 2017;18(1):30.

19. Madadi F, Aghajani M, Dabbagh A, Fani K, Sehati F, Imani A. Effects of acute potassium chloride administration on ventricular dysrhythmias after myocardial infarction in a rat model of ischemia/reperfusion. J Tehran Univ Heart Cent. 2022;17(1):15. Doi:10.18502/jthc.v17i1.9320.

20. Vietta GG, Andrades ME, Dall'Alba R, Schneider SIR, Frick LM, Matte U, et al. Early use of cardiac troponin-I and echocardiography imaging for prediction of myocardial infarction size in Wistar rats. Life Sci. 2013;93(4):139–44. Doi:10.1016/j.lfs.2013.05.026.

21. Di Filippo C, Marfella R, Capodanno P, Ferraraccio F, Coppola L, Luongo M, et al. Acute oxygen-ozone administration to rats protects the heart from ischemia reperfusion infarct. Inflamm Res. 2008;57:445–9. Doi:10.1007/s00011-008-7237-0.

22. Naseroleslami M, Sharifi M, Rakhshan K, Mokhtari B, Aboutaleb N. Nesfatin-1 attenuates injury in a rat model of myocardial infarction by targeting autophagy, inflammation, and apoptosis. Arch Physiol Biochem. 2023;129(1):122–30. Doi:10.1080/13813455.2020.1802486.

23. Van Zuylen VL, Den Haan MC, Roelofs H, Fibbe WE, Schalij MJ, Atsma DE. Myocardial infarction models in NOD/Scid mice for cell therapy research: permanent ischemia vs ischemia-reperfusion. Springerplus. 2015;4(1):336. Doi:10.1186/s40064-015-1128-y.

24. Van den Bos EJ, Mees BME, De Waard MC, De Crom R, Duncker DJ. A novel model of cryoinjury-induced myocardial infarction in the mouse: a comparison with coronary artery ligation. Am J Physiol Circ Physiol. 2005;289(3):H1291--H1300. Doi:10.1152/ajpheart.00111.2005.

25. Dittrich A, Lauridsen H. Cryo-injury induced heart regeneration in the axolotl and echocardiography and unbiased quantitative histology to evaluate regenerative progression. J Vis Exp. 2021;171(171):e61966. Doi:10.3791/61966.

26. Farag A, Mandour AS, Hendawy H, Elhaieg A, Elfadadny A, Tanaka R. A review on experimental surgical models and anesthetic protocols of heart failure in rats. Front Vet Sci. 2023;10:1103229. Doi:10.3389/fvets.2023.110322.

27. Omoto ACM, do Carmo JM, Nelson B, Aitken N, Dai X, Moak S, et al. Central Nervous System Actions of Leptin Improve Cardiac Function After Ischemia-Reperfusion: Roles of Sympathetic Innervation and Sex Differences. J Am Heart Assoc. 2022;11(21):e027081. Doi:10.1161/JAHA.122.027081.

28. Wu Y, Yin X, Wijaya C, Huang MH, McConnell BK. Acute myocardial infarction in rats. J Vis Exp. 2011;(48):2464. Doi:10.3791/2464.

29. Ong SB, Kwek XY, Katwadi K, Hernandez-Resendiz S, Crespo-Avilan GE, Ismail NI, et al. Targeting mitochondrial fission using Mdivi-1 in a clinically relevant large animal model of acute myocardial infarction: a pilot study. Int J Mol Sci. 2019;20(16):3972. Doi:10.3390/ijms20163972.

30. Kalluri R, LeBleu VS. The biology, function, and biomedical applications of exosomes. Science (80-). 2020;367(6478):eaau6977. Doi:10.1126/science.aau6977.

31. Kerkhof PL, D'iaz-Navarro R, Heyndrickx GR, Handly N. A critical analysis of ejection fraction. Rev medica de Chile. 2022;150(2):232–40. Doi:10.4067/s0034-98872022000200232.

32. Lu Y, Liu JJ, Bi XY, Yu XJ, Kong SS, Qin FF, et al. Pyridostigmine ameliorates cardiac remodeling induced by myocardial infarction via inhibition of the transforming growth factor-β1/TGF-β1-Activated Kinase Pathway. J Cardiovasc Pharmacol. 2014;63(5):412–20. Doi:10.1097/FJC.0000000000000062.

33. Bayarsaikhan D, Bayarsaikhan G, Lee J, Lee B. A study on the protective effect of sRAGE-MSCs in a rodent reperfusion model of myocardial infarction. Int J Mol Sci. 2022;23(24):15630. Doi:10.3390/ijms232415630.

How to cite this article
Karimi A, Moghadam. Matin M, Haghighitalab A, Kazemi Mehrjerdi H, Rajabioun M, Aghasizadeh M, Bahrami AR. Cryo-infarction: a method of choice for the establishment of a rat model of myocardial infarction. Iran J Vet Sci Technol.2026; 18(2): 8-21.
DOI: https://doi.org/10.22067/ijvst.2025.93330.1533
URL: https://ijvst.um.ac.ir/article_48121.html

Iranian Journal of Veterinary Science and Technology

Received: 2025- Jun-02
Accepted after revision: 2025- Nov- 29
Published online: 2025- Dec- 01

RESEARCH ARTICLE

DOI:10.22067/ijvst.2025.93754.1557

Immunohistochemical expression of EGFR, E-Cadherin, β-Catenin, and Ki67 in dogs with local and invasive cutaneous leiomyosarcoma

Fatemeh Heydarzadeh[a], Amir Amniattalab[b]

[a] Department of Clinical Sciences, Faculty of Veterinary Medicine, Ur.C., Islamic Azad University, Urmia, Iran.
[b] Department of Pathology, Faculty of Veterinary Medicine, Ur.C., Islamic Azad University, Urmia, Iran.

ABSTRACT

Cutaneous leiomyosarcoma (LMS) is a rare malignant smooth muscle tumor in dogs and humans, potentially arising from smooth muscle fibers of hair follicles, blood vessels, or genital tissues. This study examined the prevalence, clinicopathological features, hematological changes, and immunohistochemical characteristics of canine cutaneous LMS. Over a 10-year period in Urmia, Iran, six cases (three local and three invasive) of cutaneous leiomyosarcoma (LMS) were identified among 318 dogs presenting with cutaneous lesions representing a prevalence of 1.88%. The hematological analysis indicated significant leukocytosis, monocytosis, and eosinophilia in the affected dogs ($p < 0.05$) compared to the healthy dogs. Microscopically, a range of cellular pleomorphism and neoplastic smooth muscle fibers in interlacing bundles with scant stromal connective tissue were observed. Immunohistochemistry (negative for MyoD1, Myogenin, and CD31) confirmed piloleiomyosarcoma. A significant increase ($p < 0.05$) was observed in positive expression and H-score for Desmin, SMA, Vimentin, and Ki67 markers. EGFR and β-Catenin expression was significantly increased in the localized LMS group ($p < 0.05$) compared to invasive LMS and normal tissue, whereas E-Cadherin expression showed no significant difference in LMS cases. These findings indicate that EGFR is not limited to epithelial tumors but is also expressed in mesenchymal tumors like LMS. The reduction in invasive LMS cases suggests EGFR upregulation may precede metastasis. Although E-Cadherin/β-Catenin expression alone may be insufficient for prognosis, their combined evaluation with proliferative and mesenchymal markers could provide valuable insight into invasion pathways and aid in developing targeted therapies against invasive tumors.

Keywords

Cutaneous leiomyosarcoma, Dog, Immunohistochemistry, Intercellular adhesion, Proliferation

Number of Figures: 7
Number of Tables: 1
Number of References:: 30
Number of Pages: 14

Abbreviations

LMS: Leiomyosarcoma

α-SMA: α-Smooth Muscle Actin

Corresponding author: Amir Amniattalab
Email: Amir.Amniattalab@iau.ac.ir
Tel: +98(91)4441-4613

Introduction

Soft tissue sarcomas in dogs are characterized as mesenchymal tumors with local invasion, encompassing a diverse array of mesenchymal tumors exhibiting different histogenetic origins, and they constitute approximately 15% of all dermal and subdermal neoplasms in canines. Typically, mature or older dogs demonstrate a higher prevalence, with larger breeds showing an increased vulnerability. Anatomically, nearly 60% of soft tissue sarcomas in dogs are located on motor organs. In contrast, other somatic regions exhibit a comparatively lower incidence and for example the torso (35%) and head and neck (5%) are less frequently affected [1]. Malignant cutaneous smooth muscle tumors are uncommon in both humans and animals. These tumors possibly arise from the smooth muscles that erect the hair, those inside the vascular septum, or from special muscles in the genital region [2]. Cutaneous leiomyosarcoma is uncommon in both humans and animals. While multiple well-differentiated smooth muscle tumors have been reported in dogs, cats, ferrets, and horses, cutaneous smooth muscle neoplasms are typically solitary in nature [3]. Histologically, LMS is characterized by intertwined neoplastic smooth muscle cells. In humans, malignant smooth muscle tumors display marked proliferative activity, cellular uniformity, nuclear atypia, and intratumor necrosis. Human LMS is further classified into myxoid, epithelioid, and pleomorphic subtypes, while the last-mentioned subtype was only diagnosed in animal health publications, as some of them were similar to anaplastic sarcomas [2]. In human medicine, leiomyosarcoma is associated with high rates of recurrence and metastasis, resulting in a generally poor prognosis. The most frequent metastatic sites include the lungs, bone, brain, and lymph nodes. Surgical removal is the most effective treatment for leiomyosarcoma, while chemotherapy does not appear to be as effective, is largely palliative, and is typically reserved for patients with extensive metastasis. Previous reports revealed an acceptable prognosis for surgically treated dogs with spleen, stomach, small intestine, and especially the cecum leiomyosarcomas. Nevertheless, the number of studies on dogs remains limited. The anatomical site of leiomyosarcoma in dogs holds greater prognostic significance compared to human. Leiomyosarcomas originating from superficial cutaneous locations are associated with a more favorable prognosis. In contrast, osseous involvement of the human leiomyosarcoma represents a potential negative prognostic indicator.[4]. β-Catenin, encoded by the ctnnb1 gene, is a key component of intercellular junctions, and dysregulation of its expression has been implicated in the progression of animal and human tumors. Studies have demonstrated that disruption of the E-cadherin/β-catenin complex regulations affects both types of canine melanotic tumors, also disruption of the E-cadherin/β-catenin complex and increased β-catenin levels can lead to tumor progression and malignancy [5]. In conventional mature cutaneous cells, β-catenin constitutes a fundamental component of the intercellular junctions, while the Wnt/β-catenin signalling cascade significantly influences the maintenance of skin homeostasis, particularly in the preservation of hair follicle stem cells. However, data regarding the expression profile of β-catenin in normal dermal tissue, as well as in epidermal and follicular neoplasms in canines remain scarce. In malignant neoplasms, including squamous cell carcinoma, basal cell carcinoma, sebaceous gland carcinoma, apocrine gland carcinoma, and epithelial carcinoma, reduced or absent membranous β-catenin expression has been reported, suggesting that the decrease or loss of β-catenin expression is pivotal in the development of a malignant phenotype and may play a role in the invasive behaviour or metastasis of these carcinomas [6]. Cadherins are multi-family membrane glycoproteins responsible for calcium-mediated homophilic attachment. They are particularly related to the joint area and play roles in processes including tissue morphogenesis and tumorigenesis in complex organisms. E-cadherin, the predominant cadherin expressed in epithelial tissues, is widely regarded as an anti-oncogene and a developmental agent in epithelium-orig-

Abbreviations-Cont'd

EGFR: Epidermal Growth Factor Receptor
COX-2: Cyclooxygenase-2
CK: Cytokeratin
H&E: Hematoxylin and Eosin
EDTA: Ethylenediaminetetraacetic Acid
HRP: Horseradish Peroxidase
TBS: Tris-Buffered Saline
ANOVA: Analysis of Variance
H-Score: Histochemical Score
HCT: Hematocrit
Hb: Hemoglobin
RBC: Red Blood Cell
MCV: Mean Corpuscular Volume
MCHC: Mean Corpuscular Hemoglobin Concentration
PLT: Platelet
WBC: White Blood Cells
Neut: Neutrophil
Lym: Lymphocyte
MON: Monocyte
EOS: Eosinophils
VEGFr: Vascular Endothelial Growth Factor receptor
PDGFr: Platelet-Derived Growth Factor receptor
SCF: Stem Cell Factor
IHC: Immunohistochemistry
AKT/MAPK: Protein Kinase B and Mitogen-Activated Protein Kinase
TGFα: Transforming Growth Factor-alpha
SD: Standard Deviation

inated neoplasms. E-cadherin downregulation has been associated with decreased cellular differentiation, enhanced invasiveness , and metastatic behavior in a variety malignancies, including several sarcomas. Epidermal growth factor receptor (EGFR), commonly referred to as HER1 or erbB1, constitutes a member of the receptor tyrosine kinase family. Besides other ErbB family members, including ErbB2, ErbB3, and ErbB4, they can form heterodimers. These receptors are integral to essential cellular functions, encompassing cell division and specialization. Overexpression of COX-2 and EGFR has been documented in numerous malignant neoplasms. These molecules contributes to critical processes at several pivotal stages, including vascularization, inhibition of programmed cell death, suppression of immune responses, enhancement of cell division, possibility for progression, cellular specialization, and displacement. COX-2 and EGFR represent promising targets for therapeutic and chemotherapeutic interventions in the treatment of diverse pathological conditions, such as neoplasm. Therefore, due to their involvement in tumor invasiveness, malignancy, reduced survival rates, and poor prognostic, they are considered promising biomarkers and potential therapeutic targets in veterinary oncology [7]. The present study aimed to investigated the differential diagnosis of cutaneous leiomyosarcoma tumors in dogs, and the changes in the immunoexpressing of adhesion markers, including E-Cadherin, β-Catenin, in addition to the changes in the expression of markers CK, MyoD1, Myogenin, CD31, Desmin, α-SMA, Vimentin, Ki67, and EGFR in the local and invasive forms of these tumors.

Results

Skin lesions

A total of 318 dogs presenting with various diseases and disorders were examined. These included parasitic lesions (scabies) (n = 49/318, 15.40%), fungal infection (dermatophytosis) (n = 42/318, 15.20%), traumatic lesions (skin tear or wound) (n = 13/318, 4.08%), papilloma (n = 27/318, 8.49%), fibroma (n = 8/318, 2.51%), fibrosarcoma (n = 6/318, 1.88%), leiomyosarcoma (n = 6/318, 1.88%), trichoblastoma (n = 3/318, 0.94%), and squamous cell carcinoma (SCC) (n = 2/318, 0.62%). The remaining cases (n = 162/318, 50.94%) were associated with various clinical manifestations of systemic diseases and/or allergic dermatopathies.

Pathological Findings

Among the examined dogs, 6 cases were diagnosed as leiomyosarcoma (LMS) tumors, including 3 cases of localized cutaneous leiomyosarcoma (local LMS), and 3 cases of invasive cutaneous leiomyosarcoma (invasive LMS). In the local LMS group, affected dogs included one male Rottweiler, one female Terrier, and one female Iranian mixed breed dog. Their ages ranged from 6 to 10 years, and tumor diameters varied between 3 and 37 mm. Tumor locations were mainly in the lower limbs (locomotor), neck, and abdomen. In the invasive LMS group, one male Iraqi breed dog, one female Shih Tzu, and one male German Shepherd were affected. These dogs were aged between 6 and 12 years, with tumor sizes ranging from 2 to 26 mm. Tumors were primarily located in lower limbs (locomotor), neck, and abdomen regions. Metastasis spread to the conjunctiva, pulmonary system, or gastrointestinal tract was confirmed through histopathological examination (Figure 1). Histological evaluation of H&E and Masson's trichrome stained sections revealed a moderate degree of cellular and nuclear pleomorphism in both local and invasive LMS, with the nucleoli count in tumor cells ranging from 2 to 4, and the mean mitotic index for local and invasive LMS was 4.2 and 5.8, respectively. Neoplastic smooth muscle fibres exhibited an interwoven configuration characterized by an irregular morphology, with minimal intervening connective tissue. Necrosis or hemorrhage were absent in local LMS, but were observed in invasive LMS (Figure 2).

Hematological Findings

One-way ANOVA analysis demonstrated no significant difference in mean values of MCV, PLT, Neutrophils, and Lymphocytes among healthy dogs and those with local or invasive LMS ($p > 0.05$). In contrast, significant difference were detected in Hct, Hb, RBC, MCHC, WBC, Monocytes, and Eosinophils among healthy dogs and those with invasive LMS ($p < 0.05$). Within the local LMS group, mean value for RBC, MCHC, WBC, and Eosinophils did not differ significantly compared to healthy dogs ($p > 0.05$). Detailed hematological data are summarized in Table 1.

Immunohistochemical Findings

Following definitive diagnosis, immunohistochemistry staining for CD31 was negative in all six leiomyosarcoma cases. Hence, it was confirmed that all diagnosed LMS cases originated from the smooth muscles responsible for erecting hair (Figures 3 and 4). Additionally, MyoD1 and Myogenin immunohistochemical was also negative for all tumors samples that the nature of the tumors was diagnosed as definite LMS. One-way ANOVA showed no significant differences in the expression percentage or H-score of MyoD1, Myogenin, and CD 31 between healthy dogs and those with local or invasive LMS ($p > 0.05$) (Fig-

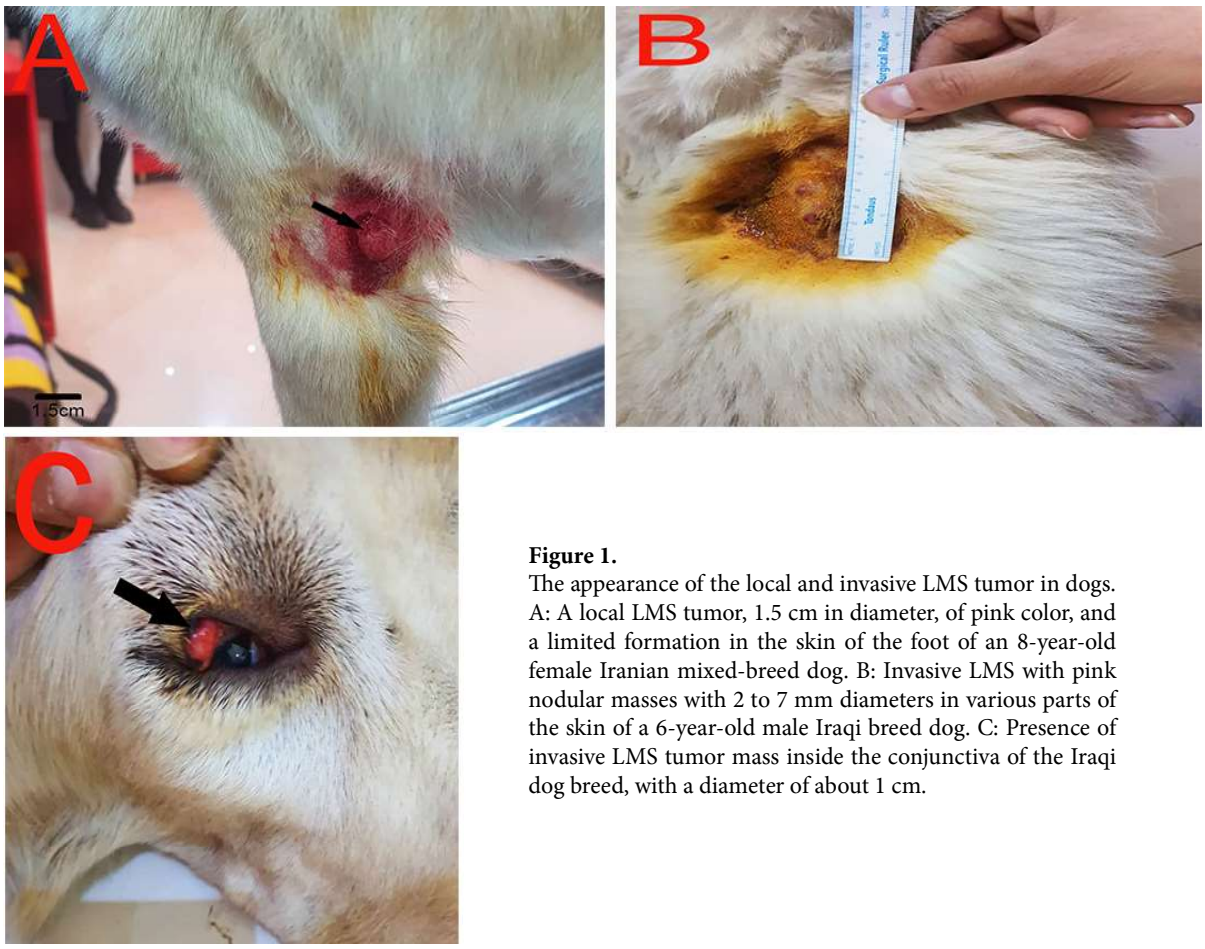

Figure 1.
The appearance of the local and invasive LMS tumor in dogs. A: A local LMS tumor, 1.5 cm in diameter, of pink color, and a limited formation in the skin of the foot of an 8-year-old female Iranian mixed-breed dog. B: Invasive LMS with pink nodular masses with 2 to 7 mm diameters in various parts of the skin of a 6-year-old male Iraqi breed dog. C: Presence of invasive LMS tumor mass inside the conjunctiva of the Iraqi dog breed, with a diameter of about 1 cm.

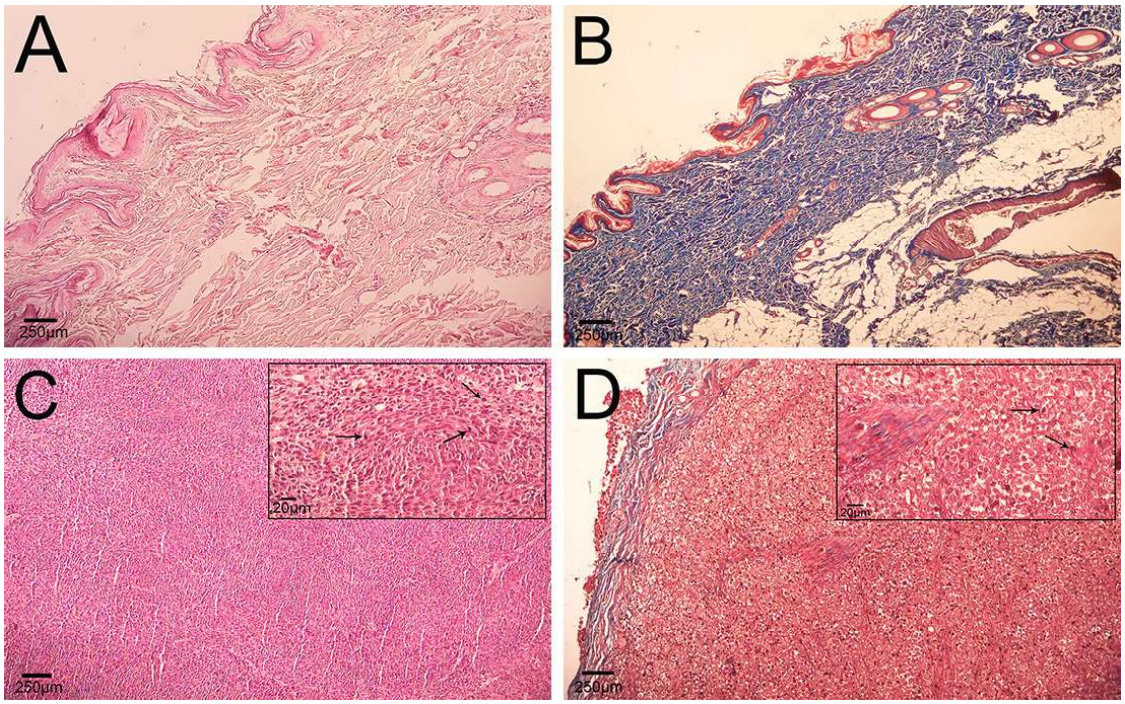

Figure 2.
Light microscope photomicrographs of LMS tumors compared with normal tissue of dog skin.
A: Organized structure of epidermis and dermis of normal dog skin (H&E). B: Organized structure of normal dog skin, despite the connective tissue (blue), dermis, and smooth muscles (red) around the blood vessels (Masson's trichrome). C: Cutaneous LMS with a view of interwoven fibers of smooth muscle, and the whirlwind view with cells formed and cut in various directions. The small picture presents the smooth muscle tumor cells with cellular pleomorphism, and the presence of mitotic figures (arrow) (H&E). D: A view of a section of LMS tumor where muscular tumor cells are visible (red) with limited connective tissue (blue) inside the tumor parenchyma. The small picture shows various forms of tumor cells and mitotic status (arrow) (Masson's trichrome).

Table 1.
Comparative hematological parameters in normal, local LMS and invasive LMS groups.

Parameter	Dogs (n= 12)			p value
	Normal (n= 6)	Local LMS (n= 3)	Invasive LMS (n= 3)	
HCT (%) (Reference: 37-55)	44.80 ± 4.82 [b]	37.60 ± 3.05 [a]	34.20 ± 2.39 [a]	0.002
Hb (g/l) (Reference: 140-190)	161.40 ± 9.24 [b]	147.20 ± 11.30 [ab]	137.00 ± 8.36 [a]	0.006
RBC (1012/l) (Reference: 5.8-8.50)	6.92 ± 0.87 [b]	6.96 ± 0.65 [b]	5.66 ± 0.61 [a]	0.023
MCV (*f*l) (Reference: 66-75)	69.20 ± 1.64	69.20 ± 1.48	70.40 ± 3.78	0.695
MCHC (g/l) (Reference: 32-36)	33.00 ± 1.58 [b]	33.40 ± 2.07 [b]	30.00 ± 1.58 [a]	0.019
PLT (109/l) (Reference: 150-400)	251.40 ± 58.44	240.00 ± 56.51	228.60 ± 67.34	0.841
WBC (109/l) (Reference: 6-13)	8.92 ± 1.25 [a]	7.84 ± 0.76 [a]	13.42 ± 2.49 [b]	0.001
Neut (109/l) (Reference: 3-10.50)	6.76 ± 1.19	6.44 ± 1.23	6.24 ± 1.32	0.806
Lym (109/l) (Reference:1-4)	2.36 ± 0.68	2.66 ± 0.40	2.72 ± 0.75	0.637
Mon (109/l) (Reference: 0.15-1.2)	0.52 ± 0.28 [a]	0.62 ± 0.25 [ab]	1.18 ± 0.46 [b]	0.023
Eos (109/l) (Reference:0-0.1.3)	0.40 ± 0.20 [a]	1.12 ± 0.37 [b]	1.34 ± 0.46 [b]	0.004

Different superscript letters (a, b, ab) designate a notable difference in every row. p <0.05 is significant.

ures 3 and 4).

In contrast, immunohistochemical analysis showed a significant increase in the percentage of Desmin-positive cells in the invasive LMS group compared to the normal skin, and significant difference were observed in H-Scores among all three groups ($p < 0.001$) (Figures 3 and 4). The increment of the number of α-SMA+ cells in the LMS groups (local and invasive) compared with the normal animals was significant, and the difference in the H-Scores of the LMS groups (local and invasive) in comparison with the normal category was also significant ($p < 0.001$). However, no significant difference was observed between local and invasive LMS groups ($p > 0.05$) (Figures 3 and 4). Vimentin expression was significantly increased, also significant difference was observed in H-Score of the LMS groups compared with the normal animals ($p < 0.001$) (Figures 3 and 4). Conversely, a significant reduction in the number of CK+ cells and the difference in the H-Score were observed in both LMS group compared with the normal animals ($p < 0.001$) (Figures 3 and 4). The number of Ki67-positive cells and the difference in the H-Score of the LMS groups compared with the normal animals were significantly increased ($p < 0.001$) (Figures 3 and 4). The number of EGFR-positive cells in the local LMS group compared with the normal and invasive LMS group was significantly Increased; also, the difference in the H-Score of the three groups was significant ($p < 0.001$). Notably, EGFR expression percentage and H-Score were significantly reduced in invasive LMS group compared with the other two groups (Figures 3 and 4). β-Catenin expression followed a pattern similar to that of EGFR, with significantly higher expression in local LMS compared with normal and invasive LMS, and significant difference in H-Score among all groups ($p < 0.001$) (Figures 3 and 4). E-Cadherin expression demonstrated a similarity with β-Catenin and EGFR, although the expression percentage and H-Score in the local LMS group were lower than those observed for EGFR and β-Catenin (Figures 3 and 4). Immunohistochemical expression patterns of all evaluated markers in the normal, local LMS and Invasive LMS are presented in Figures 5-7.

Discussion

The present study investigated the occurrence, clinicopathological features, hematological alterations, and immunohistochemical characteristics of cutaneous leiomyosarcoma (LMS) in dogs.

Results of the study, conducted over 10 years in Urmia city, revealed that among the 318 dogs with various cutaneous lesions, 6 (1.88%) were diagnosed as LMS (local and invasive). According to the occurrence rate of this tumor in other countries, information from 748 cases of neoplasm in dogs in Korea, leiomyoma and leiomyosarcoma had 0.27% and 0.4% frequencies, respectively [8]. Similarly, retrospective research conducted over seven years on dog skin tumors in analytical research center, north region of Portugal (2014 to 2020), out of the 1185 cases with

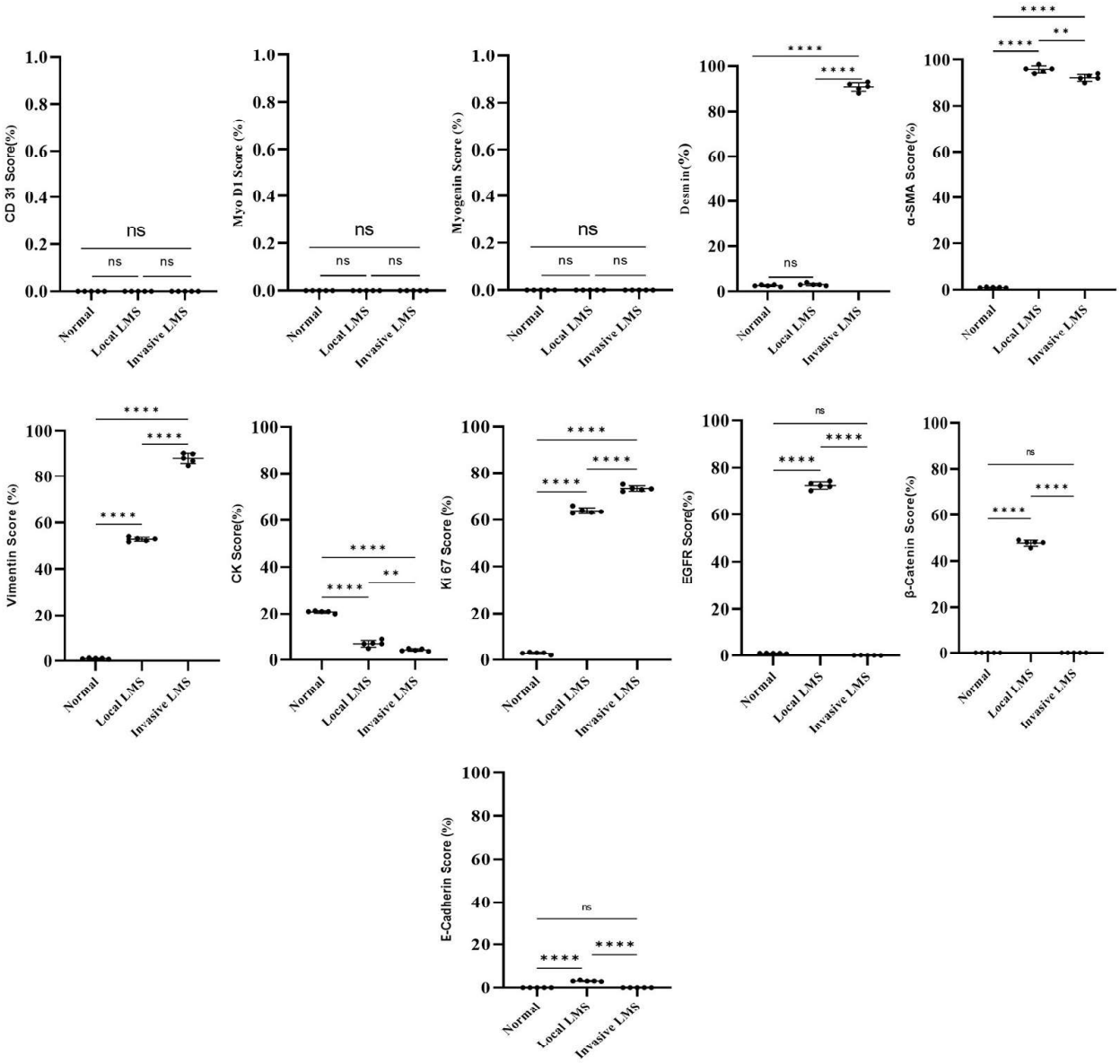

Figure 3.
The results of the one-way ANOVA for the percentage of cellular expression of various immunohistochemical markers in the normal, local LMS and invasive LMS groups. Data are presented as Mean ± SD.
*: Significant value ($p < 0.05$). ns: non-significant.

lesions identified as cutaneous neoplasms, 62.9% of them were reported as benign, and 37.1% as malignant. Mast cell tumors (22.7%) were the most common form of identified tumor, thereafter benign soft tissue neoplasms (9.7%), Sebaceous gland tumors (8.1%), vascular neoplasms (7.9%), and soft tissue sarcomas (7.6%). Cutaneous cancers were multicentric (6.14%), followed by solitary tumors in hind limb areas (12.1%), anterior motor organs (8.6%), buttocks (7.1%), abdomen (6.5%), and rib area (5.2%) [9]. In the current study, Malignant cutaneous cancers of smooth muscles affected dogs of both sexes, predominantly at high ages (between 6 and 12 years). Although two affected dogs belonged to small breeds, the majority, were medium to large breeds, supporting earlier suggestions observed in previous research [1,10], despite the fact that these tumors are rare, they are more common in larger dog breeds. On the other hand, some other studies also demonstrated that the occurrence of LMS tumors is not related to the dog's breed potential [11]. In the present study, hematological analyses showed significant decrease in indices related to red blood cells, such as Hct, Hb, RBC, and MCHC in dogs affected by LMS compared with healthy dogs ($p < 0.05$), indicating anemia. However, this anemia was more pronounced in invasive LMS group compared to local LMS group. In terms of white blood cell indices, total WBC, Mon, and Eos in LMS groups had a significant decrease compared with healthy dogs ($p < 0.05$), indicating the involvement of immune system

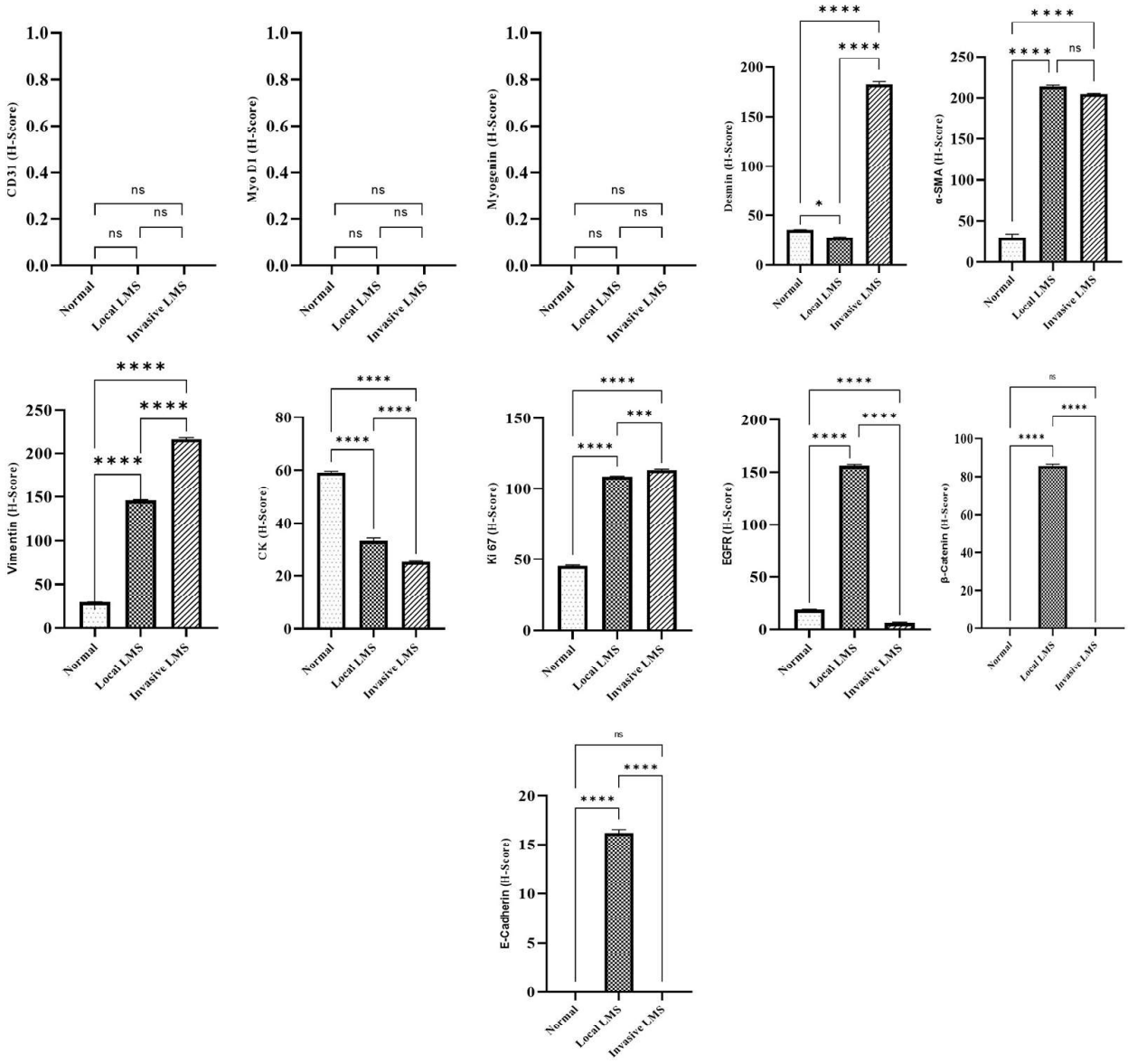

Figure 4.
The results of the one-way ANOVA for the H-Score of the different immunohistochemical markers in the normal, local LMS and invasive LMS groups. Data are presented as Mean ± SD.
*: Significant value ($p < 0.05$). ns: non-significant.

in LMS groups with the tumor and possible existence of a chronic inflammation. In another study on 44 dogs (1983-1988) with leiomyosarcoma (spleen, stomach, small intestine, cecum, and liver), every dog with liver LMS was clearly involved with metastasis, and they were euthanized during the surgery. In the remaining three groups, 79% of the infected dogs had no indication of metastasis during the surgery. In this research abnormal hematologic and biochemical findings included leukocytosis (8 cases), anemia (7 cases), azotemia (4 cases), increased serum ALP levels (6 cases), and elevated serum ALT and AST levels (3 cases) [11]. The outcomes of the mentioned study were in agreement with the findings of the present study regarding the occurrence of leukocytosis and anemia. Although the recent study did not investigate the cutaneous LMS, symptoms including anemia was observed in local LMS case and invasive LMS cases, further supporting the presence of paraneoplastic syndromes, which are commonly associated with malignant neoplasms. Besides, one of the cases with local LMS and two cases with invasive LMS indicated hypoglycemia, which is also among the symptoms of paraneoplastic syndromes [12]. In the present study, all local LMS tumors were solitary, and the invasive LMS tumors were dispersed. The local LMSs were related to surface cutaneous tissues, and no recurrence observed during a six-month follow-up after the surgery. In contrast, among the invasive LMS cases, two animals were euthanized due to disease severity and metastatic nature of the disease, While follow-up data were unavailable for the remaining case due to owner

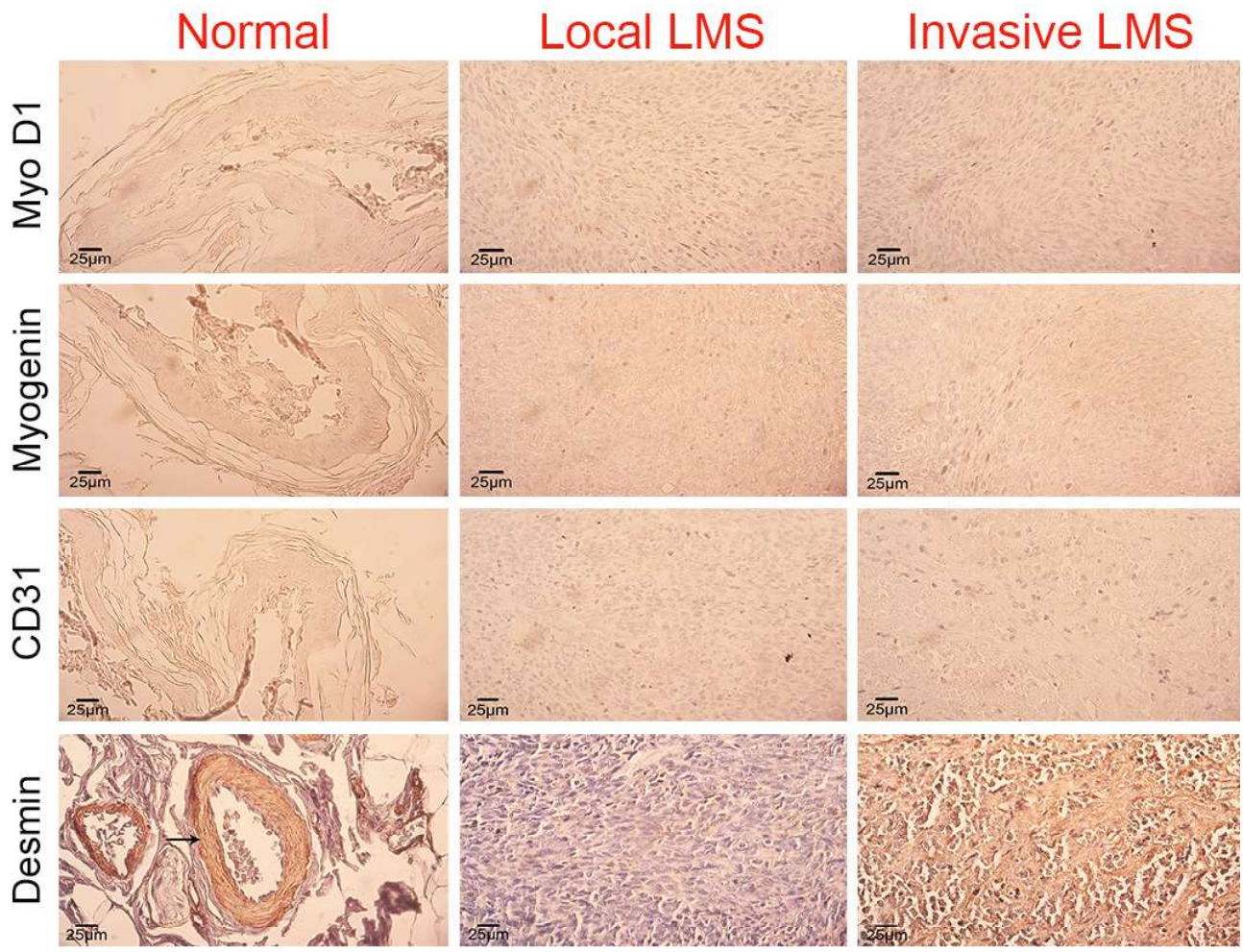

Figure 5.
Comparative immunohistochemical photomicrographs of normal skin tissue, local LMS, and invasive LMS.
The lack of MyoD1 and Myogenin markers in the normal and tumor tissue cells confirmed the LMS tumors and differentiated them from rhabdomyosarcoma tumors. Lack of CD31 marker expression in LMS tumors indicates the confirmation of piloleiomyosarcoma tumors. Desmin can be seen in normal tissue and in muscles surrounding the blood vessels (the arrow), and while it is not expressed in the local LMS, it can be seen in a dispersed form in invasive LMS (IHC).

refusal of euthanasia. These observations suggest that early surgical intervention in local LMS may result in a favorable prognosis. Previous studies have similarly reports an acceptable prognosis for cutaneous and subcutaneous smooth muscle tumors in dogs; however, such information is primarily limited to tumors originating from the smooth muscles that erect hair or from the walls of blood vessels, and there is no information on the smooth muscle tumors inside the deep soft tissues [13]. Immunohistochemistry evaluation for Myogenin, MyoD1, and CD31 showed that the negative results of LMSs for the mentioned markers confirmed their definite LMS nature and piloleiomyosarcoma type. These three markers were primarily intended for the differential diagnosis of LMS from other muscle tissue tumors, such as rhabdomyosarcoma, and the differential diagnosis of LMS types (piloleiomyosarcoma and angioleiomyosarcoma). In the present study, SMA and Desmin was significantly increased in LMS tissues compared with normal skin, although the extent of changes in their expression and intensity varied based on tumor's nature and biological behavior. Vimentin played a significant role in the metastasis process and was investigated under laboratory conditions. During the epithelial-mesenchymal transition (EMT), epithelial cells lose their basoapical and intercellular polarity, and obtain adhesion features by the downregulation of genes related to epithelial cells, including E-cadherin and cytokeratins, and while acquiring migrative and invasive characteristics related to mesenchymal cell phenotypes through genes such as N-cadherin and Vimentin [14]. In other words, the process of epithelial-mesenchymal transition (EMT) is characterized by the suppression of epithelial phenotypes and the concomitant adoption of mesenchymal properties. Cells in EMT frequently reside in a partial or intermediate state, co-expressing both epithelial and mesenchymal markers, with a fully

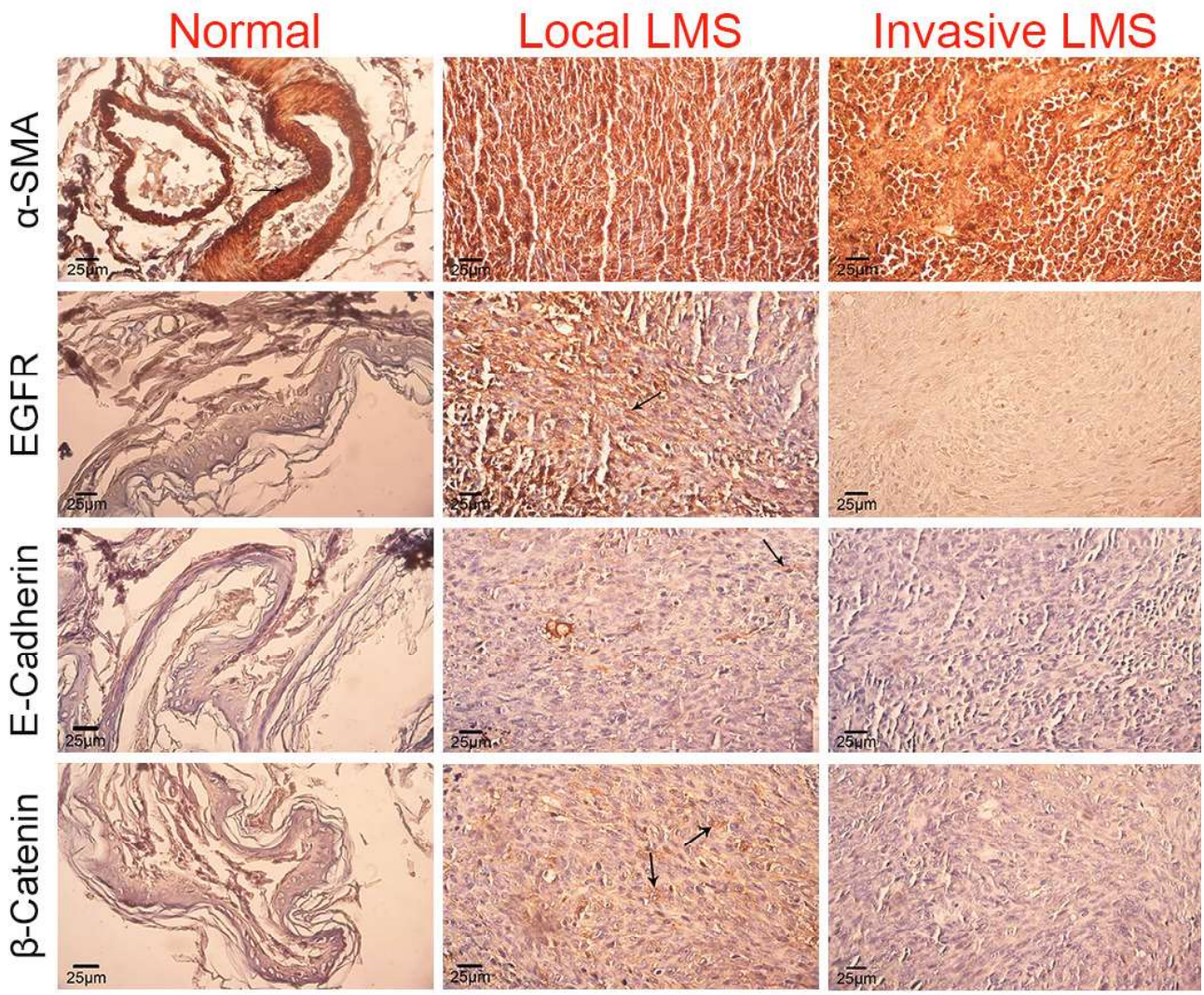

Figure 6.
The following comparative immunohistochemical photomicrographs of normal skin tissue, local and invasive LMS.
The strong and dispersed α-SMA expression in the local and invasive tumor is an indication of their smooth muscle origin for the tumor-forming cells, and its expression in normal skin can be observed only in smooth muscles around the blood vessels. EGFR expression in normal cells is negative; yet, cytoplasmic expression of EGFR (arrow) can be seen, while the marker is not expressed in the invasive tumor. E-Cadherin expression in normal skin and invasive tumor is negative, but a weak cytoplasmic expression (arrow) can be seen in the local tumor. β-catenin expression is negative in normal skin and invasive tumor; however, a cytoplasmic expression (arrow) of β-catenin in the local tumor can be seen, which is higher than E-Cadherin (IHC).

mesenchymal state being uncommon. Notably, this transition is reversible through its counterpart process, mesenchymal-epithelial transition (MET) [15]. The progressive increase in Vimentin expression with increasing tumor metastatic aggressiveness observed in the present study supports its role as an indicator effective in the degree of malignancy or invasiveness of LMS. In a report related to the first primary leiomyosarcoma occurrence in the testicles of two 10 and 12 year old dogs, the immunohistochemistry findings demonstrated a positive (moderate) immune reaction by the tumor cells to Vimentin, SMA, and Desmin markers [16]. A report from Japan on multiple polymorphic cutaneous leiomyosarcomas in a 13-year-old male Shih Tzu dog described leiomyosarcomas with poor differentiation and explained that their distinction from anaplastic sarcomas with giant cells was difficult. Immunohistochemistry examination indicated the high positivity of tumor cells to Vimentin, their relative positivity to SMA and Desmin, and a negative response to cytokeratin [3]. In a systematic review of 2616 dogs and cats with skin tumors in Britain, the occurrence rate of cutaneous leiomyomas in dogs and cats was 0.88% and 0.33%, respectively. Differentiating leiomyosarcoma, rhabdomyosarcoma, and fibrosarcoma using routine histological methods might be difficult; however, ultrastructural and immunohistochemical methods are useful for the accurate diagnosis of soft tissue sarcoma tumors. A report from Korea described one cutaneous piloleiomyoma and two angioleiomyosarcoma cases in three female dogs aged 7 to 12 years with solitary or paired nodules. In terms of

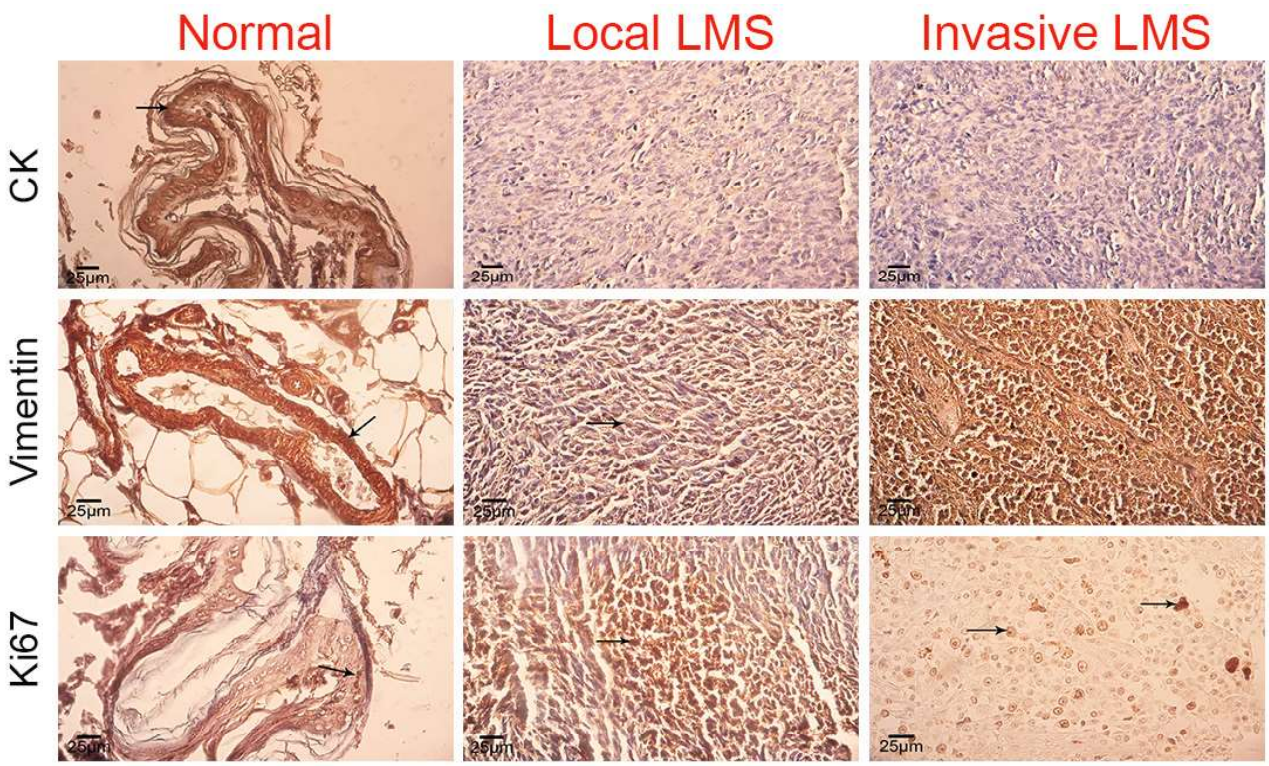

Figure 7.
The following comparative immunohistochemical photomicrographs of normal skin tissue, local and invasive LMS. The strong CK expression in normal squamous skin cells, its weak expression in the local tumors, and lack of expression in the invasive tumor confirm the mesenchymal origin of the tumor cells. The strong Vimentin expression in the smooth muscles around the blood vessels (arrow), normal skin tissue, moderate cytoplasmic expression of Vimentin in the local tumor, and its strong and dispersed expression in the invasive tumor can be seen. A weak Ki67 expression is visible inside the nuclei of several normal squamous skin cells (arrow), in addition to a strong and dispersed expression inside the nuclei of local tumor cells (arrow), and a moderate and dispersed nuclear expression in the invasive tumor cells (arrow) (IHC).

immunohistochemistry, tumor cells showed extremely positive reactions to SMA [8]. A retrospective study identified 24 dogs with histological diagnosis of definite or suspected leiomyoma and leiomyosarcoma in a non-visceral location. According to immunohistochemistry tests, more than two-thirds of the leiomyosarcoma tumor cells showed positive reactions to SMA and Laminin markers. Histochemistry also indicated a mild to moderate matrix deposition, which was identified using Masson's trichrome staining. The study data indicated the unusual nature of non-visceral leiomyosarcoma and the importance of IHC for their diagnosis [17]. In several malignant tumors related to different diseases, EGFR is overexpressed. By overexpressing these molecules in neoplasms, they will be involved in the functions of some critical stages, such as vascularization, inhibition of programmed cell death, immunosuppression, enhanced cellular multiplication, possibility of invasion, and cellular specialization and displacement. Due to the importance of EGFR and its involvement in the progression and malignancy, reduced survival rate, and poor prognosis, they are considered promising biomarker and potential therapeutic targets in veterinary oncology [7]. In a report related to a high-grade sarcoma case of an eleven-year-olds neutered female Labrador Retriever, immunohistochemistry analysis demonstrated the positive VEGFr, PDGFr, SCF, and EGFR in the tumor cells. Repeating the surgical removal and targeted treatment with toceranib led to a stable recovery for about two years. IHC results for the EGFR maker in the present study indicated a remarkable increase in the expression and intensity of this maker in the local LMS category in comparison with the normal and invasive LMS categories. Experimental studies transplanted highly tumorigenic and chemotherapy-resistant human LMS cells to mice and regenerated the tumor, and demonstrated that these cells indicated the triggering of EGFR/AKT/MAPK pathways, implying the potential of prevailing their drug resistance by blocking EGFR [18]. Moreover, TGFα-EGFR signaling pathways has been implicated in enhancing tumor growth rate and its metastasis. Moreover, the signaling activates the endothelial cells related to the tumor in addition to the tumor cells [19]. Although EGFR is specific to tumors with epithelial cell origin, the present study determined that EGFR expression occurs both in epithelial tumors and mesenchymal

tumors, such as LMS, and as EGFR expression decreases in the invasive LMS cells, it may be an indicate that EGFR upregulation plays a role during early tumor development and its expression possibly continues until the metastasis stage. However, confirming this finding requires additional molecular analyses. Analysis of E-Cadherin and β-Catenin expression demonstrated that increased β-Catenin expression and intensity in local LMS cells compared with invasive LMS and normal skin cells was significantly higher than E-Cadherin, and although E-Cadherin expression in the local LMS group was higher than invasive LMS and normal skin, when applying a 10% threshold, the increase in E-Cadherin (under 10%) expression was negligible compared with β-Catenin (40% to 60%). Epithelial cells are characterized by the expression of E-Cadherin, which is conceptualized as both a tumor suppressor gene and a morphogenic factor within the context of epithelial neoplasms. Studies have indicated a reduction or absent in E-Cadherin expression correlating with a decrease in differentiation, invasion, or metastasis among various malignancies, including multiple forms of sarcoma. An investigation into the expression of E-Cadherin, β-Catenin, and topoisomerase IIα in human leiomyosarcoma analyzed 19 paraffin-embedded primary and non-metastatic leiomyosarcoma tissue specimens for the expression of these markers utilizing immunohistochemistry (IHC), employing a threshold of 20% for determining positive cell staining results. The outcomes of this study indicated that E-Cadherin expression was uniformly negative across all leiomyosarcoma samples. Additionally, negative β-Catenin nuclear expression was found in all leiomyosarcoma samples, whereas immunopositivity for cytoplasmic expression of β-Catenin was recorded in nearly 50% of the patients [20]. β-Catenin/E-Cadherin expression was not investigated in dogs; however, a study on the mentioned issue in canine papilloma and SCC skin tumors reported through immunohistochemistry analyses that inappropriate β-Catenin/E-Cadherin expression occurred during the epidermal tumorigenesis in dogs. Such results support the hypothesis indicating that inappropriate β-Catenin/E-Cadherin expression may has a crucial importance in the pathogenesis of canine epidermal neoplasms, and not merely due to the disruption of the intercellular junctions, but also because of the irregular activating of the signaling pathways that these molecules are involved with [21]. Considering the β-Catenin/E-Cadherin IHC results in the current study, it appears that β-Catenin and E-Cadherin alone may not be sufficient prognostic markers, but may contribute to understanding tumor invasion pathways [22].

Ki67 immunoreactivity in the present study was significantly increased in both invasive and local LMS groups compared with the normal animals. Hence, considering the malignant and invasive nature of the tumor, the cell proliferation rate was high, as the percentage of Ki67-positive cell nuclei was 60% to 80%, and subsequently, the H-Score of the tumor groups had a significant increase compared with the normal group. It must be noted that Ki67 expression in canine beta tumor cells is highly dependent on the tumor type, and other factors, such as the animal's age and sex, can somewhat play roles in changing the marker's expression in tumor tissues [23]. In humans, studies suggested labelling indices (LI) over 10% as a tumor prognosis index for uterine leiomyosarcoma tumors [24]. Nevertheless, considering the aforementioned factors, LI may vary in different studies; therefore tumor prognosis should not rely solely on Ki-67 and LI, but should also consider additional histopathological parameters such as nuclear atypia and mitotic index [25]. Although CK maker is primarily used to diagnose tumors of epithelial cell origin, regarding the IHC results for this marker in the present study, considering the existing reports indicating the inappropriate expression of cytokeratin in normal and neoplastic tissues with non-epithelial origin [26], this marker was added to the immunohistochemistry panel. In the present study, CK expression was confined to squamous epithelial cells in normal skin, while LMS tumors exhibited low expression (under 10%) and negligible amount of CK immunoreactivity.

In summary, among 318 dogs with cutaneous lesions, 6 cases of leiomyosarcoma (LMS) were confirmed, including 3 local and 3 invasive. Blood test showed significant increases in leukocytes, monocytes, and eosinophils ($p < 0.05$) in affected dogs. Microscopic analysis revealed tumor fibers intermingled with connective tissue and marked cell heterogeneity. Tumor cells had a mean mitotic index of 4.2 for local cases and 5.8 for invasive ones. Immunohistochemical tests showed no MyoD1 or Myogenin, confirming LMS, and the tumors lacked CD31, indicating they were piloleiomyosarcoma. Notably, tumor cells had higher positive expressions of Desmin, SMA, Vimentin, and Ki67 compared to normal skin. Additionally, local LMS showed increased EGFR and β-Catenin compared to invasive LMS and normal tissue. The study demonstrate that, EGFR expression is not limited to epithelial tumors but is also relevant in mesenchymal tumors, such as LMS. While, β-Catenin and E-Cadherin alone are insufficient for prognostic assessment, they may help in understanding invasion pathways and aid in treatment decision making.

Materials & Methods

Ethical approval

The study was performed following approval from the Research Ethics Committee of Islamic Azad University, Urmia Branch (approval code: IR.IAU.URMIA.REC.1403.148; September 8, 2024).

Animals

Formalin fixed tissue samples and paraffin embedded blocks of canine cutaneous tumor lesions were retrospectively collected from cases referred to the Veterinary Clinic of the Islamic Azad University, Urmia Branch, and private pet clinics in Urmia city over a 10 year period (January 2014 to January 2024). During this period, a total of 318 dogs of various breeds, presenting with various cutaneous lesions were examined. These included Rottweiler (n= 25), Shih Tzu (n= 21), Iraqi (Kurdish Mastiff) (n= 15), German Shepherd (n= 33), Terrier (n= 87), and Iranian mixed breeds (n= 137).

Pathologcal Examination

For cases suspected of skin tumors, tissue samples were obtained either by biopsy (from local tumors) or during necropsy (invasive and metastatic tumors) and archived for histopathological evaluation. In macroscopic examination, first, the cutaneous lesions suspected of tumors were examined (i.e., size, number, color, consistency, hemorrhage, location, and distribution of tumors), and all the other relevant animal characteristics were recorded. Tissue samples were fixed in 10% neutral buffered formalin, stained using the H&E method and investigated using an optical microscope. In cases suspected of connective tissue and smooth muscle tumors, Masson's trichrome staining was used for differential diagnosis and to confirm the tumor. After fixation tissue samples were cut into 0.5 × 0.5 × 1 cm sections, and processed using an Autotechnicon Tissue Processor. Samples underwent dehydration, clearing, and paraffin impregnation, followed by sectioning at 6 µm thickness using a micrometers Sections were routinely stained with Hematoxylin and Eosin (H&E) method was used to stain. In cases where the cutaneous tumor mass was suspected of sarcoma, the Masson's trichrome method was applied to confirm and differentiate the diagnosis of leiomyosarcoma from fibrosarcoma and other fibromatous lesions [27]. Diagnostic criteria for cutaneous LMS, included cellular and nuclear pleomorphism (atypia), number of nucleoli, number of mitotic figures, and the presence of necrosis and hemorrhage in the tumor tissue section. Additionally, the features of the fibers with varying connective tissue amounts were investigated [13].

Hematologcal Examination

Blood samples were collected from the jugular veins of six healthy dogs and six dogs diagnosed with cutaneous leiomyosarcoma tumors using 21-gauge needles into EDTA-containing tubes. Hematological parameters were analyzed using an Abbott Cell Dyn 3500 automated hematology analyzer.

Immunohistochemistry

Immunohistochemical staining was performed using the EnVision® + HRP dual system. Sections were dewaxed with xylene and rehydrated with ethanol, followed by incubation in hydrogen peroxide (3%) for 30 minutes to inhibit non-specific peroxidase activity. Heat-induced epitope retrieval was conducted using a 0.01 M citrate buffer (pH = 6.0) for 25 minutes, and slides were incubated with albumin bovine serum (5%) in Tris buffered saline (TBS) for half an hour to suppress non-specific staining. Afterward, the sections were washed with water and TBS and held at room temperature. In the last stage, the sections were incubated overnight at 4°C with the following primary: α-SMA (Dako, USA; 1:200), Ki67 (Dako, USA;1:100), β-catenin (Dako, USA;1:100), cytokeratin (Dako, USA; 1:50), VIM (Dako, USA;1:100), MyoD1 (ThermoFisher, clone 5.8a, 1:50), Myogenin (ThermoFisher, clone FSD, 1:800), Desmin (Dako, USA; 1:100), EGFR (Zymed Laboratories, San Francisco, California, USA; 1:50), E-cadherin (Invitrogen, Carlsbad, CA, USA; 1:50), and CD31 (Dako, USA; 1:200). Following primary antibody incubation, slides were washed with phosphate-buffered saline (PBS) and incubated with streptavidin-horseradish peroxidase (HRP) for 20 minutes. After another wash with the buffer, the slides were treated with diaminobenzidine for 10 minutes, with the sections being counterstained using Harris hematoxylin [28].

CD31, which is a marker for endothelial cells of blood vessels, was used to differentiate LMS types (piloleiomyosarcoma originating from the smooth muscles around the hairs, and angioleiomyosarcoma originating from the cutaneous vessels). MyoD1 and Myogenin were used to differentiate Rhabdomyosarcoma (RMS) from LMS. cytokeratin and vimentin were used to determine epithelial or mesenchymal origin of the tumor cells, Ki67 to evaluate cellular proliferation rate, and α-SMA to confirm smooth muscle fibers differentiation. EGFR, β-catenin, and E-cadherin were evaluated to investigate possible EMT changes and prognostic in LMS tumor cells [2,7,14]. In order to rank the expression intensity of immunohistochemical markers for each sample (normal and pathological), five randomly selected microscopic fields (each measuring 2.37 mm2) were evaluated at ×40 magnification. The number of positive cells, exhibiting positive brown immunoreactivity reaction, was counted and expressed as a percentage of the total cells. The histochemical score assessment (H-Score) was calculated to assess both staining intensity and distribution using the following formula:

H-score = (P1 × 1) + (P2 × 2) + (P3 × 3)

In this formula, P indicates the percentage of positive cells (+, ++, and +++) inside the tissue, represented by P1, P2, and P3, respectively. The numerical scale for H-Score ranged between 0 and 300 [29,30].

Statistical Analysis

Statistical analyzed were performed using GraphPad Prism software (Version 9). Descriptive findings, including mean, standard deviation, and standard error, were calculated. The Shapiro-Wilk test was used for evaluating quantitative data normality. In the next step, considering the scoring data normality of the immunohistochemical percentage and H-Score data, differences among normal, local LMS, and invasive LMS groups, were analyzed using one-way analysis of variance (one-way ANOVA), followed by Tukey's post-hoc tests. Statistical significance was set at $p < 0.05$.

Authors' Contributions

F.H. and A.A. conceived and planned the experiments. F.H. and A.A. carried out the experiments. F.H. and A.A. contributed to sample preparation. A.A. contributed to the interpretation of the results. A.A. took the lead in writing the manuscript. Both authors contributed to the first draft, revising.

Acknowledgements

We would like to thank the TUMS Cancer Institute for preparing the immunohistochemical sections.

Conflict of interest

The authors declare that there is no conflict of interest.

References

1. Torrigiani F, Pierini A, Lowe R, Simčič P, Lubas G. Soft tissue sarcoma in dogs: A treatment review and a novel approach using electrochemotherapy in a case series. Vet Comp Oncol. 2019;17(3):234–41. Doi:10.1111/vco.12462.

2. Guisado FR, Castro PL. Piloleiomyosarcoma in cats: Histological and immunohistochemical features. Vet Pathol. 2022;59(1):57–62. Doi:10.1177/03009858211042582.

3. Aihara N, Sugiyama J, Baba H, Kamiie J. Multiple cutaneous pleomorphic leiomyosarcoma in a dog. J Vet Med Sci. 2019;81(11):1564–6. Doi:10.1292/jvms.19-0295.

4. Kim YJ, Jeon Y, Bae H, Shin SW, Cho Ar, Hyun J-E, et al. Oral leiomyosarcoma in a dog. J Biomed Transl Res. 2021;22(4):199–204. Doi:10.12729/jbtr.2021.22.4.199.

5. Han J, Kim Y, Kim D, Na K. Alteration in E-Cadherin/b-Catenin expression in canine melanotic tumors. Vet Pathol. 2012;50(2):274–80. Doi:10.1177/0300985812457792.

6. Bongiovanni L, Malatesta D, Brachelente C, D'Egidio S, Della Salda L. β-Catenin in canine skin: Immunohistochemical pattern of expression in normal skin and cutaneous epithelial tumours. J Comp Pathol. 2011;145(2–3):138–47. Doi:10.1016/j.jcpa.2011.01.008.

7. Files R, Santos C, Queiroga FL, Silva F, Delgado L, Pires I, et al. Investigating Cox-2 and EGFR as biomarkers in canine oral squamous cell carcinoma: Implications for diagnosis and therapy. Curr Issues Mol Biol. 2024;46:485–497. Doi:10.3390/cimb46010031.

8. Jung J-Y, Kang S-C, Park D-S, Lee E-S, Bae J-H, Kim J-H. Cutaneous smooth muscle tumors in 3 dogs. Korean J Vet Res. 2009;49(1):63–6.

9. Martins AL, Canadas-Sousa A, Mesquita JR, Dias-Pereir P, Amorim I, Gärtner F. Retrospective study of canine cutaneous tumors submitted to a diagnostic pathology laboratory in Northern Portugal (2014–2020). Canine Med Genet. 2022;9(1):2. Doi:10.1186/s40575-022-00113-w.

10. Jacobs TM, Poehlmann CE, Kiupel M. Injection-site sarcoma in a dog: clinical and pathological findings. Case Reports Vet Med. 2017;2017:1–4. Doi:10.1016/j.tips.2003.09.006.

11. Kapatkin AS, Mullen HS, Matthiesen DT, Patnaik AK. Leiomyosarcoma in dogs: 44 cases (1983-1988). JAVMA. 1992;201(7):1077–9.

12. Meuten DJ. Tumors in Domestic Animals. Fifth. Wiley Blackwell; 2017. 15–16 p.

13. Avallone G, Pellegrino V, Muscatello LV, Roccabianca P, Castellani G, Sala C, et al. Canine smooth muscle tumors: A clinicopathological study. Vet Pathol. 2022;59(2):244–55. Doi:10.1177/03009858211066862.

14. Berr AL, Wiese K, Santos G dos, Koch CM, Anekalla KR, Kidd M, et al. Vimentin is required for tumor progression and metastasis in a mouse model of non–small cell lung cancer. Oncogene. 2023;42:2074–8. Doi: 10.1038/s41388-023-02703-9.

15. Yim IS, Laronde DM. Biomarkers of epithelial-mesenchymal transition: E-cadherin and beta-catenin in malignant transformation of oral lesions. Can J Dent Hyg CJDH = J Can l'hygiene Dent JCHD. 2024;58(2):111–9.

16. Ciaputa R, Brambilla E, Godizzi F, Dzimira S, Żebrowski K, Kandefer-Gola M, et al. First report of primary testicular leiomyosarcoma in two dogs. BMC Vet Res. 2023;19:101. Doi: 10.1186/s12917-023-03658-5.

17. Brady R V., Rebhun RB, Skorupski KA, Burton JH, Al-Nadaf S, Choi E, et al. Retrospective immunohistochemical investigation of suspected non-visceral leiomyosarcoma in dogs. J Vet Diagnostic Investig. 2022;34(3):465–73. Doi:10.1177/10406387221083570.

18. Sette G, Salvati V, Memeo L, Fecchi K, Colarossi C, Di PM, et al. EGFR Inhibition Abrogates Leiomyosarcoma Cell Chemoresistance through Inactivation of Survival Pathways and Impairment of CSC Potential. PLoS One. 2012;7(10):e46891. Doi:10.1371/journal.pone.0046891.

19. Sasaki T, Hiroki K, Yamashita Y. The Role of Epidermal Growth Factor Receptor in Cancer Metastasis and Microenvironment. Biomed Res Int. 2013;2013:1–8. Doi:10.1155/2013/546318.

20. Gogou PN, Batistatou A, Pakos EE, Apostolikas N, Stefanou D, Tsekeris PG. Expression of E-cadherin, ß-catenin and topoisomerase IIα in leiomyosarcomas. Clin Transl Oncol. 2009;11:548–51. Doi:10.1007/s12094-009-0401-3.

21. Sanz Ressel B, Massone A, Barbeito C. Aberrant expression of E-cadherin/b-catenin during epidermal tumourigenesis in dogs. J Comp Pathol. 2020;176:1–9. Doi:10.1016/j.jcpa.2020.01.006.

22. Debruyne P, Vermeulen S, Mareel M. The role of the E-cadherin/catenin complex in gastrointestinal cancer. Acta Gastroenterol Belg. 1999;62:293–402.

23. Firsching TC, Dietert K, Bartel A, Gruber MGD, D A. Dependence of the Ki67 Labelling Index of Selected Canine Tumours on Patient Age, Sex and Tumour Size. J Comp Pathol. 2022;193:1–8. Doi:10.1016/j.jcpa.2022.02.001.

24. Travaglino A, Raffone A, Catena U, Luca M De, Toscano P, Prete E Del, et al. Ki67 as a prognostic marker in uterine leiomyosarcoma: A quantitative systematic review. Eur J Obstet Gynecol Reprod Biol. 2021;261:119–24. Doi:10.1016/j.ejogrb.2021.09.026.

25. Bergin IL, Smedley RC, Esplin DG, Spangler WL, Kiupel M. Prognostic Evaluation of Ki67 Threshold Value in Canine Oral Melanoma. Vet Pathol. 2011;48(1):41–53. Doi:10.1177/0300985810388947.

26. Adegboyega PA, Qiu S. Immunohistochemical profiling of cytokeratin expression by endometrial stroma sarcoma. Hum Pathol. 2008;39:1459–64. Doi:10.1016/j.humpath.2008.02.008.

27. Amoorahim S, Amniattalab A. Immunohistochemical expression of GDNF, P53 and Ki67 with Tunel assay in canine non-neoplastic esophageal nodules induced by Spirocerca lupi. Maced Vet Rev. 2025;48(1):39–51. Doi:10.2478/macvetrev-2025-0014.

28. Babanezhad-gajouti A, Amniattalab A. in the canine spleen with siderofibrotic nodules : an immunohistochemical and immunofluorescence perspective on apoptosis , ferroptosis , and oxidative stress. Turkish J Vet Anim Sci. 2023;47(4):397–412. Doi:10.55730/1300-0128.4308.

29. Piercealla WE, Wolfea M, Suschaka J, Changa H, Chena Y, Sprotta KM, et al. Strategies for H-score normalization of preanalytical technical variables with potential utility to immunohistochemical-based biomarker quantitation in therapeutic response diagnostics. Anal Cell Pathol. 2011;34:159–68. Doi:10.3233/ACP-2011-014.

30. Ruengwanichayakun P. Histochemical scoring assessment (H-score). Asian Arch Pathol. 2021;3(1):13–4.

How to cite this article
Heydarzadeh F, Amniattalab A . Immunohistochemical expression of EGFR, E-Cadherin, β-Catenin, and Ki67 in dogs with local and invasive cutaneous leiomyosarcoma. Iran J Vet Sci Technol.2026; 18(2): 23-36.
DOI: https://doi.org/10.22067/ijvst.2025.93754.1557
URL: https://ijvst.um.ac.ir/article_47596.html

Iranian Journal of Veterinary Science and Technology

Received: 2025- Jul-30
Accepted after revision: 2025- Dec- 09
Published online: 2025- Dec-09

RESEARCH ARTICLE

DOI:10.22067/ijvst.2025.94414.1574

Enhanced Antimicrobial Efficacy of Propolis Solid Lipid Nanoparticles Against Methicillin-Resistant Staphylococcus aureus Isolated from Raw beef

Jaafar Al-Hashimi[a], Amir Salari[a], Basima jasim Mohammed[b]

[a] Department of Food Hygiene and Aquaculture, Faculty of veterinary Medicin Ferdowsi University of Mashhad (FUM), Mashhad, Iran.
[b] College of veterinary Medicin , University of AL-Qadisiyah, Iraq.

ABSTRACT

Methicillin-Resistant *Staphylococcus aureus* (MRSA) in raw beef poses a serious public health threat by facilitating resistant infections, spreading through food chains, and enabling animal to human transmission. Addressing this issue requires coordinated efforts across food safety, agriculture, and healthcare sectors. A total of 112 raw beef samples were collected from the boneless outer surface of shoulder and thigh regions of beef carcasses. Methicillin-resistant S. aureus then were isolated by traditional methods. Propolis-loaded solid lipid nanoparticles (LNPs-PL) were prepared using ultra-sonication and high-shear homogenization techniques. The manufactured formulation's encapsulation efficiency, loading capacity, and physicochemical characteristics were evaluated. Morphology was examined using scanning electron microscopy (SEM), and chemical makeup of the tested regular oil and LNPs-PL was analyzed using GC/MS. The antibacterial activity of LNPs-PL was compared with that of free propolis (PL) using in vitro assays. The prevalence of MRSA among raw beef samples was 50/112 (44.6%). among which 20 isolates (40%) were confirmed as MRSA. LNPs-PL demonstrated significantly enhanced antimicrobial activity, with an inhibition zone of 36.0 mm compared to 14.0 mm for PL. The findings indicate that modifications should be made in the loading capacity, encapsulation efficiency, and physicochemical properties. Also the findings confirmed that SLNs are effective PL carriers for controlling bacterial and fungal diseases. These findings suggest that LNPs-PL could be developed as natural antimicrobial agents for food preservation or surface sanitization in the food industry

Keywords

Methicillin-Resistant S. aureus, Raw beef, Propolis nanoparticles, Antimicrobial efficacy, Foodborne pathogens

Number of Figures: 7
Number of Tables: 2
Number of References:: 25
Number of Pages: 9

Abbreviations

LNPs-PL: Propolis Solid Lipid Nanoparticles

MRSA: Methicillin-Resistant Staphylococcus aureus

Corresponding author: Amir Salari
Email: a-salari@um.ac.ir
Tel: +98(51)3880-5594

Introduction

Meat is an essential component of human nutrition, providing high quality protein, essential and non-essential essential amino acids, minerals and vitamins [1]. However, it also serves as an ideal medium for the growth and proliferation of spoilage microorganisms and serious pathogens as *Bacillus cereus*, *Escherichia. coli* O157:H7, Salmonella spp., Listeria monocytogenes and *S. aureus* [2]. Food of animal origin, such as meat and meat products, can be contaminated with *methicillin-resistant S. aureus* (MRSA) during various stages of production. Contamination may occur during slaughtering or milking processes from colonized or infected animal. This can lead to contamination of food products and environment, and ultimately the transmission of MRSA to humans through direct contact with contaminated meat [3]. The emergence of antimicrobial resistance among foodborne pathogens is largely attributed to the extensive use of antibiotics. The spread of MRSA germs to the human population can be attributed to improper hygienic standards and procedures throughout the slaughtering, transportation, and marketing processes, as evidenced by meat contamination [4]. Propolis, a natural resinous substance collected by honeybees from plant parts, buds, and exudates, has gained attention due to its potent biological activities. Its chemical composition varies depending on climates and geographical origin but is generally rich in polyphenols and flavonoids, which are responsible for its antimicrobial properties. In recent years, the use of natural antimicrobial agents has become increasingly important. Furthermore, because nanoparticles may pass through bacteria and bacterial biofilms, they may be a useful tool for limiting the spread of bacterial infections [5]. The goal of this study was to evaluate the enhanced antimicrobial efficacy of propolis-loaded solid lipid nanoparticles (LNPs-PL) against methicillin-resistant Staphylococcus aureus (MRSA) isolated from raw beef, and to compare its performance with free propolis.

Results

Prevalence of MRSA in raw beef samples

The microbiological analysis of 112 raw beef collected From different markets in Wasit city during the summer season revealed that four (MRSA) isolates, were detected from the pooled samples from different brand and locations. 50 samples (44.6 %) were positive for *S. aureus,* and among these, 20 isolates (40%) were confirmed as MRSA (Table 1, and figure 1). Also the Conventional PCR screening revealed that all the isolates were positive for intrinsic methicillin resistance (mecA) gene, producing a 163 bp amplicon (Figure 2).

Preparation and Characteristics of LNPs-PL

DLS analysis

Particle Size and Morphology

Dynamic light scattering (DLS) analysis revealed an increase in nanoparticle size from 204.16 nm to 244 nm after loading with propolis extract, confirming successful encapsulation. The SEM image of LNPs-PL

Table 1.
Prevalence of MRSA in Raw Beef Samples (n=112)

Sample Type	Total Samples (N)	*S. aureus* Positive (%)	MRSA Positive (%) (95% CI)
Raw Beef	112	50 (44.6 ± 4.7%)	20/50 (40.0 ± 6.9%)

Data analyzed by Chi-square test; $p < 0.05$
S. aureus prevalence calculated as (positive samples/N) × 100.

Figure 1.
Methicillin-Resistant *S. aureus* (MRSA) on HiCrome MeReSa Agar Base medium

Abbreviations-Cont'd

SEM: Scanning electron microscopy
GC-MS: Gas Chromatography-Mass Spectrometry
EE: Encapsulation efficiency
LC: Loading capacity
ICMSF: The International Commission on Microbiological Specification for Foods
ATCC: The American Type Culture Collection
UV–Vis: Ultraviolet–visible spectrophotometry
Au–Pd: Gold-Palladium
DSC: Differential Scanning Calorimetry
MHA: Mueller-Hinton agar
ANOVA: Analysis of Variance
PCR: Polymerase Chain Reaction
PDI: Polydispersity Index
mV: millivolt
HERP: Hydroethanolic extract of red propolis
PLGA: Poly(lactic-co-glycolic acid)
MIC: Minimum Inhibitory Concentration
3D: A three-dimensional

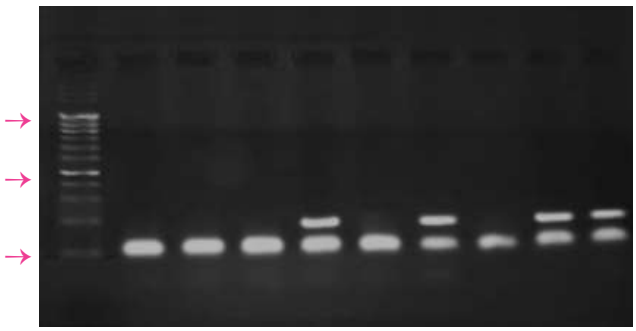

Figure 2.
Agarose gel electrophoresis image shows PCR product analysis of *S. aureus*. Lane M Marker ladder (50-1000bp), lanes (1-10): mecA gene of *S. aureus* isolate with 163bp.

is displayed in Figure 3. SEM scan revealed that the nanoparticles were spherical in shape.

Polydispersity Index (PDI)

The PDI values provide critical insights into the size distribution and homogeneity of the nanoparticle populations. A PDI of 0.421 for the free LNPs (Figure 3) suggests a moderately broad size distribution, indicating some variability in particle size. Conversely, a PDI of 0.277 for the LNPs-PL (Figure 4) indicates a more homogeneous and uniform size distribution compared to the free LNPs. This suggests that the incorporation of propolis extract has contributed to a more uniform population of nanoparticles. Generally, a PDI below 0.3 is considered acceptable for pharmaceutical applications, indicating a relatively homogeneous population. The figures 4, 5 and 6 representation clearly demonstrates the size increase post propolis loading. The peak corresponding to LNPs-PL is shifted to the right, indicating a larger size compared to the free LNPs. The narrower peak width for LNPs-PL, which is consistent with the lower PDI value, suggests a more uniform size distribution. Additionally, the presence of a small peak at the higher size range in the LNPs-PL sample indicates the aggregation of a minor fraction of the nanoparticles. In summary, the data suggests that the incorporation of propolis extract into the lipid nanoparticles has resulted in a size increase and a more uniform particle size distribution. The lower PDI value for LNPs-PL supports the notion of enhanced homogeneity, which is advantageous for pharmaceutical applications. The size distribution data, corroborated by the intensity graph, further validates these findings.

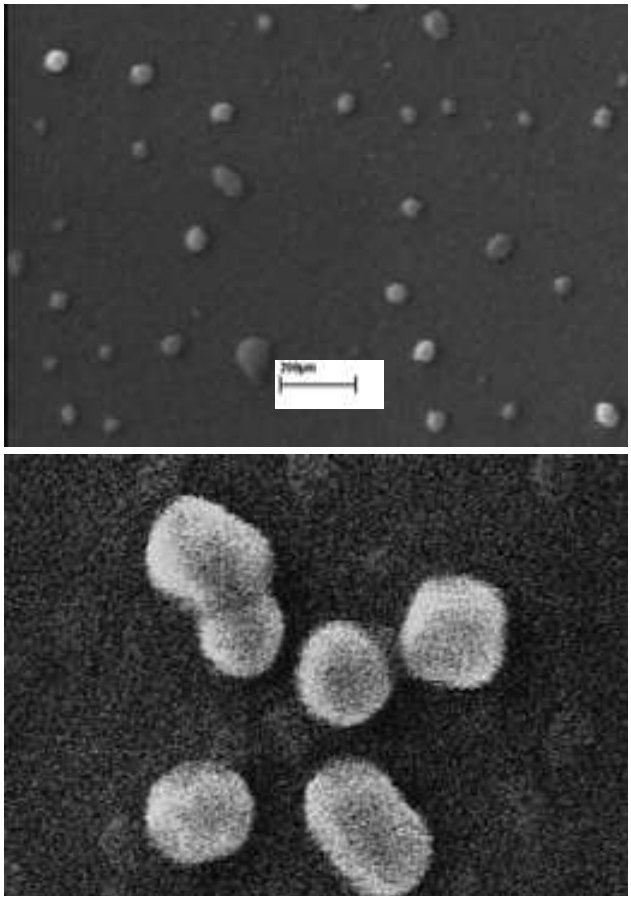

Figure 3.
Appearance of LNPs-PL under scanning electron microscopy(SEM image of LNPs-PL at 50,000× magnification. Scale bar: 200 nm)

Zeta Potential

The zeta potential of the lipid nanoparticles becomes more negative and shifted from -36.7 mV to -50.7 mV after loading with propolis extract. This increase in negative surface charge indicates a significant alteration in the surface properties of the nanoparticles. The propolis extract likely contributed negatively charged components to the nanoparticle surface, and thus enhanced the overall negative charge.

The antimicrobial activity of LNPs-PL

According to the antimicrobial activity data, LNPs-PL exhibited 74%, inhibition on the growth of MRSA. In addition, LNPs-PL exhibited significantly higher antibacterial activity against tested microorganisms compared to free PL. The inhibition zone for LNPs-PL was 36.0 ± 1.2 mm, while free propolis showed only 14.0 ± 0.8 mm (Table 2 and Figure 7). The 2.6-fold larger inhibition zones of LNPs-PL ($p < 0.001$, Cohen's d = 3.2) confirm not just statistical but practical superiority over free propolis.

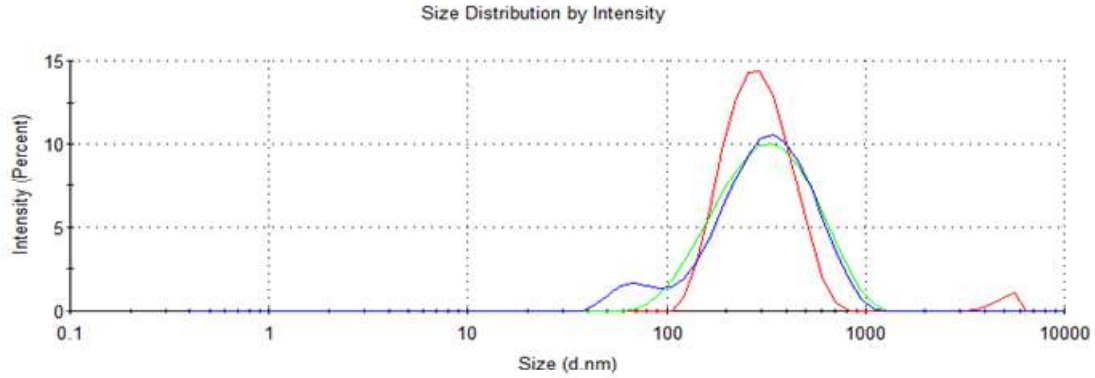

Figure 4.
(PDI) to LNPs (Size distribution profile of free LNPs showing polydispersity index (PDI = 0.421).

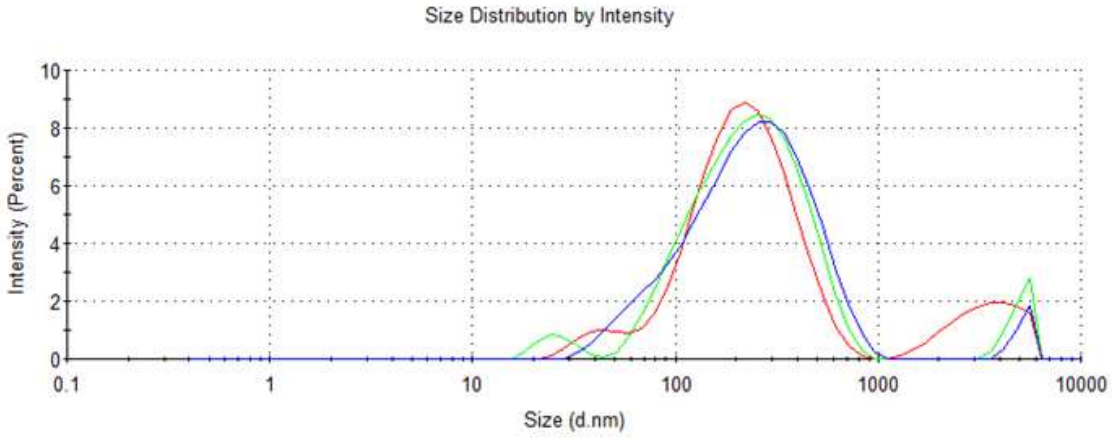

Figure 5.
(PDI) LNPs-PL (Size distribution profile of LNPs-PL showing improved homogeneity (PDI = 0.277).

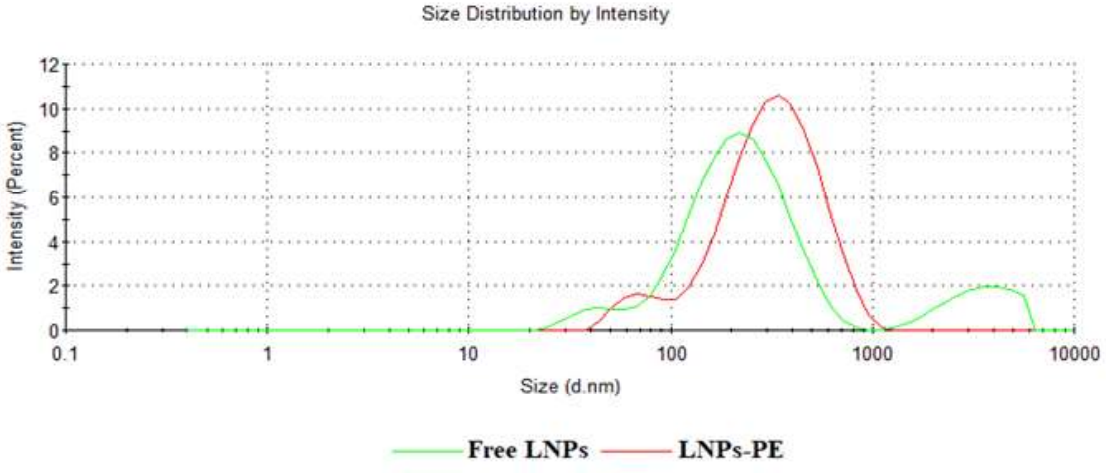

Figure 6.
LNPs-PL (Intensity-based particle size distribution of LNPs-PL demonstrating increased average hydrodynamic diameter post-propolis loading).

Table 2.
Antimicrobial Activity of LNPs-PL vs. Controls

Treatment	Zone of Inhibition (mm, Mean ± SD)	p-value (vs. PL)	Statistical Test
LNPs-PL	36.0 ± 1.2**	<0.01	One-way ANOVA
Propolis (PL)	14.0 ± 0.8	—	(Tukey's post-hoc)
Empty SLNs	0 (no activity)	—	

Data represent mean ± standard deviation of triplicate experiments.
Asterisk (**) indicates statistical significance ($p < 0.01$) vs. PL.
ANOVA assumptions (normality, homogeneity of variance) were verified.

Figure 7.
Inhibition zone as shown by LNPs-PL and regular PL on MRSA

Discussion

In this study, we aimed to compare the antimicrobial activity of propolis-loaded solid lipid nanoparticles (LNPs-PL) with that of free propolis against MRSA isolated from raw beef.

The high prevalence of MRSA in raw beef observed in this study suggests contamination from multiple sources, including infected animals and improper handling during slaughtering and processing (animal meat or workers who handled these meat may carried these bacteria as normal flora in their nasal cavity and their skin). These findings are consistent with previous studies reporting contamination sources. Scott et.al [6], reported that the meat can be contaminated with *S. aureus* during manufacture and handling. Waters et.al [7] reported a high prevalence of S. aureus isolated from fresh bovine meat, and Porpino et.al [8], reported that contamination of meat may occur through the different stages of food preparation as production, distribution, storage in the retailing supermarkets and during improper refrigeration temperature, as a results an enhance in bacterial growth can occur, leading to productions of enterotoxins. In the study done by Mohammed et.al, reported that food handlers who work with meat also can be the sourse of meat contamination by *S. aureus* [9].

This size augmentation implies that the propolis extract has been effectively integrated into the lipid matrix or adsorbed onto the surface of the LNPs. Such an increase is anticipated and confirms the presence of the propolis extract within the nanoparticle system [10].

The SEM scan revealed that the prepared SLNs had a spherical shape. Particle size distribution was similar to DLS. After loading, the nanocapsules had a spherical form, high dispersion, and a limited size distribution [11].

Because of their spherical morphology, the SLNs have the finest ability to have controlled release and to protect against encapsulated essential oil. This is because, compared to other types of nanoparticles, the spherical shape has the lowest contact surface with the aqueous medium of the dispersed phase and a longer path for the essential oil contained in the nanoparticles to flow [12].

Zeta potential is a critical parameter in assessing the stability of colloidal dispersions. Typically, zeta potential values exceeding +30 mV or below -30 mV are indicative of good colloidal stability, as the electrostatic repulsion between particles mitigates aggregation. Based on this, in the current study both the free LNPs and LNPs-PL exhibited zeta potential values within this range. Notably, the more negative zeta potential of the LNPs-PL (-50.7 mV) implies even greater stability compared to the free LNPs. This enhanced stability can be attributed to the additional negatively charged components provided by the propolis extract, which increase electrostatic repulsion and prevent particle aggregation [13, 14].

The significantly higher antimicrobial activity of LNPs-PL, in this study and in the study done by Jaiswal et.al [15], compared to free propolis can be attributed to improved growth inhibition of the tested bacteria, even at lower concentrations. The may be because the

PL is efficiently delivered by the vehicle (SLNs) and had better interaction with the bacteria [16].

Some of its constituents appear to be connected to the mechanism of propolis' antimicrobial action. Propolis's combination activity, which inhibits protein synthesis and bacterial growth by stopping cell division, is linked to its strong bacteriostatic and bactericidal actions [17]. Propolis contains high concentration of flavonoids, such as galangin, pinocembrin, and pinobanksin, which contribute to its antimicrobial (antibacterial and fungicidal) properties. These compounds may be the primary cause of the Propolis activity. For example, galangin and caffeic acids, two enzymatic inhibitory agent, are in charge of preventing the growth and multiplication of bacteria. Furthermore, several of the active ingredients in propolis have the potential to partially bacteriolyze the cell wall and cytoplasmic membrane. Flavonoids alter the permeability of the inner membrane of microorganisms and have an impact on the bacterial membrane potential [18]. Because smaller particles have better penetration and are therefore more effective, PNs' antimicrobial activity is validated. Johnson et.al [19] examined the impact of PLGA nanoparticles containing a hydroethanolic extract of red propolis (HERP) (PLG-AHERP-NPs) on the breakdown of harmful biofilms. According to this research, PLG-AHERP-NPs outperformed gram-positive bacteria in terms of MIC and biofilm formation. Variable cell wall and membrane structure in organisms can be linked to this discrepancy [19]. We mean the ingredients of propolis, specifically the flavonoids and polyphenols (such as galangin, pinocembrin, pinobanksin, and caffeic acids) that are naturally present in propolis.We do not mean adding extra or external chemicals. We mean that when propolis is loaded into nanoparticles, its natural active ingredients (flavonoids and polyphenols) are delivered more effectively, which enhances antibacterial activity.

It is also useful against abnormalities of the mouth, particularly dental problems. Propolis's polyphenols and flavonoids interact with a variety of microbial proteins to establish ionic and hydrogen connections, changing the protein's three-dimensional (3D) structure and, its function [20]. Consequently, in comparison to propolis, the addition of these chemicals in propolis nanoparticles can enhance their ability to prevent bacterial growth.

Materials & Methods

Declaration on AI use

The authors declare that no artificial intelligence (AI)-assisted technologies were used in the preparation, writing, editing, data analysis, or illustration of this manuscript.

Meat Sampling Technique

In the present research, a systematic and extensive sampling protocol was employed to examine the contamination of S. aureus and MRSA in raw beef. A total of 112 beef samples (500 g each) were collected aseptically from the boneless outer surfaces of shoulder muscles (n=56) and thigh muscles (n=56). The samples were collected from randomly chosen carcasses in three main slaughterhouses and ten licensed retail butchers across Wasit City, Iraq, to ensure proper representation of both the production and consumer points. Sampling was randomized and occurred over spring and summer periods (April to October 2024) to provide for potential temperature-dependent microbial variation, using sterile knives and pre-labeled polyethylene bags to prevent cross-contamination. The samples were transported to the laboratory in insulated iceboxes at 4 °C and processed within 6 hours to promote microbial viability. Prior to analysis, the samples were all aseptically trimmed of fat and connective tissue and homogenized in 0.1% peptone water for microorganism enumeration. To validate the integrity of sampling, negative controls (sterile swabs/blank peptone water) and positive controls (ATCC 43300 MRSA and ATCC 25923 S. aureus) were run in parallel.

This protocol, standardised in accordance with ICMSF (2002) guidelines, enabled the detection of MRSA prevalence that was statistically significant with control of confounding variables by randomisation and stratification by anatomical cut and source (60% abattoir/40% retail). Strength in the methodology provides confidence in follow-on antimicrobial efficacy testing of propolis nanoparticles on isolated MRSA strains.

Isolation of S.aureus

The bacteria were cultured on a variety of media, such as mannitol salt agar, MacConkey agar, and blood agar, which is specific to *S. aureus*. Isolated bacteria were identified based on colony morphological shape, size, colour, and pigment synthesis after incubating the samples at 37˚C for 24 hours.

Propolis exhaustive extraction (PL)

Frozen propolis samples were first put through a drying procedure in a dark environment kept at a certain temperature of 60 °C. This drying step was crucial to remove moisture content while preserving the bioactive compounds within the propolis. Following the drying process, the propolis was finely milled to obtain a uniform powder weighing 100 g. This powder was then homogenized in 100 ml of 70% ethanol, ensuring thorough mixing and extraction of the bioactive constituents. The homogenization process was allowed to proceed for 48 hours, facilitating the efficient extraction of bioactive compounds into the ethanol solvent. After the 48 hours extraction period, the homogenized sample was subjected to sonication to further enhance the extraction efficiency by disrupting cell walls and releasing intracellular contents. The sonicated mixture was then centrifuged at 10,000 rpm for 10 min to separate the solid residues from the liquid extract. The resulting supernatant was carefully filtered through Whatman No. 2 filter paper to remove any remaining particulate matter. The filtered extract was then concentrated using rotary evaporation at 60 °C, a step designed to remove the ethanol solvent and concentrate the bioactive compounds. The concentrated extracts were subsequently lyophilized, a freeze-drying process that removes water content while preserving the integrity and activity of the bioactive compounds. The final lyophilized extract, weighing 20 g, was carefully weighed and stored at 4 °C in a desiccator to prevent moisture absorption and degradation. This meticulously prepared dried extract was then stored under controlled conditions until it was required for further experimental analyses, this way the stability and consistency of the bioactive components for subsequent research applications was ensured [21].

Characterization of LNPs-PL

Particle size and zeta potential

The dynamic light scattering method (ZetaSizer Nano-ZS) was used to evaluate the SLNs formulations for particle size, polydispersity index, and zeta potential [22].

Determination of Encapsulation and Loading Efficiency

The percentage of the total amount of PL that was obtained in the formulation at the end of the process is known as the encapsulation efficiency (EE). The loading capacity (LC) was calculated by dividing the entrapped PL mass by the lipid (stearic acid) total mass. The EE and LC were calculated. Following careful weighing, 10 mg of LNPs-PL formulations were dissolved in 10 ml of methanol, and then centrifuged at 9,000 rpm for 30 minutes. The amount of PL in the supernatant was measured at 274 nm using a UV–Vis spectrophotometer (T80+ UV/VIS Spectrophotometer, PG Instruments Ltd.). To calculate the percentage of PL, a calibration curve was developed using a range of pure garlic oil concentrations. Measurements of each concentration was repeated for three times.

The sormula for calculation of the loading and encapsulation efficiency comes as follows:

$$A-B/A \times 100 = \%EE, \text{ and } A-B/C \times 100 = \%LC$$

Where:

A: The percentage of GO that was added to the formulation overall.

B: The supernatant's measured GO content.

C: The formulation's total weight of lipid (1% w/w stearic acid).

Morphology Study

The morphology of the nanoparticles has been examined using scanning electron microscopy (SEM). A thin layer of Au-Pd was sputter coated onto the nanoparticles, which were then placed on aluminum stubs and analyzed using a scanning electron microscope (SEM XL30, Philips, Netherlands) [23].

Differential scanning calorimetry (DSC)

For PL and LNPs-PL DSC scans, a Mettler DSC 821e (Mettler Toledo, Germany) was used. Five milligrams of the samples were put into pans made of aluminum oxide, sealed, and then examined. An empty aluminum pan served as a guide. The melting point of SLN dispersions was compared to that of the bulk lipid using DSC, which was carried out at a rate of 5 °C/min under N2 flow in a temperature range of 25 to 250 °C [24].

The antimicrobial activity of LNPs-PL

Mueller-Hinton agar (MHA) was the culture medium that was used for bacterial culture grow, also *S. aureus* was cultivated on mannitol salt agar. The well diffusion method was used to assess the antimicrobial activity of the tested compounds on MHA and mannitol salt agar. In the solid agar medium, 8 mm-diameter wells were made. 100 µL aliquots of every tested formulation were introduced into the wells. Using a metal caliper, the diameter of the zone of inhibition was measured and recorded in millimeters following a 24-hour stay in the incubator. The experiment was repeated for three times for each bacterium. The average zone of inhibition has been determined for each test LNPs-PL and the regular PL [25].

Statistical analysis

One-way ANOVA and Tukey's post-hoc test for inhibition zones were used to examine the data, and unpaired t-tests was used for microbial counts (α=0.05). Proportions (e.g., MRSA prevalence) included 95% Wilson score confidence intervals. All tests assumed normality ($p > 0.05$, Shapiro-Wilk) and equal variance (Levene's test).

Authors' Contributions

Conceptualization and study design, Data analysis and interpretation: AS, JA.

Methodology and laboratory work: JA, BJM.

Writing – original draft: JA.

Writing – review & editing, Supervision and project administration, Resources and ethical coordination: AS, BJM.

Acknowledgements

The authors sincerely thank the Department of Food Hygiene and Aquaculture, Faculty of Veterinary Medicine, Ferdowsi University of Mashhad, Iran, for providing laboratory facilities and technical support. Special thanks are extended to Ms. Samira Khajenasiri, for her technical assistance during the experimental phase of this study.

Conflict of interest

The authors declare that they have no conflicts of interest.

References

1. Ajayeoba TA, Kaka OM, Ajibade OA. Microbial food spoilage of selected food and food products. Food Sci Technol: Fundam Innov. 2023;173:1–15. Doi:10.1515/9783110667462-007.

2. Singh I, Roshan M, Vats A, Behera M, Gautam D, Rajput S, et al. Evaluation of Virulence, Antimicrobial Resistance and Biofilm Forming Potential of Methicillin-Resistant Staphylococcus aureus (MRSA) Isolates from Bovine Suspected with Mastitis. Current Microbiology. 2023;80(6):198. Doi:10.1007/s00284-023-03303-2

3. McClements DJ, Barrangou R, Hill C, Kokini JL, Lila MA, Meyer AS, et al. Building a resilient, sustainable, and healthier food supply through innovation and technology. Annual Review of Food Science and Technology. 2021;12(1):1-28. Doi:10.1146/annurev-food-092220-030824.

4. Sadiq A, Samad M, Saddam, Basharat N, Ali S, Roohullah, et al. Methicillin-resistant Staphylococcus aureus (MRSA) in slaughter houses and meat shops in capital territory of Pakistan during 2018–2019. Frontiers in Microbiology. 2020;11:577707. Doi:10.3389/fmicb.2020.577707.

5. Silva H, et al. The cardiovascular therapeutic potential of propolis—A comprehensive review. Biology. 2021;10(1):27. Doi:10.3390/biology10010027.

6. Scott RJ, Lian LY, Muharram SH, Cockayne A, Wood SJ, Bycroft BW, et al. Side-chain-to-tail thiolactone peptide inhibitors of the staphylococcal quorum-sensing system. Bioorganic & Medicinal Chemistry Letters. 2013;23(15):2449–2453. Doi:10.1016/j.bmcl.2013.03.018

7. Waters AE, Contente-Cuomo T, Buchhagen J, Liu CM, Watson L, Pearce K, et al. Multidrug-resistant Staphylococcus aureus in US meat and poultry. Clinical Infectious Diseases. 2011;52(10):1227–1230. Doi:10.1093/cid/cir181.

8. Porpino G, Parente J, Wansink B. Food waste paradox: antecedents of food disposal in low income households. International Journal of Consumer Studies. 2015;39(6):619-629. Doi:10.1111/ijcs.12207.

9. Mohammed NI, Alwan MJ. Isolation and Identification of Staphylococcus aureus strain from fresh and frozen meat in Karbala province. International Journal of Science and Nature. 2017;8(3):704-709. Doi:10.53730/ijhs.v6nS9.12222.

10. Ibrahim SS, Salem NY, Abd ElNaby SSI, Adel MM. Characterization of Nanoparticles Loaded with Garlic Essential Oil and Their Insecticidal Activity Against Phthorimaea Operculella (Zeller) (PTM) (Lepidoptera: Gelechiidae). International Journal of Nanoscience and Nanotechnology. 2021;17(3):147-160.

11. Layegh P, Mosallaei N, Bagheri D, Jaafari MR, Golmohammadzadeh S. The efficacy of Isotretinoin loaded solid lipid nanoparticles in comparison to Isotrex® on acne treatment. Nanomedicine Journal. 2013;1:41-51. Doi:10.7508/nmj.2013.01.005.

12. Wencui Z, Qi W, Ying W, D W. Preparation of solid lipid nanoparticles loaded with garlic oil and evaluation of their in vitro and in vivo characteristics. Eur Rev Med Pharmacol Sci. 2015;19:3742–3750. Doi:10.31083/j.fbl2807135

13. Efferth T, Koch E. Complex Interactions between Phytochemicals: The multi-target therapeutic concept of phytotherapy. Current Drug Targets. 2011;12(1):122-132. Doi:10.2174/138945011793591626.

14. Singh M, Singh S, Salgar AR, Prathibha N, Chandrahari N, Swapna LA. An in vitro comparative evaluation of antimicrobial efficacy of propolis, Morinda citrifolia Juice, sodium hypochlorite and chlorhexidine on Enterococcus faecalis and Candida albicans. Journal of Contemporary Dental Practice. 2020;20:40–45. Doi:10.5005/jp-journals-10024-2473.

15. Jaiswal N, Sinha DJ, Singh UP, Singh K, Jandial UA, Goel S. Evaluation of antibacterial efficacy of Chitosan, Chlorhexidine, Propolis and Sodium hypochlorite on Enterococcus faecalis biofilm: An in vitro study. Journal of Clinical and Experimental Dentistry. 2021;9:e1066–e1074. Doi:10.4317/jced.53777.

16. Valera MC, da Rosa JA, Maekawa LE, de Oliveira LD, Carvalh OCA, Koga-Ito CY, et al. Action of propolis and medications against MRSA bacteria and endotoxin in root canals. Oral Surgery, Oral Medicine, Oral Pathology, Oral Radiology, and Endodontology. 2020;110:e70–e74. Doi:Doi:10.1016/j.tripleo.2020.01.029.

17. Park YK, Alencar SM, Aguiar CL. Botanical origin and chemical composition of Brazilian propolis. J Agric Food Chem. 2002;50:2502–2506. Doi:10.1021/jf011432b.

18. Awawdeh L, Jamleh A, Al-Beitawi M. The Antifungal Effect of Propolis Endodontic Irrigant with Three Other Irrigation Solutions in Presence and Absence of Smear Layer: An In Vitro Study. Iranian Endodontic Journal. 2018;13(2):234–239. Doi:10.22037/iej.v13i2.19227.

19. Johnson M, Olaleye ON, Kolawole OS. Antimicrobial and antioxidant properties of propolis extract against S. aureus and Pseudomonas aeruginosa. Br Microbiol Res J. 2016;14:1–11.

20. Bueno-Silva B, Marsola A, Ikegaki M, Alencar SM, Rosalen PL. The effect of seasons on Brazilian red propolis and its botanical source: Chemical composition and antibacterial activity. Natural Product Research. 2017;31:1318–1324.

21. Shin SB, Lee JK, Ko MJ. Enhanced extraction of bioactive compounds from propolis (Apis mellifera L.) using subcritical water. Scientific Reports. 2023;13:15038. Doi:10.1038/s41598-023-42418-1.

22. Mader K, Mehnert W. Solid lipid nanoparticles concepts, procedures and physicochemical aspects. In: Nastruzzi C, editor. Lipospheres in drug targets and delivery. Florida: CRC Press; 2005. p. 1-22. Doi:10.1002/chin.200536286.

23. Jourghanian P, Ghaffari S, Ardjmand M, Haghighat S, Mohammadnejad M. Sustained Release Curcumin Loaded Solid Lipid Nanoparticles. Advanced Pharmaceutical Bulletin. 2016;6(1):17-21. Doi:10.15171/apb.2016.04.

24. Mosallaei N, Jaafari MR, Hanafi-Bojd MY, Golmohammadzadeh S, Malaekeh-Nikouei B. Docetaxel Loaded solid lipid nanoparticles: preparation, characterization, In vitro, and In vivo Evaluations. Journal of Pharmaceutical Sciences. 2013;102:1–10. Doi:10.1002/jps.23522.

25. Al-Qushawi A, Rassouli A, Atyabi F, Peighambari SM, Esfandyari-Manesh M, Shams GR, et al. Preparation and Characterization of Three Tilmicosin-loaded Lipid Nanoparticles: Physicochemical Properties and in-vitro Antibacterial Activities. Iranian Journal of Pharmaceutical Research. 2016;15(4):663-676.

How to cite this article
Alhashimi J, Salari A, Jasim Mohammed B.. TEnhanced Antimicrobial Efficacy of Propolis Solid Lipid Nanoparticles Against Methicillin-Resistant Staphylococcus aureus Isolated from Raw beef. Iran J Vet Sci Technol.2026; 18(2): 36-44.
DOI: https://doi.org/10.22067/ijvst.2025.94414.1574
URL: https://ijvst.um.ac.ir/article_47639.html

Iranian Journal of Veterinary Science and Technology

Received: 2026- Jan- 24
Accepted after revision: 2026- Feb-20
Published online: 2026- Feb-21

RESEARCH ARTICLE

DOI:10.22067/ijvst.2026.97504.1637

Technological and Sensory Characterization of Yogurt Produced with Lactic Acid Bacteria Isolated from Traditional Yogurt of Eastern Afghanistan

Sayed Attaul Haq Banuree, Abdollah Jamshidi, Amir Salari

Department of Food Hygiene and Aquaculture, Faculty of Veterinary Medicine, Ferdowsis University of Mashhad, Iran.

ABSTRACT

Traditional fermented yogurts represent an important source of indigenous lactic acid bacteria (LAB) with desirable technological, sensory, and health promising properties. However, the technological potential of LAB from Afghan traditional yoghurt remains largely unexplored. This study aimed to assess the technological and sensory attributes of LAB isolated from Afghan traditional yogurts. In this sense, four safe LAB strains, which were isolated from Afghan traditional yogurt, were used in the production of yogurts. The final product then were subjected to technological and sensory examinations through strain and product-based tests, and compared with commercial control yogurt. The results showed that all LAB isolates were positive for amylolytic activity and showed different responses to exopolysaccharide (EPS) production. All strains, particularly Pediococcus acidilactici (NSG2), showed a better response in terms of acidifying activities, reduced pH, titratable acidity, and reduced syneresis compared to the control ($p < 0.05$). The texture parameters of all four strains were significantly different, except the stiffness of yogurt compared to the control group ($p < 0.05$). Sensory evaluation by both expert and consumer panels indicated that yogurt produced with indigenous LAB isolated from Afghan yogurt samples showed superior aroma, texture, flavor, and overall acceptability. In conclusion, all isolates from Afghan traditional yogurt, particularly NSG2, showed outstanding technological and sensory attributes, reflecting their potential for industrial use.

Keywords

Lactic Acid Bacteria, Technological Properties, Sensory Attributes, Traditional Yogurt, Afghanistan

Number of Figures: 7
Number of Tables: 6
Number of References:: 33
Number of Pages: 14

Abbreviations

ANOVA: Analysis of Variance
CFU: Colony Forming Unit
EPS: Exopolysaccharide
LAB: Lactic Acid Bacteria

Corresponding author: Abdollah Jamshidi.
Email: ajamshid@um.ac.ir
Tel: +98(51)3880-5607

Introduction

Yogurt is an extensively enjoyed fermented dairy product that is popular around the globe [1]. Its consumption is linked to various health benefits, including better bone health, improved gut health, reduced cardiovascular disease risk, enhanced diabetes management, boosted immunity, and alleviation of allergy symptoms [2]. According to the Codex definition, yogurt is a type of fermented milk created through the symbiotic action of Streptococcus thermophilus and Lactobacillus delbrueckii subspecies bulgaricus [3]. Moreover, yogurts may contain additional cultures such as Lactococcus lactis, Lactobacillus casei, or various species of Bifidobacterium. In such instances, the product is classified as yogurt with added bacteria. The primary microorganisms found in yogurt belong to Lactic Acid Bacteria (LAB), which ferment lactose, the natural sugar in milk, into lactic acid [4]. Numerous studies have been carried out that have identified different LAB from naturally fermented milk products, with Lactococcus lactis subsp. cremoris and Lactococcus lactis subsp. lactis being the predominant microbiota, along with other mesophilic lactobacilli (Lactobacillus casei/Lactobacillus paracasei, Lactobacillus plantarum, Lactobacillus helveticus, Lactobacillus fermentum, or Lactobacillus acidophilus), Enterococcus faecium, Leuconostoc species, and Pedococcus [5].

The quality of yogurt is influenced by different factors, including the type and composition of the milk used, the fermentation kinetics, acidification rates, the starter cultures used, and the post-production handling and storage practices. These variables work together to define the final physicochemical, rheological, and sensory characteristics of the yogurt [6]. Even when using the commercial starter cultures Streptococcus thermophilus and Lactobacillus delbrueckii subsp. bulgaricus, the modification or inclusion of different LAB strains can alter the characteristics of yogurt, as these strains differ in their acidification processes and their capacity to generate structure-forming metabolites, especially exopolysaccharides (EPS) [7]. Experimental evidence highlights that the choice of cultures significantly impacts the final product. Yogurt cultures can improve structural stability and minimize syneresis. At the same time, adjunct/probiotic LAB (such as Lactiplantibacillus plantarum 299v or Lactobacillus acidophilus La-5) can enhance gel firmness and/or increase acidification depending on the strain and matrix. Consequently, mixed-culture systems are frequently employed to achieve an optimal balance between texture, stability, and sensory acceptance [8].

Traditional yogurt, harbor a wide variety and dense number of indigenous microbiotas, primarily consisting of LAB, which contribute unique sensory characteristics to the food. These microorganisms play a significant and well-documented role in the nutritional and dietary qualities of the product, influenced by types of mammalian milk used (e.g., cow, sheep, or goat), diverse microbial patterns, and various production techniques employed [9]. Furthermore, the acidity levels, flavor development, and texture of yogurt are directly affected by the starter culture's characteristics. While various commercial starter cultures, are available globally, they may not always accurately replicate the physicochemical and sensory attributes of traditional starter cultures in the final product. Moreover, one major risk associated with using a single starter culture for continuous yogurt production is bacteriophage contamination. Therefore, it's crucial to identify new and wild yogurt starters that possess different technological characteristics from local traditional yogurts to broaden the availability of yogurt starter cultures and improve the technological features of yogurt while maintaining traditional organoleptic qualities [10]. In this context, traditional Afghan yogurt represents a valuable opportunity for discovering new and wild cultures, particularly LAB. However, no published research currently details and assesses the various properties of LAB isolated from Afghan yogurt, particularly produced in the Eastern region of Afghanistan. Consequently, this study represents the first investigation into the technological and sensory characteristics of different LAB isolated from Afghan traditional yogurt.

Abbreviations-Cont'd

MCT: Multiple Comparison Test
MRS: de Man-Rogasa-Sharpe
PC: Principal Component
PCA: Principal Component Analysis
TA:Titratable Acidity

Results

The results of this study are presented by distinguishing between the strain-based functional characteristics of LAB and the technological and sensory attributes of the yogurts produced from these strains.

Strain-based characteristics

Amylolytic activity and exopolysaccharide production

The amylolytic activity and EPS production of the selected LAB strains are presented in Table 1. All strains showed positive amylolytic activity. Regarding EPS production, strain-dependent differences were observed depending on the carbohydrate source. KSK1 exhibited positive EPS production in the pres-

Table 1.
Amylolytic activity and EPS production of the selected isolates.

Strain	Variable				
	Amylolytic activity	EPS production			
		Lactose	Fructose	**Glucose**	**Sucrose**
KSK1	Positive	Positive	Positive	Positive	Positive
LAG2	Positive	Positive	Positive	Negative	Negative
NW2	Positive	Negative	Negative	Negative	Negative
NSG2	Positive	Negative	Negative	Negative	Negative

ence of lactose, fructose, glucose, and sucrose, while LAG2 produced EPS when grown on lactose and fructose but not on glucose or sucrose. In contrast, NW2 and NSG2 did not show EPS production with any of the tested carbohydrates.

Acidification activity

The acidification activity of the selected LAB strains was evaluated over a 24-hour incubation period, as shown in Figure 1. At the initial time point (0 h), no significant differences were observed among the strains, with initial pH values ranging from 6.51 to 6.53 ($p > 0.05$). After 6 h, all strains showed a significant decrease in pH, and differences among them became statistically significant ($p < 0.05$). Additional reductions in pH were observed at 12 and 24 h. Among the tested isolates, NSG2 consistently exhibited the lowest pH values at all fermentation times after 0 h.

Product-based characteristics

Survival of Isolates

The survival of the isolates in yogurt during 28 days of refrigerated storage, are presented in Table 2. After day one, significant differences in the viability of all isolates were observed ($p < 0.05$). Over the 28-day storage period, major difference in the survival of storage was recorded for KSK1 (0.95 Log CFU/g) followed by control (0.81), NW2 (0.48), and LAG2 (0.30). In contrast, NSG2 survival rate was increased during the storage where the Log CFU/g of the isolate was increased by approximately 0.23 Log CFU/gr.

pH and titratable acidity

The results of pH values of yogurt samples produced with different LAB strains during 28 days of refrigerated storage are presented in Figure 2. On day 1, significant differences were observed among all samples ($p < 0.05$), with pH ranging from 3.93 to 4.11. These highly significant differences persisted on days 7, 14, 21, and 28 of storage ($p < 0.01$). Although all samples showed a decreasing trend throughout storage, the extent of decrease varied among strains. By day 28, pH values ranged from 3.61 to 3.84 in LAB-fermented samples, while the control sample had higher pH at 3.84.

Changes in titratable acidity (TA) of yogurt sam-

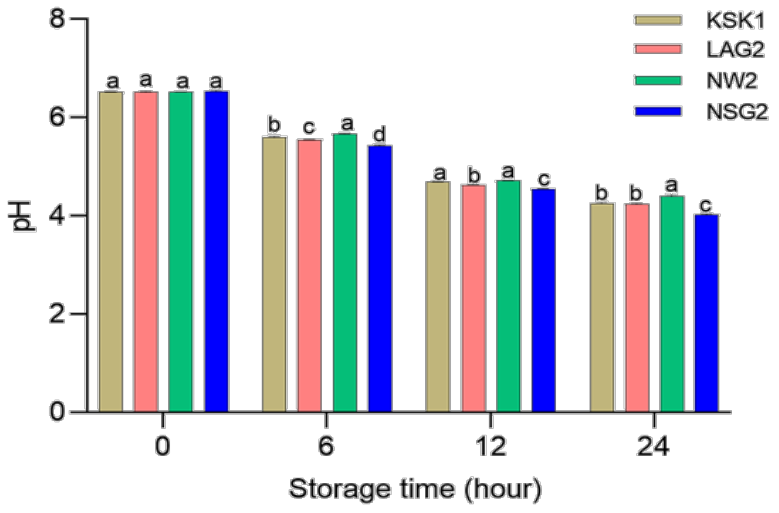

Figure 1.
Acidification activity of four selected isolates during 24 hours of storage at 37 °C.
The bars show the mean of duplicate values, and error bars represent the standard error. The data analysis showed no significant difference ($p < 0.05$), while in the subsequent storage times, a significant reduction in pH values was observed ($p < 0.05$).

Table 2.
Survival of the isolates during 28 days of refrigerated storage.

Strain	Survival (Mean±SD) *				
	Day one	7th day	14th day	21st day	28th day
KSK1	7.97 ± 0.67^{b}	8.53 ± 0.04^{c}	8.47 ± 0.03^{c}	8.08 ± 0.05^{c}	7.52 ± 0.03^{d}
LAG2	8.82 ± 0.02^{a}	9.22 ± 0.01^{a}	9.13 ± 0.03^{a}	8.85 ± 0.01^{b}	8.52 ± 0.02^{b}
NW2	8.41 ± 0.02^{ab}	8.93 ± 0.02^{b}	8.53 ± 0.03^{bc}	8.11 ± 0.02^{c}	7.93 ± 0.03^{c}
NSG2	8.62 ± 0.01^{ab}	9.22 ± 0.02^{a}	9.10 ± 0.01^{a}	8.94 ± 0.01^{a}	8.85 ± 0.05^{a}
Control	8.34 ± 0.01^{ab}	8.53 ± 0.03^{c}	8.57 ± 0.03^{b}	8.09 ± 0.02^{c}	7.53 ± 0.02^{d}

* Number in each cell represents the mean ± SD of duplicate samples.
a-d Means with different small scale alphabet superscripts in the same column are significantly different.

ples produced with different LAB strains over 28 days of refrigerated storage are presented in Figure 2 Figure 3. On day 1, titratable acidity values ranged from 0.61 to 0.69% lactic acid, and no significant differences were observed among samples ($p > 0.05$). During storage, TA increased progressively in all samples, and the difference was statistically significant in all storage days ($p < 0.05$). On day 7, 14, 21, and 28, TA values ranged from 0.66 to 0.78%, 0.73–0.85%, 0.76–0.92%, and 0.81-0.94% lactic acid, respectively.

Dry matter and syneresis

The dry matter content and syneresis of yogurt samples produced with different LAB strains during 28 days of refrigerated storage are presented in Table 3. Dry matter content differed significantly among samples ($p < 0.05$), ranging from 9.55% to 11.00%. The control sample had the highest dry matter content, while the LAB-fermented samples showed comparable values, with slight variations among strains.

Syneresis values on day 1 ranged from 13.87% to 24.05%. The control sample exhibited significantly higher syneresis compared to all LAB-fermented yogurts ($p < 0.05$). Syneresis progressively increased in all samples throughout storage, with significant differences observed among all LAB-fermented yogurts on all storage days. On day 7, syneresis values ranged from 15.27% to 27.97%. By day 14 and day 21, these values further increased to 17.87–32.42% and 19.35–39.20%, respectively. By day 28, syneresis values in LAB-fermented samples ranged from 20.47% to 26.72%, while the control sample exhibited the highest syneresis at 40.32%.

Coagulation activity

The results of the coagulation activity of yogurt samples produced with different LAB strains are presented in Table 4. Differences in coagulation time were observed among the strains. LAG2 and NSG2 exhibited rapid coagulation, occurring within 4 - 6 hours of incubation at 42 °C. KSK1 and the control sample showed intermediate coagulation activity, with coag-

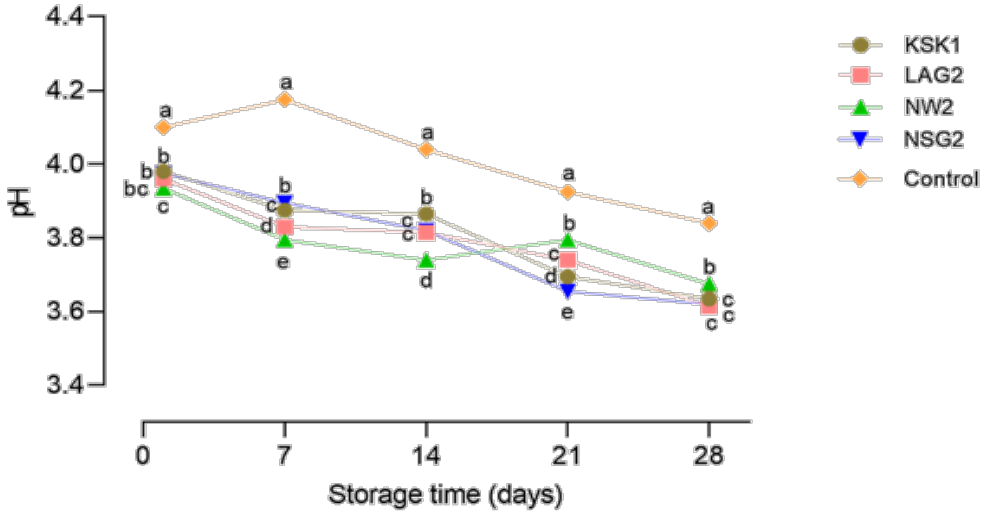

Figure 2.
pH values of different yogurt samples during 28 days of refrigerated storage.
Each symbol shows the mean of pH value calculated from duplicate samples, while the error bars show the SD. Different small alphabets in the same storage day show significant differences. The results showed significant differences among different types of yogurt in all storage days ($p < 0.05$).]

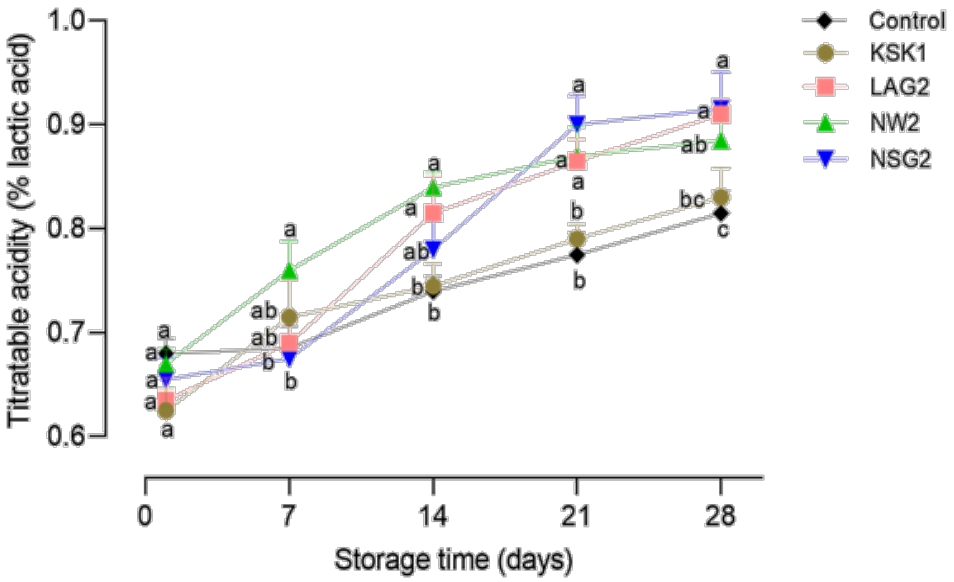

Figure 3.
Titratable acidity of different yogurt samples during 28 days of refrigerated storage.
Each symbol shows the mean of the titratable acidity value calculated from duplicate samples, while the error bars show the SD. Different small alphabets in the same storage day show significant differences. The results showed significant differences among different types of yogurts in all storage days except on day one ($p < 0.05$).]

Table 3.
Dry matter and syneresis of the produced yoghurt samples.

Strain	Dry matter	Survival (Mean±SD) *				
		Day one	7th day	14th day	21st day	28th day
KSK1	10.30 ± 0.13^{b}	14.32 ± 0.32^{c}	15.27 ± 0.25^{e}	17.87 ± 0.18^{c}	20.82 ± 0.32^{b}	22.05 ± 0.42^{d}
LAG2	9.55 ± 0.21^{c}	16.65 ± 0.28^{b}	17.57 ± 0.25^{c}	19.42 ± 0.18^{b}	19.35 ± 0.14^{c}	20.47 ± 0.32^{e}
NW2	10.50 ± 0.14^{b}	14.42 ± 0.32^{c}	18.17 ± 0.18^{b}	19.00 ± 0.28^{b}	20.55 ± 0.28^{b}	26.72 ± 0.25^{b}
NSG2	10.25 ± 0.21^{b}	13.87 ± 0.04^{c}	16.65 ± 0.14^{d}	17.95 ± 0.07^{c}	19.50 ± 0.07^{c}	23.62 ± 0.18^{c}
Control	11.00 ± 0.10^{a}	24.05 ± 0.07^{a}	27.97 ± 0.04^{a}	32.42 ± 0.25^{a}	39.20 ± 0.21^{a}	40.32 ± 0.32^{a}

* Number in each cell represents the mean ± SD of duplicate samples.
a-e Means with different small scale alphabet superscripts in the same column are significantly different.

Table 4.
Coagulation activity of LAB strains.

Strain	Coagulation*
KSK1	Intermediate
LAG2	Rapid
NW2	Slow
NSG2	Rapid
Control	Intermediate

* Rapid: 4-6 hours, Intermediate: 6-12 hours, and Slow: more than 12 hours.

ulation observed between 6 and 12 hours. In contrast, NW2 displayed slow coagulation, requiring more than 12 hours to coagulate under the same conditions.

Texture profile analysis

The findings of texture profile characteristics of yogurt samples fermented with different LAB strains are presented in Figure 4. With the exception of stiffness ($p > 0.05$), all other evaluated parameters showed significant differences among the strains ($p < 0.05$). Hardness ranged from 0.67 to 0.98 N, with higher values observed in yogurts produced with LAG2. Cohesiveness values ranged from 0.39 to 0.69, with relatively higher cohesiveness observed in the control sample (0.69) compared to most LAB-fermented samples. Springiness values were generally similar across samples, ranging from 11.01 to 14.57 mm, though yogurts fermented with LAG2 displayed higher springiness (14.57 mm) compared to the other strains. Gumminess values ranged between 0.62 and 0.72 N. Chewiness (expressed as energy) ranged from 4.88 to 5.63 mJ across all samples. Adhesiveness values ranged from 1.56 to 2.96 mJ, with higher adhesiveness observed in yogurts produced with NW2. Stiffness values, expressed as N/mm, ranged from 0.061 to 0.071.

Sensory evaluation

The sensory evaluation of the produced yogurts by the expert panel on day 7 is depicted in Figure 5.

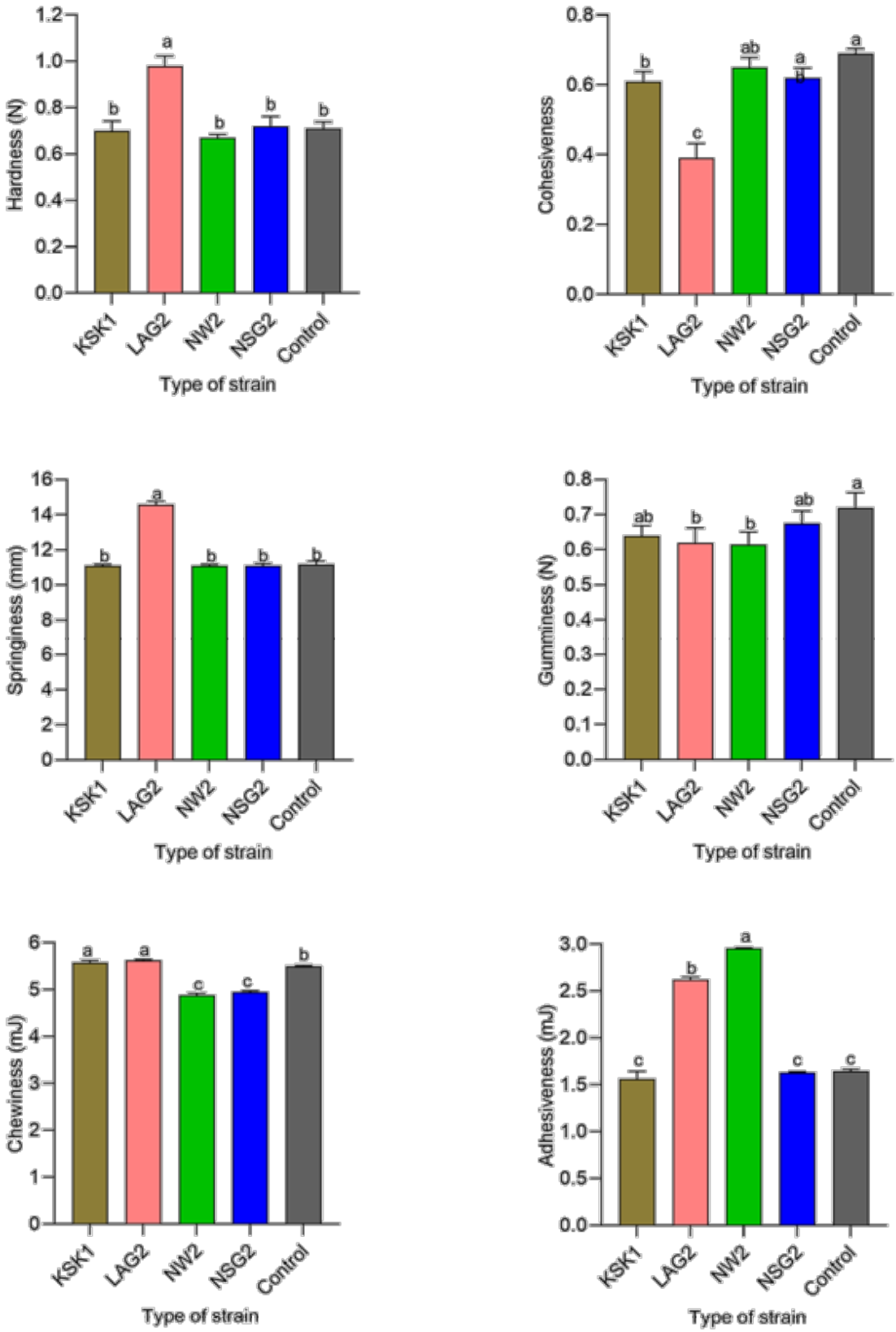

Figure 4.
Texture profile of yogurt samples produced with the isolates.
Figure 4 shows the Bars show the mean of two samples, while error bars depict the SD. Bars with different small alphabets are significantly different from each other. The results showed that all the parameters of texture profile of the yogurt samples were significantly different with each other ($p < 0.05$) except stiffness of the yogurt samples ($p > 0.05$)]

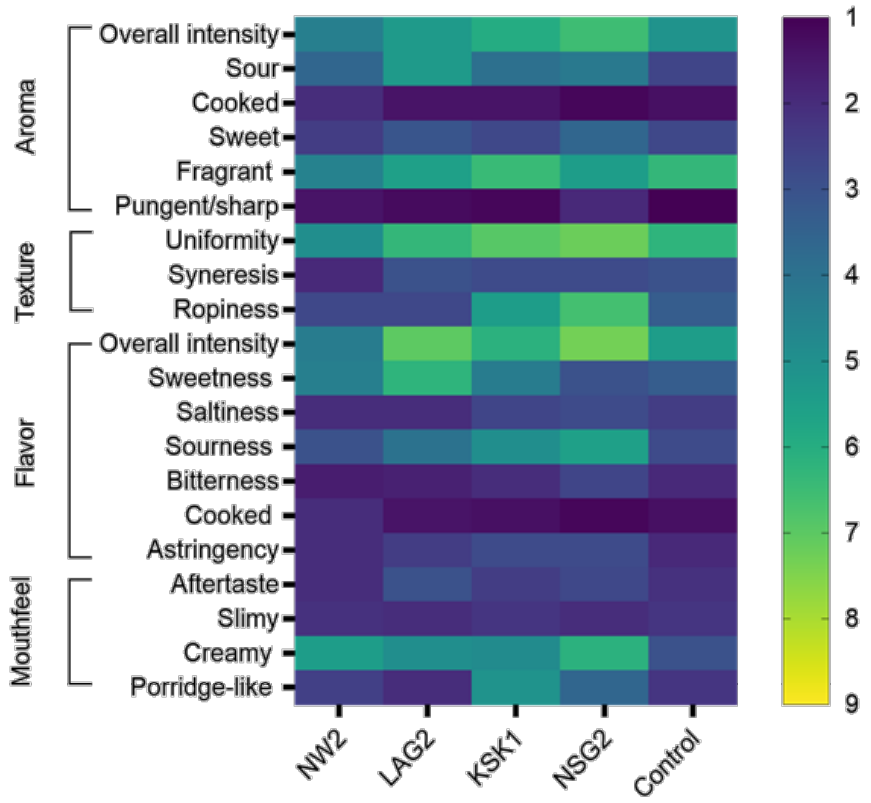

Figure 5.
Heatmap of the sensory evaluation scores by expert panel of the produced yogurt samples. Score for each attribute is the mean of 10 expert panel.

Sensory score for different attributes of the samples ranged from 1 to 7.3. NSG2 had the highest score for overall aroma intensity (6.5). For other Aroma attributes, scores were below the medium score (5) except for the fragrant attribute, where KSK1 scored highest (6.4) and NW2 lowest (4.5). Regarding texture characteristics, the high score for uniformity was reported for NSG2 (7.2), while NW2 scored lowest (4.9). Syneresis was reported with low scores for Control and LAG2 samples at 3. Ropiness was higher for NSG2 (6.6) and lower for NW2 and LAG2 (2.7). NSG2 also scored highest for overall flavor intensity (7.3), followed by LAG2 (7), KSK1 (6.1), control (5.4), and NW2 (4.3). The majority of other flavor related attributes were below the medium score (5). In terms of mouthfeel, the creamy attribute received the highest scores, with NSG2 scoring highest (6.1) and control sample lowest (3).

Principal Component Analysis (PCA) of the sensory attributes is illustrated in Figure 6. High variability (75.87%) is reported by both principal components (PC). The projection of attributes onto the factor plane indicated that, cooked and sweet flavors, cooked aroma, and slimy mouthfeel negatively influenced PC 1. Conversely, other aroma, texture, taste, and mouthfeel descriptors positively effected PC 1. On the other hand, PC 2 was positively influenced by sour, sweet, pungent, and cooked aroma, cream mouthfeel, and sweet, cooked, aftertaste, astringency, and overall intensity flavor descriptors are reported. Conversely, PC 2 was negatively influenced by mouthfeel (slimy, porridge like), aroma (fragrant, and overall intensity), flavor (bitterness and saltiness), and texture descriptors (ropiness, uniformity, and syneresis).

The PCA correlation analysis revealed a clear separation between control and treatment groups, although the distinction between LAG2 and NSG2 was not evident. LAG2 and NSG2 were characterized by sour, pungent, and sweet aroma, creamy mouthfeel, sourness, astringency, aftertaste, and overall intensity flavor descriptors. On the other hand, KSK1 was associated with texture attributes (ropiness, uniformity, and syneresis), aroma (fragrant and overall intensity), flavor (saltiness and bitterness), and mouthfeel (porridge-like). NW2 was characterized by high intensities of cooked aroma and sweet and cooked flavor. The control sample was solely intensified in slimy mouthfeel.

Consumer panel sensory evaluation scores obtained from 30-members are presented in Figure 7. NSG2 received the highest mean scores for flavor (7.35), texture (7.20), and overall acceptance of 7.15. KSK1 followed with the second-highest ratings, particularly for aroma (6.70) and texture (6.90), achieving an overall acceptance of 6.55. The control sample exhibited intermediate values with an overall acceptance of 6.40, while NW2 and LAG2 recorded the lowest scores across all attributes, both achieving an overall acceptance of 6.10.

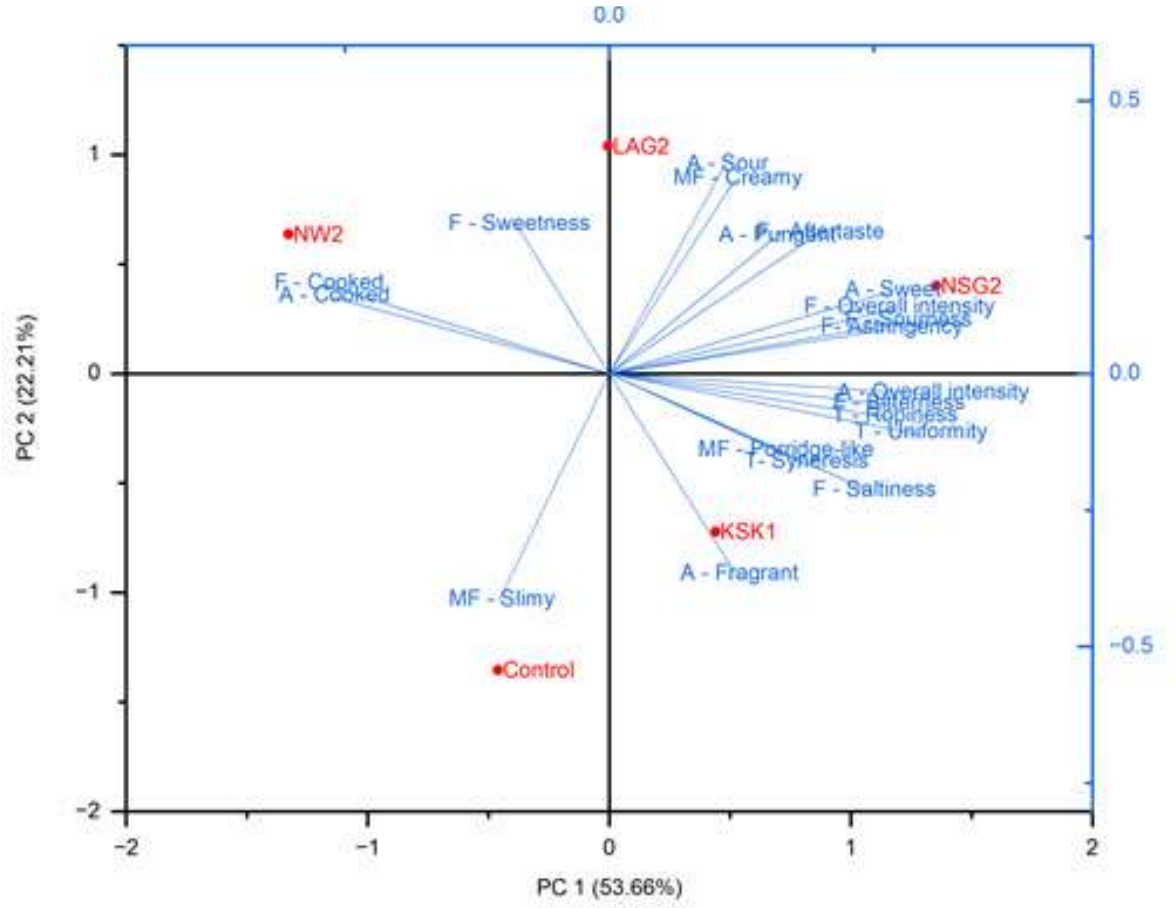

Figure 6.
PCA biplot for the distribution of different yogurt samples and its correlation with the sensory attributes.

Discussion

The present study aimed to assess the technological and sensory attributes of yogurt produced using indigenous LAB strains isolated from traditional Afghan yogurt. Notably, the study highlights the novelty of Afghan traditional yogurt as an underexplored source of indigenous LAB, demonstrating strain-specific performance in both technological and sensory aspects. The results clearly indicate that the selection of starter culture significantly impacts fermentation performance, physical stability, texture, and sensory quality. All tested strains exhibited positive amylolytic activity. However, EPS production varied influenced by the specific strain and the carbohydrate source uti-

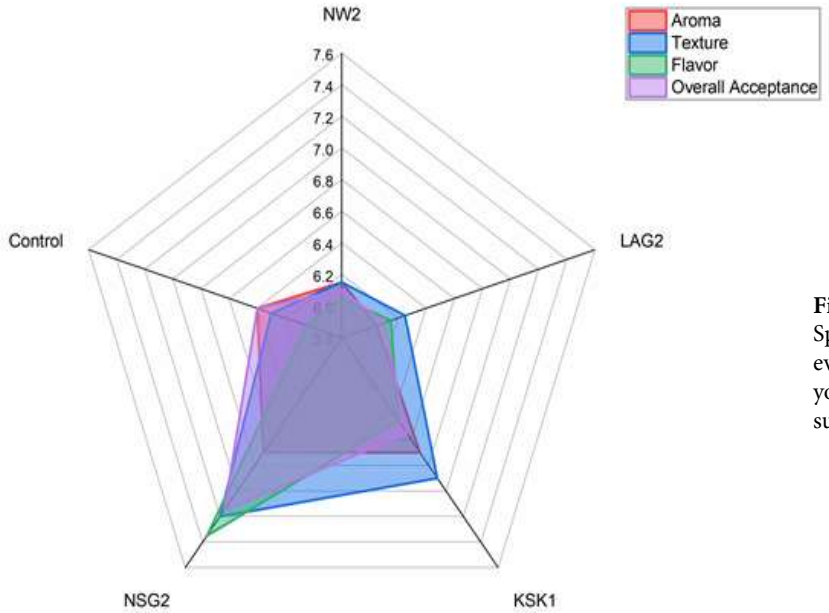

Figure 7.
Spider plot of sensory evaluation of the produced yogurt samples by consumers.

lized. Regarding fermentation dynamics, the NSG2 exhibited the most rapid acidification and maintained lower pH values during refrigerated storage, whereas titratable acidity showed a progressive increase across all samples. In terms of physical stability, yogurt produced with indigenous strains generally exhibited lower syneresis compared to the control. Coagulation times varied significantly, with LAG2 and NSG2 displaying faster activity than NW2. Texture profile analysis revealed significant variations in most parameters, with the exception of stiffness. Ultimately, sensory evaluation conducted by the expert and consumer panels revealed that yogurt produced with indigenous LAB strains offered superior quality attributes compared to the control sample.

The production of organic acids, predominantly lactic acid, by starter cultures is the primary outcome product of yogurt fermentation. This process acidifies the milk matrix, initiating milk coagulation and the formation of the yogurt gel [11-13]. Consequently, these changes are typically observed as an increase in titratable acidity and a decrease in pH over time. These acidification processes are strongly strain-dependent and influence coagulation kinetics and product quality [6, 8]. The results of the present study align with this established phenomenon, demonstrating that the indigenous LAB isolated from Afghan yogurts possess distinct acidification capacities. Notably, NSG2 showed the highest acidification activity compared with the control and the other isolates, which corresponded to shorter coagulation times. Conversely, the NW2 strain showed slower fermentation kinetics. Ziarno et al. [8] similarly reported that the acid production is strain-dependent. In their study, samples supplemented with L. plantarum 299v and L. acidophilus La-5 reached the the lowest pH levels. Furthermore, Li et al. [14] observed a strain-dependent pH decline in soy yogurt samples, where L. acidophilus N4 rapidly reached the terminal fermentation point (pH 4.6) within 240 minutes, while other strains required between 260 and 280 minutes.

Syneresis, commonly known as whey separation, is a key quality defect that negatively affects consumer acceptance. This defect is linked to the gel's water-holding capacity and the structural integrity of the protein network [15, 16]. This defect is highly strain-dependent, and studies reported the different intensities for different yogurt types produced with different LAB [17, 18]. In the present study, syneresis progressively increased in all yogurt samples during the 28-day storage period. However, yogurts produced with the indigenous LAB strains exhibited significantly lower syneresis compared to the control. Notably, the control sample, despite having the most pronounced dry matter content, showed the greatest syneresis by the end of the storage period. In contrast, yogurts fermented with indigenous strains demonstrated improved physical stability. This enhanced stability may be attributed to factors such as EPS production (e.g., KSK1) and the formation of a more compact gel structure (e.g., NSG2). These findings align with previous research indicating that EPS production by LAB contributes to reduced syneresis and enhanced textural stability in yogurt systems [19]. Additionally, strain-dependent differences in gel structure and whey separation during storage are well documented. For instance, one study reported lower syneresis in yogurt containing Lactobacillus rhamnosus and Lactobacillus paracasei compared to the control group [20].

Texture profile analysis provides an objective characterization of yogurt's structural integrity through the measurement of mechanical properties associated with gel formation [7]. In the present study, most texture parameters differed significantly among yogurt samples, with the exception of stiffness, which remained comparable. Yogurts fermented with different strains showed distinct textural profiles, with LAG2 producing a firmer/more elastic gel and NW2 showing higher adhesiveness. These findings confirm the strain-dependent nature of structure formation. Comparable strain-related variations in yogurt texture have been reported previously, where differences in texture profile were linked to the LAB strains. Ili´c et al. [7] reported that the addition of selected probiotic strains alongside commercial starters increased firmness and related texture indices compared to other formulations. In addition, EPS production also affects the rheological, sensory, and texture properties of foods, including yogurt [20, 21]. In the present study, LAG2 strain, which produced EPS from lactose, demonstrated good hardness. This observation is supported by research from Ozturkoglu-Budak et al. [22] and Tiwari et al. [23] who reported that Bifidobacterium spp. can produce EPS, thereby enhancing yogurt firmness. Tabrizi et al. [19] also reported that EPS producing LAB significantly increased the yogurt firmness throughout the storage compared to the control group using non-EPS producing LAB. Similarly, Wu et al. [18] also reported that Leuconostoc mesenteroides RSG7, an EPS producer, improved the textural properties, including hardness, cohesiveness, gumminess, chewiness, springiness, and adhesiveness compared to the control group. From an industrial standpoint, strains that enhance firmness and reduce whey separation may help decrease reliance on stabilizers and support cleaner-label yogurt formulations.

Sensory properties are among the required qualities of yogurt, serving as a reflection of the interplay between fermentation processes, matrix structure, and metabolite formation as perceived by consumers [24, 25]. In the present study, sensory evaluation conducted by a trained and consumer panel showed distinct strain-dependent differences in aroma, texture, flavor, and mouthfeel attributes. Notably, yogurt

produced with NSG2 consistently exhibited higher intensities for key positive attributes, including overall aroma intensity, uniformity, ropiness, creamy mouthfeel, and overall flavor intensity. In contrast, NW2 was associated with lower sensory scores and was characterized by undesirable cooked-related aroma and flavor notes. The control sample was mainly characterized by slimy mouthfeel and lower overall sensory intensity. PCA supported these findings, effectively separating the control from LAB-fermented yogurts and indicating distinct sensory drivers associated with each strains. These findings are consistent with previous research demonstrating that LAB strains differ significantly in their capacity to modulate yogurt sensory characteristics through strain-specific metabolic activity and structural interactions within the gel matrix [26]. In addition, Lestari et al. [27] also reported that the incorporating of probiotic LAB not only improved microbial quality but also maintained sensory acceptability comparable to control yogurt. These sensory outcomes indicate that indeginous LAB, particularly NSG2, represent promising candidate culture for producing consumer-acceptable yogurt with desirable aroma and mouthfeel profiles.

In conclusion, all LAB strains showed good performance in terms of technological and sensory properties. All strains exhibited positive amylolytic activity, produced EPS from all or some carbohydrates, maintained viability during 28 days of refrigerated storage, displayed favorable acidification activities, and sensory properties compared to the control group. Among the indigenous LAB, NSG2 (Pediococcus acidilactici) was the superior candidate. It exhibited excellent acidifying activity, coagulation, and textural profile. These characteristics collectively improved the sensory attributes of the yogurt. These findings support the practical potential of these Afghan indigenous strains as starter or adjunct cultures for industrial yogurt manufacture.

Materials & Methods

Declaration of AI use

During writing this manuscript the author(s) used AI tools to check spelling, and grammar of the content where needed. After using these tools, the author(s) reviewed and take full responsibility for the content.

Study design

This study evaluated the technological and sensory characteristics of four LAB strains isolated from traditional yogurt produced in Eastern Afghanistan (Table 5). The isolates were stored at −18 °C and reactivated prior to analysis. Assessments were conducted at two levels: (i) direct strain-based tests performed on the LAB isolates, and (ii) product-based tests involving the manufacture of yogurt using each isolate as a single-strain starter culture.

Technological and sensory attributes

The evaluation of technological properties includes two types of tests namely strain-based test which included amylolytic activity, qualitative test of exopolysaccharide production [28], acidification capacity [29], and product-based tests which included pH, titratable acidity, syneresis, dry matter [29], coagulation activity, texture profile analysis (hardness, springiness, consistency, and gumminess index) [30], and sensory analysis of the isolates. In addition, the survival of selected isolates was monitored over during 28-day refrigerated storage period [29]. All the tests were conducted in duplicate fashion. The protocols for each test are briefly described as follows:

Strain-based examinations

Amylolytic activity

The overnight culture of selected isolates of LAB in MRS medium was surface-cultured onto plates containing modified MRS agar (MRS medium without glucose but with 0.25% starch). The plates were incubated at 37°C for 48 to 72 hours. Then, a warm iodine solution was p added to the plates as a detection agent. The presence of clear halo zones surrounding the colonies indicated positive α-amylase activity.
Qualitative detection of exopolysaccharide production
For the detection of EPS, the overnight culture of the isolated LAB strains was streaked onto MRS agar supplemented with 20 g/L sugar (glucose, fructose, sucrose, or lactose). Plates then were incubated at 37°C for 36 to 48 hours. The formation of slimy colonies by the LAB isolates on the sugar-containing media was indicative of EPS production. The "Ropy" character of the colonies was also assessed by pulling the colonies with an inoculating loop.

Acidification capacity

The acidification capacity of the selected LAB strains was assessed by inoculating 1% (v/v) of the overnight culture in MRS broth of each LAB into 10 mL of reconstituted skim milk at 37°C. The pH values were measured at the beginning of incubation (0 hours), and subsequently at 6, 12, and 24 hours with a digital pH meter.
Product (yogurt)-based examinations

Yogurt production

Yogurt was prepared using commercial pasteurized whole cow's milk

Table 5.
Isolated LAB from the traditional yogurt of Eastern Afghanistan.

#	LAB strain	Accession #	Province of yoghurt sample	District of yoghurt sample	Code of sample
1	Lactiplantibacillus Plantarum H12	OQ096590.1	Kunar	Sarkani	KSK1
2	Lactobacillus brevis KLDS 1.0727	EU626012.1	Laghman	Alingar	LAG2
3	Pediococcus acidilactici HBUAS56306	MZ959430.1	Nangarhar	Spinghar	NSG2
4	Lactiplantibacillus plantarum NWAFU1559	MG551236.1	Nuristan	Wama	NW2

(Pegah, Iran). The milk was homogenized, heat-treated at 95 °C for 15 min, and then cooled to 42 °C. Selected LAB isolates were activated according to the procedure described by Faraki et al. [31]. Briefly, overnight cultures grown in MRS broth were harvested, washed twice with sterile physiological saline, and resuspended in 2 mL saline. The cell suspension was adjusted to a final concentration of 10^9 CFU/mL and inoculated into the milk at a rate of 2% (v/v). Inoculated samples were incubated at 42 °C until coagulation (indicated by a pH of 4.6). Post coagulation, the samples were stored at 4 °C for 28 days.

Survival of the isolates

The viability of the inoculated LAB during storage was monitored from day zero to day 28. To determine viability, one gram of yogurt accurately weighed and diluted in 9 mL of 0.1% (w/v) peptone water. Then, serial dilutions were performed as necessary. Subsequently, 0.1 mL of the dilutions were plated on MRS agar. The plates were incubated at 37 °C for 48-72 hours under anaerobic conditions. The number of LAB was reported as CFU/g.

pH and titratable Acidity

The pH of the prepared yogurt samples was measured using a digital pH meter. TA was measured using the titration method with 0.1 N sodium hydroxide and phenolphthalein as an indicator. TA was reported as a percentage of lactic acid, which was calculated through the following formulae:

Titratable Acidity (% Lactic acid)=(Volume (mL) NaOH*Normality of NaOH*lacit acid equivalent)/(Volume of sample used (mL))

Syneresis

To determine syneresis, 5 g of yogurt was centrifuged at 5000 rpm for 20 minutes at 4°C and the separated whey was weighed. The following equation was used to calculate the syneresis:

Syneresis (%)=(Weight of whey (g))/(Weight of yogurt (g))*100

Dry matter

The dry matter of yogurt samples was determined using the gravimetric method, and the results were reported as a percentage (w/v).

Coagulation activity

Coagulation activity was assessed based on the time required for milk to coagulate at 42°C after incubation. Strains were categorized as: (i). Rapid. Coagulation within 4-6 hours, (ii). Intermediate. Coagulation between 6-12 hours, (iii). Slow. Coagulation taking longer than 12 hours.

Texture profile analysis

Texture analysis of the prepared yogurt samples was performed using a texture analyzer (Brookfield CT3, USA) according to the manufacturer's standard protocols. Hardness (N), cohesiveness, springiness (mm), gumminess (N), chewiness (mJ), adhesiveness (mJ), and stiffness (N/mm)., were measured for texture analysis. The texture characteristics of the samples were determined on day 7 at 4 ± 2°C without removing the samples from their containers, weighing 150 g. In this test, a cylindrical probe (with a smooth cross-section of 25.5 mm in diameter, a speed of 1 mm/s, and a penetration depth of 15 mm) was used in the yogurt sample immediately after the samples were removed from 4°C [32, 33].

Sensory evaluation

Sensory evaluation of the yogurt samples was conducted on day 7 of refrigerated storage. The evaluation undertaken in a separated room under room temperature and adequate lighting. An expert panel (n = 10), comprising PhD students and lecturers experienced in yogurt sensory assessment from the food hygiene and aquaculture department, performed quantitative descriptive sensory analysis. This panel received two days of training on the definitions of the descriptors and score scale. The expert panel used a 9-point structured intensity scale (1 = very weak/low intensity; 9 = very strong/high intensity) to evaluate predefined sensory attributes encompassing aroma, texture, flavor, and mouthfeel descriptors (Table 6). In parallel, a consumer panel (n = 30) evaluated yogurt acceptability on day 7 using the 9-point hedonic scale (1 = dislike extremely; 9 = like extremely) for the aroma, texture, flavor, and overall acceptability of the yogurt samples. Scores from both panels were recorded on evaluation forms and compiled for statistical analysis.

Statistical analysis

The collected data was analyzed using SPSS statistical software (Version 23, IBM Corp, Armonk, NY, USA). One-way Analysis of Variance (ANOVA) was used to compare the means among different groups. Duncan's Multiple Comparison Test (MCT) was used for post-hoc analysis to identify specific differences between group means. All the numerical variables were reported as mean ± Standard Deviation (SD). To visualize the data for some variables, Graphpad-Prism 9.2 (Version 9.2, GraphPad Software, San Diego, CA, USA) and OriginPro (Version 2024, OriginLab Corporation, Northampton, MA, USA) software was used. A p-value less than 0.05 ($p < 0.05$) was considered as statistically significant.

Authors' Contributions

F.H. and A.A. conceived and planned the experiments. F.H. and A.A. carried out the experiments. F.H. and A.A. contributed to sample preparation. A.A. contributed to the interpretation of the results. A.A. took the lead in writing the manuscript. Both authors contributed to the first draft, revising.

Acknowledgements

We would like to thank the TUMS Cancer Institute for preparing the immunohistochemical sections.

Conflict of interest

The authors declare that there is no conflict of interest.

Table 6.
Definitions of the sensory attributes used by the expert panel.

Category of sensory attribute	Descriptor	Operational definition for scoring
Aroma	Overall intensity	Overall strength of the yoghurt smell
	Sour	Intensity of acidic/fermented sour smell.
	Cooked	Intensity of cooked/heat-treated milk odor note.
	Sweet	Intensity of sweet-smelling note (aroma-associated sweetness).
	Fragrant	Intensity of pleasant aromatic/fragrant smell.
	Pungent	Intensity of sharp/pungent odor.
Texture	Uniformity	Degree of structural evenness (smooth, consistent gel; low graininess/lumps).
	Syneresis	Degree of visible whey release/separation.
	Stretchiness	Degree of stringy/ropy behavior when handled or stirred.
Flavor	Overall intensity	Overall strength of flavor perception.
	Sweetness	Intensity of sweet taste.
	Saltiness	Intensity of salty taste.
	Sourness	Intensity of sour/acid taste.
	Bitterness	Intensity of bitter taste.
	Cooked	Intensity of cooked/heat-treated flavour note in the mouth.
	Astringency	Intensity of drying/puckering sensation in the mouth.
	Aftertaste	Intensity/persistence of taste after swallowing.
Mouthfeel	Slimy	Intensity of slippery/mucilaginous mouth-coating sensation.
	Creamy	Intensity of creamy/rich smooth mouthfeel.
	Porridge-like	Intensity of thick/pasty "porridge-like" mouthfeel impression.

References

1. Weerathilake W, Rasika D, Ruwanmali J, Munasinghe M. The evolution, processing, varieties and health benefits of yoghurt. International Journal of Scientific and Research Publications. 2014;4(4):1-10. ISSN 2250-3153.
2. Hadjimbei E, Botsaris G, Chrysostomou S. Beneficial effects of yoghurts and probiotic fermented milks and their functional food potential. Foods. 2022;11(17):2691.Doi: 10.3390/foods11172691.
3. Alimentarius C. STANDARD FOR FERMENTED MILKS CXS 243-2003. Rome, Italy: Codex Alimentarius; 2018.
4. Freitas M. The benefits of yoghurt, cultures, and fermentation. The microbiota in gastrointestinal pathophysiology: Elsevier. 2017. p. 209-23. Doi: 10.1016/B978-0-12-804024-9.00019-7.
5. Shangpliang H, Sharma S, Rai R, Tamang JP. Some technological properties of lactic acid bacteria isolated from Dahi and Datshi, naturally fermented milk products of Bhutan. Frontiers in Microbiology. 2017;8:116. Doi: 10.3389/fmicb.2017.00116..
6. Hoxha R, Evstatieva Y, Nikolova D. Physicochemical, Rheological, and Sensory Characteristics of Yogurt Fermented by Lactic Acid Bacteria with Probiotic Potential and Bioprotective Properties. foods. 2023;12(2552):1-15. Doi: 10.3390/foods12132552.
7. Ili´c N, Belovi´c M, Memiši N, Pestori´c M, Škrobot D, Pezo L, et al. Rheological Properties and Sensory Profile of Yoghurt Produced with Novel Combination of Probiotic Cultures. Foods. 2024;13(3021):1-17. Doi: 10.3390/foods13193021.
8. Ziarno M, Zar¸eba D, Kowalska E, Florowski T. A Study into the Effects of Chosen Lactic Acid Bacteria Cultures on the Quality Characteristics of Fermented Dairy, Dairy–Oat, and Oat Beverages. Applied Sciences 2025;15(3714):1-20. Doi: 10.3390/app15073714.
9. Kakabadze E, Zago M, Rossetti L, Bonvini B, Tidona F, Carminati D, et al. Characterisation of lactic acid bacteria isolated from the Georgian, yoghurt-like Matsoni. International Journal of Dairy Technology. 2019;72(3):373-80. Doi: 10.1111/1471-0307.12598.
10. İspirli H, Dertli E. Isolation and identification of exopolysaccharide producer lactic acid bacteria from Turkish yogurt. Journal of Food Processing and Preservation. 2018;42(1):e13351. Doi:10.1111/jfpp.13351.
11. Danielyan DV, Hovhannisyan HG, Baghdasaryan LG, Barseghyan AH. New generation of functional yogurts fermented with probiotic lactic acid bacteria isolated from human milk. Functional Foods in Health and Disease. 2024;14(4):232-47.Doi: 10.31989/ffhd.v14i4.1355.
12. Ayivi RD, Ibrahim SA. Lactic acid bacteria: an essential probitic and starter culture for the production of yoghurt. International Journal of Food Science and Technology

2022;57:7008-25. Doi: 10.1111/ijfs.15545.

13. Kwasi Kpodo FM, Afoakwa EO, Amoa BB, Budu AS, Saalia FK. Effect of ingredient variation on microbial acidification, susceptibility to syneresis, water holding capacity and viscosity of soy-peanut-cow milk yoghurt. Journal of Nutrition Health Food Engineering 2014;1:74-9. Doi: 10.15406/jnhfe.2014.01.00012.

14. Li S, Hu M, Wei W, Zhang P, Yu W, Fan B, et al. Effects of different strains on quality characteristics of soy yoghurt: Physicochemical, nutritional, safety features, sensory, and formation mechanism. Food Chemistry 2024;22. Doi: 10.1016/j.foodchem.2024.138800.

15. Ragab ES, Zhang S, Korma SA, Buniowska-Olejnik M, Nasser SAA, Esatbeyoglu T, et al. Physicochemical and Rheological Properties of Stirred Yoghurt during Storage Induced from High-Intensity Thermosonicated Goat and Cow Milk. Fermentation 2023;9(42):1-15. Doi: 10.3390/fermentation9010042.

16. Libberecht S, Ristevska M, Gibis M, Loeffler M. Potential of Homopolysaccharide Producing Starter Cultures in the Fermentation of Coconut Yoghurt Alternatives Enriched with Pea Protein Isolate. Foods. 2025;15(48):1-21. Doi: 10.3390/fermentation9100885.

17. Anwar A, Faiz MA, Badar IH, Jaspal MH, Hou J. Influence of Fermentation Time and Storage Conditions on the Physicochemical Properties of Different Yogurt Varieties Using Starter Cultures and Probiotic Lactobacillus rhamnosus GG. Processes. 2025;13. Doi: 10.3390/pr13020468.

18. Wu B, Guo Y, Hao L, Zuo K, Du Y, An R, et al. The Effects of Leuconostoc mesenteroides RSG7 Exopolysaccharide on the Physicochemical Properties and Flavor Compounds of Set Yoghurt. Processes. 2025;13. Doi: 10.3390/pr13020379.

19. Tabrizi P, Hesari J, Ghanbarzadeh B, Azadmard Damirchi S, Ghiasi Far S. Rheological and sensory properties and syneresis of set yogurt produced with exopolysaccharide producing starter culture YF-L811. Food Technology 2013;22(4). Doi: 10.3168/jds.S0022-0302(89)79355-3.

20. Karami M, Shahrokhi S. Comparision between Physico-Chemical, Microbiological and Reological Properties of Yoghurt Containing Lb. rhamnosus and Lb. paracasei with Convential Yoghurt Samples during the shelflife. Applied Microbiology in Food Science 2016;2(4).Doi: 10.52547/fsct.19.122.171.

21. Bibi A, Xiong Y, M.S.R R, Mehwish HM, Radicetti E, Umair M, et al. Rheological and sensory properties and syneresis of set yogurt produced with exopolysaccharide producing starter culture YF-L811. Sustainability 2021;13:1-19.Doi: 10.3390/su13094779.

22. Tiwari S, Kavitake D, Devi PB, Shetty PH. Bacterial exopolysaccharides for improvement of technological, functional and rheological properties of yoghurt. International Journal of Biological Macromolecules 2021;183:1585–95.Doi: 10.1016/j.ijbiomac.2021.05.069.

23. Ozturkoglu-Budak S, Akal HC, Buran I, Yeti¸semiyen A. Effect of inulin polymerization degree on various properties of synbiotic fermented milk including Lactobacillus acidophilus La-5 and Bifidobacterium animalis Bb-12. Journal of Dairy Science 2019;102:6901–13.Doi: 10.3168/jds.2019-16290.

24. Yilmaz-Ersan L, Kurdal E. The Production of Set-Type-Bio-Yoghurt with Commercial Probiotic Culture. International Journal of Chemical Engineering and Applications. 2014;5(5).Doi: 10.7763/IJCEA.2014.V5.418.

25. Ali MA, Shahein MR, Metwally MM, Embark HA. Physicochemical, Sensory and Microbiological Characteristics of Yoghurt Produced from Cow's Milk Supplemented with Aloe vera Extract during Cooled Storage. World Journal of Dairy & Food Sciences. 2019;14(1):108-17. Doi: 10.5829/idosi.wjdfs.2019.108.117.

26. Chen C, Shanshan Zhao, Guangfei Hao, Haiyan Yu, Huaixiang Tian, Guozhong Zhao. Role of lactic acid bacteria on the yogurt flavour: A review. International Journal of Food Properties. 2017;20(S1):S316–S30.Doi: 10.1080/10942912.2017.1347676.

27. Lestari LA, Nuriannisa F, Yuliani K, Ratnasari D, Farida IN, Azizah EF. Sensory and microbiological evaluation of probiotic yoghurt made with different types of probiotic cultures starter Lactobacillus acidophilus LA-5® and Bifidobacterium animalis subsp. lactis BB-12. Food Research. 2022;6(2):188. Doi: 10.26656/fr.2022.6(S2).014.

28. Meena KK, Taneja NK, Jain D, Ojha A, Kumawat D, Mishra V. In Vitro Assessment of Probiotic and Technological Properties of Lactic Acid Bacteria Isolated from Indigenously Fermented Cereal-Based Food Products. Fermentation. 2022;8(10):529. Doi: 10.3390/fermentation8100529.

29. Kılıç EE, Halil Kılıç İ, Koç B. Yoghurt Production Potential of Lactic Acid Bacteria Isolated from Leguminous Seeds and Effects of Encapsulated Lactic Acid Bacteria on Bacterial Viability and Physicochemical and Sensory Properties of Yoghurt. Journal of Chemistry. 2022;2022:2683126. Doi:10.1155/2022/2683126.

30. Li H, Gao J, Chen W, Qian C, Wang Y, Wang J, et al. Lactic acid bacteria isolated from Kazakh traditional fermented milk products affect the fermentation characteristics and sensory qualities of yogurt. Food Science & Nutrition. 2022;10(5):1451-60. Doi: 10.1002/fsn3.2733.

31. Faraki A, Noori N, Gandomi H, Banuree S, Rahmani F. Effect of Auricularia auricula aqueous extract on survival of Lactobacillus acidophilus La-5 and Bifidobacterium bifidum Bb-12 and on sensorial and functional properties of synbiotic yogurt. Food Science & Nutrition. 2020;0(0):1-10.Doi: 10.1002/fsn3.1541.

32. Delikanli B, Ozcan T. Effects of various whey proteins on the physicochemical and textural properties of set type nonfat yoghurt. International Journal of Dairy Technology 2014;67(4):495-503.Doi: 10.1111/1471-0307.12143.

33. Hosseinnejad M, Jafari S, Ganje M. Modeling of Changes in Physicochemical, Textural, and Sensory Properties of Fortified Yoghurt wth Zinc and Iron by Artificial Neural Networks. 2017:325-36.Doi: 10.26717/BJSTR.2017.01.000602.

How to cite this article
Banuree AH, Jamshidi A, Salari A . Technological and Sensory Characterization of Yogurt Produced with Lactic Acid Bacteria Isolated from Traditional Yogurt of Eastern Afghanistan. Iran J Vet Sci Technol.2026; 18(2): 45- 58.
DOI: https://doi.org/10.22067/ijvst.2026.97504.1637
URL: https://ijvst.um.ac.ir/article_47947.html

Iranian Journal of Veterinary Science and Technology

Received: 2025-Nov-29
Accepted after revision: 2026- Feb-02
Published online: 2026- Feb-02

RESEARCH ARTICLE

DOI:10.22067/ijvst.2026.96662.1621

Clinical, pathological, and molecular investigation and isolation of *Mycoplasma pulmonis* in a laboratory animal production and breeding colonies with murine respiratory mycoplasmosis

Roozbeh Fallahi[a], Mojtaba Moharrami[a], Mohsen Bashashati[b], Soghra Bozorgi[a]

[a] Department of Research, Breeding and Production of Laboratory Animals, Razi Vaccine and Serum Research Institute, Agricultural Research Education and Extension Organization (AREEO), Karaj, Iran.
[b] Research Department of Bacterial, Parasitic and Fungal Poultry Diseases, Razi Vaccine and Serum Research Institute, Agricultural Research, Education and Extension Organization (AREEO), Karaj, Iran.

ABSTRACT

This study investigated the prevalence of *Mycoplasma pulmonis* (*M. pulmonis*) contamination and disease within a 6 month period in a laboratory animal production center housing rats, mice, hamsters, guinea pigs, and rabbits. A total of 66 samples from different breeding colonies were subjected to culture, molecular diagnosis (PCR), and pathological examination. Sampling of the involved organs was performed in animals showed clinical signs. Clinical symptoms including tilt head and turning towards the affected ear, ruffled coat, chromodacryorrhea, and cobblestone lung, were observed in four adult rats. PCR revealed *M. pulmonis* DNA in 33 samples (50%), indicating widespread contamination. However, positive cultures and isolation were confirmed in only 12 samples (18% of total samples), all originating from rat colonies. Pathological changes such as atelectasis and bronchiectasis were observed in the samples of rats. The facility utilized a conventional breeding system with a shared air conditioner and also lacked biosecurity barriers, facilitating easy transmission of infection from infected rat to other animals. Due to the lack of sensitivity of those animals to this microorganism, no apparent issues exhibited in them, suggesting the absence of stressful and predisposing conditions for opportunistic infections such as *M. pulmonis*. Although microbial monitoring should be done regularly and periodically for various infectious agents.

Keywords

Mycoplasma pulmonis, Laboratory animals, Diagnosis, Isolation, Histopathology

Number of Figures: 7
Number of Tables: 1
Number of References:: 23
Number of Pages: 9

Abbreviations

SPF: specific pathogen-free
CAR: cilia-associated respiratory
FELASA: Federation of European Laboratory Animal Science Associations

Corresponding author: Roozbeh Fallahi
Email: r.fallahi@rvsri.ac.ir
Tel: +98(91)254-05972

Introduction

M. pulmonis is recognized as a potential rodent pathogen, even within advanced laboratory animal breeding facilities [1]. Mycoplasma represents the smallest self-replicating and polymorphic microorganism, typically ranging from 200-500 nm in diameter. Their gram-negative nature, lack of cell wall, combined with their diminutive size and flexibility, enables them to easily traverse filter membranes, posing a contamination risk [1-5]. In rats and mice, *M. pulmonis* colonizes the respiratory tract, leading to respiratory mycoplasmosis. This condition is frequently undiagnosed due to its subclinical presentation. Clinical manifestations typically emerge only when the disease has progressed significantly. Factors such as elevated ammonia levels, various stressors, and the presence of other pathogenic agents can influence the clinical progression and severity of the disease [1, 2, 6]. The prevalence of respiratory mycoplasmosis in conventional rat colonies has been reported up to 100%, while in colonies equipped with biosecurity measures, the prevalence ranges from 20% to 60%. In general, the prevalence of mycoplasma infections in laboratory rat colonies is higher than in other laboratory animals such as mice, hamsters, guinea pigs, and rabbits. Nevertheless, mycoplasmas have been identified in these other species, and they may serve as significant potential sources of infection, primarily in a subclinical form. In specific pathogen-free (SPF) colonies, the presence of mycoplasma infections is expected to be absent [3, 7, 8]. Hill (1972) noted that transmission risk is considerably higher from rats exhibiting overt disease compared to those with subclinical infections. Typical clinical manifestations include sneezing, nasal discharge, shortness of breath, and head tilt, particularly when middle or inner ear infections are present. Other common symptoms include weight loss, hunchback, wrinkled skin, and the presence of chromodacryorrhea in the eyes and nostrils, which are red secretions from harderin gland. Nasal secretions rarely become mucous and purulent, but sometimes purulent exudate may be seen in the nasal passages, ears, and trachea. Mycoplasmas usually affect the respiratory tract [1, 2, 4, 6, 9, 10]. In infected rats, the lungs may appear normal in the early stages. However, in the later and advanced stages of the infection, particularly in older rats, the lungs can develop a cobblestone texture with gray or yellow-purple discoloration. Pneumonia and chronic inflammatory infiltrates resulting from bronchiectasis abscesses may also be present [11]. Microscopic histological alterations often do not correlate with clinical symptoms or external observations. Common diagnostic methods include serology, ELISA, indirect immunofluorescence, culture, histopathology, and molecular methods like PCR. However, serological assays may be imprecise due to cross-reacting or interfering antibodies, potentially leading to false positive across different species. ELISA detects mycoplasma infections through antibody detection in serum, but cannot identify subclinical infections and may also produce cross-reactions with other species. PCR, using specific primers, can detect various mycoplasma genera and species with as little as 0.5-1 picogram of DNA. Employing the RT-PCR method to amplify ribosomal RNA sequences enhances sensitivity by up to 1000 times, effectively identifying M. pulmonis in throat swab samples from rats. While culture can confirm *M. pulmonis* presence, a negative culture result might indicate a subclinical infection. Isolating mycoplasma from rats exhibiting mild or moderate disease poses significant challenges [1, 7]. The species identified in laboratory mice and rats include *M. pulmonis*, *M. arthritidis, M. neurolyticum, M. collis,* and *M. muris*, with *M. pulmonis* being the most significant [3, 4, 7, 8, 12].

Mycoplasma cultures can be labor-intensive, time-consuming, and may lack sensitivity for certain species. Several factors influence the successful isolation of mycoplasmas, including the selection of appropriate tissues, proper sampling techniques, appropriate transportation under standard conditions, the presence of growth-inhibiting factors in the sampled tissue, and the microorganism's nutritional requirements [12]. It is advisable to collect samples from multiple tissues of the same animal. While isolation of *M. pulmonis* from rats with clinical signs is not difficult, concurrent primary or secondary bacterial and viral infections can aggravate the lesions and complicate diagnosis [7]. *M. pulmonis* is also considered as a zoonosis agent in person who deal with contaminated rats. Piasecki et al. (2017) reported a 76% infection rate in breeding technicians working with rats infected with *M. pulmonis*, detected via PCR on nasopharyngeal samples. Strain sensitivities also exist with laboratory mice. For example, the C57BL/6 is more resistant than the BALB/c and DBA/2 [8, 11, 13].

Abbreviations-Cont'd

PPLO: Pleuropneumonia-like organisms
H & E: hematoxylin and eosin
BLAST: Basic Local Alignment Search Tool
PC: Positive Control
NC: Negative Control
PS: Positive sample
fnPCR: Fluorogenic Nuclease PCR

Results

Clinical observations

Animals were monitored for clinical signs of the infection over a period of six months. Among all the tested laboratory animal colonies including Wistar and Sprague Dawley rats, non-inbred NIH and NMRI mice, BALB/c, C57BL/6 and DBA/2 inbred mice, golden Syrian hamsters, Pirbright albino and colored guinea pigs and Dutch albino rabbits, only the rat colony exhibited the related clinical signs (Table 1). Four adult male and female rats from both Wistar and Sprague Dawley strains were observed with clinical signs including head tilt and rotational movement towards the affected ear (in the direction of bending the head) when the animal was lifted by the tail (Figure 1)

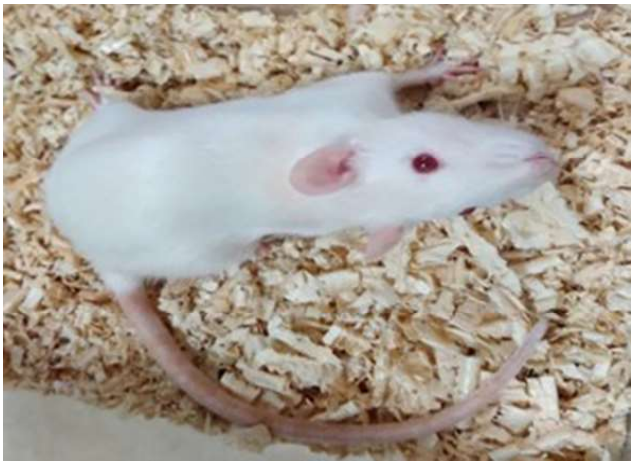

Figure 1.
Head tilt in rat with respiratory mycoplasmosis towards the right ear.

All four affected rats displayed these symptoms; one animal additionally showed hunchback, a crumpled body cover and chromodacryorrhea around the eyes. The red secretions contain porphyrin and are related to harderin gland. These secretions appeared bright fluorescent red under the UV light (Figure 2) and from this method it can be determined whether it is porphyrin or blood. Despite the presence of symptoms, fertility and reproductive in performance remained unaffected across all examined laboratory animal colonies and the breeding output continued at normal levels.

Necropsy observations

In some of the infected rats with clinical signs, lung cobblestone was observed (Figure 3).

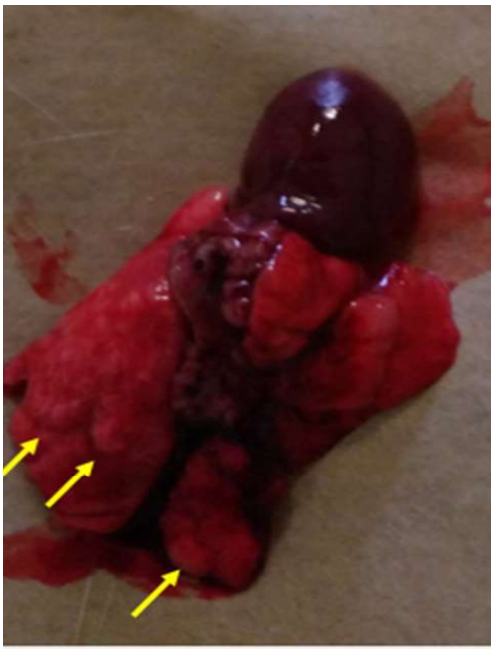

Figure 3.
Cobblestone lung in a rat with respiratory mycoplasmosis.

Cultural observations

Out of a total of 66 swab samples collected from different colonies, only 12 samples (18%) showed color change to orange and yellow in PPLO liquid medium, without any observed turbidity (Table 1). Colonies grown on PPLO agar medium appeared in the

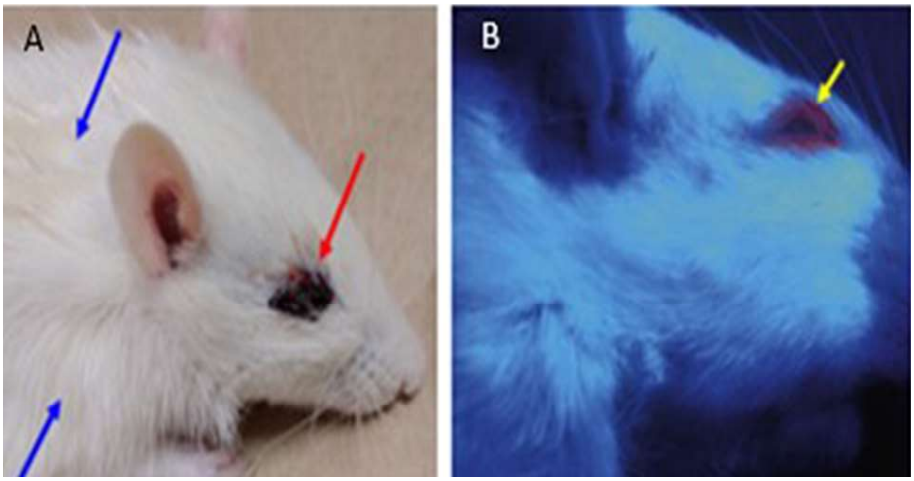

Figure 2.
A) Chromodacryorrhea around the eyes (red arrows) and ruffled coat (blue arrows), B) Observation of harderian gland discharges under the UV lamp appearing bright fluorescent red.

Table 1.
Type and number of animals and the results obtained.

Type of animal	Strain of animal	Number of male	Number of female	Number and percentage of animals with symptoms	Number and percentage of histo-pathological changes	Number and percentage of PCR-positive animals	Number of animals with positive culture results
Rat	Wistar	3	3	3 (50 %)	3 (50 %)	6 (100 %)	6 (100 %)
	Sprague Dawley	3	3	4 (66.7 %)	4 (66.7 %)	6 (100 %)	6 (100 %)
Mice	NIH	3	3	0	0	4 (66.7 %)	0
	NMRI	3	3	0	0	3 (50 %)	0
	BALB/c	3	3	0	0	0	0
	C57BL/6	3	3	0	0	0	0
	DBA/2	3	3	0	0	0	0
Hamster	Syrian	3	3	0	0	2 (33.3 %)	0
Guinea pig	Albino Pirbright	3	3	0	0	5 (83.3 %)	0
	Color Pirbright	3	3	0	0	4 (66.7 %)	0
Rabbit	Albino Dutch	3	3	0	0	3 (50 %)	0
	Total	**33**	**33**	**7 (10.6 %)**	**7 (10.6 %)**	**33 (50 %)**	**12 (18.1 %)**
		66					

form of fried-eggs (Figure 4).

Histopathology

Histopathological examination of lung tissue samples form symptomatic rats revealed hyperemia of the lung lobes. Thickening of vascular and alveolar walls was observed due to the infiltration and accumulation of lymphocytes and macrophages, which indicated infectious interstitial pneumonia (Figure 5A). The parenchyma of the lung tissue in some areas showed atelectasis, and bronchiectasis and bronchiolectasis were present in a number of bronchi. Epithelial thickening with the accumulation of nuclei (hyperplasia) and narrowing of the duct caused by a layer of cuboidal to columnar epithelium (obstructive bronchiolitis) were also observed (Figure 5B).

Identification of M. pulmonis

During PCR analyses, 33 out of 66 swab samples showed the respective DNA band of 500 bp and hence were regarded positive (Figure 6). According to these results 50% of the samples were contaminated with *M.*

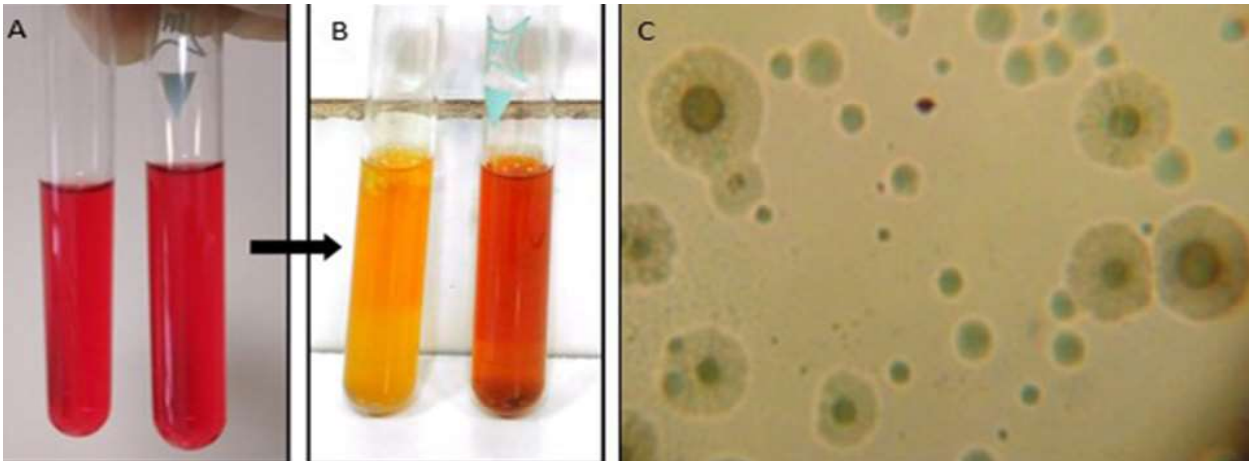

Figure 4.
PPLO broth medium A) uncultured, B) cultured with color change orange and yellow, C) typical Mycoplasma colonies on PPLO agar medium appearing as fried-egg.

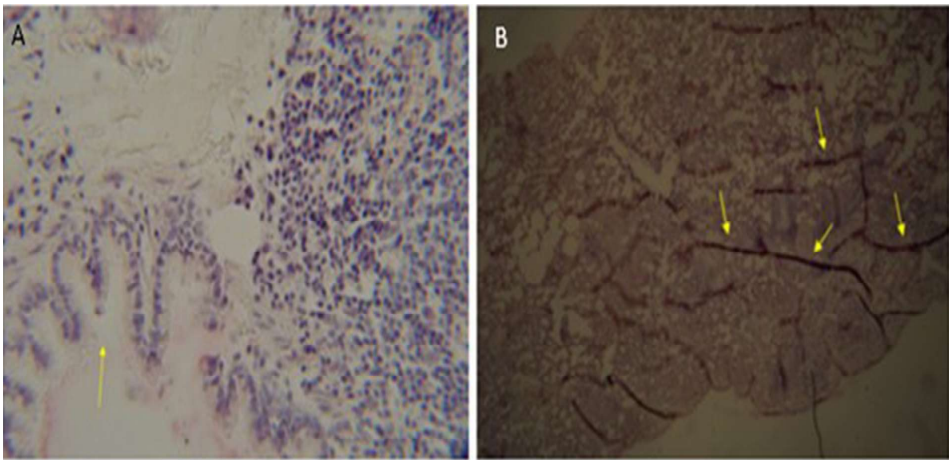

Figure 5.
A) Bronchiectasis and bronchiolectasis, thickening of the epithelium with the accumulation of nuclei (hyperplasia) and narrowing of the ducts by a layer of cuboidal to columnar epithelium (obstructive bronchiolitis) in the lung tissue of the affected rat (hematoxylin-eosin staining, magnification X 200). B) Areas of the alveolar wall thickened with the infiltration and accumulation of lymphocytes and macrophages, in the lung tissue of the infected rat, which indicates infectious pneumonia (magnification X 32).

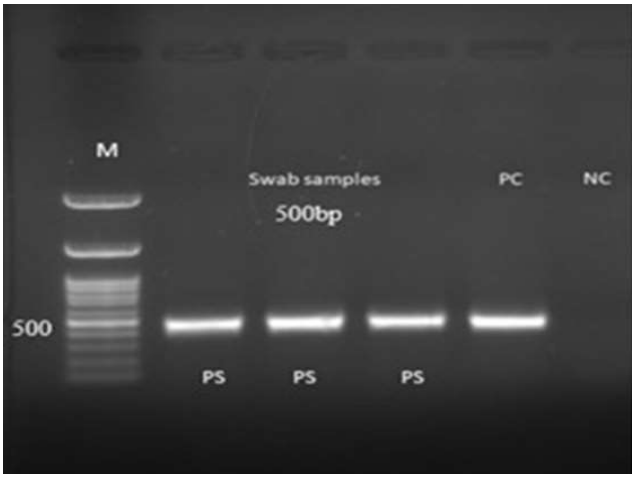

Figure 6.
PCR product performed on swab samples for *M. pulmonis* 16S/23S rRNA intergenic spacer region. [M: The Ladder DNA, 100 bp (GeneRulerTM 100 bp DNA Ladder-Fermentas) as a marker, PC: Positive Control, NC: Negative Control, PS: Positive sample].

pulmonis. According to obtained results, 50% of Wistar rats and 66.6% of the Sprague Dawley rats exhibited respiratory symptoms, while none of the other laboratory animal species showed clinical sign. Animals that showed histopathological symptoms, also showed histopathological changes (10.6%). Comparison of microbiological culture and PCR analysis a significant difference were recorded, and PCR analysis appeared more sensitive compare to microbiological culture. By culture only 18% of samples appeared positive, while PCR detected 50% positive samples. The phylogenetic tree of *M. pulmonis* is shown in Figure 7.

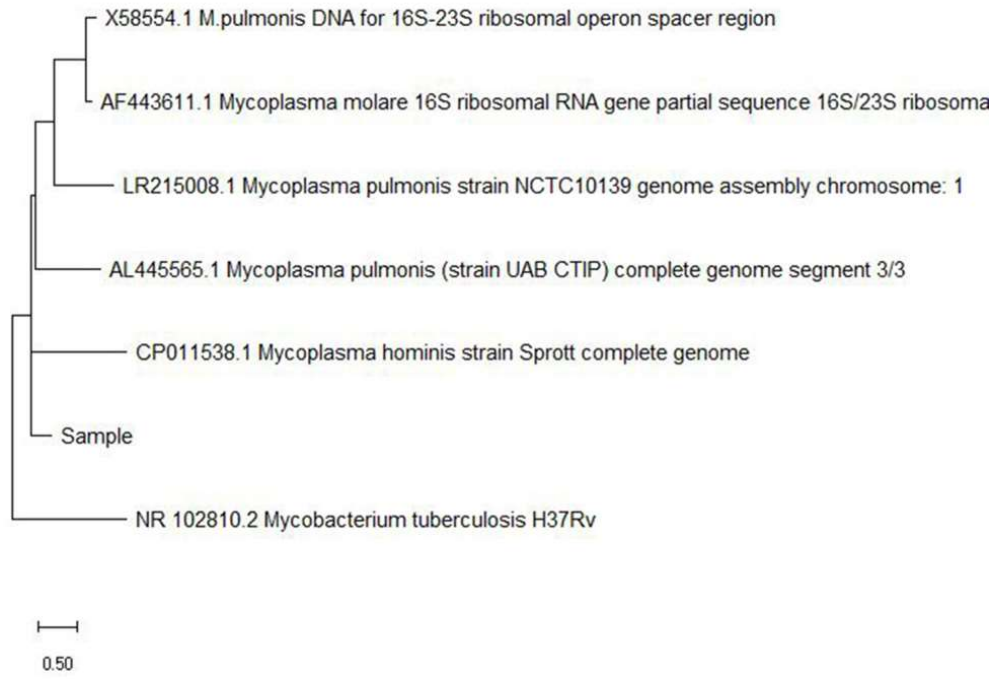

Figure 7.
Evolutionary analysis in the phylogeny tree of the samples from the current study, was constructed using the maximum likelihood method, utilizing the Mega version X (10) software. The phylogenetic tree was constructed using the nucleotide sequence of the 16S ribosomal RNA sequence gene of the *M. pulmonis*. The sample and the other nucleotide sequences Mycoplasma were grouped together in a Clustal (cluster), indicating their genetic similarity. *Mycobacterium tuberculosis* was the out group.

Discussion

Mycoplasma was initially isolated from rodents in the late 1940s, with *M. pulmonis* recognized as the predominant species in these hosts. Infection with this microorganism is of considerable importance because it can interfere with research results [7]. Rossini et al. (1983) reported the isolation of mycoplasmas from laboratory mice exhibiting symptoms of pneumonia and arthritis [7]. Furthermore, Timenesky et al. (1992) successfully isolated both *M. pulmonis* and *M. arthritidis* from rats and mice in conventional colonies [7]. Additionally, Barreto et al. (2002) identified *M. pulmonis* in mice presenting respiratory symptoms [7]. This study was investigated the precence of murine respiratory mycoplasmosis in a laboratory animal production and breeding colonies. In the study, clinical signs were observed only in four adult Wistar and Sprague Dawley rats. These signs included head tilt and a rotational movement towards the affected ear. Additionally, one rat exhibited a ruffled coat and chromodacryorrhea. In certain infected rats displaying clinical symptoms also exhibited characteristic cobblestone appearance of the lung. Overall, the incidence of mycoplasma infections in laboratory rat colonies is greater than that in other laboratory animals, such as mice, hamsters, guinea pigs, and rabbits. While mycoplasmas can be isolated from these other species, they may serve as significant potential sources of subclinical infection [3, 7, 8]. In the present study, by using culture methods, *M. pulmonis* was isolated from 12 samples from rat colonies, representing 18% of the total samples analyzed. The lung tissue samples from rats exhibiting clinical symptoms displayed pathological alterations such as hyperemia, vascular and alveolar wall thickening, atelectasis, bronchiectasis and bronchiolectasis. In contrast to culture results, PCR detected *M. pulmonis* in 33 out of 66 samples (50%) collected from colonies of rats, mice, hamsters, guinea pigs, and rabbits. According to Reyes et al. (2000), *M. pulmonis* is naturally present in the respiratory and reproductive system of rats, although susceptibility varies among strains; for example, LEW inbred rats are more sensitive to *M. pulmonis* than F344. Also, the Sprague Dawley is more sensitive to genital mycoplasmosis than the Wistar [14]. Hence, the PCR technique employed in this study might have detected the *M. pulmonis* that are natural residents of the respiratory system of these animals. In contrast, by culture technique these were not identified which might be due to the small number of these bacteria or lower sensitivity of the method used compared to PCR analysis. Shafaati et al. (2016) detected the presence of *M. pulmonis* in the respiratory system of laboratory rats through PCR targeting the SrRNA gene and successfully isolated the organism. While, many other techniques have also been employed for the identification of *M. pulmonis* in laboratory animals [2]. Goto et al. (2012) employed MALDI-TOF MS spectrophotometric technique for rapid identification of *M. pulmonis* [12]. Loganbill et al. (2005) used fnPCR (Fluorogenic Nuclease PCR) method to detect *M. pulmonis* in laboratory rats [9]. Conversely, Disastra (2019) by using PCR method, reported no detection of *M. pulmonis* infection in samples prepared from the lungs and trachea of mice, rats, guinea pigs and laboratory hamsters at Mahidol National Center of Thailand, indicating that probably animals of this facility were free of this mycoplasma [15]. *M. caviae* and *M. pulmonis* cause latent infection in the nasopharynx, brain and genital tract of guinea pigs [11]. Guinea pigs are often asymptomatic and carriers, but poor hygienic conditions and overcrowding it can elevate ammonia levels, irritates the respiratory tract and increases the risk of mycoplasma infection. In advanced cases, *M. caviae* and *M. pulmonis* cause acute lymphadenitis, metritis and arthritis in guinea pigs [16]. *M. pulmonis* has also been isolated from the rhinopharynx of rabbits with upper respiratory tract symptoms, likely due to proximity to infected rat colonies [16]. Abd-Algawad et al. (2021) reported that infection of rabbits with *M. pulmonis* increases their vulnerability to bacterial infections such as *Pasteurella multocida* and *Staphylococcus* aureus [17]. In rabbits, respiratory diseases are the second most important after digestive diseases. Respiratory bacterial infections in rabbits cause rhinitis, sinusitis, otitis media, conjunctivitis, pneumonia, lung abscess and septicemia. Although mycoplasma infections are usually subclinical; for example, *M. pulmonis* infection in rabbits is very rare, but in some cases it can lead to respiratory disorders [17]. The breeding system examined in the present study used conventional housing with shared ventilation and no biosecurity barriers between different areas, these conditions likely facilitated the transmission of infection from infected rats to other laboratory animals. The insensitivity of these animals to the microorganism did not result in any adverse effects, suggesting a lack of stressful or predisposing conditions for opportunistic infections. However, regular and periodic microbial monitoring is essential for various infectious agents.

Conclusion

This study identified *M. pulmonis* in almost 50% of the animals that showed clinical sign of respiratory mycoplasmosis. Mycoplasma infection is a recognized concern, and although preventive measures exist, it remains imperative for breeding centers to safeguard the health of their laboratory animals. Regrettably, in numerous countries, animal health certificates issued by various centers are often not authentic. Beyond the

symptoms and complications associated with mycoplasma infection, it adversely affects the outcomes of research involving these animals. Consequently, it is essential to investigate the presence of mycoplasma in the target animal population. Subclinical infections are common, and significant number of laboratory animals may carry mycoplasma infections without exhibiting clinical symptoms. The absence of SPF conditions and the use of shared ventilation likely facilitated the spread of infection within the facility examined. Therefore, the implementation of continuous and permanent health monitoring programs is crucial for quality control of these animals.

Materials & Methods

Ethical approval

The present study was conducted in accordance with the guidelines set by the Animal Ethics Committee of Razi Vaccine and Serum Research Institute, and all experiments were carried out in accordance with relevant guidelines and regulations.

Animals

During a period of 6 months, from October 2023 to March 2024, different breeds of laboratory animals from a Laboratory animal breeding facility in Iran were examined for possible contamination and disease caused by *M. pulmonis*. Laboratory animals included Wistar and Sprague Dawley rats, NIH and NMRI outbred mice, BALB/c, C57BL/6 and DBA/2 inbred mice, golden Syrian hamsters, albino and colored Pirbright guinea pigs, and albino Dutch rabbits. Each breed was housed in a separate room.

Animal Housing and management

The breeding system was conventional and the airflow was provided by a shared air conditioner. No biosecurity barriers were in place between rooms. All animals appeared clinically healthy, were free from external and internal parasite, and were provided standard compressed food (pellets) and tap water ad libitum. Laboratory mice, rats, hamsters and guinea pigs were kept in shoebox polycarbonate cages, while rabbits were kept in aluminum cages with mesh floors and standard dimensions. For polycarbonate cages, sterile aspen tree wood shavings were used as bedding. Changing the cage and wood shavings was done twice a week. The temperature of the breeding rooms was 22-24°C, the humidity was 45-55%, the air ventilation was 8-10 three minutes/hour and the light/dark period was 12:12 hours cycle with light intensity was below 325 lux.

Sampling collection

Sampling was done according to the Federation of European Laboratory Animal Science Associations (FELASA) guidelines [18-21]. Assuming the lowest probability of *M. pulmonis* presence in the mentioned colonies, for maximum sampling, 10% prevalence of infection at the animal colonies level was considered. On this basis and with the highest level of confidence (99.9%), 66 adult animals (Table 1) were randomly selected from both sexes for sampling. Swab samples from the nasopharynx of animals (two samples from each animal) were taken according to the laboratory animal ethical principles. Samples from animals with clinical signs were taken according to the animal ethical principle. After euthanasia (intraperitoneal injection of combination of ketamine and xylazine at the rate of 2-3 times the anesthesia dose) samples from the bifurcation of the trachea was taken [22].

Culturing of Samples

The collected samples were inoculated into PPLO (Pleuropneumonia-like organisms) broth medium (BBL, Sparks, MD, USA). The sample swabs were then taken out of PPLO liquid media and 1 ml of the contaminated media was passed through a 0.45µm syringe filters (Sartorious, USA) and transferred to fresh PPLO broth culture and incubated at 37°C for almost a week. If the color of the medium changed to orange or yellow (due to acidity) on three consecutive weeks with the renewal of the liquid culture medium, the results of mycoplasma culture are considered positive. Positive samples were further cultured on PPLO agar medium and observed daily up to 21 days for typical *M. pulmonis* colonies. Samples from symptomatic animals were cultured on PPLO broth, blood agar, MacConkey agar, sabouraud dextrose agar and anaerobic cultured in blood agar and placed in a 37°C.

Histopathological Examinations

In order to investigate the histopathology of lung tissue, samples from infected animals were prepared and placed in 1% neutral formaldehyde buffer solution. Tissues were routinely processed and embedded in paraffin. Paraffin blocks were cut in sections of 5-6µm and stained with hematoxylin and eosin (H & E) for observation with a light microscope. The used animal carcasses were destroyed using an infectious waste disposal device (hydroclave) [22].

DNA Extraction and PCR analysis

The swab samples were subjected to DNA extraction using the high pure PCR template preparation kit (Roche Diagnostics GmbH, Mannheim, Germany) according to the manufacturers' instructions. DNA concentration and purity were determined by absorbance using a Nano® spectrophotometer (Maestrogen, Las Vegas, USA).

The assay was performed on an ABI Veriti 96 Thermal Cycler (Applied Biosystems, Foster, CA, USA) using a primer amplifying a specific region, (16S/23S rRNA intergenic spacer region) as described earlier [23]. The reaction mixture (50 µl) contained 33 µl of nuclease-free water, 5 µl of 10X Ampliqon Ammonium Buffer, 1µl of 25mM $MgCl_2$, 2µl 10 mM of dNTP mix, 2µl of 10µM each primer, 1µl of 2.5 units/µl Ampliqon AccuPOLTM DNA Polymerase (AMPLIQON, Odense M, Denmark), and 4 µl of extracted viral DNA. The PCR conditions included; 94°C for 2 min, 35 cycles of (94°C for 30 sec, 54°C for 45 sec, and 72°C for 1 min) and 72°C for 5 min. The PCR amplified products were run and analyzed on 1% agarose gel electrophoresis.

The obtained PCR products were sequenced in both directions by a commercial DNA service company (Macrogen, Seoul, South Korea). The obtained sequences were analyzed and compared with *M. pulmonis* reference sequences in a database using Basic Local Alignment Search Tool (BLAST) at NCBI.

Authors' Contributions

All authors contributed to the study conception and design. R. F. acquisition of data: R. F. analysis and interpretation of data: R. F. drafting of the manuscript: R. F. critical revision of the manuscript for important intellectual content: M. M. review and editing: R. F. administrative, technical, and material support: M.M.

Acknowledgements

All authors would like to thank the staff of the Laboratory Animal Production and Breeding, Pathology, and Microbiology Departments of Razi Vaccine and Serum Research Institute for their cooperation.

Conflict of interest

The authors declare that there is no conflict of interest.

References

1. Chawla S, Jena S, Venkatsan B, Mahara K, Sahu N. Clinical, pathological, and molecular investigation of *M. pulmonis*-induced murine respiratory mycoplasmosis in a rat (*Rattus norvegicus*) colony. Vet World. 2017; 10 (11): 1378-1382. Doi: 10.14202/vetworld. 2017.1378-1382.

2. Shafaati MR, Khadem NS, Yazdansetad S, Momeni T, Zardadi M. Isolation and molecular identification of *Mycoplasma pulmonis* from the respiratory tract of *Rattus rattus*. Iran J Med Microbiol. 2016; 9 (4): 24-31.

3. Ferreira J B, Yamaguti M, Marques LM, Oliveira RC, Neto RL, Buzinhani M, et al. Detection of *Mycoplasma pulmonis* in laboratory rats and technicians. Zoonoses Public Hlth. 2008; 55(5): 229–234. Doi: 10.1111/j.1863-2378.2008.01122.x.

4. Masoumalinejad Z, Zinatizadeh MR, Tahmasebiabdar N. A review of mycoplasma in laboratory mice. Mod Med Lab J. 2019; 2(2):127-131. Doi: 10.30699/mmlj17.2.1.15.

5. Ceola CF, Sampaio J, Blatt SL. Mycoplasma infection and inflammatory effects on laboratory rats bred for experimental research. Rev Pan-Amaz Saude. 2016; 7(2): 59-66. Doi: 10.5123/S2176-62232016000200007.

6. Hrapkiewicz K, Colby L, Denison P. Clinical laboratory animal medicine; an introduction, 4th edition, Wiley Blackwell, 2013.

7. Barreto ML, do Nascimento ER, de Martino Campos CA, do Nascimento MGF, Brasil Lignon G, Lira MLF, et al. Detection of *Mycoplasma pulmonis* in laboratory rats. Braz J Microbiol. 2002; 33 (3):260-264. Doi:10.1590/S1517-83822002000300015.

8. Khan S, Rana R. Laboratory animal mycoplasmosis: A mini review. Indian J Anim Sci. 2021; 91 (11): 891–894. Doi:10.56093/ijans.v91i11.118116.

9. Loganbill JK, Wagner AM, Besselsen DG. Detection of *Mycoplasma pulmonis* by Fluorogenic Nuclease Polymerase Chain Reaction Analysis. Comparative Med 2005; 55 (5): 419-424.

10. Suttie AW. Boorman's pathology of rat: Reference and atlas, 2nd ed. Academic Press, 2018.

11. Fox JG, Anderson LC, Otto GM, Pritchett-Corning KR, Whary MT. Laboratory Animal Medicine, 3rd ed. Academic Press, 2015.

12. Goto K, Yamamoto M, Asahara A, Tamura T, Matsumura M, Hayashimoto N, et al. Rapid identification of *Mycoplasma pulmonis* isolated from laboratory mice and rats using Matrix-Assisted Laser desorption ionization Time-of-Flight Mass Spectrometry. Lab Anim Sci. 2012; 74(8): 1083–1086. Doi: 10.1292/jvms.12-0029.

13. Piasecki T, Chrzastek K, Kasprzykowska U. *Mycoplasma pulmonis* of rodents as a possible human pathogen. Vector-Borne Zoonot Dis. 2017; 17 (7): 475-477. Doi: 10.1089/vbz.2016.2104.

14. Reyes L, Steiner DA, Hutchison J, Crenshaw B, Brown MB. *Mycoplasma pulmonis* genital disease: Effect of rat strain on pregnancy outcome. Comparative Med. 2000; 50 (6): 622-627.

15. Disastra Y, Lestari FB, Biotech M. Identification technique of *Mycoplasma pulmonis* bacteria using polymerase chain reaction (PCR) in national laboratory animal center Mahidol University, http://etd.repository.ugm.ac.id, 2019.

16. Quesenberry KE, Orcutt CJ, Mans C, Carpenter JW. Ferrets, rabbits and rodents, 4th ed. Elsevier, 2021.

17. Abd-Algawad R, Mowafy R, Salem SMM, Atia N, Ali SF, Eltokhy EI, Kamel E, et al. Molecular characterization of snuffle-causing bacterial pathogens in rabbits in terms of prevalence and pathogenicity. Egypt J Agric Res 2021; 99 (4): 475-485. Doi: 10.21608/ejar.2021.89555.1129.

18. Mahler M, Berard M, Feinstein R, Gallagher A, Illgen-Wilcke B, Pritchett-Corning K, Raspa M. FELASA recommendations for the health monitoring of mouse, rat, hamster, guinea pig and rabbit colonies in breeding and experimental units. Lab Anim. 2014; 48:178-92. Doi:: 10.1177/0023677213516312.

19. Fallahi R, Mansouri MA. Health monitoring of Razi Institute laboratory mice (NIH strain) to *Clostridium piliforme* in 1395. Vet Res Biol Prod. 2018; 117: 78-84. Doi:10.22034/VJ.2017.109301.1263.

20. Fallahi R, Survey of Razi Institute NIH laboratory mice to *Streptobacillus moniliformis,* the causative agent of rat bite fever. New Find Vet Microbiol. 2021; 4 (1): 59-68. Doi:10.22034/NFVM.2021.141955.

21. Fallahi R, Mansouri MA, Modirrousta H. Molecular monitoring of Razi Institute NIH strain laboratory mice colony for infection with *Leptospira interogans* bacteria. Vet Res Biol. Prod 2020; 126: 9-15. Doi: 10.22092/VJ.2019.125057.1553.

22. Fallahi R, Mansouri MA. Biology, Breeding, Diseases and Principles of Working to Laboratory Animals. First edition, Razi Vaccine and Serum Research Institute Publication. 2015.

23. Lauerman LH, Chilina AR, Closser JA, Johansen D. Avian mycoplasma identification using polymerase chain reac-

tion amplicon and restriction fragment length polymorphism analysis. Avian Dis. 1995; 39(4): 804-811. Doi.10.2307/1592417.

How to cite this article
Fallahi R, Moharrami M, Bashashati M, Bozorgi S. Clinical, pathological, and molecular investigation and isolation of *Mycoplasma pulmonis* in a laboratory animal production and breeding colonies with murine respiratory mycoplasmosis. Iran J Vet Sci Technol.2026; 18(2): 59-67.
DOI: https://doi.org/10.22067/ijvst.2026.96662.1621
URL: https://ijvst.um.ac.ir/article_47848.html

Iranian Journal of Veterinary Science and Technology

Received: 2025- Nov-23
Accepted after revision: 2026- Feb-08
Published online: 2026- Feb- 10

RESEARCH ARTICLE

DOI: 10.22067/ijvst.2026.96481.1617

Synergisric effects of bacteriophages and antibiotics against Shiga toxigenic *Escherichia Coli* isolatrd from diarrheic calves

Aseem Keder Albaker[a], Maher Saleh[a], Ashraf Alaaleh[b]

[a] Department of Public Health and Preventive Medicine, Faculty of Veterinary Medicine, University of Hama, Hama, Syria.
[b] Department of microbiology, Faculty of Veterinary Medicine, University of Hama, Hama, Syria.

ABSTRACT

This study investigated the potential of coliphages as a means of decreasing the amount of antibiotics needed for treatment. Shigatoxigenic *E.Coli* (STEC) strains were isolated from diarrheic calves within the Hama governorate, Syria. Isolation was done with differential and selective media and biochemical confirmation. The presence of genes encoding Shiga toxins (stx1 and stx2) was confirmed through multiplex polymerase chain reaction (PCR). Antibiotic susceptibility testing of the bacterial isolates was also done. In addition, bacteriophages from wastewater from cattle barns were isolated and their synergistic potential was assessed when combined with the antibiotics streptomycin, oxytetracycline, and neomycin. The *STEC* isolates were resistant to antibiotics. The highest resistance rates were observed against amoxicillin (88%) and penicillin G (92%). Notably, the phage-antibiotic combination therapy proved highly effective since the addition of bacteriophages reduced the minimum inhibitory concentration (MIC) of streptomycin, oxytetracycline, and neomycin. In streptomycin, the combination MIC was significantly lower than that of streptomycin alone (40 µg/mL streptomycin + 6 $\log_{10}$ PFU/mL phages versus 250 µg/mL streptomycin alone). Similarly, the MIC for the oxytetracycline-phage combination (40 µg/mL + phages) was markedly lower than that of oxytetracycline alone (250 µg/mL). For neomycin, the combination (10 µg/mL + phages) also showed a significant MIC reduction compared to neomycin alone (200 µg/mL).

Keywords

coli phage, PCR, MIC, Antibiotic Resistance, Virulence Factors

Number of Figures: 7
Number of Tables: 6
Number of References:: 41
Number of Pages: 12

Abbreviations

STEC: Shigatoxigenic E.Coli
stx1, stx2: Shiga toxins
MIC: minimum inhibitory concentration
PFU: Plaque Forming Unit

Corresponding author: Aseem Albaker,
Email: vet-med@net.sy
Tel: +96(39)5979-4640

Introduction

Diarrhea is perhaps the most serious of all veterinary diseases, representing a primary causes of high mortality in suckling calves. This condition leads to profound weakness, reduced vitality, and poor health, making affected calves vulnerable to life-threatening secondary infections [1].

Various researchers have examined the incidence of calf diarrhea and identification of its etiologic pathogens. Escherichia coli has been identified as a major causative agent of calf diarrhea [2].

The introduction of antibiotics marked a pivotal advancement in medicine, offering effective treatments over a wide range of potentially lethal infections and enabling advanced medical procedures [3]. However, the escalating crisis of bacterial drug resistance, largely driven by the overuse and misuse of these agents, has become a virulent global health emergency. As a response to this emerging threat. The World Health Organization (WHO) and several public health agencies warn that if we do not take immediate multifactorial actions to slow resistance development and spread, the consequences will be overwhelming and most likely irreversible for human and animal health, the economy, and the environment. WHO developed a so-called One Health approach, recognizing people and animals closely connected within the shared environment [4].

In 2015, the World Organisation for Animal Health (OIE) observed highlighted the widespread availability of antimicrobial agents, in many countries, including developed nations, often with minimal regulatory restrictions. Out of 130 countries recently assessed by the OIE, more than 110 still lack appropriate legislation governing the import, manufacture, distribution, and use of veterinary products, including antimicrobials. As a result, these products circulate without control as ordinary commodities and are often falsified.

To date, there is no harmonized global system for monitoring the use and circulation of antimicrobial agents. This information is essential, however, to track and control the origin of medicines, obtain reliable import data, trace their distribution, and assess the quality of products in circulation. To address this, OIE member countries mandated the organization to collect this missing information and establish a global database to monitor antimicrobial use, integrated with the OIE's World Animal Health Information System (WAHIS). This mandate is also supported by the Food and Agriculture Organization (FAO) and the WHO's global action plan on antimicrobial resistance. The database will provide a solid foundation for the three organizations' collaborative efforts to combat antimicrobial resistance [5].

This escalating crisis has prompted the quest for alternatives to traditional antibiotics. Various approaches have been tried, including antibody therapy, antimicrobial peptides, probiotics, essential oils, metal chelation, alongside efforts to discover new antibiotics [6, 7, 8]. While these alternatives are promising, they are generally limited in that these agents are static and cannot adapt to evolving bacterial resistance. Thus, once resistance emerges, the agent becomes ineffective. This is accompanied by the huge time and financial investment necessary to get new drugs onto the market. However, bacteria can easily mutate and develop resistance to these new agents as well. This constant evolutionary battle makes the development of new antibiotics a challenging and often unsustainable endeavor [9].

On the other hand, bacteriophages (viruses that infect and kill bacteria) possess a unique capacity to co-evolve with their bacterial hosts. Combined with being the most ubiquitous biological entities on Earth (10^{31} particles estimated), such dynamic adaptability makes them a powerful alternative [10].

Phage therapy, the use of bacteriophages to treat bacterial infections, has been practiced for several decades in Eastern Europe. Recent clinical cases from the U.S. and UK have also demonstrated its potential to succeed [11, 12]. While initially applied during the 1920s in the Soviet Union, it remains a recognized treatment method for countries such as Russia and Georgia. Global interest in reassessing phage therapy as a potential antibiotic substitute has grown. Despite this, there are a number of challenges that restrict its general use in the clinical setting, including the selection of optimal phage for specific infection, the potential development of bacterial resistance to phages, and host immune responses against phages [8].

A significant advantage of phages lies in their specificity for particular bacterial species or strains. This selectivity limits collateral damage to the beneficial commensal bacteria within the host microbiome, a well-documented weakness of broad-spectrum antibiotics. Phages are also self-replicating at the infection site; they dynamically increase their numbers at the site of infection until their bacterial hosts are eliminated, after which they are cleared from the body [13].

Phages are considered to be generally recognized

Abbreviations-Cont'd

PCR: multiplex polymerase chain reaction
AMR: antimicrobial resistance
CDC: Centers for Disease Control and Prevention
WHO: World Health Organization
GRAS: generally recognized as safe
FDA: Food and Drug Administration

as safe (GRAS) by the U.S. Food and Drug Administration (FDA), given the fact that humans ingest millions of particles on a regular basis every day through food and water [14]. The natural properties of phages-safety, specificity, and self-replication make phage therapy a better candidate than traditional chemical agents. This is particularly apt when compared with the conventional drug development pipeline, a process that takes more than a decade and more than a billion dollars to produce one novel antibiotic.

Given the economic importance of calf diarrhea, its multifactorial etiology, and the pressing issue of antimicrobial resistance, this study aimed to investigate the efficacy of phage-antibiotic combination therapy as a targeted treatment strategy.

Results

Isolation of STEC

Shiga toxin-producing *E. coli* (STEC) represented 41.66% of the *E. coli* isolates obtained from diarrheic calves in Hama Governorate, Syria. Among these STEC isolates, 60% carried the stx1 gene alone, 24% carried the stx2 gene alone, and 16% carried both stx1 and stx2 genes., as shown in Fig. 1.

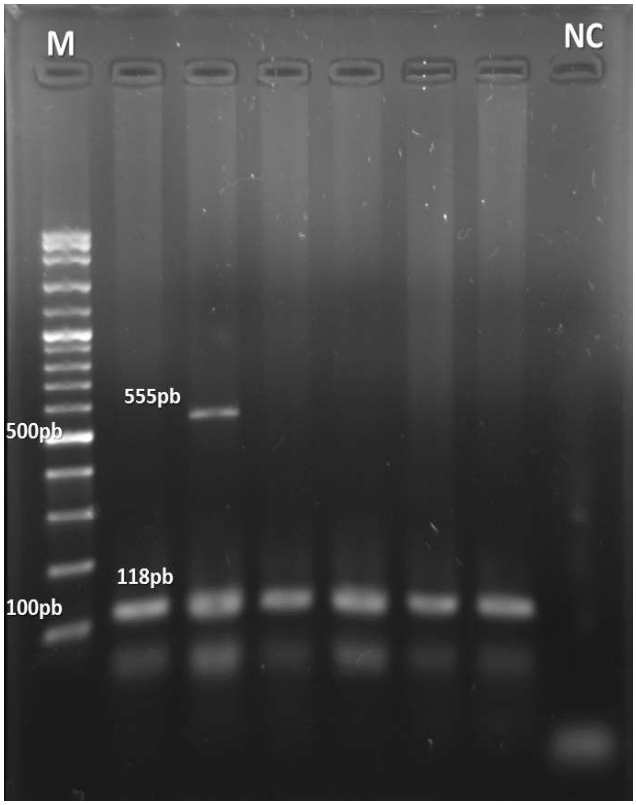

Figure 1.
Results of the multiplex polymerase chain reaction (PCR). Lane M represents the molecular weight marker (DNA ladder). Lane NC represents the Negative control. The remaining lanes display the results for the Escherichia coli isolates.

Antibiotic Susceptibility of STEC

Shigatoxigenic *E. coli* (STEC) isolates exhibited high levels of antibiotic resistance. The highest resistance was observed against Penicillin G (92%), followed by Amoxicillin (88%).

In contrast, the highest susceptibility was observed for Ceftiofur (68%), followed by Ciprofloxacin (60%). These results are presented in Table 1.

Table 1.
Antibiotic Susceptibility Profile of *Escherichia coli* Isolates

Antibiotics	Sensitive	Intermediate	Resistance
Ampicillin	36%	36%	28%
Ceftiofur	68%	20%	12%
Ciprofloxacin	60%	24%	16%
Enrofloxacin	52%	32%	16%
Streptomycin	12%	24%	64%
Gentamycin	16%	16%	68%
Neomycin	8%	16%	76%
Oxytetracycline	4%	12%	84%
Doxycycline	12%	12%	76%
penicillin G	0%	8%	92%
Amoxicillin	0%	12%	88%
Trimethoprim	16%	24%	60%

Synergistic Effect of Bacteriophages and Antibiotics against Shigatoxigenic *E. coli* (STEC):

A synergistic effect was observed between antibiotics and *E. coli* bacteriophages against the bacterial isolates. The MIC for the combination of streptomycin (40 µg/mL) and bacteriophages (6 $\log_{10}$ PFU/mL) was much lower than the MIC of streptomycin alone (250 µg/ML).

The highest bacteriophage titer (14.58 $\log_{10}$ PFU/mL) occurred at a streptomycin concentration of 20 µg/mL, while the lowest bacteriophage titer (3.63 $\log_{10}$ PFU/mL) was recorded at a higher streptomycin concentration of 250 µg/mL.

These results are illustrated in Fig. 2, Fig. 3, Table 2.

The calculated Fractional Bactericidal Concentration Index (FBIC) was 0.26, indicating a strong synergistic effect between *E. coli* bacteriophages and the antibiotic streptomycin against *E. coli.*

A similar pattern was observed for oxytetracycline. The MIC for the combination of oxytetracycline (40 µg/mL) and bacteriophages (6 $\log_{10}$ PFU/mL) was notably lower compared to the MIC of oxytetracycline alone (250 µg/mL).

The highest bacteriophage titer (14.75 $\log_{10}$ PFU/mL) occurred at a sub-inhibitory oxytetracycline con-

Albaker et al., IJVST 2026; Vol.18, No.2
DOI:10.22067/ijvst.2026.96481.1617

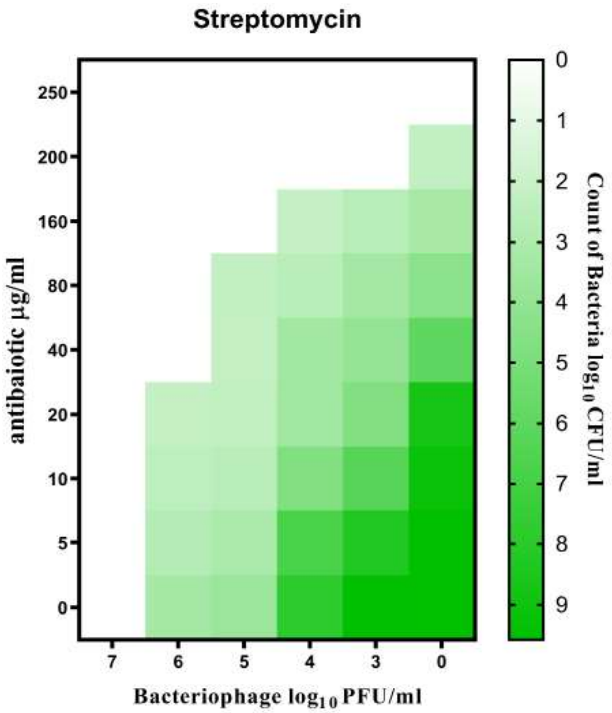

Figure 2.
The heat map shows the concentration of Escherichia coli germs after 24 hours of incubation at 37°C with the synergistic effect of the antibiotic streptomycin and Escherichia coli phages.

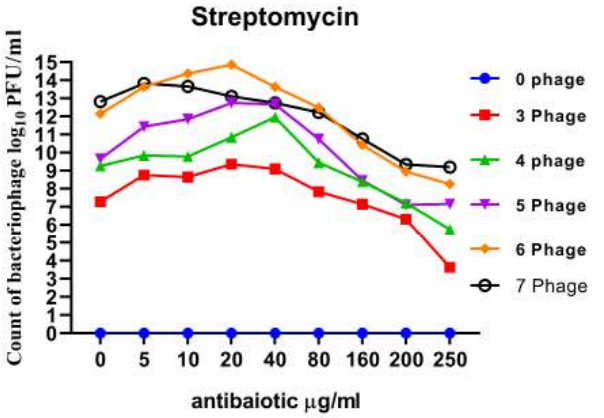

Figure 3.
Titers of bacteriophage on synergistic action with streptomycin against STEC.

centration of 10 µg/mL, while lowest bacteriophage titer (4.77 $\log_{10}$ PFU/mL) was recorded in conjunction with the higher oxytetracycline concentration of 250 µg/mL.These results are illustrated in Fig. 4, Fig. 5, Table 3.

The calculated Fractional Bactericidal Concentration Index (FBCI) was 0.26, confirming a robust syn-

Table 2.
The table demonstrates the synergistic effect of bacteriophages with the antibiotic streptomycin, where the blue color represents the colony count of Escherichia coli, and the green color indicates the bacteriophage titer.

antibaiotic µg/ml						
250	**0**	**0**	**0**	0	0	0
	0	3.63 ± 1.2	5.74 ± 1.4	7.15±2.3	8.25±2.6	9.2±3.5
200	2.25 ± 0.8	0	0	0	0	0
	0	6.31 ± 2.1	7.21 ± 2.8	7.11 ± 2.7	8.94 ± 3.4	9.35 ± 2.8
160	3.23 ± 1.7	2.68 ± 0.7	2.14 ± 0.9	0	0	0
	0	7.14 ± 2.3	8.38 ± 3.5	8.46 ± 3.1	10.42 ± 2.8	10.75 ± 2.3
80	4.26 ± 2.2	3.35 ± 2.1	2.61 ± 1.1	2.24 ± 0.6	0	0
	0	7.83 ± 2.4	9.45 ± 3.4	10.74 ± 2.7	12.48 ± 3.3	12.22 ± 3.4
40	5.94 ± 2.7	3.95 ± 1.8	3.47 ± 1.5	2.21 ± 1.2	0	0
	0	9.1 ± 3.2	11.96 ± 4.2	12.67 ± 3.8	13.63 ± 2.9	12.74 ± 3.1
20	8.73 ± 2.8	4.67 ± 2.2	3.51 ± 1.8	2.33 ± 0.8	2.18 ± 1.1	0
	0	9.36 ± 3.7	10.85 ± 2.8	12.74 ± 4.2	14.85 ± 3.9	13.1 ± 2.8
10	9.15 ± 3.3	6.73 ± 2.7	4.68 ± 2.6	2.59 ± 1.5	2.42 ± 0.4	0
	0	8.64 ± 3.8	9.78 ± 3.2	11.85 ± 3.7	14.37 ± 4.7	13.65 ± 3.5
5	9.52 ± 3.2	8.31 ± 3.3	6.73 ± 2.9	3.17 ± 2.1	2.75 ± 0.8	0
	0	8.75 ± 3.6	9.85 ± 2.1	11.43 ± 3.5	13.63 ± 3.2	13.82 ± 3.2
0	9.57 ± 3.7	9.53 ± 3.8	7.82 ± 3.7	3.71 ± 1.8	3.34 ± 1.4	0
	0	7.28 ± 3.2	9.26 ± 2.6	9.64 ± 2.8	12.14 ± 2.9	12.82 ± 2.9
A	0	3	4	5	6	7
P	**Count of bacteriophage log10 PFU/ml**					

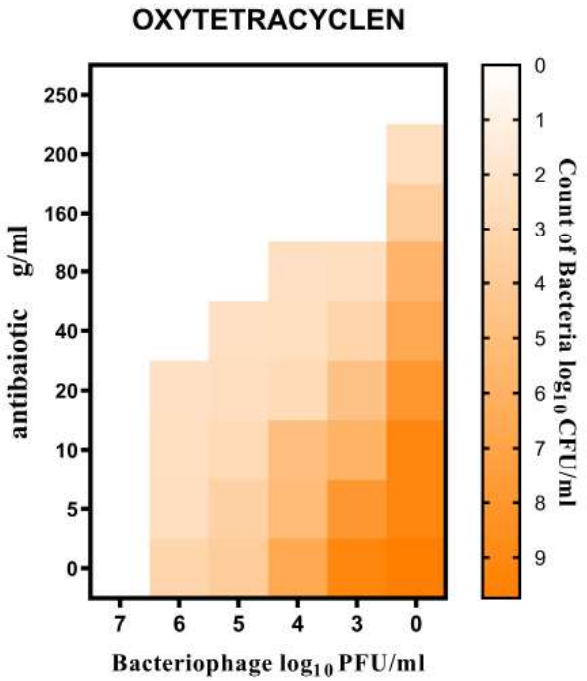

Figure 4.
The heat map shows the concentration of *Escherichia coli* germs after 24 hours of incubation at 37°C with the synergistic effect of the antibiotic oxytetracycline and Escherichia coli phages.

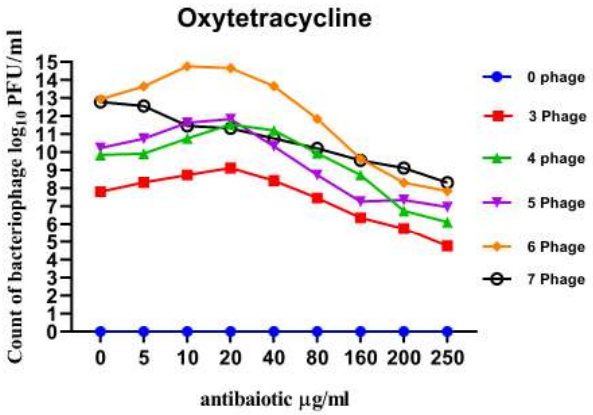

Figure 5.
Bacteriophage titres under synergistic use of oxytetracycline against STEC.

ergistic interaction between *E. coli* bacteriophages and oxytetracycline against the Shiga toxin-producing *E. coli* (STEC) strains.

The antibiotic neomycin also produced a synergistic effect. The MIC the combination of neomycin (10 µg/mL) and bacteriophages (6 $\log_{10}$ PFU/mL) was much lower than the MIC of neomycin alone (200 µg/ML). The highest bacteriophage titer (13.63 $\log_{10}$

Table 3.
The table demonstrates the synergistic effect of bacteriophages with the antibiotic oxytetracycline, where the blue color represents the colony count of Escherichia coli, and the green color indicates the bacteriophage titer.

antibaiotic µg/ml	A	0	3	4	5	6	7
	P	**Count of bacteriophage $\log_{10}$ PFU/ml**					
250		**0**	0	**0**	0	0	0
		0	4.77 ± 1.7	6.12 ± 1.9	6.95 ± 1.4	7.84 ± 2.1	8.31 ± 2.8
200		2.43 ± 0.6	0	0	0	0	0
		0	5.74 ± 1.5	6.74 ± 2.1	7.35 ± 2.8	8.31 ± 2.6	9.12 ± 2.2
160		3.75 ± 1.2	0	0	0	0	0
		0	6.36 ± 2.7	8.73 ± 2.2	7.25 ± 2.6	9.63 ± 3.2	9.54 ± 2.7
80		5.62 ± 2.1	2.43 ± 1.4	2.32 ± 0.8	0	0	0
		0	7.46±2.3	9.95 ± 3.5	8.73 ± 2.6	11.85 ± 3.6	10.21 ± 2.6
40		6.54 ± 1.9	3.16 ± 1.6	2.37 ± 1.2	2.31 ± 0.9	0	0
		0	8.42 ± 2.8	11.21 ± 4.2	10.32 ± 3.2	13.65 ± 4.2	10.76 ± 3.1
20		7.95 ± 3.1	4.61 ± 2.3	2.74 ± 1.8	2.38 ± 1.6	2.2 ± 0.6	0
		0	9.12 ± 3.3	11.53 ± 3.7	11.83 ± 2.8	14.65 ± 4.1	11.32 ± 2.6
10		9.12 ± 3.6	5.8 ± 2.8	4.84 ± 2	2.75 ± 1.2	2.35 ± 0.7	0
		0	8.73 ± 2.9	10.75 ± 2.3	11.63 ± 4	14.75 ± 3.6	11.46 ± 3.5
5		9.18 ± 3.2	7.84 ± 3.6	5.12 ± 2.1	3.47 ± 1.3	2.41 ± 1.2	0
		0	8.32 ± 2.6	9.92 ± 3.2	10.74 ± 3.5	13.64 ± 3.8	12.56 ± 3.6
0		9.73 ± 3.5	9.17 ± 3.8	6.53 ± 2.5	3.82 ± 1.6	3.14 ± 1.5	0
		0	7.82 ± 2.5	9.84 ± 2.2	10.23 ± 3.8	12.93 ± 4.3	12.78 ± 3.7

PFU/mL) occurred at neomycin concentration of 10 µg/mL, while lowest bacteriophage titer (4.56 $\log_{10}$ PFU/mL), was recorded at the highest neomycin concentration of 160 µg/mL. These results are illustrated in Figs. 6 and 7, Table 4.

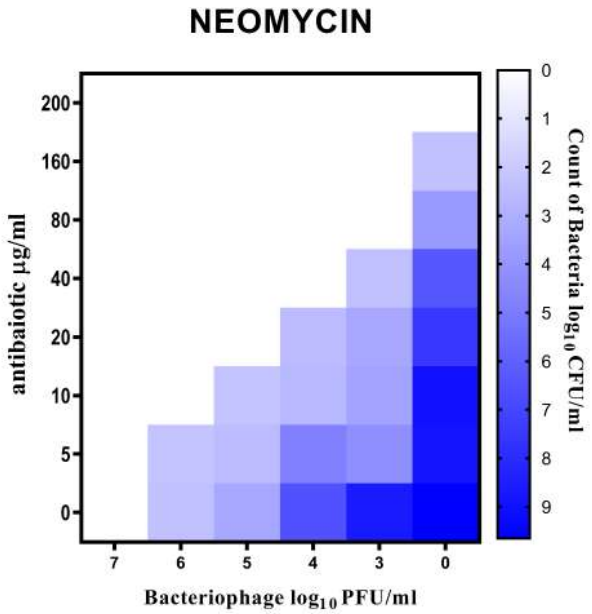

Figure 6.
The heat map shows the concentration of Escherichia coli germs after 24 hours of incubation at 37°C with the synergistic effect of the antibiotic Neomycin and Escherichia coli phages.

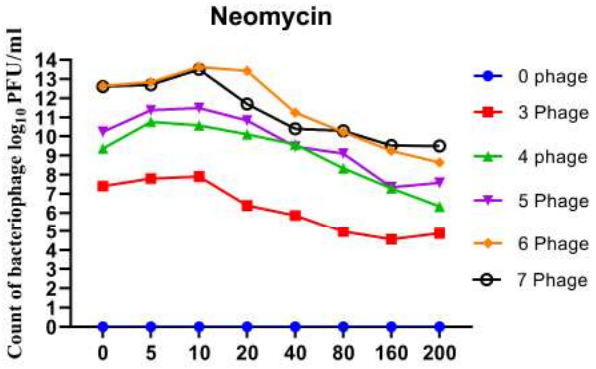

Figure 7.
Bacteriophage titers during synergistic application of neomycin against STEC.

The calculated Fractional Bactericidal Concentration Index (FBCI) was 0.15, indicating potent synergistic bactericidal activity between *E. coli* bacteriophages and the antibiotic neomycin against the targeted *E. coli*.

Table 4.
The table demonstrates the synergistic effect of bacteriophages with the antibiotic Neomycin, where the blue color represents the colony count of Escherichia coli, and the green color indicates the bacteriophage titer.

antibaiotic µg/ml	0	3	4	5	6	7
250	0	0	0	0	0	0
	0	4.87±2.1	6.34±2.8	7.58±2.4	8.64±3.5	9.5±3.8
160	2.32±0.6	0	0	0	0	0
	0	4.56±2.6	7.29±3.1	7.34±3.5	9.24±3.6	9.53±2.8
80	3.86±0.8	0	0	0	0	0
	0	4.97±2.4	8.34±2.3	9.11±3.3	10.23±3.7	10.3±3.7
40	6.35±1.2	2.31±0.7	0	0	0	0
	0	5.86±2.8	9.58±3.5	9.47±3.5	11.24±3.2	10.4±3.4
20	7.56±2.1	3.28±1.8	2.5±1.4	0	0	0
	0	6.39±3.6	10.11±4.2	10.83±4.1	13.42±4.1	11.7±4.2
10	9.01±2.5	3.43±1.8	2.63±1.1	2.21±1.2	0	0
	0	7.9±3.2	10.58±4.2	11.37±3.2	13.63±4.3	13.5±3.7
5	8.86±2.5	4.21±2.3	4.76±2	2.53±1.4	2.22±0.7	0
	0	7.8±2.5	10.76±3.9	11.37±3.7	12.84±3.5	12.7±3.5
0	9.65±3.1	8.64±3.1	6.56±2.4	3.28±1.7	2.32±0.6	0
	0	7.4±3.2	9.36±4.1	10.24±3.2	12.64±3.7	12.6±3.8
A	0	3	**4**	**5**	**6**	7
	p		**Count of bacteriophage $\log_{10}$ PFU/ml**			

Discussion

The aim of this study was to investigate the synergistic effects of bacteriophages combined with antibiotics against STEC isolated from diarrheic calves. The present study revealed a high prevalence of STEC among *E. coli* isolates obtained from diarrheic calves. In comparison with previous studies, Wang et al. [15] documented an STEC prevalence of 13.79% among *E. coli* isolates of calf diarrhea, with 37.5% of them possessing stx1, 12.5% possessing stx2, and 50% possessing both stx1 and stx2. Nguyen et al. [16] reported that 19.08% of *E. coli* isolates of diarrheic calves possessing stx1, 30.29% possessing stx2, and 24.48% possessing both stx1 and stx2. In contrast, Andrade et al. [41] documented 82.8% of *E. coli* isolates of diarrheic calves possessing stx1 and only 4% possessing stx2. Similarly, Cengiz and Adiguzel [17] reported that 3.03% of isolates possessing stx1 and 9.09% possessing stx2.

Differences of STEC prevalence reported in the present study compared to earlier studies may result from differences inF geographical location, epidemiological conditions, and farm management practices.

Moreover, the STEC isolates of diarrheic calves from the present study were significantly resistant to a number of antibiotics. Extensive and often indiscriminate application of antibiotics likely play a central role in the emergence of resistant strains. For instance, Abdulridha and Ibrahim [2] observed 100% resistance of *E. coli* isolates of diarrheic calves against ampicillin and amoxicillin but only 30% susceptibility to ciprofloxacin. Wang et al. [18] documented 100% resistance of *E. coli* isolates against sulfadiazine sodium, enrofloxacin, and ciprofloxacin. while Ibrahim et al. [19] documented 100% resistance of *E. coli* isolates against colistin, tetracycline, amoxicillin/clavulanic acid, and trimethoprim sulfamethoxazole.

Variability in resistance profiles between studies likely reflect variations in local antibiotic usage practices.

The combination of *E. coli* bacteriophages with antibiotics showed markedly increased effectiveness when compared with the use of either treatment individually. This synergistic interaction substantially reduced the MIC of the used antibiotics. These results align with earlier investigations; for example, Narulita et al. [20] reported that combining phages with tetracycline or amoxicillin lowered antibiotic MICs. Moradpour et al. [21] reported strong synergy effect between ampicillin (6 µg/mL) and phages, achieving 95% *E. coli* growth inhibition compared with to 85% for phages alone and 82% for ampicillin alone. Similarly, Shamsuzzaman et al. [22] reported that the combination of phages and colistin caused a 4-8-fold reduction in the MIC, and synergy with meropenem and tigecycline caused a 4-fold reduction of the MIC.

The synergistic effects between phages and antibiotics may be explained by antibiotics weakening the bacterial cell wall, facilitating enhanced phage entry and bacterial lysis. Alternatively, antibiotics may suppress bacterial replication, allowing phages to proliferate within cells, ultimately enhancing bacterial death and the release of new phage particles [23].

The efficacy of the synergistic effect between bacteriophages and antibiotics may be attributed to several reasons, including the occurrence of mutations conferring resistance to phage infection. Although such mutations prevent phage infection, they also provide a unique opportunity to significantly influence or steer the pathogen's evolutionary trajectory toward a therapeutically beneficial phenotype. In particular, phages that target structures involved in antimicrobial resistance may promote evolutionary tradeoffs that enhance the activity of otherwise ineffective antibiotics [24].

The primary defense against phages arises through mutation or concealment of phage receptors [40]. Such surface modifications often impose a consistent, non-adaptive, and pleiotropic cost on the host bacteria [25] and can have a direct impact on antibiotic resistance if the phage receptor plays a role in antibiotic resistance mechanisms. Synergy involving phage interaction with efflux systems was first suggested with the discovery of phage OMKO1, which binds to the outer membrane porin protein OprM during infection of P. aeruginosa. OprM forms the outer membrane channel of the multidrug efflux systems MexAB-OprM and MexXY-OprM. Under selection by OMKO1, spontaneous phage-resistant mutations in P. aeruginosa exhibited increased susceptibility to ciprofloxacin, tetracycline, ceftazidime, and erythromycin, likely due to reduced drug efflux capacity caused by altered or nonfunctional efflux pumps [24]. Thus, phages that target components of efflux systems can synergize with antibiotics that are substrates of those specific systems. Furthermore, phage-mediated antibiotic sensitization has been observed for phages that target cell envelope structures such as lipopolysaccharides (LPS) [26] and capsular polysaccharides [27], suggesting increased membrane permeability or improved drug target accessibility as a potential evolutionary mechanism for phage-antibiotic synergy.

Qin et al., [28] found that incubating Klebsiella pneumoniae with phage H5 alone produced phage-resistant mutants with increased metabolic activity and competitive fitness compared to an untreated control group. These mutants, which arose from missense mutations in wcaJ, a gene involved in capsule production, were more susceptible to ceftazidime.

Although some examples showed a direct rela-

tionship between loss of the phage receptor and antibiotic susceptibility, the heterogeneity of mutational responses to phage infection suggests that sensitization may also occur indirectly. Accordingly, researchers have proposed that mutations likely conferred phage resistance, while increased drug susceptibility may be associated with reduced antibiotic efflux. Collectively, these findings suggest that deploying phages targeting efflux-enhancing structures or entry determinants represents a novel and promising mode of phage-antibiotic synergy [28].

Alternatively, the synergistic effect observed in this study may be attributed to complementary mechanisms of action. Aminoglycosides such as streptomycin and neomycin inhibit bacterial protein synthesis by binding to the 30S ribosomal subunit. This growth inhibition may impair the bacterium's ability to mount effective defenses against phage infection, such as CRISPR-Cas system or receptor modifications, thereby facilitating phage replication. Oxytetracycline, a protein synthesis inhibitor also targeting the 30S subunit, likely operates through a similar principle, leading to a compromised physiological state. Additionally, at subinhibitory concentrations these antibiotics may induce mild membrane stress or alter cell surface architecture, potentially enhancing phage adsorption and genome injection [24]. These mechanisms are consistent with the well-established documented observations that antibiotics can potentiate phage therapy by weakening bacterial homeostasis and suppressing resistance mechanisms, resulting in a more effective combined bactericidal outcome.

Limitations

This study acknowledges several limitations. Firstly, the lack of transmission electron microscopy analysis precluded precise morphological classification of the phages, which is essential for taxonomic identification and understanding infection dynamics. Secondly, resource constraints prevented whole-genome sequencing of the phages. Such genomic data would be invaluable for assessing their lysogenic potential, identifying virulence factors, and assessing safety profiles. Finally, the findings derived based solely from in vitro assays; the absence of in vivo validation in a relevant animal model limits the translational relevance of our conclusions regarding therapeutic efficacy and safety within a complex biological system.

Materials & Methods

Declaration of Generative AI and AI-assisted technologies in the writing process

During the preparation of this manuscript, the authors used AI-assisted tools solely for language translation and grammatical phrasing. All scientific content, data interpretation, and conclusions are the original work of the authors.

Ethical approval

Ethical approval was provided by the College of Veterinary Medicine, Hama University, Hama, Syria (No. 479, Date 20/2/2024). Rectal fecal samples were obtained from animals without anesthesia or tranquilizers after obtaining the permission of the farmers.

Sample Collection

A total of 60 samples were collected from diarrheic calves (aged 1 day to 6 months) in different parts of the Hama governorate between July 2, 2024, to December 23, 2024. Samples consisted of swabs taken from affected animals, with one swab per animal inoculated directly into sterile tube containing peptone water. All samples were transferred to the laboratory for analysis on the same day.

Bacterial Isolation

Swabs were incubated on MacConkey agar (HiMedia®) at 37°C for 24 hours. Lactose-fermenting colonies were subcultured onto Eosin Methylene Blue (EMB) agar (HiMedia®) and re-incubated at 37°C for another 24 hours.

Colonies exhibiting a characteristic dark green metallic luster on EMB agar were considered presumptive *E. coli* positive and were subjected to secondary biochemical confirmation. The isolates were tested using a battery of biochemical tests: Indole, Methyl Red, Voges-Proskauer, and Citrate (IMViC) as enumerated by Gibbons et al. [29].

DNA Extraction

For DNA template preparation, 1-2 colonies from a pure isolate were transferred onto agar plates and were transferred into 50 µL sterile distilled water. The suspension was incubated in a boiling water bath for 10 minutes and centrifuged at 12,000 × g for 15 minutes. The resulting supernatant was carefully collected and used as the DNA template for the multiplex polymerase chain reaction (PCR) assay [17].

Multiplex Polymerase Chain Reaction (PCR)

Stx1 and Stx2 Shiga toxin genes were detected using specific primers, as shown in Table 5. The PCR reaction mixture comprised a total volume of 25 µL, containing the following components: 3 µL DNA template,1 µL forward and reverse primer each, 2.5 µL 10X PCR buffer, 1.5 µL Magnesium Chloride (25 mM), 0.5 µL dNTP mix (10 mM each), 0.5 µL Taq DNA polymerase (5 U/µL) and Nuclease-free water. Amplification was carried out using the Franck et al. [30] protocol with the following cycling conditions: Initial Denaturation: 94°C for 3 minutes, 30 cycles of) :Denaturation: 94°C for 30 seconds, Annealing: 50°C for 45 seconds, Extension: 72°C for 1.5 minutes (90 seconds) Final Extension: 72°C for 10 minutes.

Detection of PCR Amplicons

PCR products were analyzed by electrophoresis on a 2% agarose gel prepared in TBE buffer and stained with ethidium bromide (1 µg/mL). Electrophoresis was performed at 100 V for one hour. Gel was visualized using a UVIpro Platinum transilluminator equipped with a UV light source and a camera. Images were captured using the accompanying software. DNA bands corresponding to the expected amplicon sizes for each virulence factor (Table 5) were identified by comparison with a DNA molecular weight ladder.

Antibiotic Susceptibility Testing

Antibiotic susceptibility testing was performed using the Kirby-Bauer disc diffusion method on Muller-Hinton Agar. Bacterial suspensions were adjusted to a turbidity equivalent to a

Table 5.
Primers used in Shigatoxigenic *E. coli* gene detection (Franck et al., 1998)

Virulence factor		Primer sequence 5'-3'	Size of product (bp)
st_1	F	TTCGCTCTGCAATAGGTA	555
	R	TTCCCCAGTTCAATGTAAGAT	
st_2	F	GTGCCTGTTACTGGGTTTTTCTTC	118
	R	AGGGGTCGATATCTCTGTCC	

Table 6.
Antibiotics Used in Antimicrobial Susceptibility Testing of Shigatoxogenic *E. coli* Isolates

Antibiotic Name	Code	Concentration (µg/disc)
Ampicillin	Am	µg (10)
Ceftiofur	Cef	µg (30)
Ciprofloxacin	Cip	µg (5)
Enrofloxacin	Enr	µg (5)
Streptomycin	S	µg (10)
Gentamycin	Gen	µg (10)
Neomycin	N	µg (30)
Oxytetracycline	TE	µg (30)
Doxycycline	Do	µg (30)
pincillin G	P	µg (25)
Amoxicillin	Ax	µg (25)
Trimethoprim	Tm	µg (5)

0.5 McFarland standard and swabbed onto the agar plates. Antibiotic Unidiscs were aseptically located on the inoculated floor. The antibiotics tested, along with their concentrations and abbreviations, are listed in Table 6.

Plates were incubated at 37°C for 24 hours. Following incubation, the diameter of the zone of inhibition around each antibiotic disc was measured in millimeters using a calibrated ruler. Results were interpreted according to the Clinical and Laboratory Standards Institute guidelines [31].

Isolation of E. coli Bacteriophages

Sample Collection and Processing

Twenty wastewater samples (n = 20) were collected from dairy cattle barns in the study region for the isolation of *E. coli*-specific bacteriophages. Samples were transported under refrigeration (4°C) and processed immediately. Solid particulates were suspended in 100 mL of sterile peptone water, filtered through coarse filter paper, and then centrifuged at 2000 rpm for 15 minutes to remove coarse debris. The supernatant was sequentially filtered through 0.8 µm, 0.45 µm, and 0.22 µm membrane filters [32] to obtain a bacteria-free phage lysate. Following three consecutive cycles of plaque purification, a single, well-isolated phage clone was selected for all subsequent synergy experiments.

Host Bacterial Culture

E. coli isolates, originally obtained from diarrheic calves, were cultured in Nutrient Broth, and incubated at 37°C. These cultures served as the host bacteria for phage propagation and isolation [33].

Plaque Assay and Phage Isolation

Double agar overlay technique was employed for phage isolation. A base layer of nutrient agar supplemented with calcium nitrate was prepared in sterile Petri dishes. For the overlay, 300 µL of filtered phage lysate was mixed with 300 µL of host *E. coli* culture and incubated at 37°C for 10 minutes with constant agitation. This mixture was then blended with 3 mL of soft agar and overlaid on the base layer of agar. Plates were incubated at 37°C for 48 hours post solidification. Clear zones of lysis (plaques), indicative of bacteriophage activity, were observed [34, 35, 36].

Phage Purification and Propagation

Single plaques were purified using the method described by Kobayashi and Palumbo [34]. A single plaque was picked using a sterile cork borer and inoculated into a sterile 100 mL PYCA peptone-yeast extract and calcium nitrate broth tube, containing 5 mL of pre-cultured host *E. coli*. The tube was vortexed for 30 seconds to release phages and incubated at 37°C for 48 hours. The resulting lysate was centrifuged at 2000 rpm for 15 minutes to remove bacterial debris. The supernatant was filtered successively through 0.45 µm and 0.22 µm filters and stored at 4°C.

Phage Spot Assay

An *E. coli* bacterial suspension, adjusted to a 0.5 McFarland standard, was spread onto Mueller-Hinton agar plates. A 10 µL droplet of phage lysate was then spotted directly onto the inoculated agar surface. After allowing the droplet to absorb briefly, plates were inverted and incubated at 37°C for 24 hours. Following incubation, the presence of plaques was assessed, and any observed plaques were purified [35].

Phage Titration

Phage titers were determined using the double agar overlay technique. Ten-fold serial dilutions were prepared by adding 100 µL of phage stock to 900 µL of PYCA broth. For each dilution, 300 µL was added to 300 µL of an 18-hour log-phase host *E. coli* culture, incubated for 10 minutes, and then combined with 3 mL of soft agar. This mixture was overlaid onto base agar plates and incubated at 37°C for 24 hours. Plates exhibiting 100–200 plaques were selected, and phage titer was expressed as Plaque-Forming Units per mL (PFU/mL) [35].

Synergistic Effect Between Bacteriophages and Antibiotics

The synergistic activity between the isolated coliphage and three antibiotics (neomycin, oxytetracycline, streptomycin) was evaluated using a quantitative checkerboard method in 96-well microtiter plates. Working concentrations of both phage and antibiotics were prepared from stock solutions using the standard dilution formula ($C_1V_1 = C_2V_2$). Two-fold serial dilutions of each antibiotic were combined with ten-fold serial dilutions of the phage across the plate matrix, according to established protocols [37]. Bacterial growth was assessed after 24 hours of incubation at 37°C. Instead of turbidity measurements, synergy was quantified by determining viable bacterial counts (CFU/mL) through ten-fold serial dilutions from each well and plating on Eosin Methylene Blue (EMB) agar [38].

The Fractional Bactericidal Concentration Index (FBCI) was calculated using the following formula [39]:

FBCI = (MBC A+Ph / MBC A) + (MBC Ph+A / MBC Ph)

Where:

- MBC A+Ph: Minimum Bactericidal Concentration (MBC) of the antibiotic when combined with the phage.
- MBC A: Minimum Bactericidal Concentration (MBC) of the antibiotic when used alone.
- MBC Ph+A: Minimum Bactericidal Concentration (MBC) of the phage when combined with the antibiotic.
- MBC Ph: Minimum Bactericidal Concentration (MBC) of the phage when used alone.

Interpretation of the FBCI value

- FBCI ≤ 0.5: Synergistic bactericidal effect (Synergy).
- 0.5 < FBCI ≤ 1: Additive bactericidal effect (Additive).
- 1 < FBCI ≤ 2: No interaction (Indifference).
- FBCI > 2: Antagonistic effect (Antagonism).

Statistical analysis

Data processing and graphical representation were performed using Microsoft Excel 2019 and GraphPad Prism (v8.2.1).

Authors' Contributions

Aseem Keder Albaker is the primary researcher, implementer, and writer of the research, as this research is part of the doctoral thesis that is currently being prepared. Dr. Maher Saleh supervises the research as a scientific supervisor and assistant in directing and writing the thesis, and Dr. Ashraf Alaaleh is the assistant practical supervisor during the implementation of the research.

Acknowledgements

This study was funded by Eagle For Veterinary Medicines and Feed Additives.

Conflict of interest

The authors declare that there is no conflict of interest.

References

1. Foster DM, Smith GW. Pathophysiology of diarrhea in calves. Vet Clin North Am Food Anim Pract. 2009;25:13–36. Doi:10.1016/j.cvfa.2008.10.013.
2. Abdulridha RN, Ibrahim OMS. Activity Of Bacterial Antibiotics Against Some Pathogenic Bacteria Isolated From Calves Diarrhoea In Baghdad (PartI). Iraqi Journal of Agricultural Sciences. 2018;49(5):248-54. Doi:10.36103/ijas.v49i5.45.
3. Munita JM, Arias CA. Mechanisms of antibiotic resistance. Microbiol Spectr. 2016;4(2):4-2. Doi: 10.1128/microbiolspec.VMBF-0016-2015.
4. Sobierajski T, Mazińska B, Chajęcka-Wierzchowska W, Śmiałek M, Hryniewicz W. Antimicrobial and antibiotic resistance from the perspective of Polish veterinary students: an inter-university study. Antibiotics (Basel). 2022;11(1):115. Doi:10.3390/antibiotics11010115.
5. OIE. Antimicrobial Resistance. World Organization for Animal Health. 2015. www.oie.int. Accessed 22 May 2016.
6. Al wendawi SH, Al Rekaby SM. The Effeciency Of Enteric Lactobacillus In Preventing Hemorrhagic Colitis And Blocking Shiga Toxins Productions In Rats Models Infected With Enterohemorrhagic Escherichia Coli (EHEC). Iraqi Journal of Agricultural Sciences. 2021;52(6):1346-55. Doi:10.36103/ijas.v52i6.1474.
7. Majda B, Barchan AA, Aarab A, Bakkali M, Arakrak A, Laglaoui A. Evaluation Of The Antibacterial Activity Of Essential Oils Against E. Coli Isolated From Rabbits. Iraqi Journal of Agricultural Sciences. 2022;53(4):802-9. Doi:10.36103/ijas.v53i4.1592.
8. Oechslin F. Resistance development to bacteriophages occurring during bacteriophage therapy. Viruses. 2018;10(7):1-23. Doi:10.3390/v10070351.
9. Marwa Sh, Ibrahim MAH. Correlation Between Antibiotic Resistance Phenotypes With Mobile Genetic Elements (Integron Class I) In Uropathogenic E. Coli. Iraqi Journal of Agricultural Sciences. 2024;55(4):1280-91. Doi:10.36103/shxqpf87.
10. Keen EC. A century of phage research: bacteriophages and the shaping of modern biology. Bioessays. 2015;37:6–9. Doi: 10.1002/bies.201400152.
11. Hesse S, Adhya S. Phage therapy in the twenty-first century: facing the decline of the antibiotic era; is it finally time for the age of the phage? Annu Rev Microbiol. 2019;73:155–74. Doi:10.1146/annurev-micro-090817-062535.
12. McCallin S, Sacher JC, Zheng J, Chan BK. Current state of compassionate phage therapy. Viruses. 2019;11:1–14. Doi: 10.3390/v11040343.
13. Payne RJ, Phil D, Jansen VA. Phage therapy: the peculiar kinetics of self-replicating pharmaceuticals. Clin Pharmacol Ther. 2000;68:225–30. Doi:10.1067/mcp.2000.109520.
14. FDA (US Food and Drug Administration). Food additives permitted for direct addition to food for human consumption; bacteriophage preparation. Silver Spring, MD: US Food and Drug Administration; 2006.
15. Wang L, Bai Y, Shi X, Zheng X, Liu Y, Zhang Y, et al. The Virulence Gene and Drug Resistance Analysis of Shiga Toxin-Producing Escherichia coli from Diarrhea Calves in Xinjiang, China. Foodborne Pathog Dis. 2025. Doi:10.1089/fpd.2024.0056.
16. Nguyen TD, Vo TT, Vu-Khac H. Virulence factors in Escherichia coli isolated from calves with diarrhea in Vietnam. J Vet Sci. 2011;12(2):159-64. Doi:10.4142/jvs.2011.12.2.159.
17. Cengiz S, Adigüzel MC. Determination of virulence factors and antimicrobial resistance of E. coli isolated from calf diarrhea, part of eastern Turkey. Ankara Univ Vet Fak Derg.

2020;67(3):365–71. Doi:10.33988/auvfd.640990.

18. Wang Z, Sun M, Guo S, Wang Y, Meng L, Shi J, et al. Detection of drug resistance in Escherichia coli from calves with diarrhea in the Tongliao region: an analysis of multidrug-resistant strains. Front Vet Sci. 2024;11:1466690. Doi:10.3389/fvets.2024.1466690.

19. Ibrahim HS, Abdelhamed GS, Elgohary AH, Fathi M. Relationship between virulence and antibiotic resistant genes in some Gram negative bacteria causing diarrhea in calves. J Adv Vet Res. 2025;15(1):6-12. Available from: https://advetresearch.com/index.php/AVR/article/view/2055.

20. Narulita E, Aji GP, Wahono B, Murdiyah S, Yulian R. Synergism of Phage ϕPT1b and Antibiotics for Reducing Infection of Escherichia coli. Biogenesis. 2020;8:22-8. Doi:10.24252/bio.v8i1.11280.

21. Moradpour Z, Yousefi N, Sadeghi D, Ghasemian A. Synergistic bactericidal activity of a naturally isolated phage and ampicillin against urinary tract infecting Escherichia coli O157. Iran J Basic Med Sci. 2020;23:257-63. Doi:10.22038/ijbms.2019.37561.8989.

22. Shamsuzzaman M, Kim S, Kim J. Therapeutic potential of novel phages with antibiotic combinations against ESBL-producing and carbapenem-resistant Escherichia Coli. J Glob Antimicrob Resist. 2025;43:86–97. DOI: https://doi.org/10.1016/j.jgar.2025.04.005.

23. Supina BSI, Dennis JJ. The Current Landscape of Phage–Antibiotic Synergistic (PAS) Interactions. Antibiotics. 2025;14:545. Doi:10.3390/antibiotics14060545.

24. Chan BK, Sistrom M, Wertz JE, Kortright KE, Narayan D, Turner PE. Phage selection restores antibiotic sensitivity in MDR Pseudomonas aeruginosa. Sci Rep. 2016;6:26717. Doi:10.1038/srep26717.

25. Chen Q, Dharmaraj T, Cai PC, Burgener EB, Haddock NL, Spakowitz AJ, et al. Bacteriophage and bacterial susceptibility, resistance, and tolerance to antibiotics. Pharmaceutics. 2022;14(7):1425. Doi:10.3390/pharmaceutics14071425.

26. Ruest MK, Supina BSI, Dennis JJ. Bacteriophage steering of Burkholderia cenocepacia toward reduced virulence and increased antibiotic sensitivity. J Bacteriol. 2023;205(12):e00196-23. Doi:10.1128/jb.00196-23.

27. Wang X, Loh B, Gordillo Altamirano F, Yu Y, Hua X, Leptihn S. Colistin-phage combinations decrease antibiotic resistance in Acinetobacter baumannii via changes in envelope architecture. Emerg Microbes Infect. 2021;10(1):2205-19. Doi:10.1080/22221751.2021.2002671.

28. Qin K, Shi X, Yang K, Xu Q, Wang F, Chen S, et al. Phage-antibiotic synergy suppresses resistance emergence of Klebsiella pneumoniae by altering the evolutionary fitness. mBio. 2024;15(2):e01393-24. Doi:10.1128/mbio.01393-24.

29. Gibbons JF, Boland F, Buckley JF, et al. Patterns of antimicrobial resistance in pathogenic Escherichia coli isolates from cases of calf enteritis during the spring-calving season. Vet Microbiol. 2014;170:73-80. Doi:10.1016/j.vetmic.2014.01.010.

30. Franck SM, Bosworth BT, Moon HW. Multiplex PCR for enterotoxigenic, attaching and effacing, and Shiga toxin-producing Escherichia coli strains from calves. J Clin Microbiol. 1998;36(6):1795–7. Doi:10.1128/jcm.36.6.1795-1797.1998.

31. CLSI. Performance standards for antimicrobial susceptibility testing. 30th ed. CLSI supplement M100. Wayne, PA: Clinical and Laboratory Standard Institute; 2020.

32. Beaudoin R, DeCesaro D, Durkee D, Barbaro S. Isolation of a Bacteriophage From Sewage Sludge and characterization of its bacterial host cell. Rivier Academic Journal. 2007;3(1):1-8.

33. Alexyuk P, Bogoyavlenskiy A, Alexyuk M, Akanova K, Moldakhanov Y, Berezin V. Isolation and Characterization of Lytic Bacteriophages Active against Clinical Strains of E. coli and Development of a Phage Antimicrobial Cocktail. Viruses. 2022;14(11):2381. Doi:10.3390/v14112381.

34. Kobayashi DY, Palumbo JD. Bacterial endophytes and their effects on plants and uses in agriculture. In: Bacon CW, White JF, editors. Microbial Endophytes. New York, USA: Marcel Dekker, Inc.; 2000.

35. Pallavali RR, Degati VL, Lomada D, Reddy MC, Durbaka VRP. Isolation and in vitro evaluation of bacteriophages against MDR bacterial isolates from septic wound infections. PLoS One. 2017;12(7):1-16. Doi:10.1371/journal.pone.0179245.

36. Santos SB, Carvalho CM, Sillankorva S, Nicolau A, Ferreira EC, Azeredo J. The use of antibiotics to improve phage detection and enumeration by the double-layer agar technique. BMC Microbiol. 2009;9(1):1-10. Doi:10.1186/1471-2180-9-148.

37. Gu Liu C, Green SI, Min L, Clark JR, Salazar KC, Terwilliger AL, et al. Phageantibiotic synergy is driven by a unique combination of antibacterial mechanism of action and stoichiometry. mBio. 2020;11:e01462-20. Doi:10.1128/mbio.01462-20.

38. Cheesbrough M. Medical Laboratory Manual for Tropical Countries. 1st ed. London: English Language Book Society; 1987. p. 400–480.

39. Moody, J. Synergism testing: Broth microdilution checkerboard and broth macrodilution method. In Clinical Microbiology Procedures Handbook; ASM Press: Washington, DC, USA, 2004; 1–28.

40. Labrie SJ, Samson JE, Moineau S. Bacteriophage resistance mechanisms. Nat Rev Microbiol. 2010;8(5):317-27.

41. Andrade GI, Coura FM, Santos EL, Ferreira MG, Galinari GC, Facury Filho EJ, et al. Identification of virulence factors by multiplex PCR in Escherichia coli isolated from calves in Minas Gerais, Brazil. Trop Anim Health Prod. 2012;44(7):1783-90. Doi:10.1007/s11250-012-0139-8.

How to cite this article
Albaker A.K, Saleh M , Alaaleh A. Synergisric effects of bacteriophages and antibiotics against Shiga toxigenic *Escherichia Coli* isolatrd from diarrheic calves. Iran J Vet Sci Technol.2026; 18(2): 68-79.
DOI: https://doi.org/10.22067/ijvst.2026.96481.1617
URL:https://ijvst.um.ac.ir/article_47907.html

Iranian Journal of Veterinary Science and Technology

Received: 2025- Sep-07
Accepted after revision: 2026- Feb-09
Published online: 2026- Feb- 10

Case Report

DOI:10.22067/ijvst.2026.94756.1591

Non-Surgical Resolution of Dystocia in a Captive Zebra (*Equus quagga*) Due to Fetal Malposture

Muhammad Usman Mehmood[a], Shahid Ali[a], Shahzad Akram[b], Madia Ashraf[c], Abdul Sattar[a]

[a] Department of Theriogenology, Faculty of Veterinary Sciences, University of Veterinary and Animal Sciences, Lahore, Pakistan.
[b] Department of Veterinary Biosciences, Faculty of Veterinary Medicine, Chiang Mai University, Chiang Mai, Thailand.
[c] Lahore Zoological Garden, Shahrah-e-Quid-e-Azam, Lahore, Pakistan.

ABSTRACT

Dystocia can pose serious obstetrical problems, especially if it results from fetal malposition, although it is not rare in mares. This report details an uncommon case of dystocia in a four-year-old captive plains zebra (*Equus quagga*) at Lahore Zoo in Pakistan. The mare was diagnosed with anterior longitudinal presentation, dorsopubic position, and posture deficits, including significant lateral deviation of the head and bilateral carpal flexion, after displaying symptoms of prolonged second-stage labor of 10-12 hours. After examination, the fetus was determined to be deceased. Obstetrical correction was accomplished through mutation, repulsion, and forced extraction under general anesthesia administered via remote darting. This manual correction, completed in approximately four hours, and facilitated a successful vaginal delivery, without the need for a fetotomy or cesarean surgery. Post-procedure care included antibiotics, anti-inflammatory drugs, and fluid therapy. The mare recovered without any injuries to the reproductive tract or retained fetal membranes. To our knowledge, this is the first documented case of successful assisted vaginal delivery for dystocia in a zebra in Pakistan, offering valuable clinical insights for managing similar obstetric situations in equids and other wildlife species.

Keywords

Fetal malposition, Dystocia, Mutation, Forced extraction, Zebra

Number of Figures: 1
Number of Tables: 0
Number of References:: 17
Number of Pages: 5

Abbreviations

UVAS: University of Veterinary and Animal Sciences
NSAIDs: Nonsteroidal anti-inflammatory drugs

Corresponding author:
Muhammad Usman Mehmood
Email: usman.mehmood@uvas.edu.pk
Tel: +92(33)4612-6693

Introduction

Zebras belong to the genus Equus and include four species: the plains zebra (*Equus quagga*), Cape mountain zebra (*Equus zebra*), Hartmann's mountain zebra (*Equus hartmannae*), and Grevy's zebra (*Equus grevyi*) [1]. The most geographically widespread specie is the plains zebra, also known as Burchell's or common zebra, ranging from eastern South Africa to southern Ethiopia and South Sudan [1]. Despite their adaptability, human encroachment, habitat degradation, and competition with livestock pose risks to plains zebras, which has resulted in a drop in their population, leading to their classification as near threatened and raising conservation concerns [1].

Mares usually reach puberty between 1 and 3 years of age [2, 3], with first estrus occurring around 2–3 years. The gestation period ranges from 361-396 days [4], and first foaling occurs at 3-4 years of age [3]. Parturition commonly occurs during the early morning hours [5]. Although, dystocia is relatively rare in mares, it represents a true veterinary emergency and needs to be treated promptly due to risks to both the mare and fetus [6]. The most frequent cause of dystocia in mares is malposition from normal alignments, especially postural abnormalities, while anterior presentation, dorsal position, extension of the limbs and head posture are normal [7]. Approximately 99% of parturition occurs in the anterior presentation. Williams [8] and Noakes, Parkinson [9] reported that there is 1.1 % incidence of dystocia in equines. This report describes a case of dystocia in a four-year-old captive plains zebra mare (*Equus quagga*) housed at Lahore Zoo, Punjab, Pakistan. In thai case, dystocia resulted from fetal malposition, a commom cause in equids, leading to a challenging condition but ultimately successful manual correction was performed.

Case Presentation

The administration of Lahore Zoo requested assistance from the University of Veterinary and Animal Sciences (UVAS), Lahore, Pakistan, to manage a suspected case of dystocia in a captive zebra. A clinical team from UVAS arrived at the zoo (90 Mall Road, Lahore, Punjab, Pakistan; 31.556°N, 74.325°E) in the afternoon. Feeding and drinking of the animal were compromised. The affected animal was a four-year-old plains zebra (*Equus quagga*) mare exhibiting symptoms of prolonged labor. According to zoo staff, the mare's water broke earlier that morning but no progress toward delivery had occurred by afternoon.

This was the mare's first parturition. Upon physical examination, the animal appeared to be standing but dull, depressed, and exhibited a staggering gait. Vaginal examination indicated completion of the first stage of laber, but the second stage had been prolonged for 10-12 hours without progress. The mare was struggling continuously. Clinical signs included sacrosciatic ligaments relaxation, vulvar edema, and ruptured fetal membranes. During the initial obstetrical assessment, fetal viability, orientation, and condition of the birth canal were evaluated. The fetus was confirmed dead based on the absence of reflexes such as suckling and pedal response. Detailed palpation revealed an anterior longitudinal presentation, dorsopubic position, and multiple postural defects, including carpal flexion of both forelimbs and severe lateral deviation of the head. The diagnosis of dystocia related to fetal malposition was confirmed by these abnormalities.

Obstetrical procedure and treatment

General anesthesia was administered via remote darting (Figure 1. A) using a Teleinject Vario 4 system. Butorphanol (0.01 mg/kg; total 120 mg) and detomidine (0.1 mg/kg; total 50 mg) were administered for induction. The mare was kept under anesthesia after sedation with intravenous boluses of xylazine (500 mg) and ketamine (1,500 mg) [10]. dart placement targeted the heavy thigh musculature using an 18-gauge, 1.5-inch specialized needle [11]. Because of the low musculature and risk of injury, darting in the thoracic or abdominal regions was avoided. The darting area was inspected for rough ground, pools of water, debris and fencing. To reduce the risk of capture myopathy, the procedure was performed in a quiet, enclosed stall free of obstacles. After the dart was fired (Figure 1. A), the dart stuck effectively in the animal's muscle. Sedation took effect within 20 to 25 minutes, and the dart successfully discharged and detached appropriately. The mare was examined for external abnormalities such as sarcoids [12], hoof deformities, mucous membrane state, and oral health prior to the obstetrical intervention. Additional ketamine boluses (100–200 mg IV) were administered as needed to prolong the anesthesia [10]. Intravenous glucose-saline (1,500 ml) was provided to address dehydration and support energy requirements.

Obstetrical correction began with mutation to address the fetal postural defects. Both forelimbs were flexed at the carpal joints. To provide additional working space, the fetus was gently repelled into the uterus. Flexion of the left carpus was converted to fetlock flexion. The proximal metacarpus was oriented laterally, and the hoof was manually cupped and rotated medially. An obstetrical chain (Figure 1. C) was used to secure the limb once it had been stretched. The right limb was corrected using the same tech-

nique. Both legs were pushed back into the birth canal. The head showed severe rightward deviation. A soft rope was used to snare the head at the mandible, a gentle repulsion allowed improved access. Controlled upward traction realigned the head, after which both limbs were simultaneously tractioned. After some time, legs and head were correctly positioned on the pelvic floor. Copious amounts of obstetrical lubricant was applied to minimize trauma or reduce the risk of uterine rupture by rotating the fetus around its longitudinal axis into the dorsosacral position. Final traction was applied in a horizontal, downward, and posterior direction toward the hock joints (Figure 1. C). After approximately two hours, the fetus was successfully delivered vaginally. The foal weighed 35 kg and displayed a typical neonatal zebra coat pattern of brown and white (Figure 1. D).

The mare received supportive therapy during recovery, which included a second 1,500 ml glucose-saline infusion and multivitamins (Amivicom, 30 ml). Ceftiofur hydrochloride (1.1–2.2 mg/kg; total 7 ml) was administered to prevent the infection. Systemic non-steroidal anti-inflammatory drugs (NSAIDs) were administered to treat pain (5 ml, 2–4.4 mg/kg). The mare regained the ability to stand without assistance roughly four hours after treatment began. Post procedure care included continued administration of phenylbutazone (2.2–4.4 mg/kg IV every 12 hours for 48–96 hours, then decreased and continued for 5 days) and ceftiofur (1.1-2.2 mg/kg, for 5 days). An antispasmodic drug (Spasfon) was administered as a preventative measure since lateral recumbency during sedation carries a risk of colic.

Results & Discussion

Dystocia in mare is less common than in other domestic animals, but when it occurs, it is a serious obstetrical emergency that needs to be treated immediately [6, 13]. There is less documentation regarding dystocia in mares [14]. The most common cause of dystocia in equines is postural abnormality, especially lateral deviation of the head. Although other presentation and positional abnormalities can also contribute, they are observed less frequently [9]. Fetotomy is frequently necessary in these situations in order to protect the mare's life and future reproductive poten-

Figure 1.
Stages of Dystocia Management in a Zebra (*Equus quagga*)
(a) Chemical immobilization (darting) using a remote injection system; (b) Physical restraint for clinical examination; (c) Manual forced extraction of the malpositioned fetus; (d) Outcome showing the dead foal post-extraction.

tial [9]. Despite its effectiveness, cesarean section poses additional risks, including decreased post-surgical fertility, uterine laceration, retained fetal membranes, laminitis, metritis, and peritonitis [6, 15]. An assisted vaginal delivery using mutation, repulsion, and controlled extraction may be preferable to cesarean section when fetal viability is lost and surgical facilities are unavailable [6, 16]. Furthermore, the availability of surgical facilities, fetal state, gestational age, and the veterinary team's experience must all be taken into account while making decisions. In equine, assisted vaginal delivery or fetotomy is often favored over cesarean section due to lower risks of mare mortality, retained placenta and reduced fertility [17].

In the present case, multiple fetal abnormalities, including dorsopubic positioning, bilateral carpal flexion, and extreme lateral displacement of the head, resulted in dystocia. Despite the complexity of dystocia caused by these combined abnormalities, resolution was achieved without recourse to cesarean section or fetotomy. Successful manual correction was facilitated by timely intervention, accurate diagnosis, appropriate sedation, and skilled obstetrical manipulation. The use of remote dart administered anesthesia was particularly important given the wildlife context and was well tolerated without significant complications. To the authors' knowledge, represents the first documented case in Pakistan of dystocia in a captive plains zebra successfully managed via assisted vaginal delivery. No post delivery complications such as retained fetal membranes, vaginal lacerations, or laminitis were observed. This case highlights the potential of non-surgical management of complex dystocia in wild equids under field conditions and provides practical guidance for wildlife veterinarians confronted with similar scenarios.

Conclusion

This case demonstrates that even complex dystocia in zebras resulting from fetal malposition can be successfully treated through mutation and controlled extraction without the need for a fetotomy or cesarean section. The positive outcome was largely dependent on early diagnosis, appropriate anesthesia, skilled obstetrical manipulation, and attentive supportive care. Beyond adding to the limited literature on dystocia in wild equids, this report provides useful guidance for veterinarians managing similar cases in wild equines in field conditions, this article contributes to the scant literature on equine dystocia.

Authors' Contributions

The case of this mare was first attended by M.U.M., S. Ali, M.A. and A.S. after thorough obstetrical examination it was decided to perform manual correction and assisted vaginal delivery. Consequently, M.U.M., M.A. and S. Akram conceived the idea of reporting the procedure and findings for this case. M.U.M., S. Akram and M.A. equally contributed on this case report–research; manuscript drafting; M.U.M. and A.S. equally contributed on patient care and monitoring. All authors have checked the final draft.

Acknowledgements

The authors extend their sincere gratitude to the administration of Lahore Zoo for their cooperation, provision of necessary resources and timely communication during this emergency case. The successful completion of the obstetrical intervention and safe handling of the animal were made possible by their proactive help. Without their support and dedication to animal welfare, this case could not have been resolved successfully.

Conflict of interest

The authors declare that there is no conflict of interest.

References

1. King S, Moehlman P. Equus quagga. The IUCN Red List of Threatened Species 2016: e. T41013A45172424. 2021. Doi:10.2305/IUCN.UK.2016.

2. Klingel H. Notes on the biology of the plains zebra Equus quagga boehmi Matschie. African Journal of Ecology. 1965;3(1):86-8. Doi:10.1111/j.1365-2028.1965.tb00739.x.

3. Smuts G. Reproduction in the zebra stallion (Equus burchelli antiquorum) from the Kruger National Park. African Zoology. 1976;11(1):207-20. Doi:10.1080/00445096.1976.11447525.

4. Nunez CM, Asa CS, Rubenstein DI. Zebra reproduction. Equine reproduction 2nd ed Wiley-Blackwell, Ames, IA2011. p. 2851-65. Doi:10.1111/j.1751-0813.2012.00920.x.

5. Wackernagel H. GRANT'S ZEBRA, Equus burchelli boehmi, AT BASLE ZOO-A CONTRIBUTION TO BREEDING BIOLOGY. International Zoo Yearbook. 1965;5(1):38-41. Doi:10.1111/j.1748-1090.1965.tb01567.x.

6. Freeman D, Hungerford L, Schaeffer D, Lock T, Sertich P, Baker G, et al. Caesarean section and other methods for assisted delivery: comparison of effects on mare mortality and complications. Equine veterinary journal. 1999;31(3):203-7.

Doi:10.1111/j.2042-3306.1999.tb03173.x.

7. Freeman D, Hungerford L, Schaeffer D, Lock T, Sertich P, Baker G, et al. Caesarean section and other methods for assisted delivery: comparison of effects on mare mortality and complications. Equine veterinary journal. 1999;31(3):203-7. Doi:10.1111/j.2042-3306.1999.tb03173.x.

8. Williams WL. Veterinary obstetrics: The author; 1917.

9. Noakes DE, Parkinson TJ, England GC. Veterinary reproduction and obstetrics 2009. Doi:10.1016/C2014-0-04782-X.

10. Wiedner EB, Lindsay WA, Isaza R. Management of zebras and zebra hybrids (zebroids). Compend Contin Educ Vet. 2012;34(9):E4. PMID: 23705207.

11. Allen JL. Immobilization of Hartmann's mountain zebras (Equus zebra hartmannae) with carfentanil and antagonism with naltrexone or nalmefene. Journal of Zoo and Wildlife Medicine. 1994:205-8. Doi:10.1109/CSR-SWTC60855.2023.10427260.

12. Bergvall KE. Sarcoids. Veterinary Clinics: Equine Practice. 2013;29(3):657-71.Doi:10.1016/j.cveq.2013.09.002.

13. Lu KG, Barr BS, Embertson R, Schaer BD. DystociaA true equine emergency. Clinical Techniques in Equine Practice. 2006;5(2):145-53. Doi:10.1053/j.ctep.2006.03.008.

14. Jeffcott L, Rossdale P. A critical review of current methods for induction of parturition in the mare. Equine veterinary journal. 1977;9(4):208-15. Doi:10.1111/j.2042-3306.1977.tb04033.x.

15. Carluccio A, Contri A, Tosi U, De Amicis I, De Fanti C. Survival rate and short-term fertility rate associated with the use of fetotomy for resolution of dystocia in mares: 72 cases (19912005). Journal of the American Veterinary Medical Association. 2007;230(10):1502-5. Doi:10.2460/javma.230.10.1502.

16. Walters K. Obstetrics: Mutation, Forced Extraction, and Fetotomy. Bovine Reproduction2021. p. 608-18. Doi:10.1002/9781119602484.ch51.

17. Maaskant A, De Bruijn C, Schutrups A, Stout T. Dystocia in Friesian mares: Prevalence, causes and outcome following caesarean section. Equine Veterinary Education. 2010;22(4):190-5. Doi:10.1111/j.2042-3292.2010.00046.x.

How to cite this article
Mehmood MU, Ali Sh, Akram Sh, Ashraf M, Sattar A. Non-Surgical Resolution of Dystocia in a Captive Zebra (*Equus quagga*) Due to Fetal Malposture. Iran J Vet Sci Technol.2026; 18(2): 80-84.
DOI: https://doi.org/10.22067/ijvst.2026.94756.1591
URL: https://ijvst.um.ac.ir/article_47905.html

Iranian Journal of Veterinary Science and Technology

Received: 2025- Sep-04
Accepted after revision: 2026- Feb-09
Published online: 2026-Feb-10

Abstracts (in Persian)

شناسایی مورفولوژیک و ملکولی گونه های شایع ایمریا درگوسفندان وبزهای شهرستان بجستان

محمد عبداللهی[1]، اسما کیوانلو[2]، غلامرضا رزمی[3]**

[1]دانش آموخته دکتری عمومی، دانشکده دامپزشکی، دانشگاه فردوسی مشهد، مشهد، ایران.
[2]دانش آموخته دکتری تخصصی انگل شناسی، دانشکده دامپزشکی، دانشگاه فردوسی مشهد، مشهد، ایران.
[3] گروه پاتوبیولوژی، دانشکده دامپزشکی، دانشگاه فردوسی مشهد، مشهد، ایران.

چکیده

کوکسیدیوزنوعی بیماری گوارشی است توسط گونه‌های ایمریا در نشخوارکنندگان کوچک ایجاد می‌شود. تاکنون طلاعات کمی در مورد گونه‌های ایمریا شناسایی شده در گله‌های گوسفند در استان خراسان رضوی وجود دارد. هدف از این تحقیق شناسایی گونه‌های رایج ایمریا و تشخیص گونه‌های بیماری‌زا در گله‌های گوسفند در منطقه بجستان است. از اکتبر ۲۰۲۱ تا ژوئن ۲۰۲۲، چهارصد نمونه مدفوع از رکتوم گوسفند و بز گرفته شد. نمونه‌های مدفوع ابتدا با روش ویلیس از نظر وجود آلودگی ایمریا بررسی شدند و سپس میزان OPG با استفاده از روش کلیتون لین تعیین گردید. نمونه‌هایی که OPG بالایی داشتند در محلول ۲/۵ ٪ دی کرومات پتاسیم کشت داده شدند. پس از هاگ‌دار شدن نمونه کشت داده شده، گونه ایمریا با استفاده از مشخصات مورفولوژیکی شناسایی شدند. همچنین، DNA اووسیست‌های ایمریای هاگ‌دار گوسفند و بز استخراج و با روشPCR مورد آزمایش قرار گرفتند. دو نمونه مثبت واجد واکنش قوی PCR از هر یک از این حیوانات انتخاب و برای تعیین توالی ارسال شدند. در این مطالعه، فراوانی آلودگی به آیمریا در گوسفندان ۶۹/۵ ٪ (۱۳۹/۲۰۰) و در بزها ۶۹ ٪ (۱۳۸/۲۰۰) بودند. در مطالعات ریخت‌شناسی، گونه‌های آیمریا فاوری و آیمریا اووینوئیدالیس در گوسفندان و گونه‌های آیمریا آلیجوی، آیمریا هیرسی و آیمریا کریستنسنی در بزها شناسایی شدند. نتایج PCR وجود آلودگی به آیمریا را در نمونه‌های مدفوع گوسفندان و بزها تأیید کرد. نتایج بدست امده نشان‌دهنده شیوع بالای آلودگی مخلوط گونه‌های آیمریا در گوسفندان و بزها در منطقه بجستان بود. همچنین فقط دو گونه آیمریا در گوسفندان و سه گونه در بزها از نظر ریخت‌شناسی شناسایی شدند.

واژگان کلیدی

میزان شیوع، شناسایی ، آیمریا، بز، گوسفند

* **نویسنده مسئول**: غلامرضا رزمی
razmi@um.ac.ir

Iranian Journal of Veterinary Science and Technology

Received: 2025- Jul-13
Accepted after revision: 2025- Nov-29
Published online: 2025-Dec-01

Abstracts (in Persian)

انفارکتوس–کرایو: روشی برگزیده برای ایجاد مدل رت انفارکتوس میوکارد

علیرضا کریمی[1]، مریم مقدم متین[1،2]، آزاده حقیقی طلب[1،3]، حسین کاظمی‌مهرجردی[4]، مسعود رجبیون[4]، مهرداد آقاسی‌زاده[1]، احمدرضا بهرامی*[1،2]

۱ گروه زیست‌شناسی، دانشکده علوم، دانشگاه فردوسی مشهد، مشهد، ایران.
۲ پژوهشکده فناوری زیستی، دانشگاه فردوسی مشهد، مشهد، ایران.
۳ گروه سلول‌های‌بنیادی و پزشکی‌بازساختی، جهاد دانشگاهی-خراسان رضوی، مشهد، ایران.
۴ گروه علوم‌بالینی، دانشکده دامپزشکی، دانشگاه فردوسی مشهد، مشهد، ایران.

چکیده

بستن شریان کرونری قدامی نزولی چپ (LAD) یکی از روش‌های رایج برای ایجاد انفارکتوس میوکارد (MI) در مدل‌های تجربی است، اما این روش با محدودیت‌هایی از جمله مرگ‌ومیر بالا، خونریزی بیش از حد و تغییرپذیری در اندازه انفارکتوس همراه است. انفارکتوس-کرایو به عنوان یک جایگزین نویدبخش مطرح شده که می‌تواند با بهبود بقا و افزایش تکرارپذیری، بر این چالش‌ها غلبه کند. در این مطالعه، هدف ما بررسی کارایی روش کرایو برای ایجاد یک مدل قابل اعتماد و عملی انفارکتوس میوکارد در رت بود. رت‌های نر بالغ ویستار تحت جراحی توراکوتومی و تهویه مکانیکی قرار گرفتند و MI به‌وسیله بستن LAD با گره یا با روش کرایو القا شد. اعتبارسنجی مدل با استفاده از رنگ‌آمیزی تری‌کروم‌ماسون و ایمونوفلورسانس، اندازه‌گیری سرمی تروپونین I و ارزیابی الکتروکاردیوگرافی انجام گرفت. شدت انفارکتوس نیز با اکوکاردیوگرافی سنجیده شد. یافته‌های حاصل از رنگ‌آمیزی هماتوکسیلین-ائوزین و تری‌کروم‌ماسون نشان داد که انفارکتوس-کرایو در مقایسه با لیگاسیون مرسوم، از نظر سادگی، کارایی و کاهش مرگ‌ومیر، مزایای قابل توجهی دارد. این نتایج پتانسیل انفارکتوس-کرایو را برای استفاده به‌عنوان یک رویکرد استاندارد در توسعه مدل‌های حیوانی مختلف برای تحقیقات پایه و کاربردی قلب و عروق برجسته می‌کند.

واژگان کلیدی

انفارکتوس میوکارد، انفارکتوس-کرایو، قلب، حیوان مدل

* **نویسنده مسئول**: احمدرضا بهرامی
ar-bahrami@um.ac.ir

Iranian Journal of Veterinary Science and Technology

Received: 2025-Jun-02
Accepted after revision: 2025-Nov-29
Published online: 2025-Dec-01

Abstracts (in Persian)

بیان ایمونوهیستوشیمیایی β-Catenin، E-cadherin ، EGFR و Ki67 در سگ‌های مبتلا به لیومیوسارکوم پوستی موضعی و مهاجم

فاطمه حیدرزاده[1]، امیر امنیت طلب*[2]

[1]گروه علوم درمانگاهی، دانشکده دامپزشکی، واحد ارومیه، دانشگاه آزاد اسلامی، ارومیه، ایران.
[2]گروه پاتولوژی، دانشکده دامپزشکی، واحد ارومیه، دانشگاه آزاد اسلامی، ارومیه، ایران.

چکیده

لیومیوسارکوم پوستی (LMS) یک تومور بدخیم عضلانی صاف نادر در سگ‌ها و انسان‌ها است که بالقوه از الیاف عضلانی صاف فولیکول‌های مو، عروق خونی یا بافت‌های تناسلی منشأ می‌گیرد. هدف از این مطالعه، بررسی شیوع، ویژگی‌های بالینی-آسیب‌شناختی، تغییرات هماتولوژیکی و خصوصیات ایمونوهیستوشیمیایی لیومیوسارکوم پوستی در سگ بود. در یک دوره ۱۰ ساله در ارومیه، ایران، شش مورد (سه مورد موضعی و سه مورد مهاجم) لیومیوسارکوم پوستی (LMS) از میان ۳۱۸ سگ با ضایعات پوستی شناسایی شد که نشان‌دهنده شیوع ۱.۸۸ ٪ بود. تجزیه و تحلیل هماتولوژیکی نشان‌دهنده لکوسیتوز (افزایش گلبول‌های سفید)، مونوسیتوز و ائوزینوفیلی معنی‌دار در سگ‌های مبتلا در مقایسه با سگ‌های سالم بود ($p < 0.05$). از نظر میکروسکوپی، طیفی از پلئومورفیسم سلولی و الیاف عضلانی صاف نئوپلاستیک در دسته‌های درهم‌تنیده با بافت همبند استرومای کم مشاهده شد. ایمونوهیستوشیمی (منفی برای MyoD1، Myogenin و CD31) وجود پیلولیومیوسارکوم را تأیید کرد. افزایش معنی‌داری ($p < 0.05$) در بیان مثبت و امتیاز H برای نشانگرهای Vimentin، SMA، Desminو Ki67 مشاهده شد. بیان EGFR و β-Catenin در گروه LMS موضعی به‌طور معنی‌داری در مقایسه با LMS مهاجم و بافت طبیعی افزایش یافت ($p < 0.05$) در حالی که بیان E-Cadherin تفاوت معنی‌داری در موارد LMS نشان نداد. این یافته‌ها نشان می‌دهد که EGFR محدود به تومورهای اپیتلیال نیست، بلکه در تومورهای مزانشیمی مانند LMS نیز بیان می‌شود. کاهش موارد LMS مهاجم نشان می‌دهد که افزایش تنظیمی EGFR ممکن است پیش از متاستاز رخ دهد. اگرچه بیان E-Cad-herin/β-Catenin به‌تنهایی ممکن است برای پیش‌آگهی کافی نباشد، ارزیابی ترکیبی آنها همراه با نشانگرهای تکثیری و مزانشیمی می‌تواند بینش ارزشمندی درباره مسیرهای تهاجم فراهم کند و به توسعه درمان‌های هدفمند علیه تومورهای مهاجم کمک کند.

واژگان کلیدی

لیومیوسارکوم پوستی، سگ، ایمونوهیستوشیمی، چسبندگی بین سلولی، تزاید

* **نویسنده مسئول**: امیر امنیت طلب
Amir.Amniattalab@iau.ac.ir

Iranian Journal of Veterinary Science and Technology

Received: 2025- Jul-30
Accepted after revision: 2025- Dec- 09
Published online: 2025-Dec-09

Abstracts (in Persian)

افزایش کارایی ضدمیکروبی نانوذرات لیپیدی جامد پروپولیس در برابر استافیلوکوکوس اورئوس مقاوم به متیسیلین جداشده از گوشت خام گاو

جعفر الهاشمی[۱]، امیر سالاری[۱]*، بسیما جاسیم محمد[۲]

[۱]گروه بهداشت مواد غذایی و آبزیان، دانشکده دامپزشکی، دانشگاه فردوسی مشهد، مشهد، ایران.

[۲]دانشکده دامپزشکی، دانشگاه القادسیه، عراق.

چکیده

استافیلوکوکوس اورئوس مقاوم به متی‌سیلین (MRSA) در گوشت گاو خام، با ایجاد عفونت‌های مقاوم، گسترش از طریق زنجیره‌های غذایی و ایجاد پل انتقال حیوان-انسان، سلامت عمومی را تهدید می‌کند. مقابله با آن نیازمند تلاش‌های هماهنگ در زمینه ایمنی مواد غذایی، کشاورزی و مراقبت‌های بهداشتی است. مواد و روش‌ها: ۱۱۲ نمونه گوشت گاو خام از سطح بیرونی بدون استخوان شانه و ران لاشه گاو گرفته شد. سپس استافیلوکوکوس اورئوس مقاوم به متی‌سیلین با روش‌های سنتی جداسازی شد. LNPs-PL با استفاده از تکنیک‌های فراصوت و همگن‌سازی با برش بالا تهیه شدند. راندمان کپسوله‌سازی، ظرفیت بارگیری و ویژگی‌های فیزیکوشیمیایی فرمولاسیون تولید شده ارزیابی شد. با استفاده از میکروسکوپ الکترونی روبشی (SEM)، مورفولوژی LNPs-PL بررسی شد. ترکیب شیمیایی روغن معمولی و LNPs-PL آزمایش شده با استفاده از آنالیز GC/MS ارزیابی شد. برای مقایسه فعالیت ضد باکتریایی LNPs-PL و PL معمولی، آزمایش‌های آزمایشگاهی انجام شد. نتایج: شیوع MRSA در بین نمونه‌های گوشت گاو خام ۵۰/۱۱۲ (۴۴.۶٪) بود. از ۵۰ جدایه MRSA (20/50 (40%)، *S. aureus*) بودند. نتایج فعالیت ضدمیکروبی LNPs-PL نشان داد که سطح مهار رشد روی باکتری MRSA به (۳۶ میلی‌متر) در مقایسه با (۱۴ میلی‌متر) بره موم (PL) افزایش یافته است. تفاوت بسیار معنی‌داری ($p < 0.01$) وجود دارد. LNPs-PL به طور قابل توجهی هاله‌های مهار رشد بزرگتری نسبت به PL نشان داد. نتیجه‌گیری: بر اساس یافته‌های این مطالعه، باید در ظرفیت بارگذاری، راندمان انکپسولاسیون و خواص فیزیکوشیمیایی اصلاحاتی انجام شود. یافته‌های ما تأیید کرد که SLNها حامل‌های PL مؤثری برای کنترل بیماری‌های باکتریایی و قارچی هستند و تحقیقات بیشتری در مورد آنها مورد نیاز است.

واژگان کلیدی

استافیلوکوکوس اورئوس مقاوم به متیسیلین، گوشت خام گاو، نانوذرات پروپولیس، کارایی ضد میکروبی، عوامل بیماریزای منتقله از غذا

* **نویسنده مسئول**: امیر سالاری
a-salari@um.ac.ir

Iranian Journal of Veterinary Science and Technology

Received: 2026- Jan- 24
Accepted after revision: 2026- Fen-20
Published online: 2026-Feb-21

Abstracts (in Persian)

ویژگی‌های تکنولوژیکی و حسی ماست تولید شده با باکتری‌های اسید لاکتیک جدا شده از ماست سنتی شرق افغانستان

سید عطاءالحق بنوری، عبدالله جمشیدی*، امیر سالاری

گروه بهداشت مواد غذایی و آبزیان، دانشکده دامپزشکی، دانشگاه فردوسی مشهد، مشهد، ایران.

چکیده

ماست‌های تخمیری سنتی منبع مهمی از باکتری‌های اسید لاکتیک بومی با خواص مطلوب تکنولوژیکی، حسی و سلامتی‌بخش هستند. با این حال، پتانسیل تکنولوژیکی باکتری های اسیدلاکتیک از ماست سنتی افغانستان تا حد زیادی ناشناخته مانده است. این مطالعه با هدف ارزیابی ویژگی‌های تکنولوژیکی و حسی باکتری های اسیدلاکتیک جدا شده از ماست‌های سنتی افغانستان انجام شد. در این راستا، چهار سویه ایمن باکتری های اسیدلاکتیک که از ماست سنتی افغانستان جدا شده بودند، در تولید ماست مورد استفاده قرار گرفتند و از طریق آزمایش‌های مبتنی بر سویه و محصول، تحت بررسی‌های تکنولوژیکی و حسی قرار گرفتند و با ماست تجاری کنترل مقایسه شدند. نتایج نشان داد که همه جدایه‌ها از نظر فعالیت آمیلولیتیک مثبت بودند و پاسخ‌های متفاوتی به تولید اگزوپلی‌ساکارید ها نشان دادند. همه سویه‌ها، به ویژه پدیوکوکوس اسیدیلاکتیسی (NSG2)، از نظر فعالیت‌های اسیدی، کاهش pH، اسیدیته قابل تیتراسیون و کاهش آب‌اندازی در مقایسه با گروه کنترل، پاسخ بهتری نشان دادند ($p < 0.05$). پارامترهای بافت هر چهار سویه به جز سفتی ماست در مقایسه با گروه کنترل، تفاوت معنی‌داری داشتند ($p < 0.05$). ارزیابی حسی توسط هر دو گروه متخصص و مصرف‌کننده نشان داد که ماست تولید شده با باکتری های اسیدلاکتیک بومی جدا شده از نمونه‌های ماست افغانی، عطر، بافت، طعم و پذیرش کلی بهتری را نشان داد. در نتیجه، همه جدایه‌های ماست سنتی افغانستان، به ویژه NSG2، ویژگی‌های تکنولوژیکی و حسی برجسته‌ای را نشان دادند که نشان‌دهنده پتانسیل آنها برای استفاده صنعتی است.

واژگان کلیدی

باکتری‌های اسید لاکتیک، ویژگی‌های تکنولوژیکی، ویژگی‌های حسی، ماست سنتی، افغانستان

* **نویسنده مسئول**: عبدا... جمشیدی
ajamshid@um.ac.ir

Iranian Journal of Veterinary Science and Technology

Received: 2025- Nov-29
Accepted after revision: 2026- Feb-02
Published online: 2026- Feb-02

Abstracts (in Persian)

بررسی بالینی، پاتولوژی، مولکولی و جداسازی مایکوپلاسما پولمونیس عامل مایکوپلاسموز تنفسی موشی در کلنی‌های یک مرکز تولید و پرورش حیوانات آزمایشگاهی

روزبه فلاحی*[1]، مجتبی محرمی[1]، محسن بشاشتی[2]، صغری بزرگی[1]

[1]بخش تحقیق، تولید و پرورش حیوانات آزمایشگاهی، مؤسسه تحقیقات واکسن و سرم سازی رازی، سازمان تحقیقات، آموزش و ترویج کشاورزی، کرج، ایران.
[2]بخش تحقیق، بیماریهای باکتریایی، انگلی و قارچی طیور، مؤسسه تحقیقات واکسن و سرم سازی رازی، سازمان تحقیقات، آموزش و ترویج کشاورزی، کرج، ایران.

چکیده

این مطالعه به منظور بررسی میزان شیوع آلودگی به مایکوپلاسما پولمونیس و بیماری حاصل از آن در طول شش ماه، در کلونی های یک مرکز تولید حیوانات آزمایشگاهی شامل رتها، موش، همسترها، خوکچههای هندی و خرگوشها انجام گرفت. ۶۶ نمونه از کلونی-های مختلف پرورشی برای کشت، تشخیص مولکولی (PCR) و بررسی آسیب شناسی تهیه گردید. نمونهبرداری از اندامهای درگیر در مواردی که حیوانات علائم بالینی را نشان میدادند، صورت گرفت. علائم بالینی شامل کج بودن سر و چرخاندن به سمت گوش آسیب دیده، ژولیده شدن پوشش بدن، ترشحات قرمز رنگ در چشمها و قلوه سنگی شدن ریهها در ۴ سر رت بالغ مشاهده شد. در روشPCR، در ۳۳ نمونه (۵۰ ٪) ، باندهای مثبت DNA که نشاندهنده آلودگی به مایکوپلاسما پولمونیس بودند، مشاهده گردید. در ۱۲ نمونه از کلونیهای رتها (۱۸ ٪ از کل نمونهها) نتایج کشت مثبت بود. در بررسیهای آسیب شناسی بافت ریه رت-ها، تغییراتی مانند آتلکتازی و برونشکتازی مشاهده گردید. از آنجاکه سیستم پرورش، از نوع متعارفی بوده است که در آن جریان هوای ورودی توسط یک دستگاه تهویه مطبوع معمولی تأمین میشود و نیز موانع محافظت کننده وجود ندارد، گسترش عفونت از رتهای آلوده به سایر حیوانات آزمایشگاهی، به سادگی صورت گرفته است. با این وجود، به دلیل عدم حساسیت این حیوانات به این میکروارگانیسم، هیچ نمونه مثبتی شناسایی نشد که نشاندهنده عدم وجود شرایط استرسزا یا مستعدکننده برای عفونتهای فرصتطلب مانند مایکوپلاسما پولمونیس میباشد. لذا پایش میکروبی منظم و دورهای برای عوامل عفونی مختلف توصیه می گردد.

واژگان کلیدی

مایکوپلاسما پولمونیس، حیوانات آزمایشگاهی، تشخیص، جداسازی، هیستوپاتولوژی

* **نویسنده مسئول**: روزبه فلاحی
r.fallahi@rvsri.ac.ir

Author Index

Author index

Guide for authors

SCOPE

Iranian journal of Veterinary Science and Technology (IJVST) publishes important research advances in veterinary medicine and subject areas relevant to veterinary medicine including anatomy, physiology, pharmacology, bacteriology, biochemistry, biotechnology, food hygiene, public health, immunology, molecular biology, parasitology, pathology, virology, large and small animal medicine, poultry diseases, diseases of equine species, and aquaculture. Articles can comprise research findings in basic sciences, as well as applied veterinary findings and experimental studies and their impact on diagnosis, treatment, and prevention of diseases. IJVST publishes four kinds of manuscripts: Research Article, Review Article, Short Communication, and Case Report.

Guide for Authors

GENERAL GUIDELINES

1. Submitted manuscripts should not be previously published elsewhere and should not be under consideration by any other journal.
2. The corresponding author should provide all co-authors with information regarding the manuscript, and obtain their approval before submitting any revisions.
3. The submitted manuscript should be accompanied by a written statement signed by the corresponding author on behalf of all the authors that its publication has been approved by all co-authors, stating that the whole manuscript or a part of it has not been published.
4. Ethics: Authors must state that the protocol for the research project has been approved by the Ethics Committee of the institution within which the work was undertaken. Authors are responsible for animal welfare and all statements made in their work.

OPEN ACCESS POLICY

Iranian Journal of Veterinary Science and Technology is a fully Open Access journal in which all the articles are available Open Access. There is no cost to the reader or author. All costs are covered by the Ferdowsi University of Mashhad Press.

COPYRIGHT

Copyright on any open access article in the Iranian Journal of Veterinary Science and Technology, published by Ferdowsi University of Mashhad Press is retained by the author(s).

- Authors grant Ferdowsi University of Mashhad Press a license to publish the article and identify itself as the original publisher.
- Authors also grant any third party the right to use the article freely as long as its integrity is maintained and its original authors, citation details, and publisher are identified.

The Creative Commons Attribution License 4.0 formalizes these and other terms and conditions of publishing articles. The Copyright assignment form can be downloaded from the IJVST website.

SUBMISSION

Copyright on any open access article in the Iranian Journal of Veterinary Science and Technology, published by Ferdowsi University of Mashhad Press is retained by the author(s).

- Authors grant Ferdowsi University of Mashhad Press a license to publish the article and identify itself as the original publisher.
- Authors also grant any third party the right to use the article freely as long as its integrity is maintained and its original authors, citation details, and publisher are identified.

The Creative Commons Attribution License 4.0 formalizes these and other terms and conditions of publishing articles. The Copyright assignment form can be downloaded from the IJVST website.

Guide for Authors

PREPARATION OF MANUSCRIPT

Manuscripts submitted to IJVST should neither be published previously nor be under consideration for publication in another journal. The main article types are as follows:

Research Articles should contain Title page, Abstract, Keywords, List of Abbreviations, Introduction, Results, Discussion, Materials and methods, References, and Figure legends. Tables and figures should be appended as individual files.

Review Articles should contain Title page, Abstract, Keywords, List of Abbreviations, Introduction, appropriate sections dependeing to the subject, Conclusions and future directions. Tables and figures should be appended as individual files. The review article should provide an update on recent advances in a particular field. Authors wishing to submit review articles should contact the Editor with an outline of the proposed paper prior to submission.

Case Reports should include Title page, Abstract, Keywords, List of Abbreviations, Introduction, Case Presentation, Results and Discussion, and References. Case reports should not exceed 2000 words (excluding the references) and should include no more than two tables or figures. Tables and figures should be appended as individual files.

Short Communications should not exceed 2000 words (excluding the references) and include no more than two tables or figures. They should include Title page, Abstract, Keywords, List of Abbreviations, the text summarizing results with no other divisions, and References. Tables and figures should be appended as individual files.

Submission Process

Manuscripts for IJVST should be submitted online at https://ijvst.um.ac.ir/ .

The submitting author, who is generally the corresponding author, is responsible for the manuscript during the submission and peer-review process. The submitting author must ensure that all eligible co-authors have been included in the tittle page and that they have all read and approved the submitted version of the manuscript.

To submit your manuscript, register and log in (https://ijvst.um.ac.ir/contacts?_action=loginForm). All co-authors can see the manuscript details in the submission system, if they register and log in using the e-mail address provided during manuscript submission.

Reviewer Suggestions: During the submission process, please suggest three potential reviewers with the appropriate expertise to review the manuscript. The editors will not necessarily approach these referees. Please provide detailed contact information (address, homepage, phone, e-mail address). The proposed referees should neither be current collaborators of the co-authors nor have published with any of the co-authors of the manuscript within the last three years. Proposed reviewers should be from different institutions to the authors. You may identify appropriate Editorial Board members

of the journal as potential reviewers. You may suggest reviewers from among the authors that you frequently cite in your paper. For detailed information regarding the qualifications and responsibilities of the reviewers, please visit Review Guide.

Ethics: Authors must state that the protocol for the research project has been approved by the Ethics Committee of the institution within which the work was undertaken. Authors are responsible for animal welfare and all statements made in their work.

Accepted file format

Authors are encouraged to use the Microsoft Word template to prepare their manuscript. Using the template file will substantially shorten the time to complete copy-editing and publication of accepted manuscripts. The total amount of data for all files must not exceed 120 MB. If this is a problem, please contact the Editorial Office ijvst@um.ac.ir. Accepted file formats are:

Microsoft Word: Manuscripts prepared in Microsoft Word must be written in English, with Abstract in both English and Persian (where applicable), typewritten in MS Word program, double-spaced, in 12-point "Times New Roman" font on A4 paper size. Authors are requested to reserve margins of 2.5 cm all around the pages. Manuscript should also have line numbers. All pages of the manuscripts should also be enumerated.Templates can be downloaded from the following links:

Template MS Word file for Title page (https://ijvst.um.ac.ir/page_3.html).
Template MS Word file for Original articles (https://ijvst.um.ac.ir/page_3.html).
Template MS Word file for Short Communication (https://ijvst.um.ac.ir/page_3.html).
Template MS Word file for Case Report (https://ijvst.um.ac.ir/page_3.html).
Template MS Word file for Tables (https://ijvst.um.ac.ir/page_3.html).
Template MS Word file for Persian Abstract (https://ijvst.um.ac.ir/page_3.html).

Tables: Please submit tables as individual files and editable text and not as images. Place all table notes below the table body. Each table should have a title which is followed by explanation of results shown in the table. Use of vertical rules must be avoided. Tables should be self-explanatory, and clearly arranged. Tables should provide easier understanding and not duplicate information already included in the text or figures. Each table should be typewritten with double spacing on a separate file and numbered in order of citation in the text with Arabic numerals. Each table should have a concise heading that makes it comprehensible without reference to the text of the article. Explain any non-standard abbreviations in a footnote to the table.

Figures: Figures must be submitted in individual files (format: TIFF, Dimensions: Width: 789 – 2250 pixels at 300 dpi Height maximum: 2625 pixels at 300 dpi, Resolution: 300 – 600 dpi, file size: less than 10 MB, Text within figures: Arial or Symbol font only in 8-12 point). The text and other labels should be placed in the figure as un-compressed layers. Each figure should have a title which is followed by explanation of results shown in the figure. Figures should be numbered in order of citation in the text with Arabic numerals. If a published figure is used, the publisher's permission needs to be presented to the office, and the figure should be referenced in its legend.

diagrams : For the use of bar diagrams the following publication should be consulted:

Weissgerber TL, Milic NM, Winham SJ, Garovic VD. Beyond bar and line graphs: time for a new data presentation paradigm. PLoS Biol. 2015 Apr22;13(4):e1002128. The bar diagrams should be provided in color and in a well-designed and professional format. Please do not use different shades of gray. The axes of diagrams should have titles and units. Also, the source file of the image (Excel etc.) should be provided for typesetting.Illustrations should be numbered as cited in the sequential order in the text, with a legend at the end of the manuscript. Color photographs are accepted at no extra charge. The editors and publisher reserve the right to reject illustrations or figures based upon poor quality of submitted materials.

Title Page information

Full Title Page should include title (concise and informative), author(s) (including the complete name, department affiliation, and institution), running head (condensed title) (≤ 50 characters, including spaces), name and address of the authors to whom correspondence and reprint requests should be addressed, Acknowledgements, Author contributions, and Conflict of interest.

Acknowledgements: Personal acknowledgement, sources of financial support, contributions and helps of other researchers and everything that does not justify authorship should be mentioned in this section, if required.

Author contributions: Authors are required to include a statement to specify the contributions of each author. The statement describes the tasks of individual authors referred to by their initials. Listed below is an example of author contributions statement:

" Conceived and designed the experiments: HD, SS. Performed the experiments: SS. Analyzed the data: HD, SS, MMM, ARB.

Research space and equipment: HD, MMM, ARB. Contributed reagents/materials/analysis tools: HD. wrote the paper: SS, HD."

Conflict of interest: All authors must disclose any financial and personal relationships with other people or organizations that could inappropriately influence (bias) their work. Examples of potential conflicts of interest include employment, consultancies, stock ownership, honoraria, paid expert testimony, patent applications/registrations, and grants or other funding. If there are no conflicts of interest then please state 'The authors declare that there is no conflict of interest'. This form can be downloaded from the IJVST website.

Abstract: Abstract (in English and Persian) no more than 250 words should contain the purpose of the study, findings and the conclusion made on the basis of the findings. Authors who are not native Persian speakers may submit their manuscript with an abstract in English only. Abbreviations and reference citations may not be used in the abstracts.

Keywords: For indexing purposes, each submitted manuscript should include three to seven keywords, following the abstract and preferably chosen from the Medical Subject Headings (MESH). Keywords should express the precise content of the manuscript.

Abbreviations: Define abbreviations that are not standard in this field in a list to be placed on the tit-

tle page. Such abbreviations that are unavoidable in the abstract must be defined at their first mention there, as well as in the tittle page. Ensure consistency of abbreviations throughout the article.

Main Text

Introduction: Introduction should be as concise as possible, and clearly explain the main objective and hypothesis of the investigation.

Results: Results indicate the results of an original research in a clear and logical sequence. Do not repeat data that are already covered in tables and illustrations. In manuscripts describing more than one animal, all animals should be assigned a case number.

Discussion: Discussion should include the answer to the question proposed in the introduction and emphasize the new and important aspects of the study and the conclusions that follow from them. It could include the implication, application, or speculation of the findings and their limitations, relate the observations to other relevant studies, and links the conclusions with the goals of the study. Recommendations, when appropriate, may be included.

Materials and Methods: Materials and methods should be described in sufficient details to allow other researchers to reproduce the results. Specify any statistical computer programs used .The methods of data collection and use of statistical analysis will be checked by the referees and if necessary, a statistician. Drugs and therapeutic agents, reagents, softwares and equipments should be given in the format: name (trade name, manufacturer name, city, country), e.g. Statview 5 (SAS Institute, Inc., Cary, NC, USA).

Animals: All animal experiments should comply with the ARRIVE guidelines and the authors should clearly indicate in the manuscript the ethical code of the study.

Gene names: The standard gene names, as provided by HGNC should be used. Gene names must be italicized. If the case of mammalian species and if gene names refer to rodent species, they must be upper case; if they refer to non-rodent species they must be written in capitals. If they refer to other species, they must written lower case. Protein names are written in capitals and are not italicized. As an example:

Mouse beta actin gene: Actb

Bovine beta actin gene: ACTB

Chicken beta actin gene: actb

Beta actin protein: ACTB

Quantitative PCR: If the quantitative PCR method has been used, the related section in Materials and Methods and Results must be written following the reference:

Bustin SA, Benes V, Garson JA, Hellemans J, Huggett J, Kubista M, Mueller R, Nolan T, Pfaffl MW, Shipley GL, Vandesompele J, Wittwer CT. The MIQE guidelines: minimum information for publica-

tion of quantitative real-time PCR experiments. Clin Chem. 2009 Apr;55(4):611-22.

Protocol for DNA/RNA extraction, including quantification and determination of purity.

Reverse transcription (if used): amount of RNA, concentration of all reagents: primers conce ntration (either random primers or oligonucleotides), reverse transcriptase and master mix components.

qPCR: sequence of forward and reverse primers, probes, amplicon size, accession number of Genebank;

thermocycler parameters (i.e. denaturation, annealing and extension steps, number of cycles, melting curves);

validation of PCR products; non-template controls for reverse transcription and qPCR should be included in all reactions; and

Data analysis: details for the quantitative or relative analysis.

Use of antibodies: Authors must show that the antibodies are validated and their specificity sis confirmed.

References: Must be up-to-dated and limited to those that are necessary. Lists of references should be given in numerical order in the text, and in the reference list. Please use Vancouver style. To download the Vancouver Style follow the link in the IJVST website which could be used in the Endnote software.

Example piece of text and reference list :
An unhealthy diet, obesity and physical inactivity play a role in the onset of type 2 diabetes, but it has been shown that increased physical activity substantially reduces the risk [1], and participation in regular physical activity is one of the major recommendation of the evidence based guidelines for the primary prevention of diseases [2]. According to the 2004-05 National Health Survey, more than half a million Australians (3.5% of the population) have diabetes mellitus which had been medically diagnosed and most of these people have the Type 2 condition [3]. Gestational diabetes is also on the increase, rising steadily between 2000-01 and 2005-06 [4]. Approximately two thirds of those with diabetes have been prescribed medication [3], but it is of concern that a recent review of the literature found that many people do not take their medication as prescribed [5]. Many patients also self monitor the disease by measuring their blood glucose levels with a glucose meter but Song and Lipman [6] have concerns about how well this is managed.

References for the above example:
1. Hull J, Forton J, Thompson A. Paediatric respiratory medicine. Oxford: Oxford University Press; 2015.
2. Eckerman AK, Dowd T, Chong E, Nixon L, Gray R, Johnson S. Binan goonj: bridging cultures in Aboriginal health. 3rd ed. Chatswood, NSW: Elsevier Australia; 2010.
3. Johnson C, Anderson SR, Dallimore J, Winser S, Warrell D, Imray C, et al. Oxford handbook of expedition and wilderness medicine. Oxford: Oxford University Press; 2015.
4. McLatchie GR, Borley NR, Chikwe J, editors. Oxford handbook of clinical surgery. Oxford: Oxford University Press; 2013.

5. Petitti DB, Crooks VC, Buckwalter JG, Chiu V. Blood pressure levels before dementia. Arch Neurol. 2005 Jan;62(1):112-6. Doi: 10.1001/archneur.62.1.112 .
6. Liaw S, Hasan I, Wade, V, Canalese R, Kelaher M, Lau P, et al. Improving cultural respect to improve Aboriginal health in general practice: a multi-perspective pragmatic study. Aust Fam Physician. 2015;44(6):387-92.Doi: 10.1001/archneur.62.1.112 .
Use of Italics

Gene symbols, Latin terms (i.e. in vivo, in vitro, ex vivo, in utero, in situ, and etc.) and species scientific names (using the binomial nomenclature), should be typed in italics, while the first letter of the genus name must be capitalized (i.e. Homo sapiens).

Copyright

PUBLICATION ETHICS

Iranian Journal of Veterinary Science and Technology is a member of the Committee on Publication Ethics (COPE), best practice guidelines for dealing with ethical issues in journal publishing and adopts the COPE guidelines. The journal members (editor, editorial board and the journal manager) have agreed to meet the purposes and objectives of the Journal.

Ethical guidelines for authors:

- Manuscripts must be submitted with the understanding that they have not been previously published and are not currently under consideration by another journal.
- Authors are expected to submit manuscripts with enough detail and references to enable others to replicate the work.
-Authors may be requested to provide the original data from their study for editorial review and should be ready to make the data publicly available if feasible.
-The corresponding author is responsible for ensuring that all co-authors have approved the manuscript prior to submission.
- Only individuals who meet the authorship criteria should be listed as authors in the manuscript, as they are expected to take public responsibility for the content. The "Conflict of interest declaration and author agreement form" must be signed and completed by all authors. This statement and sig-

natures certifies that all authors have seen and approved the manuscript being submitted. Also, the authors by signing this form warrant that the article is the Authors' original work, that the article has not received prior publication and is not under consideration for publication elsewhere, and that the corresponding author shall bear full responsibility for the submission.

Before submission, all authors are required to review the Article Submission Checklist.

- Authors should disclose any conflicts of interest that might be perceived as influencing the results or their interpretation in the manuscript at the earliest stage possible. This can be done by uploading the Conflicts of Interest Form along with the manuscript submission.

-The authors are responsible for ensuring that the submitted manuscript is a complete and original work, free from any form of plagiarism. All authors are advised to use plagiarism prevention software to check for similarities.

-Authors are required to identify in their manuscript if their work involves chemicals, procedures, or equipment that have any inherent unusual hazards.

- All researchers should have a written and signed informed consent form from whom voluntarily participate in their researches. This signed form shows obviously the consent of the subject to participate. All steps of the experiment were carried out based on the Guidelines for Animal Care at Ferdowsi University of Mashhad in Iran that are approved by the Committee of Biological Ethics, Faculty of Veterinary Medicine, Ferdowsi University of Mashhad, Iran (https://ethics.research.ac.ir/docs/pages/Guideline-En.pdf). The experiments that are carried outside the university should have a written and signed informed consent form related to ethic protocols of university or institute that they are carried.

- If the decision is 'Needs Revision,' authors are expected to respond systematically and promptly to the reviewers' comments, addressing point by point, and revising their manuscript accordingly. The revised manuscript should then be submitted to the journal within the given deadline.

- Authors are requested to clearly identify who financially supported the research and/or preparation of the manuscript and briefly describe the role of the founder/ sponsor in any part of the work at the end of their manuscript under "Acknowledgements" section.

-It is a condition for submission of a manuscript that the authors permit editing of the paper for readability.

- All authors agree to allow the corresponding author to serve as the correspondent with the Journal's editorial office, to review the edited manuscript and proof.

-Under open access license, authors retain ownership of the copyright for their content, but allow anyone to download, reuse, re-print, modify, distribute, and/or copy the content as long as the original authors and source are cited properly.

- When author(s) discover(s) a significant error or inaccuracy in his/her own published work, it is the author's obligation to promptly notify the Journal editor or publisher to retract or correct the manuscript.

- All authors must know that the submitted manuscripts under review with the IJVST are subject to screening, using Plagiarism Prevention Software. Plagiarism is a serious violation of publication ethics and in all its forms constitutes unethical publishing behavior and is unacceptable.

- Editors and members of editorial board as authors should be excluded from publication decisions

when they are authors or have contributed to a manuscript.

-The artificial intelligence (AI) tools such as ChatGPT or Large Language Models cannot meet the requirements for authorship. Authors who use AI tools in the writing of a manuscript, production of images or graphical elements of the paper, or in the collection and analysis of data, must be transparent in disclosing in the Materials and Methods (or similar section) of the paper how the AI tool was used and which tool was used. Authors are fully responsible for the content of their manuscript, even those parts produced by an AI tool, and are thus liable for any breach of publication ethics(Authorship and AI tools).

Ethical guidelines for Peer reviewers

- Reviewers are expected to provide insightful comments that assist the editors in making a decision about whether or not to publish the submitted manuscript.

- Reviewers are expected to maintain the confidentiality of the manuscripts they are invited to review.

-Reviewers are expected to disclose any conflicts of interest they have with the authors, companies, or institutions associated with the manuscripts they are invited to review. If a conflict of interest exists, reviewers should immediately notify the Editor-in-Chief, decline the invitation to review, and suggest alternative reviewers.

- If reviewers feel unqualified to review an assigned manuscript or are unable to provide a timely review, they should inform the Editor-in-Chief and excuse themselves from the review process. If they know of any other expert reviewers, they may suggest them to the Editor-in-Chief through the dedicated email/comments section in the Reviewer Dashboard.

- Reviewers are expected to maintain the confidentiality of the manuscripts they review and not discuss any information from the manuscript with anyone other than the Editor-in-Chief, unless they have obtained explicit permission to do so. This also applies to invited reviewers who decline the review invitation.

- Reviewers are obligated to treat the manuscripts they receive for peer review as confidential and must not use any information obtained through this process for personal gain.

-Reviewers are expected to provide technical, professional, and objective comments on the manuscripts they are invited to review.

-Reviewers are expected to avoid personal biases in their comments and judgments, and express their views clearly with supporting arguments that assist the author in improving the manuscript.

-Reviewers are expected to identify any relevant published work that has not been cited by the authors. If a statement has been previously reported elsewhere, it should be accompanied by the appropriate citation.

-Reviewers should also bring to the attention of the Editor-in-Chief any significant similarity or overlap between the manuscript under consideration and any other publications of which they are personally aware.

The process has been explained in the section “Peer Review Process”.

Publication Ethics

Ethical guidelines for Editor

-The editors should evaluate submitted manuscripts to determine if they fall within the scope of the journal. Additionally, the editors should recommend expert reviewers based on their integrated recognition of specialized reviewers.

-The Editor-in-Chief is responsible for deciding whether to accept or reject submitted manuscripts for the journal. This decision takes into consideration several factors, such as the judgment of the editorial board members, the validation of the work in question, its significance to researchers and readers, as well as any feedback from reviewers. Furthermore, the decision must also comply with legal requirements regarding libel, copyright infringement, and plagiarism, which are currently in force. The Editor-in-Chief works closely with other editors and reviewers to ensure that all submissions are fairly evaluated.

-The editors ought to uphold the anonymity of both reviewers and authors.

-The editors should disclose any potential conflicts of interest and make efforts to avoid them. If such circumstances arise, they are expected to delegate the handling of the manuscript to another member of the editorial board.

-The editors, particularly the Editor-in-Chief, should demonstrate a willingness to investigate cases of plagiarism and fraudulent data. When ethical concerns are raised about a submitted manuscript or published paper, the editors will take appropriate measures in response. Any reported incidents of unethical publishing behavior will be thoroughly examined, even if they come to light years after publication.

-When dealing with cases of suspected misconduct, the Editor-in-Chief follows the COPE Flowcharts. If an investigation supports the ethical concern, the journal will publish a correction, retraction, expression of concern, or any other relevant note.

-The editors must not share any information about submitted manuscripts with anyone until they are published, as appropriate.

-The Editor-in-Chief and members of the editorial board will not use unpublished materials disclosed in a submitted paper for their own research purposes without obtaining explicit written consent from the author.

-Editors are expected to give fair consideration to all manuscripts submitted for publication, evaluating each on its own merits and without prejudice based on the author(s)' country, race, religion, nationality, sex, seniority or institutional affiliation. Decisions about editing and publishing are made solely based on the quality and relevance of the manuscript and are not influenced by external policies of governments or other agencies beyond the scope of this journal.

-The Editor-in-Chief has complete authority over the editorial content of the journal as well as the timing of its publication.

Ethical guidelines for Publisher

"Ferdowsi University of Mashhad press (FUM)" is promising to ensure that the decision on manuscript submissions is only made based on professional judgment and will not be affected by any

commercial interests.

- FUM is committed to maintain the integrity of academic and research records.

- FUM is monitoring the ethics by Editor-in-Chief, Associate Editors, Editorial Board Members, Reviewers, Authors, and Readers.

- FUM, together with the Journal's editors, shall take reasonable steps to identify and prevent the publication of manuscripts where research misconduct has occurred, and under no circumstances encourage such misconduct or knowingly allow taking place.

- FUM is always checking the plagiarism and fraudulent data issues involving in the submitted manuscripts and willing to publish corrections, clarifications and retractions involving its publications as and when needed.

-FUM as the publisher supports the Journal for each published issue by paying a defined budget according to its published annual rank in the Portal of Scientific Journals of Iranian Ministry of Science, Research and Technology for costs including those pertaining to setup and maintenance of the publication infrastructure, routine operation of the Journal, processing of manuscripts through peer-reviews, editing, publishing, maintaining the scholarly record, and archiving.

Violation of Publication Ethics

The Editorial board of IJVST acknowledges that plagiarism is unacceptable in any of its forms:

Plagiarism:

Plagiarism is intentionally using someone else's ideas or other original material as if they are one's own. Copying even one sentence from someone else's manuscript, or even one of your own that has previously been published, without proper citation is considered by the JAM as plagiarism. All manuscripts under review or published with JAM are subject to screening using plagiarism prevention software (e.g. iThenticate). Thus, plagiarism is a serious violation of publication ethics.

Simultaneous Submission:

Care should be taken to ensure that the work has not been published elsewhere, in any language and is not simultaneously submitted to other journals.

Duplicate Publication:

Duplicate publication occurs when two or more articles, without full cross referencing, share essentially the same hypotheses, data, discussion points, and conclusions.

Redundant Publications:

Redundant publications involve the inappropriate division of study outcomes into several articles, most often consequent to the desire to plump academic vitae.

Data Fabrication:

Data fabrication means the researcher did not really carry out the study, but made up data or results and had recorded or reported the fabricated information. Data falsification means the researcher did the experiment, but manipulated, changed, or omitted data or results from the research findings.

Citation Manipulation:

Citation Manipulation implies excessive citations in the submitted manuscript that do not contribute to the scholarly content of the article and have been included solely for the purpose of increasing citations to a given author's work, or to articles published in a particular journal. This leads to misrepresenting the importance of the specific work and journal in which it appears and is thus a form of scientific misconduct.

Improper Author Contribution or Attribution:

All listed authors must have made a significant scientific contribution to the research in the manuscript and approved all its claims. Do not forget to list everyone who made a significant scientific contribution, including students and laboratory technicians.

Handling Misconduct Cases

The Editorial board of IJVST takes the necessary measures to examine the incoming papers on their originality, reliability of contained information and correct use of citations.

-If any of the unethical publishing behavior is detected by the Journal Editorial board or by one of the reviewers, the first action is to inform the Editor-in-chief by supplying copies of the relevant material and a draft letter to the corresponding author asking for an explanation in a nonjudgmental manner.

- If the infraction is less severe, the Editor, upon the advice of the Committee on Publication Ethics, sends the author a letter of reprimand and reminds the JAM publication policies; if the manuscript has been published, the Editor may request the author to publish an apology in the journal to correct the record.

- If the author's explanation is unacceptable and it seems that serious unethical conduct has taken place, the matter is referred to the Publication Committee via Editorial board. After deliberation, the Committee will decide whether the case is sufficiently serious to warrant a ban on future submissions.

Post-Publication Discussions and Corrections

This journal allows debate post publication on journal's site, through "Send comment about this article" section to the editor up to one month before final publication. Our mechanisms for correcting, revising or retracting articles after publication depends on the content of the received comment and if the sent comments are useful and applicable for readers/authors, they will be showed under reference section of the articles pages.

Complaint Policy

If the authors disagree with the editorial decision on their manuscripts, they have a right to appeal. Authors who wish to appeal an editorial decision should contact the Editor-in-Chief of the Iranian Journal of Veterinary Science and Technology. In such cases the Editor-in-Chief will review the manuscript, the editorial and peer reviewers' comments and gives his/her decision for accepting or rejecting a manuscript. Editor-in-Chief may, if so required, send the manuscript to a new handling editor for a fresh editorial review and to new reviewer for further peer reviewing. In such case, the

final decision maker will be the Editorial board of the journal.

How to Make a Complaint

The procedure to make a complaint is quite simple. The complaint can be made by writing an e-mail to: ijvst@um.ac.ir. All complaints will be acknowledged within a week.

PEER REVIEW PROCESS

Iranian Journal of Veterinary Science and Technology peer reviews all submitted manuscripts with contents within the scope of the journal.

Initial assessment

The submitted manuscript will be subjected to a primary review by the editor or a member of the editorial board for suitability and relevance of the findings to the scope of the journal and quality of the science presented in the paper (sufficient originality, having a message that is important to the general field of Veterinary Medicine, quality of data, novelty, English language, and overall manuscript quality) within two weeks. If the paper is evaluated to be relevant to the scope of the journal and having enough scientific rigor and novelty, it will be sent for the next stage. Otherwise, those manuscripts which are evaluated as not-appropriate in the initial review will be rejected at this stage.

Initial screen

The initial screen will be performed by the editorial office for the structure and format of the manuscript.

Peer review (double-blind)

The manuscripts which are found to be appropriate after the initial screen will be sent for external review by experts in the related field. We have prepared a checklist for reviewers that summarizes their evaluation of the manuscript. The items in this checklist are:

1. TITLE is clear and adequate
2. ABSTRACT clearly presents objects, methods, and results.
3. INTRODUCTION well-structured and provides a rationale for the experiments described.
4. MATERIALS AND METHODS are sufficiently explained and is detailed enough to be reproduced.
5. RESULTS are clearly presented and supported by figures and tables.
6. DISCUSSION properly interprets the results and places the results into a larger research context, and contains all important references.
7. Conclusions are logically derived from the data presented.
8. English Language/style/grammar is clear, correct, and unambiguous.
9. Figures and tables are of good quality and well-designed and clearly illustrate the results of the study.
10. References are appropriate.
11. Regarding this article are you concerned about any issues relating to author misconduct such as plagiarism and unethical behavior.

12. Comments on the importance of the article.

Final Decision

Based on the reviewers' recommendations a final decision is made by the editor and if needed the help of a member of the editorial board (depending on the field of study). Decisions will include accept, minor revision, major revision with and without re-review, and reject. We aim to reach a final decision on each manuscript as soon as their review results are available.

Iranian Journal of Veterinary Science and Technology

Faculty of Veterinary Medicine, Ferdowsi University of Mashhad, Azadi Square, Mashhad, IRAN
P.O. Box: 1793; Postal Code: 9177948974

Tel: 0098 51 3880 3742
Fax: 0098 51 3876 3852

Web: ijvst.um.ac.ir
Email: ijvst@um.ac.ir